MOLECULAR MECHANISMS INVOLVED IN THE ANTICANCER ACTIVITY OF BISPMB IN OESOPHAGEAL CANCER CELLS

Thesis presented by

VUYOLWETHU PENELOPE SIYO

In fulfilment of the requirements of the degree of

DOCTOR OF PHILOSOPHY

In

Medical Biochemistry

Supervisor: Prof. M. Iqbal Parker

Co supervisor: Dr Catherine H. Kaschula

Faculty of Health Science, University of Cape Town

International Centre for Genetic Engineering and Biotechnology

September 2015

University of Cape Town

The copyright of this thesis vests in the author. No quotation from it or information derived from it is to be published without full acknowledgement of the source. The thesis is to be used for private study or non-commercial research purposes only.

Published by the University of Cape Town (UCT) in terms of the non-exclusive license granted to UCT by the author.

University of Cape Town

DEDICATION

This thesis is dedicated to my family who have been my rock and have supported me in every way possible throughout my studies.

The completion of this thesis also bears tribute to my late grandmother, who always had faith in me and foresaw the conclusion of my studies. I hope I have made you proud.

ACKNOWLEDGEMENT

I would like to thank my supervisors Prof. M. Iqbal Parker and Dr. Catherine H. Kaschula for taking the time to guide, encourage, and motivate me during the course of my PhD studies. I have learnt a lot from working with you, thank you for the opportunity.

I am also grateful for the support and the willingness to help that I received from my ICGEB colleagues throughout the years. To Dr. Kevin Dzobo and Dr Lamech Mwaphagha, for reading sections of this thesis and providing constructive feedback. To the soon to be Dr Akhona Vava, for proof reading this thesis, bearing with me and being a good friend through my mood swings. Thank you for seeing me through challenging periods.

I whole heartedly thank the following funders; NRF innovation and doctoral extension scholarship, UCT Equity Scholarship, UCT Doctoral Research scholarship, Marion Beatrice Waddell Scholarship and KW Johnstone Bequest for providing me with financial support for my studies. Without your support, this work would not be possible.

I would also like to thank the CPGR team, for conducting the microarray and providing me with the bioinformatics assistance during my microarray analysis.

I am eternally grateful to my mother and aunt (Nosisi Siyo, Nomfanelo Siyo), sister (Wendy Siyo) and the rest of my beloved family for their unconditional love, words of encouragement and believing in me throughout the years.

“It always seems impossible, until it is done”..... *Nelson Mandela*

Above all, I praise God for blessing me, for seeing me through it all and for giving me strength and means to complete this project.

“I can do all things, through Him who gives me strength”..... Philippians 4:13

ABBREVIATIONS

ABTS	2, 2'-azino-bis (3-ethylbenzothiazoline-6-sulphonic acid)
APS	Ammonium persulfate
ATCC	American type culture collection
ATF	Activating Transcription Factor
BiP	Immunoglobulin heavy chain-binding protein
BisPMB	(E,Z)-1,8-(Bis-p-methoxyphenyl)-2,3,7-trithiaocta-4-ene 7-oxide)
BSA	Bovine Serum Albumin
CHOP	C/EBP [CAAT/enhancer- binding protein]- homologous
DAG	Directed acyclic graph
DEGs	Differentially expressed genes
DMEM	Dulbecco's modified eagle medium
DMSO	Dimethyl sulfoxide
DNA	Deoxynucleotide nucleic acid
dNTPs	Deoxynucleotide triphosphates
EDTA	Ethylenediaminetetraacetic acid
EGF	Epidermal growth factor
EGTA	Ethylene glycol tetraacetic acid
ER	Endoplasmic reticulum
ERAD	Endoplasmic Reticulum Associated Degradation
ERSE	Endoplasmic Reticulum Stress Element
FBS	Foetal bovine serum
FDR	False Discovery Rate
GAPDH	Glyceraldehyde-3-phosphate dehydrogenase
GO	Gene Ontology
HRP	Horseradish peroxidise
Hsp90	Heat shock protein 90
IPA	Ingenuity Pathways Analysis
IPAKB	Ingenuity Pathway Analysis Knowledge Base
IRE1	Inosotol-requiring Enzyme 1
JNK	c-Jun N-terminal kinase
KEGG	Kyoto Encyclopedia of Genes and Genomes

MAPK	Mitogen-activated protein kinase
MEF	Mouse embryonic fibroblast
MTT	Thiazoyl blue tetrazolium bromide
ORF	Open Reading Frame
OSCC	Oesophageal Squamous Cell Carcinoma
P/S	Penicillin/ Streptomycin
PBS	Phosphate buffered saline
PCA	Principle Component Analysis
PCR	Polymerase chain reaction
PERK	PRK-like endoplasmic reticulum kinase
RefSeq	Reference Sequence
RMA	Robust Multi-array Average
RNA	Ribonucleic acid
SCC	Squamous cell carcinomas
qRT-PCR	Quantitative Reverse Transcriptase- Polymerase Chain Reaction
siRNA	Short interference RNA
TEMED	N, N, N', N' Tetramethylethylenediamine
TG	Thapsigargin
TNF-α	Tumour necrosis factor alpha
Ub	Ubiquitin
UPR	Unfolded Protein Response
UPRE	Unfolded Protein Response Element
WHCO1	Wits Human Carcinoma of the Oesophagus
XBP1	X-box binding Protein 1

TABLE OF CONTENTS

LIST OF TABLES

LIST OF FIGURES

ABSTRACT

BisPMB (E, Z)-1,8-(Bis-p-methoxyphenyl)-2,3,7-trithiaocta-4-ene 7-oxide) is a synthetic analogue of the garlic compound ajoene. It is 12 times more active at inhibiting the growth of oesophageal squamous cell carcinoma WHCO1 cells and displays selectivity for cancer cells over normal cells. BisPMB is therefore attractive as a potential cancer therapeutic.

In this study, bisPMB was found to inhibit WHCO1 cancer cell proliferation in a time and concentration dependent manner with 24 hour IC_{50}'s between 6.7 – 8.1 μM against a range of oesophageal cancer cell lines including WHCO1, KYSE30 and WHCO6. The normal oesophageal epithelial cell line, HET1A was found to be five times less responsive to bisPMB. Furthermore, bisPMB was found to induce apoptosis and G_2/M cell cycle arrest in WHCO1 cells. Gene expression data obtained from the microarray analysis showed that bisPMB primarily targets the unfolded protein response (UPR) in WHCO1 cells. We also found that bisPMB deregulated the ER stress genes involved in protein processing in the endoplasmic reticulum and also deregulated MAPK pathways in WHCO1 cells. At a protein level, bisPMB was found to induce an increase in protein ubiquitination and in the expression of ER stress and UPR genes ATF4, Grp78 and CHOP in WHCO1 cells. We also observed a decrease in ATF6 90 kDa protein and transient XBP-1 mRNA splicing. The activation of p38, JNK and ERK MAPK pathways in bisPMB treated WHCO1 cells was also observed. Furthermore siRNA mediated knock-down of CHOP abolished the anti-proliferative effect of bisPMB in WHCO1 cells. However, inhibition of JNK and p38 MAPK by chemical inhibitors, SP600125 and SB 203580 respectively, had no effect on bisPMB antiproliferative activity against WHCO1 cells. On the other hand, inhibition of ERK1/2 MAPK by U0126 enhanced the anti-proliferative effect of bisPMB in WHCO1 cells. These results support the hypothesis that ER stress and MAPK signalling pathways are essential for bisPMB induced cytotoxicity in oesophageal cancer cells.

CHAPTER 1: LITERATURE REVIEW

Oesophageal cancer (OC) presents a significant health burden in South Africa, being the third most prevalent cancer amongst black South African males. The average 5 year survival rate for these patients is reported to be less than 10% (Wong and Malthaner, 2000, Hendricks and Parker, 2002, Cotton et al., 2014, Dandara et al., 2015, Somdyala et al., 2015) and this is commonly attributed to late stage diagnosis of the disease. In addition, current OC treatment options have low success rates and poor prognosis (Barabas et al., 2008, Cohen and Leichman, 2015). Consequently, more effective and less toxic chemotherapeutic treatment options are needed. In this thesis, we investigate a new compound called bisPMB for OC therapeutic that has been developed based on the structure of the garlic compound ajoene. We present data on its cytotoxicity, its effect on gene transcription and the signalling pathways it modulates in WHCO1 oesophageal cancer cells. We also show that bisPMB induces its cytotoxic effects primarily via the ER stress and UPR pathway.

1.1 Treatment of oesophageal cancer

The treatment of OC is challenging because most patients present late for therapy and current treatment options result in low survival rates. For example, the 5 year survival rate for OC patients that have undergone surgery alone is 5 - 30% (Allum et al., 2009). Furthermore, this outcome is mainly applicable to patients diagnosed at the early stages of the OC disease development.

Consequently, multimodal approaches are often used to improve the prognosis for OC patients, consisting of a combination of surgery, chemotherapy, radiotherapy, chemoradiotherapy, laser treatment, stent insertions and radiofrequency ablation (RFA) (Desai et al., 1989, Koshy et al., 2004, Tong and Law, 2009, Dandara et al., 2015). However the benefit of a multimodal treatment approaches is not clear with several clinical trials reporting conflicting outcomes (Bosset et al., 1997, Kelsen et al., 1998, Cooper et al., 1999, Urba et al., 2001, Stahl et al., 2005). Despite the inconclusive outcomes of the clinical trials, the most promising therapies are selected for treatment. The treatment options selected for therapy are dependent on multiple factors including the disease stage, as defined by the tumour node metastasis (TNM) system (Edge and Compton, 2010, Rice et al., 2010). Stage 0 OC tumours are defined as non-invasive high grade dysplasia of the epithelial cells lining the oesophagus and are mainly treated by surgery alone (Rice et al., 2010). In stage I, when the

cancer has grown into the submucosa layer of the oesophagus (Rice et al., 2010), combination of chemo-radiation followed by surgery or surgery alone is administered (figure 1.1) (Mackay and Stefanou, 2006, Graham et al., 2007, Tong and Law, 2009). Late stage cancers (stage II and III) which invade all the oesophageal muscle layers and spread into the local lymph nodes (Rice et al., 2003, Rice et al., 2010) are usually treated with a combination of chemoradiotherapy and surgery or surgery alone or chemo-radiotherapy alone. The final stage IV cancer obstructs the oesophagus lumen and metastasizes to local and distant lymph nodes and possibly tissues (Rice et al., 2003). It is the stage that most patients are diagnosed in because OC patients typically present with dysphasia (Schlansky et al., 2006). For stage IV, the treatment options are primarily for palliative purposes and they include chemo radiation followed by surgery, stent insertions and chemotherapy (figure 1.1) (Tong and Law, 2009, Kato and Nakajima, 2013). In most cases, OC treatment options (i.e. surgery, chemotherapy and radiotherapy) need to be improved with new and effective chemotherapeutic options

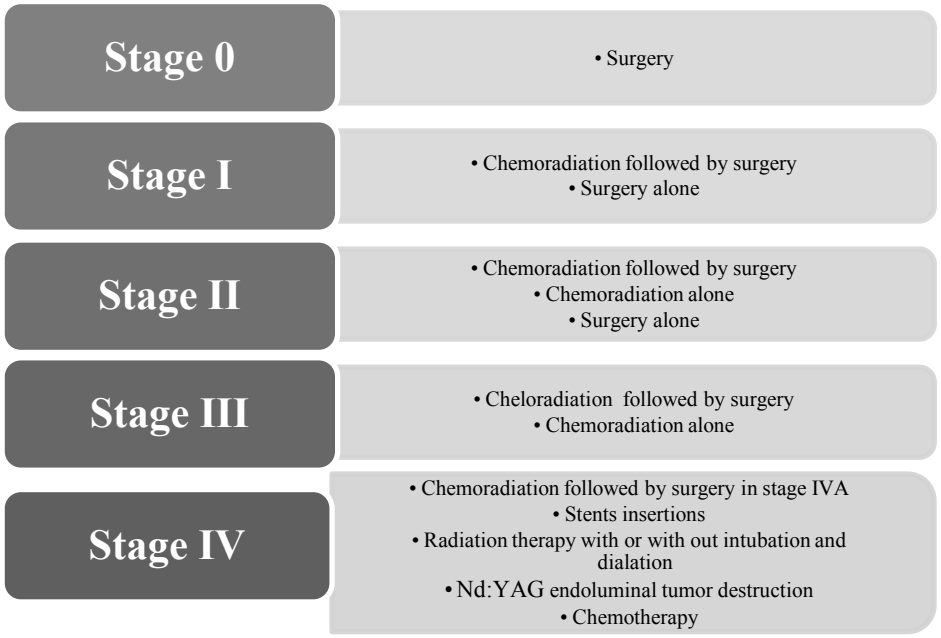

Figure 1.1 Standardized treatment options for each OC stage. Stage 0 non-invasive OC tumours are surgically removed. Stage I OC tumours are treated with chemoradiation in combination with surgical removal. Late metastatic stage II, III and IV OC tumours are subjected to palliative treatment including chemo radiation, surgery, stent insertions, radiation and chemotherapy.

The chemotherapeutic drugs currently used in OC treatment are cisplatin, 5-fluorouracil (5-FU), paclitaxel and docetaxel. These drugs targets different pathways in cancer cells. For

example, cisplatin exerts its cytotoxic effects by interacting with DNA, forming DNA adducts and inhibiting DNA synthesis and repair (Dasari and Tchounwou, 2014). 5-FU is metabolised to form fluorodeoxyuridine monophosphate (FdUMP) which inhibits the synthesis of deoxythymidine monophosphate (dTMP) by thymidilate synthase and thus blocks DNA repair and replication (Longley et al., 2003). Paclitaxel and docetaxel are anti-mitotic agents which target microtubules by directly interacting with β-tubulin (Horwitz, 1994, Stein, 1999). The net effect of the aforementioned chemotherapeutic drugs is inhibition of growth and induction of apoptosis in rapidly dividing cancer cells.

Cisplatin is the most widely used chemotherapeutic drug for OC treatment, however toxic side effects and drug resistance remain problematic (Barabas et al., 2008, Galluzzi et al., 2012, Galluzzi et al., 2014). In order to reduce toxicity, drug combination regimens with cisplatin have been developed which have enabled reduction of the cisplatin dose (Ali and Al Moundhri, 2006). Cisplatin is commonly combined with 5-FU, docataxel or paclitaxel to result in a synergistic outcome .

The most widely used cisplatin based combination is cisplatin/5-FU. In a phase II randomised trial, it was reported that the outcome of patients treated with cisplatin/5-FU combinations compared to cisplatin alone displayed an overall survival rate of 35 % compared to 19 % with cisplatin alone although still with unwanted side effects (Bleiberg et al., 1997). This has led to the development of the cisplatin/5-FU/paclitaxel or cisplatin/paclitaxel combinations, which are reported to be active with tolerable side effects (Petrasch et al., 1998, Kim et al., 1999).

Drug synergism arises in most cases from combinations that target multiple pathways such as the combination of a DNA binding compound (cisplatin) together with an anti-mitotic (Paclitaxel) (Jekunen et al., 1994, Cai et al., 2015). Furthermore, toxicity can be reduced in combination therapy due to a lowering of the effective drug concentration required for activity with drugs acting synergistically (Clark et al., 2010). Although drug combinations for the treatment of OC are currently acceptable, the survival rate is still low and the development of new and less toxic chemotherapeutics is needed.

1.2 Plants as a source of anticancer drugs

Plants contain reservoirs of compounds active both in cancer prevention and treatment. The potential of plants to yield compounds for cancer therapeutic development led to the establishment of the United States National Cancer Institute (US NCI), plant collection program, in the early 1960's.

During the period of 1967 – 1971, Hartwell and colleagues reported over 3000 plant species that possessed anti-cancer properties. To date over 275 000 structures of compounds have been recorded in the national cancer institute (NCI) database (Hartwell, 1969c, Hartwell, 1969b, Hartwell, 1969a, Hartwell, 1971, Graham et al., 2000, Shiryaev et al., 2011). In addition, over 60 % of the newly approved anticancer drugs documented in *Annual Reports of Medicinal Chemistry* during the 1984 - 1995 originated from natural sources (Cragg et al., 1997).

Currently available plant derived anticancer drugs, either in clinical use or trials are categorised into vinca alkaloids, camptothecin derivatives, epipodophyllotoxins, anthracyclines and taxanes (Cragg and Newman, 2005, Nobili et al., 2009). Taxol is the success story of the NCI plant collection program. This clinical anticancer drug was discovered from extracts of the bark of the Pacific Yew, *Taxus brevifolia* found in the Pacific Northwest of North America (Cragg, 1998).

There are a number of plant based foods that contain compounds (table 1.1) able to inhibit initiation and progression of cancer (Surh, 2003). One of these compounds, ajoene; is derived from garlic and is the compound of interest in this project.

Table 1.1 Dietary plant derived compounds with cytotoxic effects against cancer cell lines and *in vivo*

Source	Compound	Structure	Cancer Cell Lines	Reference
Turmeric	Curcumin	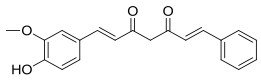	Skin,colon, myeloid leukaemia and multiple myeloma	(Singh and Aggarwal, 1995, Plummer et al., 1999, Bharti et al., 2003)
Chilli Peppers	Capsaicin	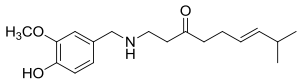	Mouse skin tumour and human leukaemia cells, melanoma cells and Jurkat cells	(Han et al., 2001)
Ginger	[6]-Gingerol	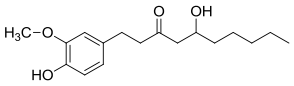	Mouse skin	(Park et al., 1998)
Green tea	Epigallocatechin-3-gallate	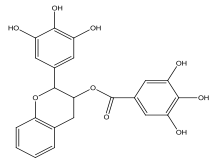	Mouse epidermal keratinocytes JB6 cell line, human breast, head and neck cancer cell lines	(Afaq et al., 2003, Masuda et al., 2002)
Soybeans	Genistein	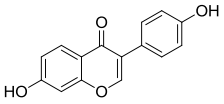	Human breast, prostate cancer cell lines, hepatocarcinoma cells, alveolar epithelial carcinoma cells	(Tacchini et al., 2000, Davis et al., 1999)
Grapes	Resveratrol	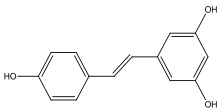	Human mammary epithelial cells, Rat and human pancreatic carcinoma cells, human breast cancer cells, mouse epidermal bj6, HeLa cells.	(Subbaramaiah et al., 1998, Subbaramaiah et al., 1999, Mouria et al., 2002, Banerjee et al., 2002)
Garlic	Ajoene	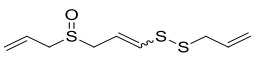	Human promyeloleukamia, Basal cell carcinoma	(Dirsch et al., 1998, Antlsperger et al., 2003, Tilli et al., 2003)

1.3 The anti-cancer activity of garlic organosulfur compounds (OSC)

1.3.1 The composition of OSC in a garlic clove

A garlic clove contains an array of organosulfur compounds (OSC) which are proposedly responsible for its cancer preventative activity (Siegers et al., 1999, Bianchini and Vainio, 2001, Nicastro et al., 2015). When an intact garlic clove is crushed, previously compartmentalised alliin and the enzyme alliinase come into contact followed by an enzymatic reaction which generates allicin, a diallyl thiosulfinate compound (figure 1.2) (Block et al., 1986). Allicin then spontaneously decomposes into an array of water and oil soluble second generation OSC (figure 1.3) (Shukla and Kalra, 2007, Kaschula et al., 2010) of which the major constituents are diallyl sulphide (DAS), diallyl disulfide (DADS), diallyl trisulfide (DATS) and Ajoene ((*E*,*Z*)-4, 5, 9-thrithiadodeca-1, 6, 11-triene-9-oxide) (table 1.2). The concentrations of these compounds in crushed garlic vary according to the type of extraction technique used (table 1.3) (Block et al., 1992, Amagase et al., 2001, Lee et al., 2003f, Kimbaris et al., 2006, Shukla and Kalra, 2007). Therefore different garlic preparations have different concentrations of respective OSC compounds.

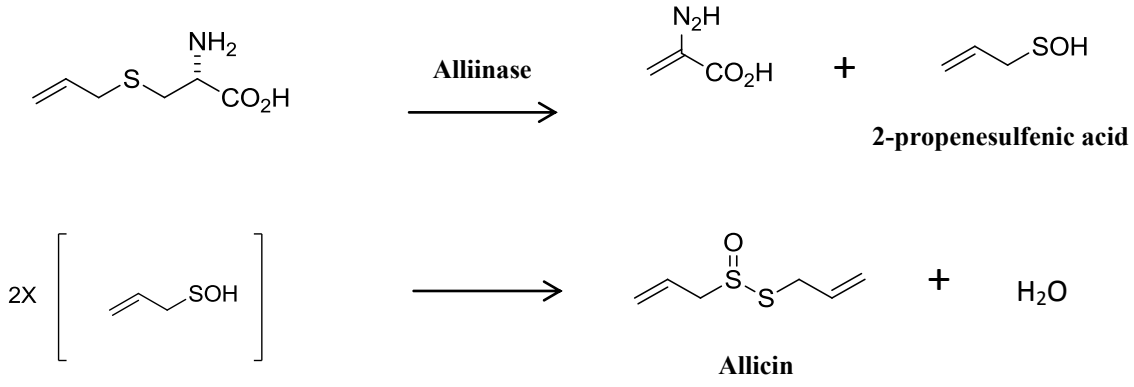

Figure 1.2 The enzymatic reaction between alliin and the enzyme alliinase in a crushed garlic clove. A Initial reaction between alliin and alliinase produce 2-propenesufenic acid. B Spontaneous condensation of two 2-propenesufenic acid molecules produces allicin.

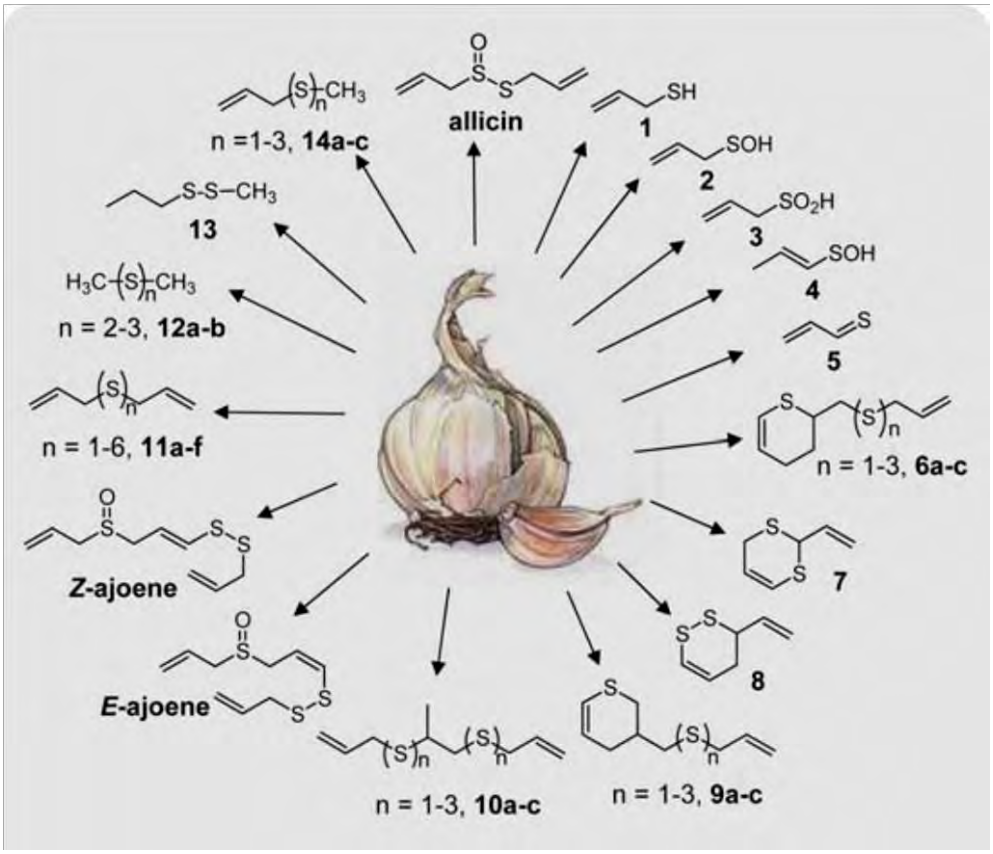

Figure 1.3. Chemical structures of allicin degradation products isolated from macerated garlic extracts. Allicin spontaneously degrades into an array of soluble OSCs including (1) 2.propensulphenic acid, (2) 2-propenesulfinic acid, (3) propenesulphenic acid, (4) 1-propenesulfenic acid, (5) thioacrolein, (6a-c) 2-(allylthiomethyl), 2-(allyldithiomethyl), 2-(allyltrithiomethyl)-3,4-dihydro-2H-thiopyran (7) 2-vinyl-2,4-dihydro-1,3-dithiin, (8) 3-vinyl-3,4-dihydro-1,2-dithiin, (9a-c) 3-[(allylthiomethyl), (allyldithiomethyl), (allyltrithiomethyl)-] -3,4-dihydro-2H-thiopyran (10a-c) 5-methyl-4,7-dithiaundeca-1,9-diene for n 5 1, E- and Z-4,5,9-trithiadodeca-1,6,11-triene 9-oxide (E- and Z-ajoene (11a-f) diallyl sulfides,n 5 1–6, (12a-b) dimethyl sulphides n 5 2–3, (13) 1-(methyldithio)propane, (14a-c) allyl methyl sulphides (Kaschula *et al*., 2010).

Table 1.2 Chemical structures of the garlic derived organosulfur compound DAS, DADS, DATS and ajoene.

Garlic Organosulfur Compound	Chemical Structure
Diallyl sulphide (DAS)	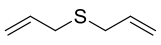
Diallyl disulphide (DADS)	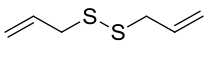
Diallyl trisulphide (DATS)	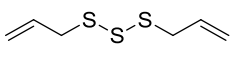
Ajoene	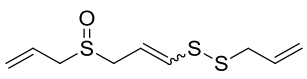

Table 1.3 Reported Concentrations of garlic derived OSCs prepared using different extraction methods

Garlic Compound	Method of extraction	Concentration	References
Allicin	Blended crushed garlic in water	2.5 to 3.1 mg/g	(Block et al., 1986, Lawson et al., 1991, Lawson and Gardner, 2005)
DAS	simultaneous distillation extraction	579µg/g	(Munchberg et al., 2007)
	Steam Distillation	898 µg/g	
DADS	simultaneous distillation extraction	236 µg/g	(Munchberg et al., 2007)
	Steam Distillation	24 µg/g	
DATS	simultaneous distillation extraction	114 µg/g	(Munchberg et al., 2007)
	Steam distillation	39 µg/g	
***E*-ajoene**	Fresh garlic in rice oil at 80 ℃	172 µg/g	(Shukla and Kalra, 2007, Naznin et al., 2008)
	Marketed garlic oil at 80 ℃	127 µg/g	
***Z*-ajoene**	Fresh garlic in rice oil at 80 ℃	476.3 µg/g	(Shukla and Kalra, 2007, Naznin et al., 2008)
	Marketed garlic oil at 80 ℃	170 µg/g	

1.3.2 The chemopreventitive activity of OSC

Garlic (*Allium sativum L*), an *Allium* family member, has been used for centuries as a herbal remedy against a number of ailments. Epidemiological studies have demonstrated that garlic consumption reduces prevalence and cancer related death of oesophageal, gastric, skin, colon and lung cancer (Agarwal, 1996, Shukla and Kalra, 2007, Jin et al., 2013, Turati et al., 2015). In China, gastric cancer cases from regions that consume higher amounts of garlic (20 g/day) were found to have 12 times lower mortality rates from gastric cancer compared to the lower consumption regions and subsequent meta-analysis findings have illustrated this protective role (Agarwal, 1996, Kodali and Eslick, 2015). Moreover, the consumption of high amounts of *Allium* vegetables were found to associate with reduced risk of oesophageal and stomach cancer in Jiangsu province in China (Gao et al., 1999). On the other hand, the epidemiological reports on the protective role of garlic consumption against colorectal cancer have been inconsistent. Data from a meta-analysis study was found to demonstrate that high garlic consumption (>28 g/wk) has a protective role against colorectal and stomach cancer (Fleischauer et al., 2000). However, recent meta-analysis and prospective cohort studies have shown that garlic consumption or intake of garlic supplements is not associated with the

reduced risk of colorectal cancer (Meng et al., 2013, Zhu et al., 2014, Chiavarini et al., 2015). The variation in the meta-analysis reports have been attributed to the type of studies analysed, for example case-control studies seemingly found garlic to be protective against colorectal cancer while cohort studies did not (Chiavarini et al., 2015). Despite the somewhat conflicting evidence, the majority of epidemiological studies conducted suggest that garlic consumption has a protective role against different cancer types.

1.3.3 Molecular mechanisms underlying OSC chemopreventitive activity

Several reports have suggested that garlic extracts and more specifically, the OSC found in the garlic extracts may hinder cancer initiation by inhibiting mutagenesis and DNA adduct formation as well as altering the activity of xenobiotic metabolising enzymes and scavenging free radicals.

Garlic extract is reported to inhibit the activation of the mutagens such as aflatoxin B_1 and 4-nitroquinoline-1-oxide in *Salmonella typhimurium* and *Escherichia coli* while ajoene inhibits the binding of aflatoxin B1 to calf thymus DNA in rat liver (Zhang et al., 1989, Tadi et al., 1991, Soni et al., 1997). Furthermore, ajoene is reported to inhibit the activation of benzo[*a*]pyrene and 4-nitro-1, 2 phenylenediamine (NPD) in *Salmonella typhimurium* Strains (Tadi et al., 1991, Ishikawa et al., 1996). DAS is reported to delay the onset of polycyclic aromatic hydrocarbon (PAH) induced skin and lung carcinogenesis in mice (Singh and Shukla, 1998a, Singh and Shukla, 1998b, Yang et al., 2001). In addition, garlic powder and ajoene have been reported to inhibit 7, 12 dimethylbenzo[a]athracene (DMBA) - induced DNA adduct formation in rat liver and the mammary gland (Mehta et al., 1991, Liu et al., 1992, Amagase and Milner, 1993).

In addition to inactivation of mutagens and DNA adduct formation, garlic constituents are reported to modulate the activity of enzymes responsible for detoxifying carcinogens. For an example, garlic powder, DAS and DADS were found to enhance the activity of *S*-glutathione transferase (GST) and nicotinamide adenine dinucleotide phosphate (NADPH)-dependent oxidoreductase activity in rat liver (Reddy et al., 1993, Munday and Munday, 1999, Sheen et al., 1999). DAS was also found to decrease the activity of cytochrome P450 CYP2E1 in hepatic microsomes (Brady et al., 1988). Whereas garlic oil was found to enhance the activity of glutathione peroxidase, an enzyme that protects against free radicals, in epidermal cells (Perchellet et al., 1986). Furthermore, aged garlic extracts have been reported to exhibit antioxidant properties in the liver microsomal fractions (Imai et al., 1994). These

experimental reports suggest that garlic extracts and OSC may inhibit the initiation of mutagen and chemical induced cancer through similar mechanisms.

1.3.4 Cytotoxicity of garlic extracts and OSCs in cancer cells

Garlic extracts and OSC have been shown to prevent cancer progression through anti-proliferative and apoptosis-inducing effects on growing tumour cells. Fresh garlic extracts and oil are reported to inhibit the growth of MCF-7 breast cancer, hepatoma HepG2, colon carcinoma Caco-2 and promyelocytic leukaemia HL-60 cells (Siegers et al., 1999, Seki et al., 2000, Modem et al., 2012). DADS and DATS were found to inhibit prostate cancer PC-3 cell proliferation with 24 h 7 μM values of 35 μM and 22 μM respectively (Xiao et al., 2004). Furthermore, the 48 h 7 μM value of ajoene in human leukaemia HL-60, nasopharyngeal KB, cervical Bel-780, colon HCT, gastric BGC-823, breast MCF-7 gliobastoma cancer stem cells GBM CSC, hepatocellular Bel 7402, basal cell carcinoma TE354T, B cell lymphoma BJA-B and mouse melanoma cancer cells B16/BL6 (Scharfenberg et al., 1990, Dirsch et al., 1998, Li et al., 2002a, Tilli et al., 2003, Xu et al., 2004, Taylor et al., 2006, Jung et al., 2014) was found to lie in the range 5.2 - 26.1 μM (Li et al., 2002a). The 7 μM therefore does not appear to vary greatly with different cancer cell lines although a level of specificity has been reported for cancer over normal cell lines (see next section). DAS however is reported to have greatly reduced activity against the human SW-480 colon cancer and PC-3 prostate cancer cell lines with an 7 μM greater than 100 μM (Xiao et al., 2004).

The anti-proliferative activity of garlic derived OSC has been associated with the induction of G_2/M cell cycle arrest and apoptosis. Ajoene has been shown to induce a G_2/M cell cycle arrest and apoptosis in human basal cell carcinoma BCC (Tilli et al., 2003), HT-29, leukaemia HL-60 (Dirsch et al., 2002, Li et al., 2002a) and Burkitt lymphoma BJA-B (Scharfenberg et al., 1990). DADS is reported to trigger G_2/M cell cycle arrest in gastric cancer MGC803 cells (Ling et al., 2014) and oesophageal cancer cells (Yin et al., 2014). DATS is reported to induce G_2/M cell cycle arrest and apoptosis in prostate DU145, basal cell carcinoma BCC, melanoma A375 and bladder cancer T24 cells (Herman-Antosiewicz et al., 2010, Wang et al., 2010a, Wang et al., 2010b). In addition to the *in vitro* studies, ajoene has been shown to have an inhibitory effect on the growth of hepatocellular 22 and sarcoma 180 tumour xenografts in Kunming mice and to reduce the tumour size of nodular or superficial basal cell carcinoma (BCC) in humans (Nakagawa et al., 2001, Li et al., 2002a,

Tilli et al., 2003). The reduction in the BCC tumour growth in human patients has been attributed to ajoene-induced apoptotic activity in these cells (Tilli et al., 2003). On the other hand, DADS and DATS were found to hinder leukaemia cell growth in a WEHI-3B mouse model by inducing apoptosis (Yang et al., 2006a, Hung et al., 2014). In summary, the garlic derived OSC compounds DADS, DATS and ajoene have been shown to counter cancer cell growth both *in vitro* and *in vivo* by inhibiting cell proliferation, and apoptosis. In addition garlic OSC also induced G_2/M cell cycle arrest in various cancer cells.

1.3.5 Selectivity of OSC for cancer cells

As with many anticancer agents, the potential of OSC for selectivity against cancer rather than normal cells is a critical requirement. Data presented on the selectivity of garlic OSC for cancer cells is controversial. For example ajoene was found to have similar cytotoxicity against the normal HER2 immortalized mouse fibroblast NIH 3T3 cell line as against a panel of cancer cell lines including mouse melanoma BL6/B6 and human colon HT-29, lung adenocarcinoma A549 and pancreatic adenocarcinoma PANC-1 cells (Taylor et al., 2006). However, marsupial Ptk2 cells, baby hamster kidney BHK21 and primary fibroblast FS_4 cells were shown to be more resistant to ajoene than human leukemic HL60, Burkitt lymphoma BJA-B, breast MCF7, nasopharyngeal KB, hepatocellular Bel 7402, gastric BGC 823 and colon cancer HCT cells (Scharfenberg et al., 1990, Li et al., 2002o). Moreover, DADS was found to display increased toxicity against oesophageal squamous cell carcinoma ESCC than against the corresponding normal liver L02 cells (Yin et al., 2014). Generally, DATS has been reported to be more active in cancer than in normal cell lines. Melanoma A375, prostate cancer DU145 and PC-3 and breast cancer MCF-7 and MDA-MB-231 and human lung cancer H358 and H460 cells have been shown to be more sensitive to DATS induced apoptosis than normal melanocytes, prostate epithelial PrEC, human mammary MCF-10A and normal bronchial epithelial BEAS-2B cells (Xiao et al., 2005, Xiao et al., 2009, Murai et al., 2012, Chandra-Kuntal et al., 2013). Some of the most striking evidence comes from the complete selectivity of ajoene for normal peripheral mononuclear blood (PBMC) cells from healthy humans compared to leukemic cells collected from patients (Dirsch et al., 1998). In brief, the majority of reports suggest that garlic derived OSC are more active against cancer cells than their normal counter parts. The selectivity of anticancer agents for cancer cells is critical in cancer therapy as it reduces toxic side effects.

1.3.6 Signalling Pathways identified in OSC apoptotic activity against cancer cells

The mechanism of action behind the cytotoxicity of garlic derived OSC in cancer cells is reported to be dependent on the activation of a number of signalling pathways. OSC induced apoptosis has been shown to proceed via the intrinsic pathway. Signalling pathways which may converge on this apoptotic pathway include activation of mitogen activated protein kinase (MAPK) pathways, intracellular calcium mobilization and the production of reactive oxygen species (ROS)

DADS, DATS and ajoene have been found to induce apoptosis in a variety of cancer cells by triggering the mitochondrial dependent caspase cascade (Nakagawa et al., 2001, Dirsch et al., 2002, Kwon et al., 2002, Tilli et al., 2003, Oommen et al., 2004, Xiao et al., 2004, Wang et al., 2010b, Chiu et al., 2013, Dasgupta and Bandyopadhyay, 2013, Shin et al., 2014). This involves activation of caspase 3, disruption of mitochondrial membrane potential, release of cytochrome c from the mitochondria into the cytosol and the down-regulation and phosphorylation of Bcl2 (Shi, 2001, Dirsch et al., 2002, Xiao et al., 2004, Wang et al., 2010b, Wang et al., 2012).

Various studies have implicated MAPK activation by garlic OSC in cancer cells. The MAPK intracellular signalling pathways are activated in response to extracellular stimuli and are characterised into JNK, p38 and MEK/ERK MAPK (Yang et al., 2013). Activation of the JNK MAPK signalling pathway by stress stimuli promotes apoptosis (Pritchard and Hayward, 2013). The JNK signalling pathway mediates apoptosis induced by DATS in prostate cancer PC-3 and DU154 (Xiao et al., 2004) and in bladder cancer T24 cells (Shin et al., 2014). Moreover, DADS has been reported to induce apoptosis in prostate DU145 cancer cells by activating the JNK pathway (Shin et al., 2014, Shin et al., 2012). Although JNK is activated in ajoene treated human leukaemia HL60 (Antlsperger et al., 2003) and 3T3L-adipocytes, it does not play a central role in ajoene induced apoptosis. The other stress activated MAPK is p38 and it also promotes apoptosis when activated (Obata et al., 2000). Garlic derived OSCs DAS and DADS trigger p38 induced apoptosis in glioblastoma T98G and U87MG (Das et al., 2007), colon cancer COLO 205 (Yang et al., 2009) (Das et al., 2007, Yang et al., 2009, Wang et al., 2012). On the other hand, the MEK/ERK MAPK pathway is known to be activated by growth factors (Boulton et al., 1991). Once activated the ERK1/2 pathway promotes cell proliferation and differentiation (Yang et al., 2013). The earliest report of ERK1/2 activation by DADS was reported in human colon cancer HCT cells (Knowles

and Milner, 2003). In addition, MEK1/2 inhibitors PD98059 and U0126 significantly enhanced ajoene and DADS induced apoptosis in human leukemic HL-60 and ESCC cancer cells respectively (Antlsperger et al., 2003, Xiao et al., 2004). Thus, all MAPK pathways are activated by different OSC, with the JNK pathway playing a major role in OSC induced apoptosis with the exception of ajoene. Furthermore, the p38 and MEK/ERK pathways are also activated by OSC, with the MEK/ ERK pathway negatively affecting ajoene induced apoptotic activity. The stress activated MAPK are sometimes activated by increased intracellular ROS levels

ROS is produced as the by-product of metabolic reactions such as cellular respiration (Saybasili et al., 2001), with different types including superoxide and hydrogen peroxide (Richter et al., 1995). Since cancer cells have high metabolic rates, ROS production is reported to be elevated in cancer cells (Behrend et al., 2003). Consequently, production of ROS plays a major role in therapy cancer cell death (Benhar et al., 2002) and is reported to mediate OSC induced apoptosis in cancer cells. ROS mediates DADS induced apoptosis in mouse-rat hybrid ganglion cells (N18) (Lin et al., 2006) and lung A549 carcinoma cells (Wu et al., 2005), human glioblastoma T98G and U87MG (Das et al., 2007), leukaemia HL60 cells (Kwon et al., 2002) and neuroblastoma SH-SY5Y (Filomeni et al., 2003). Furthermore, DATS is reported to enhance ROS levels in prostate cancer LNCaP cell line (Kim et al., 2007), PC-3 and DU145 (Xiao et al., 2005). ROS production is key in ajoene induced apoptosis in human lymphoma U937 cells (Kelkel et al., 2012), leukaemia HL60 (Dirsch et al., 1998) and adipocytes 3T3-L1(Yang et al., 2006b). Thus, garlic derived OSC possibly promotes cancer cell oxidative stress condition caused by high ROS levels, to kill cancer cells.

Garlic derived OSC have also been found to enhance intracellular calcium concentration. In this regard, DAS and DADS were found to increase intracellular calcium concentrations in SW480 colon cancer cells (Chen et al., 2012) and in human glioblastoma T98G and U87MG cells (Das et al., 2007). DADS was found to inhibit the growth of human colon, lung and skin cancer by reducing the expression of calcium ATPase activity and consequently increasing intracellular calcium levels (Sundaram and Milner, 1996). Similarly, DADS and DATS were found to enhance intracellular calcium levels in lung A549 cancer cells (Sakamoto et al., 1997). The increase in intracellular calcium levels have been implicated in cellular processes such as ER stress (Pyrko et al., 2007a).

ER stress has not been as extensively studied as an OSC mechanism of action as the above mentioned intracellular events. However, Certain ER stress markers have been identified in garlic OSC treated cells. Increased expression of caspase 4 and Calpain has been observed in human glioblastoma T96G and U87MG cells treated with DAS and DADS (Das et al., 2007). Subsequently, C/EBP [CAAT/enhancer- binding protein]- homologous (CHOP), glucose regulated protein 78/ binding immunoglobulin protein (GRP78/BIP) and caspase 4 have been identified in human colon COLO 205 and basal cell carcinoma BCC cell treated with DADS (Yang et al., 2009, Wang et al., 2012). More recently, ajoene has been reported to increase GRP78/BIP in breast cancer MDA-MB-231 cells (Kaschula et al., 2015). These reports show that ER stress is activated by the garlic derived OSC in cancer cells. However none of them have demonstrated the role that it plays in OSC induced apoptosis. Furthermore, nothing is known about whether ER stress is a secondary or primary response to OSC treatment.

Although various mechanisms of action have been cited, their relation to the chemical structure and intracellular target of garlic OSC is yet to be elucidated.

1.4 Structure-activity relationships in garlic related OSC's

The cytotoxicity of garlic derived OSC in cancer cells is associated with the presence of a polysulphide or sulphide group. The potency of these OSC is related to the number of sulphur atoms in the backbone of the structure (Xiao et al., 2004) in which various studies have shown that the OSC from the least active to the most active against cancer cell growth is of the order: DAS < DADS < DATS = ajoene (table 1.2) (Scharfenberg et al., 1990, Sundaram and Milner, 1996, Sakamoto et al., 1997). Structure-activity studies conducted in our lab with ajoene analogues substituted with R^1 end-groups demonstrated that the allyl end group is not critical in the anti-proliferative activity of ajoene against transformed fibroblast (CT-1), and WHCO1 cells (Hunter et al., 2008). In fact, some of the R^1-substituted analogues were found to be more active than the parent ajoene with the most active analogue being that substituted with *p*-methoxybenzyl at both the R^1 and R^2 terminal ends (Hunter et al., 2008, Kaschula et al., 2011). This compound, designated bisPMB, was found to have enhanced anti-proliferative activity against breast MDA-MB-231, cervical HeLa, oesophageal WHCO1 and Kyse520, and transformed fibroblast cancer CT1 cell lines by 2 - 12 fold relative to the natural product *Z*-ajoene (Kaschula et al., 2011).

In a follow up SAR study on bisPMB, the pharmacophore was found to be the disulfide with the vinyl group serving to further enhance the activity (see table 1.4) (Kaschula et al., 2012). Furthermore, stereoisomerism was found to be important in the cytotoxicity of ajoene with the *E*-stereoisomers being marginally less active than the corresponding *Z*-stereoisomers against WHCO1 or CT-1 cell proliferation (Hunter et al., 2008, Kaschula et al., 2011). Additionally, these reports suggest that the anticancer activity of ajoene and ajoene analogues may also be governed by certain stereospecific interactions such as in the interactions with proteins.

Table 1.4 IC_{50} values of ajoene and structural analogues in WHCO1 oesophageal cancer cells.

Name	Chemical Structure	WHCO1 7 µM ±SD (µM)
***E*-ajoene**	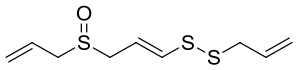	39 ± 7.8
***Z*-ajoene**	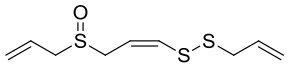	25± 2.8
bisPMB	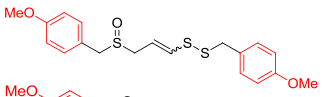	2.1 ± 0.4
vinyl sulphide	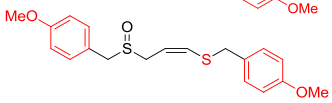	>200
vinyl sulphide	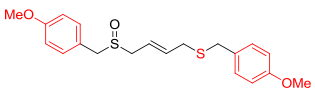	>200
saturated disulphide	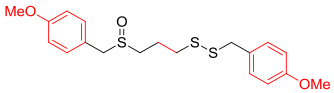	16 ± 3.7

1.5 Mixed disulphide bond formation through OSC induced protein *S*-thiolation

Disulfides are considered as thiol oxidising agents able to thiolate cysteine thiols in proteins through a mixed disulfide bond. There are specific reports in which garlic derived OSC *S*-thiolate cysteine thiols to form mixed disulfides (Gallwitz et al., 1999). DATS is reported to form a mixed disulfide with β-tubulin at Cys12β and Cys354β in a cell free *in vitro* system (Hosono et al., 2005) and this is reported to be responsible for the inability of β-tubulin to

polymerise into microtubules (Li, Carcinogenesis 2002). In addition, ajoene has been shown to inhibit the activity of human gastric lipase, which contains a thiol, by forming a mixed disulfide bond with the enzyme (Gargouri et al., 1989). An X-ray crystallography study demonstrated that a reaction occurs between the cysteine (Cys58) of glutathione reductase (GR) and the vinyl sulfur atom of *E*-ajoene, in a cell free system to form an *S*-thiolated protein product CH2=CH-CH2-SO2-CH2-CH=CH-S-Cys58-GR (Gallwitz et al., 1999). The proposed rationale for mixed disulfide bond formation between a protein and ajoene was demonstrated in a model reaction between *N*-Boc-L-cysteine ethyl ester and the ajoene analogue bisPMB (Kaschula et al., 2011). The product of the *S*-thiolation reaction demonstrated regioselectivity of the mixed disulfide reaction with the thiolate nucleophile attacking the allyl sulfur of the disulfide (figure 1.4) (Kaschula et al., 2011). The allyl sulfur is therefore transferred to the protein during thiolysis, producing alkylated proteins.

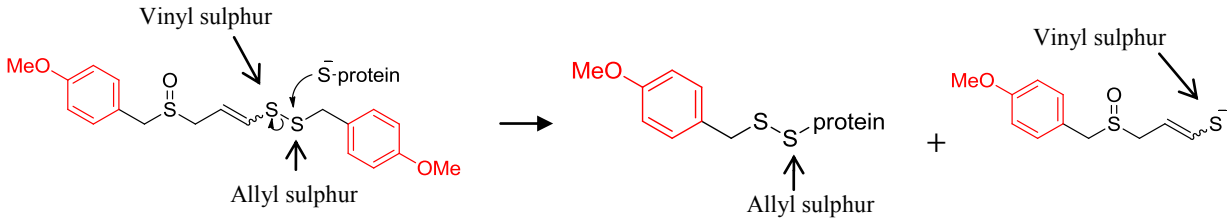

Figure 1.4 Proposed rationale of *S*-thiolation between bisPMB and cellular protein thiols. Sulphur atom from a cysteine residue attacks the allyl sulphur of ajoene (demonstrated using bisPMB). The product of this reaction is a thiolated protein with the vinyl sulphur as the leaving group.

A combination of both thiol/disulfide exchange reactions with protein cysteine residues in conjugation with single electron transfer (SET) processes of the disulfide with production of reactive oxygen species (figure 1.5) are proposed to contribute to the cytotoxicity of ajoene in cancer cells (Kaschula et al., 2011).

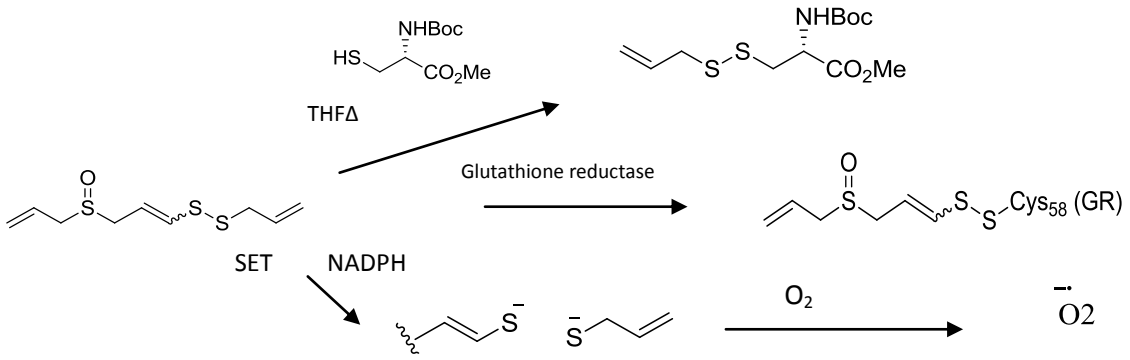

Figure 1.5 Proposed chemical reactivity of the ajoene disulphide bond (Kaschula et al., 2011).

Until recently, the interaction of garlic derived OSC with prospective protein targets have only been illustrated in cell-free systems. In order to identify the *intracellular* ajoene targets, we have recently published data on fluorescently tagged ajoene analogues: dansyl tagged (DP) and flourescein tagged (FOX) which were designed & synthesized in our lab (figure 1.6) and used to track the localization of ajoene within the human breast cancer cell line MDA-MB-231 (Kaschula et al., 2015). DP and FOX were found for the first time to localize to the endoplasmic reticulum (ER) in these cells (figure 1.7) Based on an *S*-thiolation reaction, ajoene was found to *S*-thiolate multiple protein targets in MDA-MB-231 breast cancer cells and this interaction was found to interfere with the folding of newly synthesized proteins (Kaschula et al., 2015). Protein aggregation and an increase in protein ubiquitination was also observed in MDA-MB-231 breast cancer cells treated with ajoene supporting induction of ER stress (Kaschula et al., 2015).

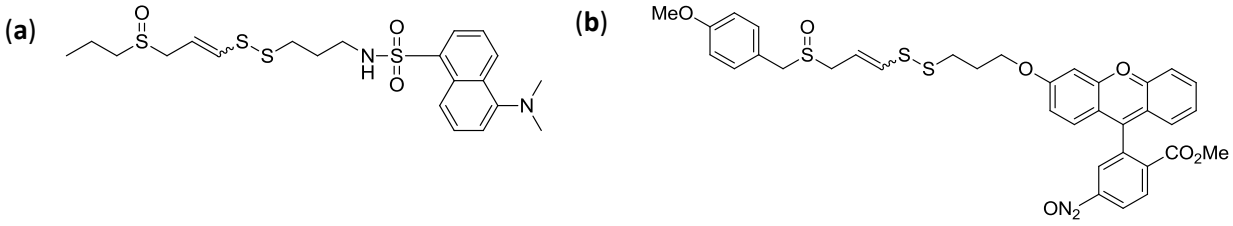

Figure 1.6 Chemical structures of fluorescent ajoene analogues (a) DP and (b) FOX (Kaschula et al., 2015).

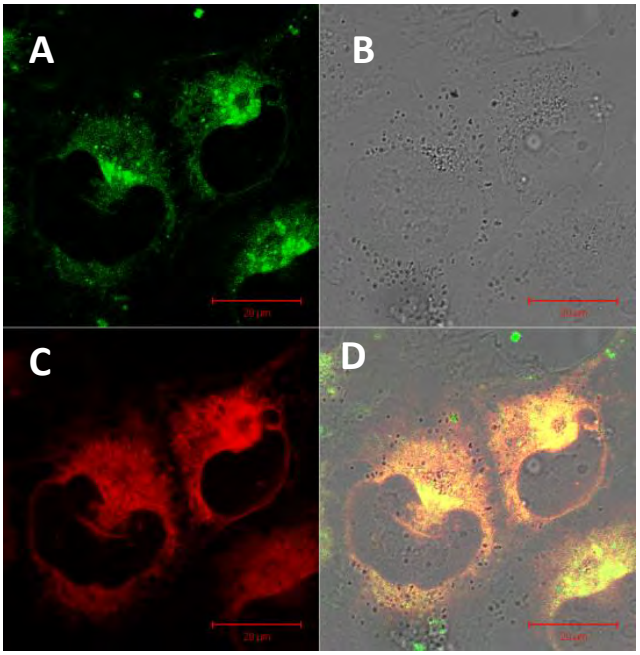

Figure 1.7 Flourescein ajoene (FOX) localises to the ER in MDA-MB 231 breast cancer cells. A) FOX ajoene analogue in green transmitting light B) Phase contrast image of MDA MB 231 cells C) ER tracker in red transmitting light and D) Overlay of the three images (Kaschula et al., 2015).

1.6 Endoplasmic Reticulum Stress and the Unfolded Protein Response

The rough endoplasmic reticulum (ER) is an intracellular organelle and the site for the synthesis of secreted and membrane proteins. Newly synthesised polypeptides are targeted to the ER by signal sequences (Walter and Johnson, 1994). After entering the ER, post-translational modification such as *N*-glycosylation and disulfide bond formation occur to stabilize the polypeptides. These polypeptides are then recognized by and bind to ER resident molecular chaperones such as protein disulphide isomerase (PDI), GRP78/BIP and glucose regulated protein 94 (GRP94) (Wang and Tsou, 1993, Griesemer et al., 2014, Halperin et al., 2014). The molecular chaperones assist in the folding of polypeptides so that they can acquire their native/functional protein conformation. In addition to molecular chaperones, proteins are subjected to molecular foldases such as protein disulfide isomerase (PDI) and peptidyl-prolyl *cis-trans* isomerase (PPI) (Schiene and Fischer, 2000, Hebert and Molinari, 2007) which catalyse the rate limiting reactions occurring during folding which include disulfide bond formation and isomerisation of the *cis* to *trans* conformation of proline residues in protein (Freedman et al., 1994, Schiene and Fischer, 2000). Only properly folded proteins are transported to the Golgi apparatus, *en route* to the extracellular environment and cell membranes, in coat protein II (COPII) vesicles (figure 1.8).

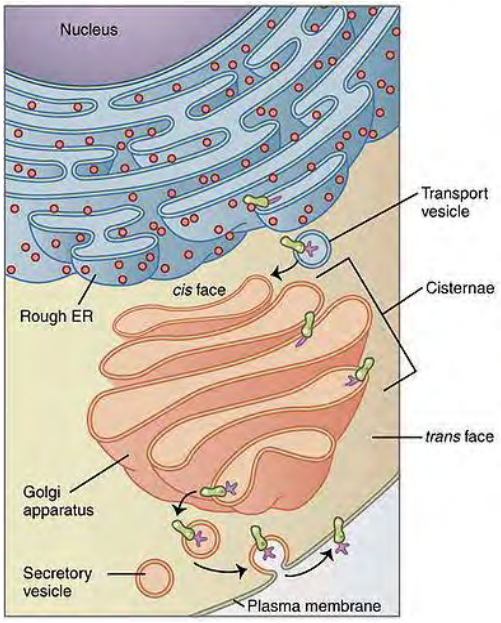

Figure 1.8 The route of transportation of secretory and membrane proteins from the rough ER to the cell membrane via the Golgi apparatus. Newly synthesized proteins in the rough ER are transported by COPII membrane vesicles "transport vesicles" to the *cis* face of the Golgi apparatus and exported through the *Trans* face in secretory vesicles towards the plasma membrane where they are secreted to the extracellular space in secretory vesicles. The Picture was taken from; http://en.wikipedia.org/wiki/Golgi_apparatus.

Approximately 30 % of newly synthesized proteins in normal eukaryotic cells undergo degradation mainly due to unsuccessful folding (Schubert et al., 2000, Goldberg, 2003). In the event of an abnormal accumulation of misfolded proteins in the ER, the formation of protein aggregates which are highly toxic to cells ensues (Bucciantini et al., 2002, Stefani and Dobson, 2003). Cells have evolved to cope with misfolded proteins through the unfolded protein response (UPR). The UPR reduces misfolded protein load by (i) attenuating translation by stopping protein production, (ii) increasing expression of the protein folding machinery to guide the re-folding of misfolded proteins (Takayanagi et al., 2013) and (iii) enhancing the degradation of terminally misfolded proteins through ER associated degradation (ERAD) (Meusser et al., 2005, Raasi and Wolf, 2007, Walter and Ron, 2011).

The UPR is orchestrated by three ER transmembrane proteins namely: protein kinase like ER kinase (PERK), activating transcription factor 6 (ATF6) and Inositol requiring enzyme-1 (IRE-1) (Ron and Walter, 2007, Walter and Ron, 2011). Once the ER transmembrane proteins are activated, they trigger a cascade of cellular reactions such as phosphorylation of eIF2- α resulting in selective translation of ATF4 and other reactions include ATF6 cleavage and XBP-1 mRNA splicing by IRE1 (figure 1.9). These molecular events lead to the localization of active transcription factors (ATF4, ATF6 and XBP-1s) to the nucleus to drive the transcription of molecular chaperones and genes involved in the ERAD process (figure 1.9).

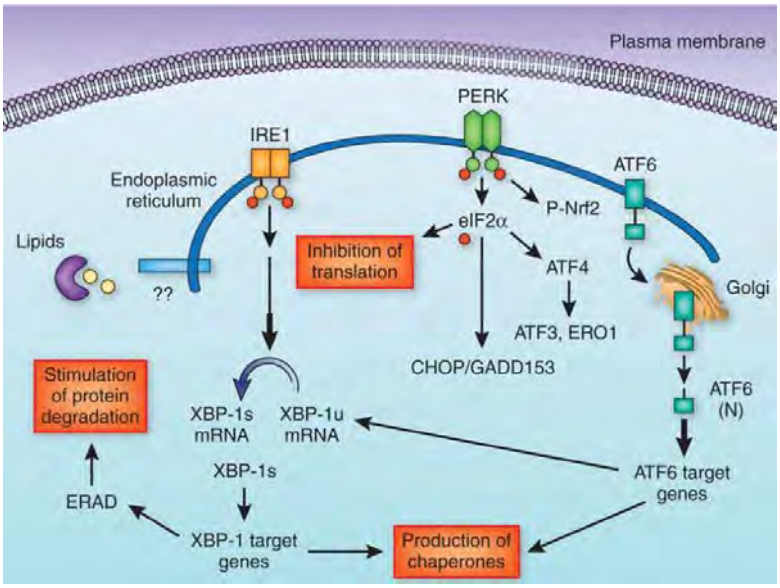

Figure 1.9 The events that occur during the Unfolded Protein Response. UPR pathways (IRE1, PERK and ATF6) inhibit global protein translation, enhance the transcription of molecular chaperones and foldases and activate ER associated degradation (ERAD) for degradation of misfolded proteins. The picture was taken from www.nature.com/nm/journal/v16/n4/images/nm0410-396-F1.

In addition, the activation of all UPR transmembrane proteins is regulated by GRP78/BIP binding to their ER luminal domain upon an accumulation of misfolded proteins (Shen et al., 2002, Ron and Walter, 2007). Thus, an increase in GRP78/BIP expression commonly indicates ER stress and UPR induction. This increase in GRP78/BIP has been observed in garlic derived OSC treated cancer cells. For instance, the increase GRP78/BIP expression was reported in DADS treated human colon cancer COLO205 (Yang et al., 2009), DATS treated basal cell carcinoma BCC (Wang et al., 2012) and ajoene treated breast cancer MDA-MB-231 cells (Kaschula et al., 2015).

1.6.1 The protein kinase like – endoplasmic reticulum kinase (PERK) pathway

PERK is a serine/ threonine kinase that serves as an ER stress sensor and UPR transducer. Following an increase in misfolded proteins, PERK undergoes dimerization, *trans*-autophosphorylation and activation. Activated PERK phosphorylates and inactivates the eukaryotic translation initiation factor 2 alpha (eIF2α), which is required for polypeptide synthesis. This results in the attenuation of global protein synthesis (Koumenis et al., 2002). Interestingly, phosphorylated eIF2α selectively enhances the translation of several mRNAs including activating transcription factor 4 (ATF4) (figure 1.10). The garlic derived OSC DATTS was found to upregulate ATF4 expression in human colon HCT 116 cells (Saidu et al., 2013) Genes that are downstream targets of ATF4 include Growth Arrest and DNA Damage 34 (GADD34), CAAT/ Enhancing binding protein homologous protein (CHOP), Activating Transcription Factor 3 (ATF3), Tribbles Pseudo-Kinase 3 (TRIB3), genes involved in protein folding and ERAD (Ma et al., 2002, Teske et al., 2011). The activation of these genes suggest that the PERK/ATF4 pathway is cytoprotective and primarily restores ER homeostasis through the reduction of ER misfolded protein load. On the other hand genes such as CHOP are implicated in ER stress induced apoptosis (Matsumoto et al., 2013). This suggested that the PERK/ATF4 pathway is also involved in ER stress induced apoptosis. The PERK/ATF4 pathway has also been implicated in crosstalks with other UPR pathways. The PERK/ATF4 arm of the UPR pathway has been shown to be essential for the transcription, and activation of ATF-6 in mouse embryonic fibroblast (MEF) cells (Teske et al., 2011). In contrast, the ATF6 pathway possibly lowers the expression of ATF4 through a negative feedback mechanism by mediating the $p58^{IPK}$ induction (van Huizen et al., 2003).

1.6.2 Activating Transcription Factor 6 (ATF6) Pathway

ATF6 is an ER transmembrane protein reported to have two isoforms ATF6α (90kDa) and ATF6β (110 kDa). In unstressed cells, the ATF6 protein is bound to GRP78/BIP, an ER resident chaperone. However, in response to ER stress, ATF6 dissociates from GRP78/BIP and translocates to the Golgi apparatus where it is sequentially cleaved by site 1 protease (S1P) and site 2 protease (S2P) (Ye et al., 2000, Shen et al., 2002). The cleaved products of ATF6α (50 kDa) or β (60kDa) are bZIP transcription factors that translocate to the nucleus and bind to the ATF/cAMP responsive element (CRE) and the ER responsive element (ERSE) (Guan et al., 2009, Yoshida et al., 2001g). The most active isoform is ATF6α and its activity is reportedly regulated by ATF6β. Glycosylated ATF6β represses the transcriptional activity of ATF6α possibly by competing for the promoter binding site (Guan et al., 2009). ATF6α has been shown to induce the transcription of GRP78/BIP, PDIA5, XBP-1, CHOP and GRP96 in MEF cells (Yamamoto et al., 2007).

1.6.3 Inositol Requiring Enzyme 1 (IRE1) Pathway

The IRE1 branch of the UPR is the most evolutionary conserved arm and has been extensively studied (Mori et al., 2000, Mori, 2009). The mammalian IRE1 homologs are IRE1α and IRE1β (Tirasophon et al., 1998, Mori et al., 2000). IRE-1 functions as a sensor for ER stress and is a UPR transducer (Mori et al., 2000). Two models have been proposed for the activation of IRE1. The first model proposes that inactive monomeric IRE-1 is bound to GRP78/BIP which dissociates in response to increased misfolded proteins. The dissociation of GRP78/BIP triggers IRE1 oligomerization and transphosphorylation (Ron and Walter, 2007). The second model proposes that direct contact of unfolded proteins in the ER to IRE1 leads to IRE1 oligomerization and activation (Credle et al., 2005, Gardner and Walter, 2011, Walter and Ron, 2011). In both models though, activation is induced by the presence of misfolded proteins. Active IRE1 functions as a kinase and endoribonuclease (RNase) (Tirasophon et al., 1998, Mori et al., 2000) and exerts its endoribonuclease activity by cleaving the mRNA encoding membrane and secretory proteins in a process termed regulated IRE1 dependent decay (RIDD). Additionally, IRE-1 mediates unconventional splicing of XBP-1 mRNA in the cytoplasm in response to ER stress, as opposed to conventional splicing that occurs in the nucleus (Yoshida et al., 2001a, Calfon et al., 2002, Hirota et al., 2006, Iwawaki and Akai, 2006, Uemura et al., 2009). Spliced XBP-1 codes for a transcription

factor that has been shown to induce genes involved in protein folding and degradation including GRP78/BIP, DNAJ/Hsp40 genes, $p58^{IPK}$, ERdj4, HEDJ, and EDEM (Lee et al., 2003a, Hirota et al., 2006). There is a regulatory mechanism which controls XBP-1s induced protein degradation, whereby levels of XBP-1s mRNA are reported to progressively decline in response to IRE1α inactivation when ER Stress persists and is also regulated through ATF6 (Yoshida et al., 2001a, Lee et al., 2003a, Lisbona et al., 2009). Additionally, p53 upregulated modulator of apoptosis (PUMA) has been suggested to regulate sustained activation of IRE-1 through direct interaction in mouse embryonic fibroblasts MEF cells (Rodriguez et al., 2012). Together, these reports suggest that IRE-1 is activated in response to the accumulation of misfolded proteins, where it activates downstream targets that facilitate the transcription of genes involved in protein folding.

1.6.4 ER stress induced apoptosis

When ER stress persists and the UPR is unable to restore ER homeostasis, apoptosis is triggered. The precise mechanisms involved in the UPR switch, from pro-survival to pro-death in response to ER stress, are not well understood. However, an altering switch between autophagy and apoptosis has implicated the expression of ATF4 and CHOP UPR proteins. ATF4 is responsible for ER stress induced autophagy and CHOP has been shown to trigger the switch to apoptosis in HepG2 cells (Matsumoto et al., 2013). CHOP has been suggested to induce apoptosis by enhancing the expression of GADD34, which promotes the de-phosphorylation of eIF2α leading to enhanced protein translation and ER protein load (figure 1.10) (Brush et al., 2003, Marciniak et al., 2004). The increase in ER protein load and in translation of pro-apoptotic proteins overwhelm the UPR protective processes and triggers apoptosis (Sano and Reed, 2013). On the other hand, CHOP has also been shown to repress the transcription of Bcl-2, an anti-apoptotic protein (McCullough et al., 2001). This suggests that CHOP mediated ER stress induced apoptosis seemingly involves the PERK and the mitochondrial-dependent caspase cascade pathways.

Then again, ER stress associated apoptosis is also linked to UPR via M-Calpain, which is activated by caspase 12 (figure 1.10) (Nakagawa and Yuan, 2000). Crosstalks between the JNK and IRE-1 signalling pathway have also been shown to be implicated in apoptotic induction (figure 1.10). The cytoplasmic domain of IRE-1 is reported to recruit and interact with the tumour necrosis factor receptor associated factor 2 (TRAF2) and apoptosis signal-regulated kinase-1 (ASK-1), and this recruitment is regulated by the c-Jun NH_2 terminal

inhibitory kinase (JIK). The TRAF2/ASK complex then phosphorylates and activates c-Jun kinase (JNK) (Nishitoh et al., 2002). The JNK/MAPK substrates include transcription factors such as c-Jun, c-Fos, ATF-2, AP-1, p53 and Elk (Hibi et al., 1993, Minden et al., 1994, Whitmarsh et al., 1995). JNK/MAPK is also reported to phosphorylate members of the Bcl-2 family such as BCL2 and BIM (Lei and Davis, 2003, Wei et al., 2008). Consequently, the JNK pathway promotes cellular death by enhancing the expression and activation of proteins involved in apoptosis in response to stress stimuli (figure 1.10). These reports support ER stress mediated apoptosis occurring via CHOP, caspase 12 and JNK/MAPK pathway activation.

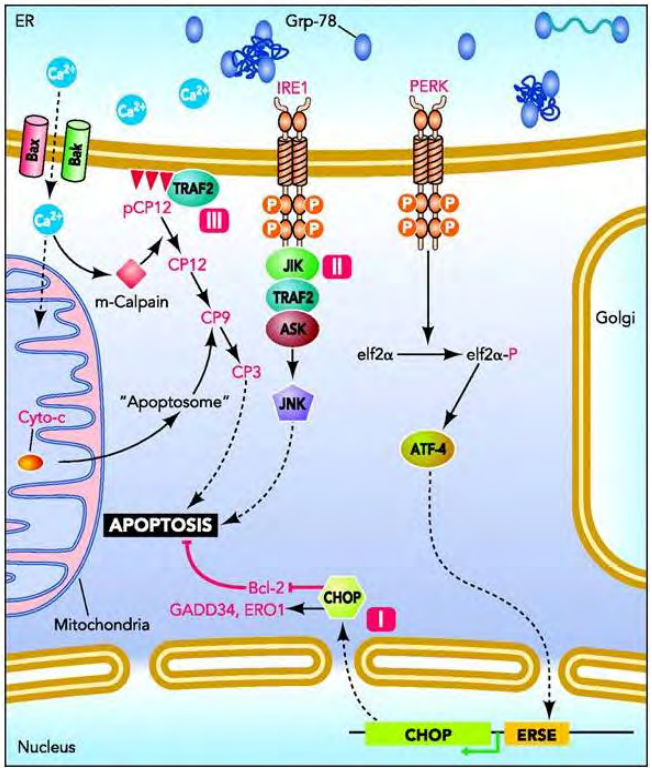

Figure 1.10 Pathways involved in ER stress induced apoptosis. CHOP expression is up-regulated by UPR pathways. CHOP down-regulates bcl-2 and promotes the transcription of GADD34 and ERO1. GADD34 and ERO1 exacerbate ER stress by promoting protein synthesis and disrupting redox homeostasis respectively. Activated IRE1 forms a complex with JIK, TRAF2 and ASK1 leading to the phosphorylation of JNK. TRAF2 dissociation from pro-caspase 12 (pCP12) and activated m-Calpain activates pCP12 leading to subsequent activation of caspase 9 and 3. Bcl-2 family proteins BAK and BAX oligomerise in the ER membrane to permit the movement of calcium form the ER to the cytosol. The increased intracellular calcium levels activate m-Calpain and diffuse into the mitochondria, disrupting the mitochondrial membrane potential and cytochrome c (Lai et al., 2007).

1.6.5 Cross-talk between the p38 and MEK/ERK and the ER stress/UPR pathways

Apart from the IRE1/JNK signalling pathway, UPR pathways have been reported to interact with other MAPK signalling pathways which include p38 and the MEK/ERK pathways. Recently, accumulating evidence has shown that intracellular stress signals such as ER stress can activate the MAPK pathways (Darling and Cook, 2014).

The UPR pathway transmembrane proteins are also reported to be activated both upstream and downstream of MAPK (figure 1.11) (Darling and Cook, 2014). Once triggered, the MAPK pathways are activated through sequential phosphorylation/activation of a three tiered signalling cascade composed of protein kinases MKKKs, MKKs and MAPK (figure 1.11) (Yang et al., 2013, Darling and Cook, 2014).

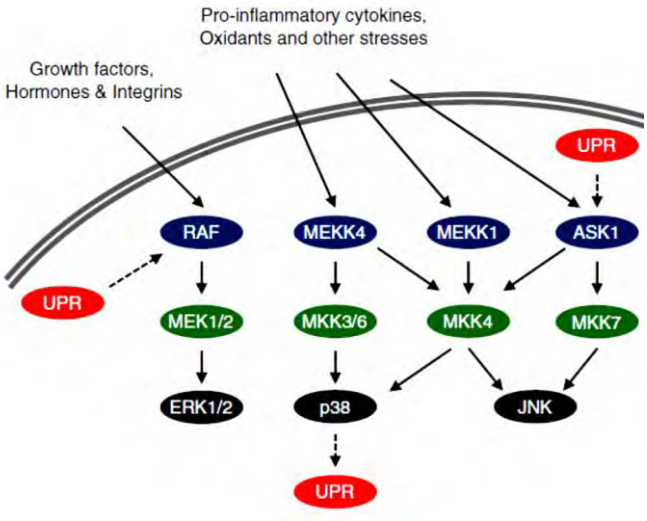

Figure 1.11 Activation of the three tiered MAPK signalling cascade and points of interaction with the UPR pathways (red). The three tired signalling cascade consists of the MKKKs (blue), the MKK (green) and the MAPK (black). The MEK/ERK MAPK signalling cascade is activated by growth factors, hormones and intergrins and the UPR. The p38 and JNK MAPK signalling cascade are activated by pro-inflammatory cytokines and extracellular stress signals. JNK is also activated through the IRE1 pathway and p38 phosphorylates CHOP (Darling and Cook, 2014).

Under ER stress conditions, the IRE-1 pathway potentiates cell survival by activating the MEK/ERK pathway (Nguyen et al., 2004). For instance, ER stress induced IRE-1 is reported to dissociate from adaptor protein non catalytic region of tyrosine kinase (Nck) and activate ERK1/2 (Nguyen et al., 2004). Once activated, ERK1/2 phosphorylates/activates various transcription factors such as fos, elk1 and p53, cytoskeletal elements and components of

MAPK pathway (Pritchard and Hayward, 2013). Since the MEK/ERK pathway promotes cell survival, the IRE-1 activated MEK/ERK pathway may also promote cell survival.

The p38/MAPK belongs to the stress activated protein kinase family; it is activated by inflammatory cytokines, irradiation, heat shock, stress inducing chemical agents and also by ER stress (Obata et al., 2000, Ranganathan et al., 2006, Cuenda and Rousseau, 2007, Yang et al., 2013). The substrates of p38/MAPK include the MAP kinase activated protein kinase 2 (MAPK) interacting kinase 1 (Mnk1), MAPK interacting kinase 1 (Mnk2) and components of the ER stress pathways such as activating transcription factor 6 (ATF6), Nrf2, c-Jun, XBP-1 and CHOP (Cohen, 1997, Ben-Levy et al., 1998, Thuerauf et al., 1998, Ma and Hendershot, 2004, Ranganathan et al., 2006). Several studies have suggested that CHOP is phosphorylated by p38 at the trans-activation sites (Wang and Ron, 1996, Darling and Cook, 2014). The transcriptional activity of ATF6 is reported to be enhanced by phosphorylation with p38/MAPK in myocardial cells, promoting the transcription of GRP78/BIP (Thuerauf et al., 1998). On the one hand, the p38/MAPK pathway has also been shown to be activated downstream of the PERK/ATF4 UPR pathway. There is therefore evidence that the p38/MAPK pathway is activated both upstream and downstream of ER stress induction, interacting with various components of the ER stress and UPR pathways.

1.6.6 ER Stress and UPR in cancer therapy

The pro-survival function of ER stress and UPR pathways render it a good target for cancer therapy as it has been implicated in promoting malignancy (Yadav et al., 2014). For example, UPR cytoprotective pathways have been shown to significantly alter cellular transformation and progression of multiple myeloma, hepatocellular carcinoma, gastric cancer and breast cancer (Song et al., 2001, Shuda et al., 2003, Carrasco et al., 2007, Papandreou et al., 2011). In triple negative breast cancer cells, hetero-dimerization of XBP-1 with hypoxia-inducible factors 1 alpha (HIF1α) has been shown to regulate the transcription of HIF1α target genes, which promote tumour progression (Chen et al., 2014). Suggesting that activation of the unfolded protein response and ER stress may offer a potential chemotherapeutic target.

The pro-death function of ER stress and UPR pathways plays a major role in enhancing cancer therapy (Yadav et al., 2014). The UPR is commonly quiescent in normal cells, whereas cancer cells are exposed to stress stimuli including proteotoxic stress, metabolic stress, hypoxia and nutrient starvation and therefore have latent adaptive UPR activity (Pyrko

et al., 2007b, Hersey and Zhang, 2008, Luo et al., 2009). The latent UPR activation in cancer cells predisposes them to apoptosis when treated with agents that elevate misfolded protein load, as these agents overwhelm the UPR adaptive signals and trigger apoptosis. As a result, the UPR and ER stress pathways have been implicated in a number of chemotherapeutic approaches (Boelens et al., 2007). For example, photo sensitizer photodynamic therapy (PS 1 PDT), which is used for treatment of various cancers, is reported to induce apoptosis via the ER stress pathway (Li et al., 2015). Therefore activation of the unfolded protein response and ER stress is an attractive potential chemotherapeutic target.

Thapsigargin (TG) is a well established ER stress inducer used as a positive control in this study (Andersen et al., 2015) and is a natural product obtained from the roots and fruits of wild *thapsia garganica.* TG (figure 1.12) is known to induce ER stress by inhibiting the sarcoplasmic reticulum Ca^{2+} ATPase (Thastrup et al., 1990, Treiman et al., 1998a). At high concentrations, TG is cytotoxic in cancer cells. Accordingly, TG has been shown to induce apoptosis in human prostatic carcinoma TSU and rat prostate cancer cell lines by increasing intracellular calcium concentrations (Tombal et al., 2000). Emerging evidence suggests that thapsigargin based pro-drugs have potential as anticancer agents in humans (Denmeade et al., 2003) (Denmeade et al., 2003) with the pro-drug currently being on phase II human clinical trials (Doan et al., 2015).

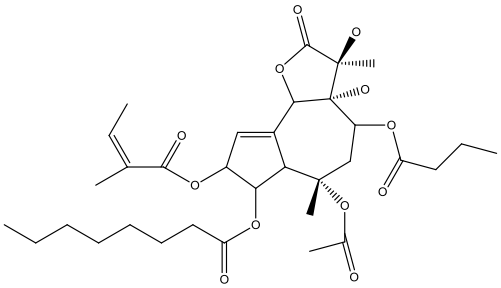

Figure 1.12 Chemical structures of Thapsigargin.

Other ER stress and UPR stress inducing agents that are in human clinical trials or FDA approved for cancer therapy, include proteosome inhibitors, HSP90 inhibitors and ER stress inducers (Li et al., 2011). Proteosome inhibitors included Boterzomib, salinosporamide A, Carfizomib, PS-341, CEP- 18770 (San Miguel et al., 2008, O'Connor et al., 2009, Chauhan et al., 2010, Lee et al., 2010). HSP90 inhibitors included Retaspimycin (Heath et al., 2008,

Hanson and Vesole, 2009, Richardson et al., 2010, Pacey et al., 2012). Delta (9)-Tetrahydrocannabinol (THC) is on phase I clinical trials, exerts its anticancer activity against glioblastoma multiforme and is classified as an ER stress inducer (Guzman et al., 2006).

Furthermore, chemotherapeutic drugs commonly used for oesophageal cancer such as cisplatin and paclitaxel have been reported to induce ER stress in human melanoma 224, colon cancer HCT 116 cell lines and neuroblastoma SK-N-SH (Mandic et al., 2003, Tanimukai et al., 2013, Xu et al., 2014).

Thus, from the aforementioned reports it can be said that ER stress and UPR may be targeted in cancer therapy using two different approaches. Anticancer drugs that inhibit UPR in cancer cells can abrogate the adaptation of cancer cells to stressful environment leading to cancer cell death. Alternatively, the induction of ER stress by anticancer agents can overwhelm pro-survival UPR activity in cancer cells and trigger cell death. Either way, ER stress and UPR targeting agents possess great potential as anticancer drugs.

1.7 PROJECT OUTLINE

In the study conducted by Kaschula et al., (2015); the ER was identified as the intracellular target for ajoene. On a chemical level, ajoene was shown to *S*-thiolate multiple protein targets through mixed disulfide formation in cancer cells. This was found to lead to an accumulation of misfolded protein aggregates. This thesis plans to build on these findings by elucidating whether ER stress and UPR are central to the cytotoxicity of bisPMB in oesophageal cancer cells. We further present a potential new candidate for OS chemotherapy, bisPMB.

1.7.1 Hypothesis

The ajoene analogue bisPMB induces cytotoxic activity in WHCO1 cells by activating the UPR and MAPK pathway.

1.7.2 Study Objectives

2 To determine whether bisPMB affects proliferation, cell cycle progression and induces apoptosis in WHCO1 cells

3 To investigate the effect of bisPMB on global gene transcription in WHCO1 cells.

To investigate the intracellular signalling pathways that lead to the cytotoxicity of bisPMB in WHCO1 cells

CHAPTER 2: CYTOTOXIC EFFECT OF BISPMB ON OESOPHAGEAL CELLS

2.1 INTRODUCTION

BisPMB (figure 2.1 **A**), a R^1 and R^2 *para*-methoxybenzyl substituted ajoene (figure 2.1 **B**) is more active than *Z*-ajoene against oesophageal squamous cell carcinoma WHCO1 cells (Hunter et al., 2008, Kaschula et al., 2011, Kaschula et al., 2012). BisPMB also demonstrated selectivity for cancer cells including CT1, PC3, MDA-MB-231 and WHCO1 oesophageal cancer cells over the WI31, PNT1A, MCF12A and EPC2 normal cell counterparts (Kaschula et al., 2011). The greatest bisPMB selectivity and activity was observed against oesophageal cancer WHCO1 cells making it an attractive compound for OS cancer (Kaschula et al., 2011). Therefore, we investigated the mechanism of action of bisPMB against the WHCO1 oesophageal cancer cell line.

In addition to the anti-proliferative effect of ajoene against cancer cell lines, it has been also shown to induce a G_2/M cell cycle arrest and apoptosis. Given that bisPMB is a synthetic analogue of ajoene and the two compounds share a common pharmacophore (Kaschula et al., 2011, Kaschula et al., 2012, Hunter et al., 2008), it is possible that bisPMB acts via the same molecular mechanisms as its parent compound.

A

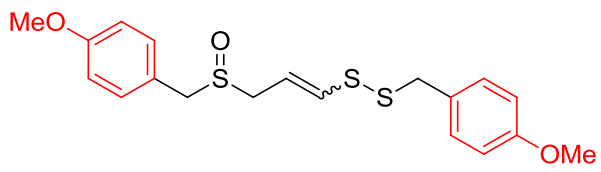

***E/Z* BISPMB**

B

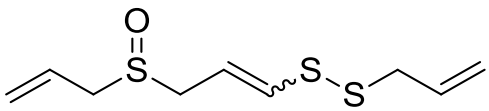

***E/Z* - AJOENE**

Figure 2.1 The Chemical structures of *E/Z* bisPMB and its parent compound E/Z ajoene represented as isomeric mixtures. The substituted R^1 and R^2 *p*-methoxybenzyl end groups are highlighted in red.

2.1.1 Overall strategy and experimental approach

In this chapter, different biochemical techniques were used to characterize bisPMB induced cytotoxicity in oesophageal cell lines. We determined the 24 h IC_{50} concentrations required to inhibit growth of three oesophageal cancer cell lines to include; WHCO1 and WHCO6 of South African origin and were gifted to our lab by Prof Robin Veal from Witwatersrand University and KYSE30 of Japanese origin. KYSE30 cell line was purchased from the German Resource Center for Biological Material, DSMZ GmbH (Braunschweig, Germany).
In addition, the 24 h IC_{50} of the Het-1A cell line (ATCC® CLR-2692™), a normal oesophageal epithelial cell line of American origin transformed with the SV-40 T-antigen was determined. Het-1A cell (ATCC® CRL2692™) was purchased from the American Type Culture Collection (ATCC), Mannasas, USA. We then investigated the time-dependent effect of bisPMB on WHCO1 cell proliferation, cell cycle progression, apoptosis and secondary necrosis/ late-stage apoptosis.

2.2 RESULTS

2.2.1 The effect of bisPMB on WHCO1 cell viability

In order to investigate the effect of bisPMB on WHCO1 cell viability, the colorimetric water soluble tetrazolium salt WST (4-[3-(4-Iodophenyl-2-(4 nitrophenyl)-2H-5-tetrozolio]-1,3-benzene disulfonate) based assay was performed as described in section 6.2.1. The WST assay indirectly quantifies cell proliferation by quantitating the formation of formazan dye from the cleavage of the WST tetrazolium salt by the mitochondrial dehydrogenase in viable cells. The WST assay is similar to the MTT assay except its formazan product is soluble as opposed to the insoluble formazan crystals produced by MTT cleavage.

Our results demonstrated that 0.1% DMSO is not cytotoxic to WHCO1 cells, as the cell viability profile was similar to the media only control (figure 2.2). Furthermore, the loss of WHCO1 cell viability was significantly higher in cells treated with 10 µM bisPMB compared to 1 µM bisPMB or untreated controls (figure 2.2). In addition 1 µM bisPMB had no effect on WHCO1 cell viability, with a profile similar to untreated controls. A time-dependent effect was seen in which WHCO1 cells treated with 10 µM bisPMB for 48 h ($p = 0.0004$) and 24 h ($p = 0.034$) time points, with the significantly enhanced reduction in cell viability when observed in the 48 h treated WHCO1 cells (figure 2.2). This data demonstrated 10 µM

bisPMB inhibits WHCO1 cell proliferation and the inhibitory effect is more pronounced at 48 hours.

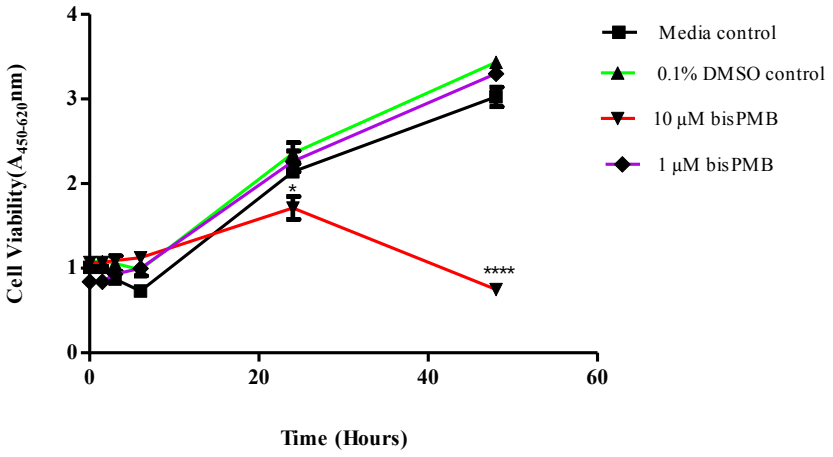

Figure 2.2 Time and concentration dependent inhibitory effect of bisPMB on WHCO1 cell viability. WHCO1 cells were incubated with 1 µM (purple) or 10 µM (red) bisPMB in 0.1% DMSO or 0.1% DMSO alone (green) or media alone (black) for up to 48 h. The WST assay was conducted as described in section 6.2.1. An absorbance value of 450 nm with the reference of 620 nm was used to read the photometric signal. Each point is an average ± SD of three independent experiments. A student t-test was statistical analysis was performed using GraphPad Prism, * indicated $p < 0.05$ and**** indicated $p < 0.0001$

2.2.2 Cytotoxicity of bisPMB in different oesophageal cancer and normal cell lines

To compare the effect of bisPMB on different oesophageal squamous cell carcinoma cell lines and a normal cell line (described in section 6.1.1), we quantified this effect by determining bisPMB's 50% inhibitory concentration (IC_{50}). The IC_{50} was used as a quantitative measure of the effectiveness of bisPMB at inhibiting cell proliferation using the MTT assay as described in section 6.2.2. The MTT assay indirectly quantifies cell proliferation by measuring the formazan produced from the cleavage of the MTT tetrazolium salt in metabolically active cells at A595nm, thus measuring cell viability. To interpret results obtained from this assay, it is assumed that higher cell numbers are directly correlated with high cell viability.

From the dose response curves cell viability was defined as absorbance at 595nm against log [bisPMB], the IC_{50} value was calculated for WHCO1, WHCO6 and KYSE30 and Het-1A cells (figure 2.3) as described in section 6.3.2. It was found that cell viability decreased with increasing bisPMB concentration, with the 7 µM, 14 µM and 3.5 µM concentrations displayed on the WHCO1 graph. As expected the 7 µM correlated with 50 % cell viability, the 14 µM displayed 27 % cell viability and the 3.5 µM concentration resulted in 81 % cell viability (table

2.1). This demonstrated that the 3.5 µM concentration was the least toxic concentration and14 µM displayed high cytotoxic levels in WHCO1 cells.

The average of three independent determinations of 24 h IC_{50}'s obtained for cell lines WHCO1, WHCO6, KYSE30 and Het-1A are displayed in Table 2.1. As can be seen, the bisPMB IC_{50} concentrations observed for the WHCO1 and WHCO6 cell lines were found to be similar being 6.97 ± 0.08 µM and 6.70 ± 1.64 µM respectively (Table 2.2). Furthermore, bisPMB was found to be marginally although significantly (1.2 fold) more active in WHCO1 cells compared to KYSE30 ($p < 0.001$) (Table 2.1).

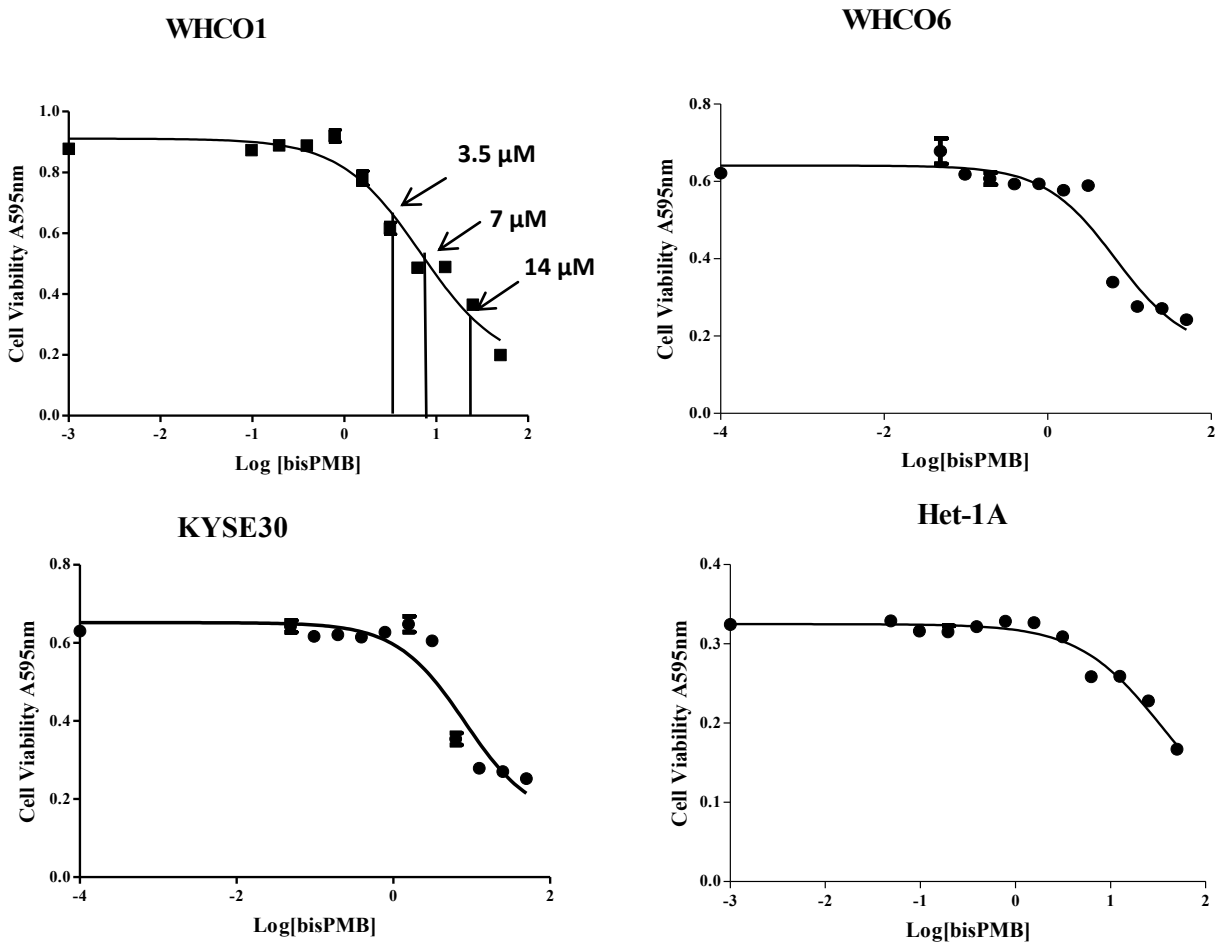

Figure 2.3 Dose response curves used for 24 hour IC_{50} determination in WHCO1, WHCO6, KYSE30 and Het-1A cells. Oesophageal cell lines were incubated with varying concentrations of bisPMB for 24 hours and subjected to an MTT assay as described in section 6.2.2. The bisPMB concentration (µM) is log transformed and plotted on the x–axis. Each dot indicates the average cell viability of four technical replicates from each concentration.

Table 2.1 Average percentage WHCO1 cell viability for three bisPMB concentrations. The average of the percentage WHCO1 cell viability ± SD was calculated from the dose response curves of three independent determinations.

BisPMB Concentration	Percentage WHCO1 cell viability ± SD
3.5 μM	79 ± 5
7 μM	50± 3
14 μM	27± 6

Table 2.2. 24 h IC_{50} values (μM) with ± SD from bisPMB-treated oesophageal cell lines, obtained using the MTT assay. Average IC_{50} values of three independent biological replicates.

CELL LINE	AVERAGE IC_{50} ± SD μM
WHCO1	6.97 ± 0.08
WHCO6	6.70 ± 1.64
KYSE30	8.09 ± 0.06
HET-1A	33.7 ± 2.15

The bisPMB IC_{50} concentration on the non-cancer epithelial cell line Het-1A was found to be 33.7 ± 2.15 μM (Table2.2). This indicated that bisPMB displayed 5 fold increased cytotoxicity in WHCO1 cells compared to the Het-1A cells. These findings demonstrated that bisPMB had a similar inhibitory effect on the proliferation of the different oesophageal cancer cell lines, and selectivity for cancer over the Het-1A normal oesophageal cell line.

For the purposes of this study, we used the 3.5 μM, 7 μM and14 μM bisPMB concentration values obtained from the WHCO1 cells to investigate the molecular mechanisms of action of bisPMB in oesophageal cell lines. These concentrations would provide insight into the molecular response of oesophageal cancer cells to different cytotoxic concentrations of bisPMB. Furthermore, we chose WHCO1 cells as the model cell line for further experiments.

2.2.3 Effect of bisPMB on WHCO1 cell morphology

To evaluate the effect of bisPMB on cell morphology, WHCO1 cells were treated with 24 h 3.5 μM, 7 μM and14μM bisPMB concentrations and images of the treated cells were captured with an Olympus SC30 camera as described in section 6.1.6.

The untreated WHCO1 cells displayed a multinucleated morphology (figure 2.4**A**). The WHCO1 cells treated with 3.5 μM bisPMB concentration for 24h displayed similar

morphological characteristics to the untreated cells (figure 2.4**B**). However the morphology of WHCO1 cells treated with 7 µM appeared flat, rounded and contained vacuole like structures in the cytoplasm (figure 2.4**C**). The WHCO1 cells treated with 14 µM appeared round and shrunken, but also had membrane bound sac like structures (figure 2.4**D**).

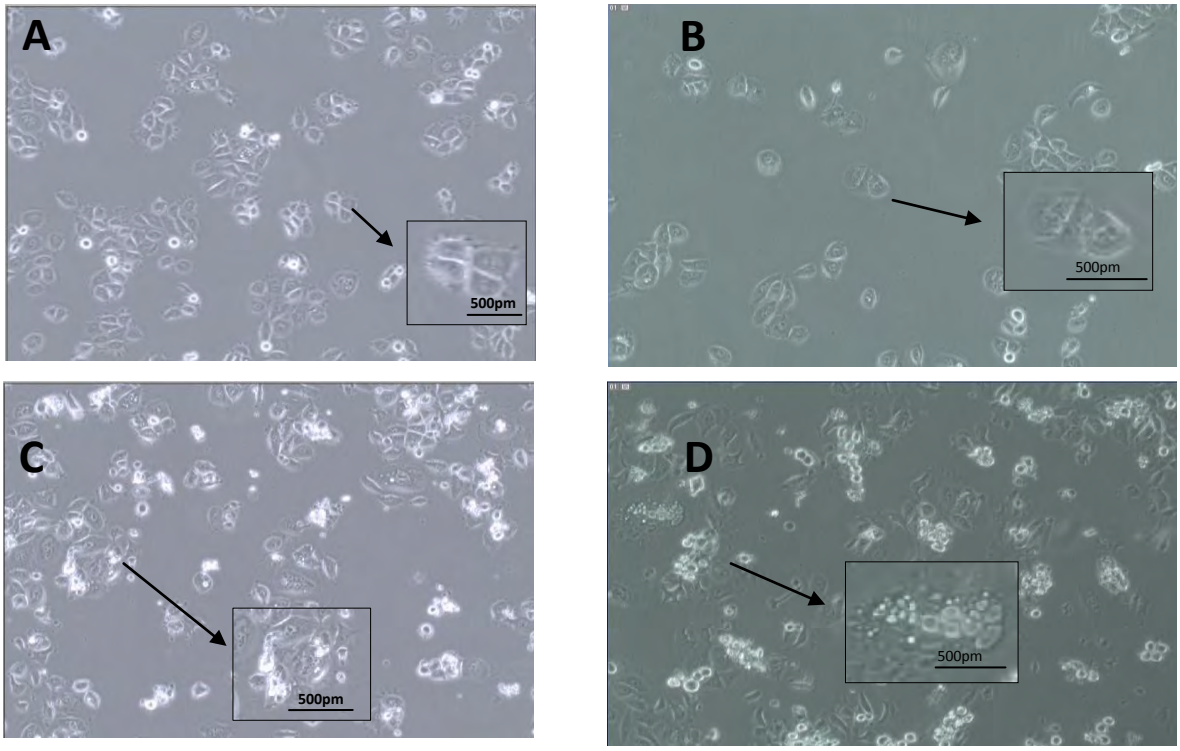

Figure 2.4 Morphological changes of WHCO1 cells treated with increasing concentrations of bisPMB. Images for WHCO1 cells were captured using a phase contrast image with an Olympus SC30 camera. (**A**) Untreated WHCO1 cells, (**B**) WHCO1 cells treated with bisPMB at 3.5 µM, (**C**) 7 µM and (**D**) ×14 µM concentration at 10 × magnification. The inserts in C and D show cells with membrane bound sacs.

2.2.4 Effect of BisPMB on the Cell Cycle

In order to determine whether bisPMB has any effect on the cell cycle progression in WHCO1 cells, flow cytometry using propidium iodide staining was performed as outlined in section 6.5. BisPMB was found to induce a concentration dependent G_2/M cell cycle arrest in WHCO1 cells (figure 2.5). The untreated cell cycle profile of WHCO1 cell cells displayed a greater population of cells at the G_0/G_1 than the S and G_2/M phase (figure 2.5**A**). The cell cycle profile of WHCO1 cells treated with 3.5 µMwas similar to the untreated control (figure 2.5 B). The 7 µM (figure 2.5 **C**) and 2 7 µM (figure 2.5 **D**) bisPMB concentrations demonstrated a 3.8 ($p < 0.001$) and 3.3 ($p < 0.001$) fold increase respectively in the number of cells in the G_2/M phase compared to the untreated control. The number of cells at the G_0/G_1 phase of the cell cycle were found to decrease by 5.7 ($p < 0.001$) and 3.6 ($p < 0.001$) fold in WHC01 cells treated with bisPMB at 7 µM and 14 µM concentrations respectively compared

to untreated control. Additionally, we observed a 1.6 and 20 fold increases in cells occupying the $SubG_1$ peak in WHCO1 cells treated only with the higher 7 µM and 14 µM concentrations respectively (table 2.2). Therefore evidence from both morphology & cell cycle support the cell viability data that suggests that bisPMB is cytotoxic toWHCO1 cells at 7 µM and 14 µM concentrations.

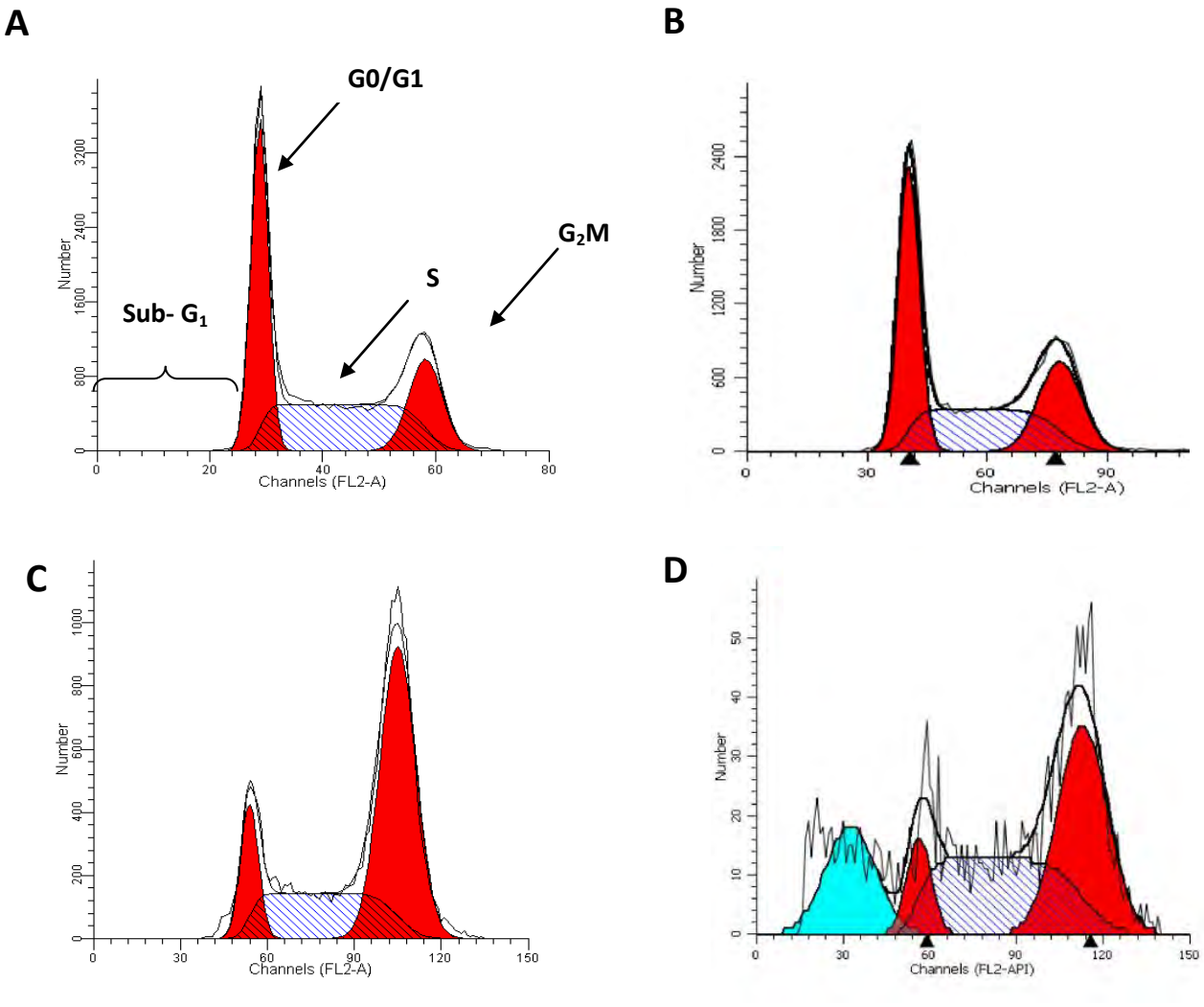

Figure 2.5. The cell cycle profile of WHCO1 cells treated with increasing concentrations of bisPMB. Cell cycle analysis of (**A**) Untreated WHCO1 cells, (**B**) WHCO1 cells treated with bisPMB at 3.5 µM, (**C**) 7 µM and (**D**) 14 µM of bisPMB with $subG_1$ peak was performed by flow cytometry using propidium iodide staining as described in section 6.5. The x-axis indicates the amount of fluorescence and the y-axis the number of cells. Each experiment was performed in triplicate and these results are representative of three independent experiments.

Table 2.2 Cell cycle analysis of WHCO1 cells treated with bisPMB. Average percentage ± SD of 3 independent experiments of WHCO1 cell populations treated with 3.5 μMor 7 μM or 14 μM bisPMB for 24 h.

BisPMB (μM)	Sub- G_1 (%)	G_0/G_1 (%)	S (%)	G_2M (%)
Untreated	0	44.5 ± 3.5	39.8 ± 1.2	15.7 ± 2.4
3.5 μM	0	44.1 ± 2.9	34.9 ± 3.1	26.9 ± 5.4
7 μM	1.61	7.7 ± 2.7	31.8 ± 3.4	60.0 ± 6.8
14 μM	19.9 ± 8.4	12.3 ± 2.2	36.2 ± 6.5	51.5 ± 5.0

2.2.5 BisPMB induces apoptosis in WHCO1 but not in Het-1A oesophageal cell lines at the concentrations used.

Apoptosis is defined as programmed cell death and is characterised by biochemical changes which is known to include internucleosomal genomic DNA fragmentation. In order to determine whether bisPMB induced apoptosis in WHCO1 or Het-1A cells, histone-associated DNA fragments (mono and oligonucleosomes) were quantified in the cytoplasm after treatment using the Roche cell death ELISA kit. Briefly, WHCO1 or Het-1A cell lysate was sandwiched between anti-histone and anti-DNA conjugated to horseradish peroxidise (HRP) antibodies in streptavidin coated multiwell plates. The histone associated DNA fragments were then photometrically quantified using the colour development from the HRP substrate ABTS (2,2'-Azinobis [3-ethylbenzothiazoline-6-sulfonic acid]-diammonium salt). The absorbance value obtained correlated with the amount of histone associated DNA fragments, indicating apoptosis.

We observed a 1.2, 1.8 and 3 fold increase in the induction of apoptosis in WHCO1 cells treated with 3.5 μM, 7 μM and 14 μM bisPMB concentrations respectively over a 24 h period and compared to the untreated control (Figure 2.6**A**). This result demonstrated the ability of bisPMB to induce apoptosis in WHCO1 cells, in a concentration dependent manner. However, no apoptotic induction in Het-1A cells treated with the same bisPMB concentrations was observed (figure 2.6**B**). Thus, the 7 μM and the 14 μM concentrations of bisPMB induced membrane blebbing, an increase in sub-G_1peak and histone associated DNA fragments in WHCO1 cells.

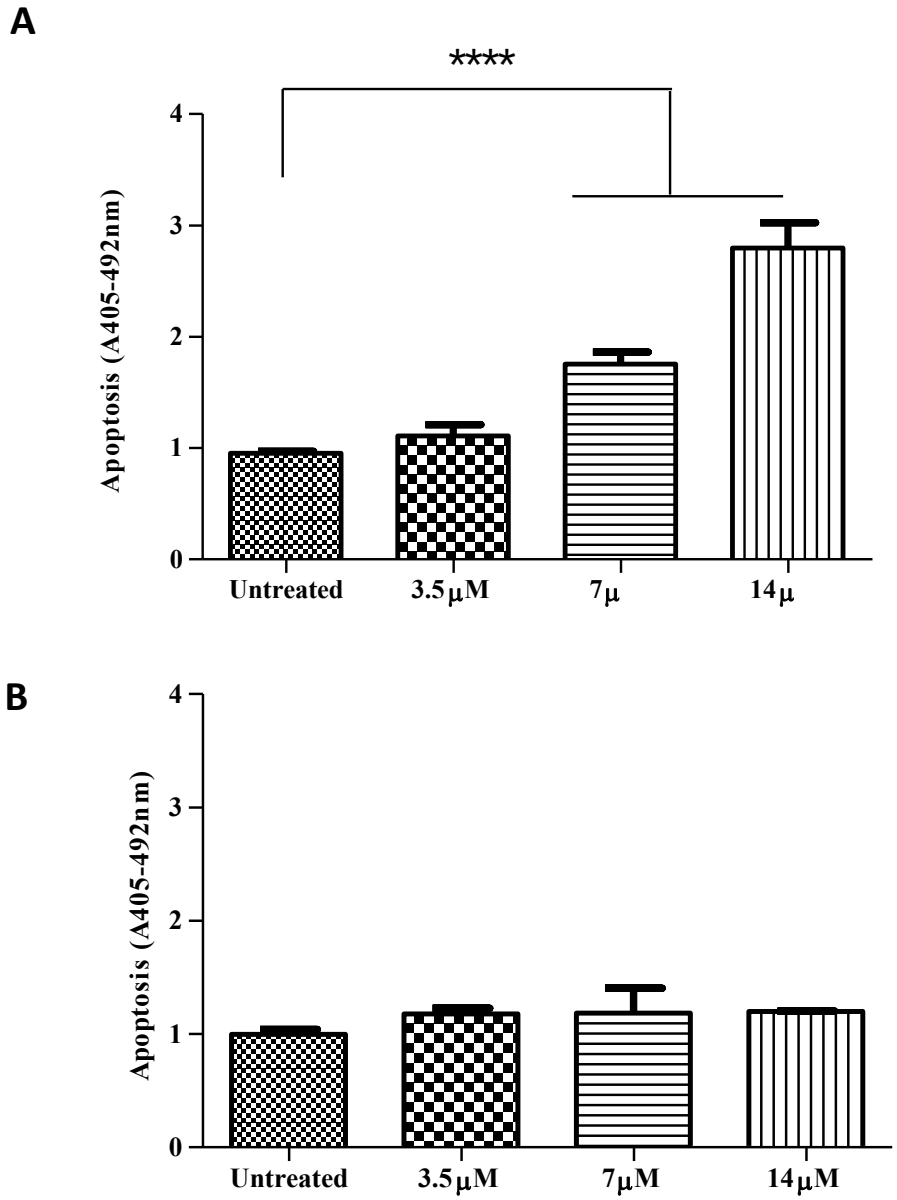

Figure 2.6. Induction of apoptosis in WHCO1 and Het-1A cells by bisPMB. WHCO1 cells or Het-1A cells were incubated with bisPMB at 3.5 μMor 7 μM or 14 μM for 24 h, and apoptosis was quantified by measuring histone associated DNA fragments in the cytoplasm. **A**) WHCO1 cells and (**B**) Het-1A. An absorbance value of 405 nm with the reference of 492 nm was used to read the photometric signal, measuring cell apoptosis. Each bar represents the mean absorbance ± SD of two independent experiments. Student t-test and one way ANOVA statistical analysis were performed using GraphPad Prism, ****indicated p <0.0001.

2.2.6 The effect of bisPMB on cell membrane integrity.

To further examine the cytotoxicity of bisPMB in WHCO1 cells, the lactate dehydrogenase (LDH) activity assay was detected in cells undergoing late stage apoptosis/secondary necrosis. This assay quantifies the activity of the LDH expelled from the cytoplasm of cells as a result of a damaged plasma membrane.

WHCO1 cells in media or 0.1% DMSO alone served as negative controls for this study. We demonstrated that 0.1% DMSO does not have a cytotoxic effect on WHCO1 cells, as there was no change in LDH activity in the cytoplasm of these cells over a 48 h period compared to the media only sample. Furthermore, our results indicate that 10 µM bisPMB increased LDH released by WHCO1 cells after 48 h (Figure 2.7). In contrast, 1 µM bisPMB did not damage WHCO1 cell membrane integrity, as we observed no change in LDH activity, even after 48 h of treatment (Figure 2.7).

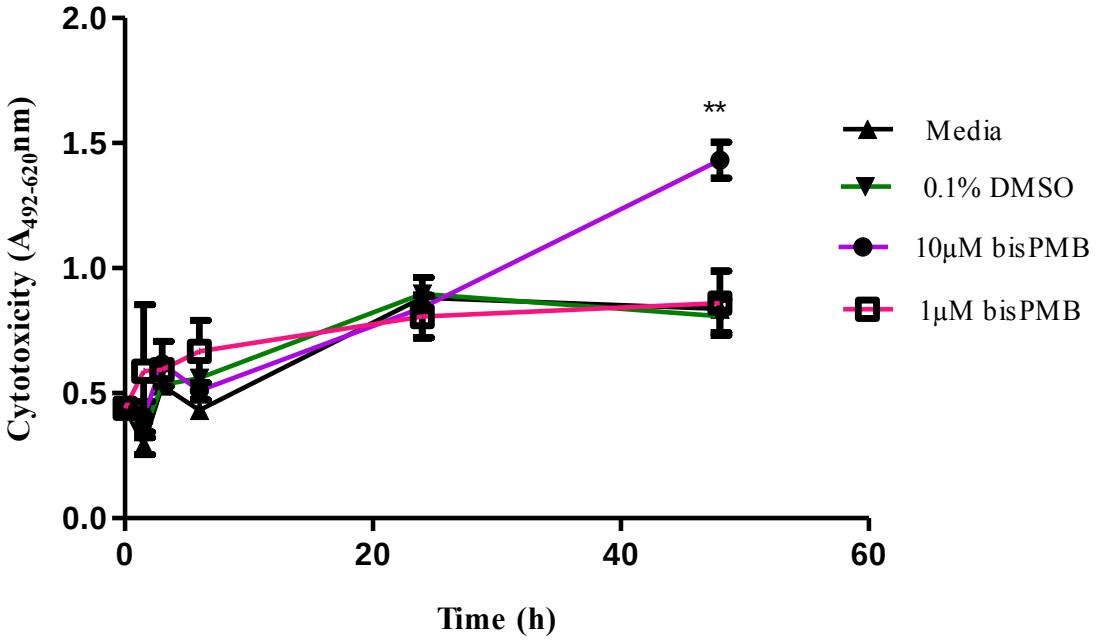

Figure 2.7 Time and concentration dependent cytotoxic effect of bisPMB on WHCO1 LDH release. WHCO1 cells were incubated with 1 µM (red) or 10 µM (purple) bisPMB, 0.1% DMSO (green) or media alone (black) for 3, 6, 24 and 48 h. LDH activity released from the cells was measured. An absorbance value of 450nm with the reference of 620nm was used to read the photometric signal, measuring cell cytotoxicity.

2.3 DISCUSSION

The compound bisPMB contains the same vinyl disulfide pharmacophore as ajoene. However, *para*-methoxybenzyl substitution at the terminal ends was found to enhance the potency of ajoene against WHCO1 cell proliferation (Hunter et al., 2008, Kaschula et al., 2011, Kaschula et al., 2012). Kaschula et al., (2011) reported the inhibition of breast cancer MDA-MB-231 and SiHa, cervical HeLa, oesophageal cancer WHCO1 and Kyse520 and

transformed fibroblast CT1 cell proliferation by *Z*-ajoene and bisPMB with the 48 IC_{50} range of 13.7 – 42.1 μM for *Z*-ajoene and 1.4 – 13.8 μM for bisPMB. BisPMB displayed the greatest improvement of ajoene antiproliferative activity against oesophageal cancer WHCO1 cells with 12 fold enhancement (Kaschula et al., 2011). Thus, this study focused on bisPMB cytotoxic activities against WHCO1 cells. Here we demonstrated that bisPMB inhibited proliferation of three different oesophageal cancer cell lines with 24 hour IC_{50}'s in the range of 6.7 – 8.09 μM. The 24 hour IC_{50} values for cisplatin treated oesophageal cancer cell lines TE-2 and TE-13 is 37.5 and 56.3 μM respectively (Tanaka et al., 2010). This implied that bisPMB is more potent than the clinically used drug cisplatin against oesophageal cancer cells. Suggesting that bisPMB could be a good candidate for OC therapy.

We also observed that the inhibition of WHCO1 cell viability increased following treatment with 10 μM bisPMB from 24 h to 48 h. This suggested that bisPMB inhibitory effect was also time dependent. In line with this, ajoene is reported to inhibit the proliferation of Burkitt lymphoma BJA-B, glioblastoma multiforme cancer stem cells (GBM CSC), breast MDA-MB-231, pancreatic adenocarcinoma PANC1, lung adenocarcinoma A5949, colon HT29 and cervical cancer Hela cells (Scharfenberg et al., 1990, Li et al., 2002a, Ye et al., 2005, Taylor et al., 2006, Jung et al., 2014, Kaschula et al., 2011)

The anti-proliferative activity of ajoene may be attributed to its ability to block cell cycle progression. BisPMB was found to induce a G_2/M cell cycle arrest in WHCO1 cells in a concentration dependent manner. This result is consistent with the reports that ajoene blocks the cell cycle progression of HL-60 and U937 cells at the G_2/M phase (Li et al., 2002a, Xu et al., 2004, Ye et al., 2005). BisPMB induced cell cycle arrest can be linked to the disruption of microtubule network which has been shown for *Z*-ajoene treated normal marsupial kidney Ptk2 cells (Li et al., 2002a). Our FACS cell cycle analysis also revealed that bisPMB induced a concentration dependent increase in subG1 peak in WHCO1 cells which is indicative of cells undergoing apoptosis and has also been observed in HL60 cells treated with ajoene (Dirsch et al., 1998).

Apoptosis is widely implicated in the anticancer activities of chemotherapeutic drugs. Further analysis showed that bisPMB induced apoptosis in WHCO1 cells following a 24 h treatment at both 7 μM and 14 μM, where both concentrations induced a rounded up and shrunken WHCO1 cell morphology. These morphological features resembled the characteristics apoptotic cells that include; cell shrinkage, membrane blebbing and loss of cell membrane

integrity (Sen and D'Incalci, 1992, Green and Kroemer, 2004). Subsequently, we demonstrated that WHCO1 cells displayed a concentration dependent increase of histone-associated DNA fragments indicative of apoptosis when treated with 7 μM and 14 μM concentrations of bisPMB. This agrees with data in the literature where ajoene was found to induce apoptosis in leukaemia HL-60 (Dirsch et al., 1998) and basal cell carcinoma BCC cells (Tilli et al., 2003) in a concentration dependent manner. Furthermore, *Z*-ajoene was found to trigger apoptosis in leukaemia HL-60 and U937 (Li et al., 2002a, Li et al., 2002o)

After the induction of apoptosis, secondary necrosis is initiated in cells (Saraste, 1999). This event is sometimes referred to as late-stage apoptosis and is characterized by the loss of cell membrane integrity (Patel et al., 2005). Cells with damaged cell membranes release intracellular enzymes such as LDH and this is an indication of late stage apoptosis (Kaja et al., 2015). We observed that bisPMB triggered a time and concentration-dependent increase in LDH activity in WHCO1 cells, which was apparent after 48 hours. As expected, this finding suggests that LDH released by WHCO1 cells treated with bisPMB occurs at a later stage to inhibition of viability and apoptosis induction where an effect is seen at 24h, which is suggestive of damaged WHCO1 cell membrane integrity. The observed secondary necrosis may not be a phenomena that bisPMB induces *in vivo* and may have been a consequence of the limitations in *in vitro* cell culture technique, as cells undergoing apoptosis are not cleared by macrophages resulting in their intracellular contents are expelled into the media (Hochreiter-Hufford and Ravichandran, 2013). Moreover, this observation is consistent with reports that show that ajoene triggered the release of LDH in A549 lung cancer cells in a concentration dependent manner with an EC_{50} of 200 μM (Jakobsen et al., 2012).This demonstrated that bisPMB cytotoxic activity was superior to that of ajoene as LDH release was observed at 10 μM in WHCO1 cells.

We also observed that bisPMB was approximately five fold more active at inhibiting WHCO1 cancer cell proliferation compared to the normal oesophageal epithelial (Het-1A) cell line. In addition, no apoptosis was observed in Het-1A cells treated with the same bisPMB concentration as in WHCO1 cells. This demonstrated that bisPMB was less cytotoxic to non-cancer cell lines and is in agreement with the reported three fold selectivity of bisPMB against the normal esophageal epithelial cells (EPC2) (Kaschula et al., 2011), although the effect with HET-1A cells was more dramatic. The Het-1A cell line is transformed with the SV-40 large T-antigen, which binds and inactivates p53 (tumour

suppressor), rendering it having tumour features. Unlike the Het-1A cells, the EPC2 cells have a functional p53 (tumour suppressor) and are immortalised with human telomerase reverse transcriptase (Harada et al., 2003). However, both Het-1A and EPC2-hTERT have been reported to have tumour like characteristics; EPC2-hTERT cells have been reported to yield basal cell hyperplasia in an organotypic tissue culture system, while Het-1A cells have been demonstrated to possess a dysplastic appearance (Harada et al., 2003, Underwood et al., 2010). The Het-1A cell line was chosen as a "normal" model cell line in this chapter because it was available in the lab, it's easier to work with and is cultured with the same media (DMEM) as the cancer WHCO1 cells, thus the experimental data is more comparable to that of WHCO1 cells. Other reports have shown selectivity of ajoene for cancer over non-cancer cell lines. Ajoene has been shown to be two fold more active in Burkitt lymphoma (BJA) than the normal baby hamster (BHK21) cells (Scharfenberg et al., 1990). Similarly, normal marsupial kidney cells (Ptk2) were less sensitive to ajoene cytotoxic activity than the promyeloleukemia (HL-60) and nasopharyngeal carcinoma (KB) cell lines (Li et al., 2002a). Similarly, marsupial Ptk2 cells and the primary fibroblast FS_4 cells were found to be less sensitive to ajoene than cancer cell lines (Dirsch et al., 1998, Scharfenberg et al., 1990, Li et al., 2002o). Furthermore, ajoene has been shown to induce apoptosis in human leukaemia cell line, but it did not induce apoptosis in peripheral mononuclear blood cells (Dirsch et al., 1998).

Our results on bisPMB are consistent with published data on cytotoxicity of ajoene in cancer cells. It is evident from our data that bisPMB is cytotoxic to WHCO1 cells although the mode of action and molecular mechanisms underlying these events are still unknown. In order to further our investigation into the molecular mechanisms leading to the apoptotic effect of bisPMB, we performed a DNA microarray in WHCO1 cells treated with bisPMB at 3.5 μM concentration. The 3.5 μM concentration was selected as we had already confirmed that this is a non–toxic concentration to WHCO1.

Since bisPMB displays excellent cytotoxic activity against OC cancer cells lines and in addition has a longer shelf life, as unpublished nuclear magnetic resonance spectroscopy (NMR) data did not show any decomposition of the compound after 3 years of storage and therefore it is easier to work with than ajoene, we decided to probe into the mechanism leading to the cytotoxicity in oesophageal cancer cell lines with a view to its development as a OC therapeutic.

CHAPTER 3: TRANSCRIPTIONAL PROFILING OF WHCO1 OESOPHAGEAL CANCER CELLS TREATED WITH BISPMB

3.1 INTRODUCTION

In chapter 2 we observed the cytotoxic effects of bisPMB in the oesophageal squamous cell carcinoma (WHCO1) cell line. This observation was consistent with the cytotoxicity reported for ajoene on various cancer cell lines which include human leukaemia HL-60 (Dirsch et al., 1998), nasopharyngeal KB, cervical Bel-780, colon HCT, gastric BGC-823 and breast MCF-7 cancer (Li et al., 2002a) and breast cancer MDA-MB-231 and SiHa, oesophageal cancer WHCO1 and Kyse520, transformed fibroblast CT1 and cervical HeLa cell lines (Kaschula et al., 2011). The focus of this chapter is on the mechanistic events leading to the cytotoxicity of bisPMB in WHCO1 cancer cells.

Although not widely reported, there is emerging evidence that garlic derived OSC may be implicated in ER stress. More specifically, both DADS and DATS are reported to trigger ER stress associated apoptosis in colon cancer COLO 205 cells and basal cell carcinoma BCC cells respectively (Yang et al., 2009, Wang et al., 2012). Importantly, we have found and reported that ajoene targets and localizes to the ER in breast cancer MDA-MB-231 cells (Kaschula et al., 2015). Moreover, *Z*-ajoene was found to *S*-thiolate a multitude of proteins, promote protein aggregate formation and cause an increase in the expression of GRP78/BIP in MDA-MB-231 cells (Kaschula et al., 2015). GRP78/BIP is an ER resident chaperone and is commonly known to be upregulated under ER stress conditions. Therefore ajoene is proposed to target the ER where it interferes with protein folding to generate misfolded aggregates which may then activate an ER stress response in MDA-MB- 231 breast cancer cells. Based on the similar structures of ajoene and bisPMB and that they both contain the vinyl disulfide pharmacophore, we propose that bisPMB may also induce apoptosis by triggering ER stress in WHCO1 cells. We therefore chose thapsigargin (TG) as a positive control for ER stress induction in WHCO1 cells. TG is a natural compound isolated from the *Thapsia garganica* L plant (figure 3.1) and is a potent inhibitor of the sarco-endoplasmic reticulum Ca^{2+} ATPase (SERCA) in the nanomolar range, and induces apoptosis in the micromolar range (Treiman et al., 1998a). Moreover, TG is also reported to exert cytotoxic

effects in cancer cells *in vitro*. For example, TG has been shown to induce apoptosis in human TSU and rat prostate cancer cell lines (Tombal et al., 2000).

In this chapter, WHCO1 cells were treated with the previously determined non-cytotoxic 3.5 μMconcentration of bisPMB. It was anticipated that this sub-toxic concentration of bisPMB may give insights into early stage gene transcriptional changes in WHCO1 cells that occur prior to apoptosis induction. In addition, 1 μM TG was used as this concentration is reported to induce ER stress in cancer cells (Uemura et al., 2009, Andersen et al., 2015). Thereafter, the treated WHCO1 cells were subjected to microarray analysis to examine gene global expression changes

3.2 RESULTS

3.2.1 Effect of bisPMB or thapsigargin on WHCO1 cell morphology and apoptosis.

To evaluate the effect of bisPMB and TG on WHCO1 cell morphology, WHCO1 cells were treated with 3.5 μM bisPMB concentration or 1 μM TG and images of these cells were captured with an Olympus SC30 camera. As expected, the morphology of the WHCO1 cells treated with bisPMB at 3.5 μMconcentration was similar to the untreated control sample (figure 3.1 **A** and **B**); whereas 1 μM TG treated WHCO1 cells had a shrunken appearance (figure 3.1**C**).

In order to determine whether bisPMB or 1 μM TG induced apoptosis in WHCO1 cells, histone-associated DNA fragments were quantified in the cytoplasm after treatment. In agreement with figure 2.6 A, the 3.5 μM concentration of bisPMB did not induce apoptosis and was similar to the untreated control. However, 1 μM TG significantly enhanced apoptosis by 2 folds in WHCO1 cells compared to the untreated control (figure 3.2). Taken together, these observations suggested that the 3.5 μM bisPMB was not toxic to the cells however 1 μM TG is a cytotoxic concentration as apoptosis was induced

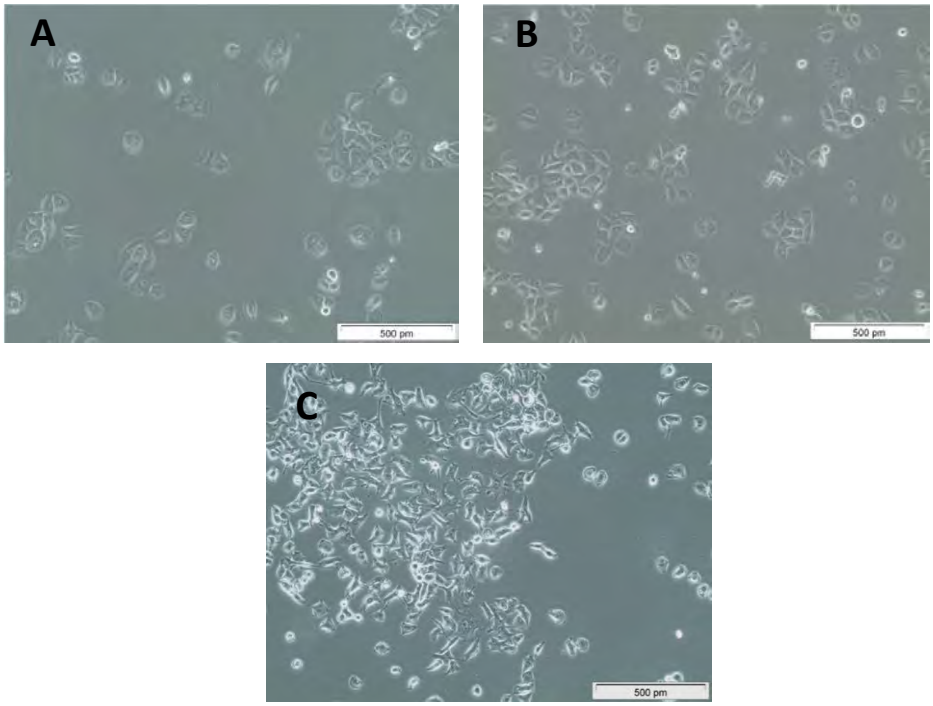

Figure 3.1 WHCO1 cell morphological changes after bisPMB and thapsigargin treatment. WHCO1 cells were treated with bisPMB at3.5 µM concentration or 1µM thapsigargin (TG) for 24 h and morphology observed under phase contrast at 10 × magnification **(A)** Untreated WHCO1 cells; **(B)** WHCO1 cells treated with bisPMB at 3.5 µMconcentration; **(C)** WHCO1 cells treated with 1µM TG.

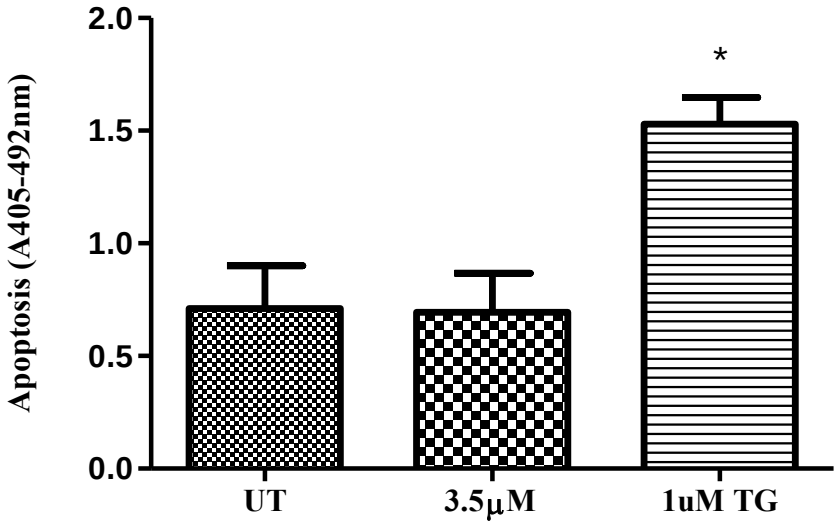

Figure 3.2 Apoptotic induction in WHCO1 cells treated with bisPMB or TG. WHCO1 cells were treated with bisPMB at 3.5 µM concentration or 1µM thapsigargin (TG) for 24 h. Subsequently, total cell lysate was used to determine histone associated DNA fragments in the cytoplasm. An absorbance of 405 nm with the reference of 492 nm was used to read the photometric signal, measuring cell apoptosis. Each bar represents the mean absorbance ± SD of three independent experiments. A t-test statistical analysis was performed using GraphPad Prism, * indicated $p < 0.05$.

3.2.2 Analysis of RNA extracted from bisPMB-treated WHCO1 cells

3.2.2.1 RNA Quality Control

Total RNA was extracted in quadruplicate from untreated, bisPMB or TG treated WHCO1 cells, followed by RNA quality assessment. Examination of RNA integrity is an important step when conducting gene expression studies as intact RNA is key to obtaining accurate data from downstream analysis such as qRT-PCR and microarrays (Fleige and Pfaffl, 2006). In this study, the quality of the total RNA extracted was assessed at the Centre of Proteomic and Genomic Research (CPGR). RNA integrity numbers (RIN) were found to be between 9.9 and 10 (Table 3.1), indicative that the RNA was of good quality and not degraded; intact RNA is considered to have a RIN value between 7 and 10 (Kawasaki, 2006). These results demonstrated that the RNA samples used in this study were of good quality and suitable for downstream cDNA microarray analysis.

Table 3.1. Quantification of the integrity of RNA samples used for cDNA microarray analysis. Total RNA was extracted in quadruplicate from the untreated, bisPMB and TG treated WHCO1 cells. The RNA integrity number (RIN) obtained from the samples was between 9.9 and 10. All the samples passed the quality control examination.

RNA Sample	RIN	Comment
Untreated	10	Pass
Untreated	10	Pass
Untreated	10	Pass
Untreated	10	Pass
BisPMB	10	Pass
BisPMB	10	Pass
BisPMB	10	Pass
BisPMB	10	Pass
TG	10	Pass
TG	10	Pass
TG	10	Pass
TG	10	Pass

3.2.2.2 cDNA microarray analysis in WHCO1 cells

Affymetrix human gene ST 2.0 arrays were used to conduct microarray analysis at the CPGR. The procedure depicted in figure 3.3 was conducted on an affymetrix platform and used to perform the cDNA microarray analysis, where labelled cRNA was fragmented and hybridized onto Affymetrix array ST 2.0 GeneChip. The raw probe intensity values obtained from the gene ST 2.0 arrays were computed on affymetrix .CEL files (figure 3.3). Thereafter, Partek®Genomics Suite™ (Partek Inc., 2014) software was used for data analysis.

The raw probe intensity values from the .CEL files were imported in the Partek®Genomics Suite™ (Partek Inc., 2014) software and normalized using the robust multi-array average (RMA) (Irizarry et al., 2003). The RMA normalizes the raw probe intensity values from different arrays by adjusting for the background, performing Log2 transformations, quantile normalisation and summarisation (Irizarry et al., 2003).

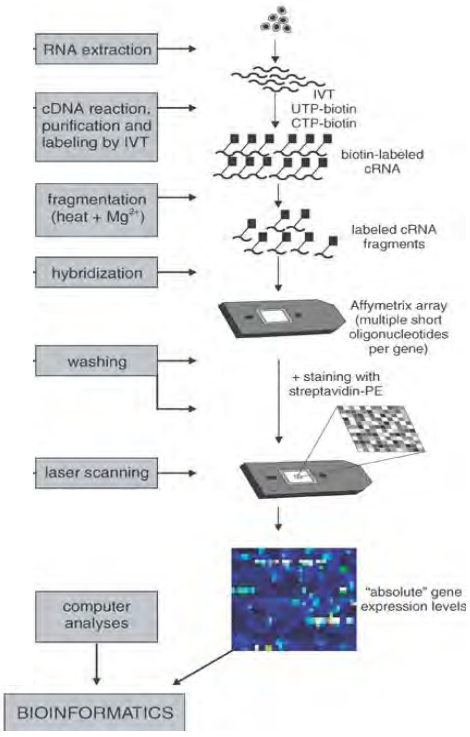

Figure 3.3. Workflow of cDNA microarray analysis with affymetrix GeneChip 2.0 array platform. The RNA extracted from bisPMB or TG treated WHCO1 cells were reverse transcribed into cDNA which was subsequently fragmented, labelled and hybridized into Affymetrix gene ST 2.0 array GeneChip. After hybridization, the array was washed and stained. Subsequently, the array was scanned using the GeneChip® scanner 3000 which stored the resulting intensity values as .CEL files. The picture was taken from http://www.nature.com/leu/journal/v17/n7/images/2402974f1.jpg.

Following normalization of the arrays, the similarities and differences in the gene expression profiles of untreated, bisPMB or TG samples was examined using the principal component analysis (PCA) and hierarchical clustering methods (Peterson, 2002). The PCA takes into account the variability of the gene expression data set within each sample group and also between the three sample groups studied. The PCA demonstrated that the biological replicates within each sample group clustered together with a single outlier observed in one of the thapsigargin treated samples (figure 3.4 **A**). The hierarchical clustering confirmed the reproducibility of the biological replicates within each sample group (figure 3.4**B**). Thus no variations were observed in biological replicates each of sample (untreated, bisPMB or TG).

A **B**

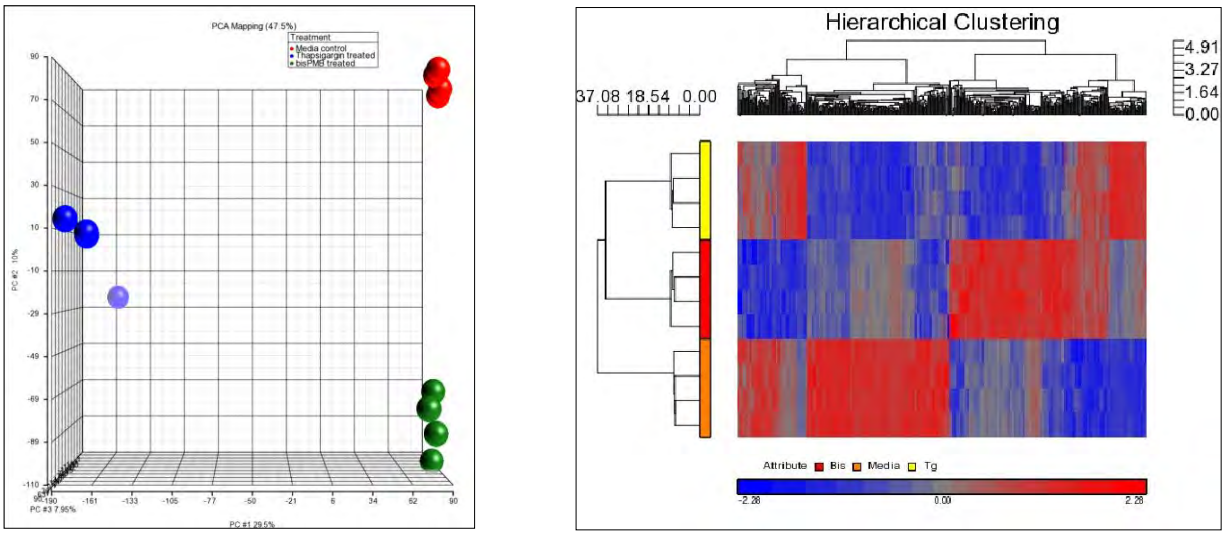

Figure 3.4. The Principal Component Analysis (PCA) score plot and hierarchical clustering heat map of microarray data in WHCO1 cells. (A) PCA plot of the gene expression data that was generated by Affymetrix GeneChip® Human Gene 2.0 ST Array from 12 samples of untreated WHCO1 cells (Red, n = 4) or treated with BisPMB (Green, n = 4) or TG (Blue, n = 4). Each dot represents a single array sample. The samples from each treatment group clustered well, except for the one outlier that was detected in the TG sample. (**B)** The hierarchical clustering of the genes in WHCO1 cells. The dendogram branches on y-axis represent the biological replicates of the untreated WHCO1 cells (Orange), treated with bisPMB (Red) and TG (Yellow) while the x-axis is indicative of the genes in the array. The red columns represent upregulated genes and the blue columns represented down regulated genes.

The differentially expressed genes (DEGs) derived from the bisPMB or TG samples were subsequently determined. Two way analysis of variance (ANOVA) was used to select the significantly deregulated genes, in bisPMB and TG treatment samples compared to the untreated control, by determining *p*-values. Multiple testing of these *p*-values using the Bonferroni test was conducted in order to calculate the false discover rate (FDR). The FDR conceptualized the rate of type I error in null hypothesis testing (Storey, 2002). The cut off for the DEGs from the

bisPMB or TG samples was set at 1.5 fold with a statistically significant FDR value set at $\alpha \leq 0.05$.

The number of DEGs uniquely expressed in the bisPMB or TG sample and those shared in both samples was then visualised using a Venn diagram (figure 3.5). A higher number of DEGs were observed in the TG sample compared to the bisPMB samples. A total of 6341 DEGs were found in the TG sample with 488 DEGs in the bisPMB sample. Of these, 295 DEGs were found to be common between both bisPMB and TG samples. The shared DEGs accounted for 60.5% and 4.7% of the total DEGs in bisPMB and TG samples respectively. Collectively, this demonstrated that the majority of the DEGs from the bisPMB sample were shared with TG sample but many of the TG DEGs were not shared with bisPMB.

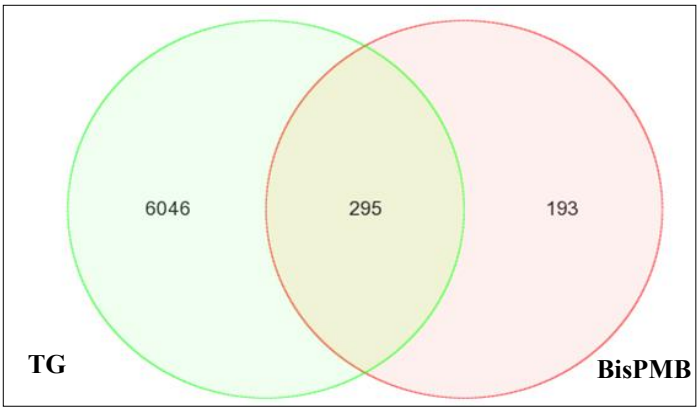

Figure 3.5. Venn diagram displaying the DEGs in WHCO1 cells treated with bisPMB (Red circle) and TG (Green circle) and those shared between the two treatments (overlap). There are 6046 and 193 unique DEGs in the TG and bisPMB treated WHCO1 cell samples respectively while 295 DEG's were common between oth samples

3.2.2.3 Validation of selected microarray DEGs involved in protein processing by qPCR

The results obtained from the cDNA microarray were validated by q - RT PCR on the same RNA samples used for the microarray analysis; and also independently repeated by extracting new RNA from two independent repeats. The validation was conducted using 23 DEGs shared between the bisPMB and TG groups (Table 3.2). A line representing the untreated control was set at one and drawn across the bar chart (See figure 3.6). Consequently, all data above the line indicated upregulated DEGs in the indicated samples and data below the line represent down regulated DEGs compared to untreated control. The DEGs selected were based on involvement in ER stress and protein processing pathways in the ER. The qPCR results for 4 (DDOST, Ubc6, GRP94 and CASP4) of the 23 DEGs in the bisPMB sample did not agree with the direction of

fold change of the microarray data. We observed consistency in 19 of the 23 DEGs in the bisPMB sample and in all DEGs in the TG sample with regards to the direction of fold change in gene expression between the qPCR and cDNA microarray results. Thus we were satisfied that the RNA sent for microarray analysis gave the correct results, that the fold changes observed were reproducible and that the independent biological replicates displayed striking similarities with the RNA used for microarray. This authenticated the microarray results and rendered them suitable for use in functional enrichment analysis studies.

Table 3.2 Genes selected of relevance to ER stress and protein processing pathways. BisPMB and TG DEGs with cDNA microarray fold changes. The negative fold changes represent downregulated genes and the positive fold changed indicate upregulated genes relative to the untreated control.

GENE	DESCRIPTION	BISPMB	TG
Sec61	Translocation protein *Saccharomyeces Cerevisiae* 61 homolog	-1.67757	2.98533
Sec63	Translocation protein *Saccharomyeces Cerevisiae* 63 homolog	-1.02034	2.51986
rrbp1	Ribosome binding protein 1	-1.54513	2.00086
tram	Translocating chain – associated membrane	-1.60647	2.50978
ero1l	Endoplasmic reticulum oxidoreductin-1-like protein B	-1.52044	5.49922
vimp	VCP-interacting membrane protein	-1.72005	2.8603
sel1L	Suppressor of lin-12-like	-1.50057	5.95984
ssr3	Signal sequence receptor subunit gamma	-1.7	4.5663
ddost	Dolichyl-diphosphooligossacharide-protein glycosyltransferase	1.14939	2.24069
lmna1	Lamin A related sequence 1	1.57643	3.72986
ask	Apoptosis signal regulating kinase 1	-1.619	-5.79027
sec24D	Translocation protein *S. Cerevisiae* family member 24D	-1.66651	2.16198
ire1	Inositol –Requiring enzyme 1	1.05086	2.20624
ubc6	Ubiquitin-conjugated enzyme E2	1.6063	2.629
grp94	Glucose regulated protein 94	1.53431	4.88002
edem	ER degradation- enhancing alpha-mannosidase like protein	1.92258	-2.35283
pdia4	Protein disulfide isomerise A4	1.65048	5.68534
atf6	Activating transcription factor 6	1.50036	2.0337
casp4	Caspase 4	1.72382	2.10505
xbp-1s	X-box binding protein 1 spliced variant	1.54864	3.48261
grp78	Glucose regulated protein 78	1.56787	3.66649
ddit3	DNA damage inducible transcript 3	1.60875	11.4566

A

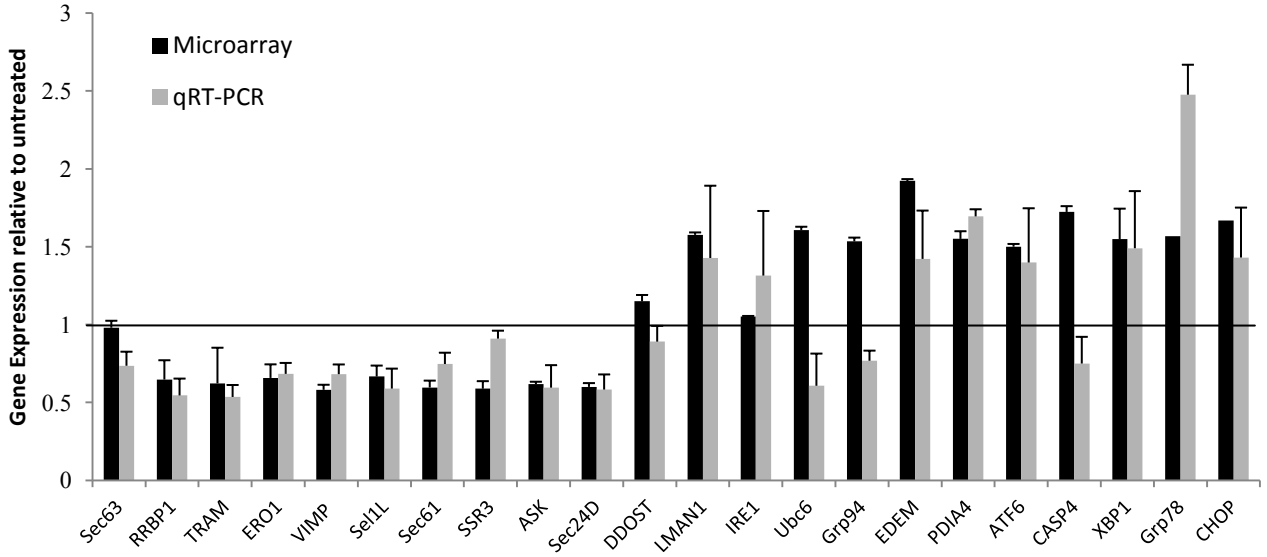

B

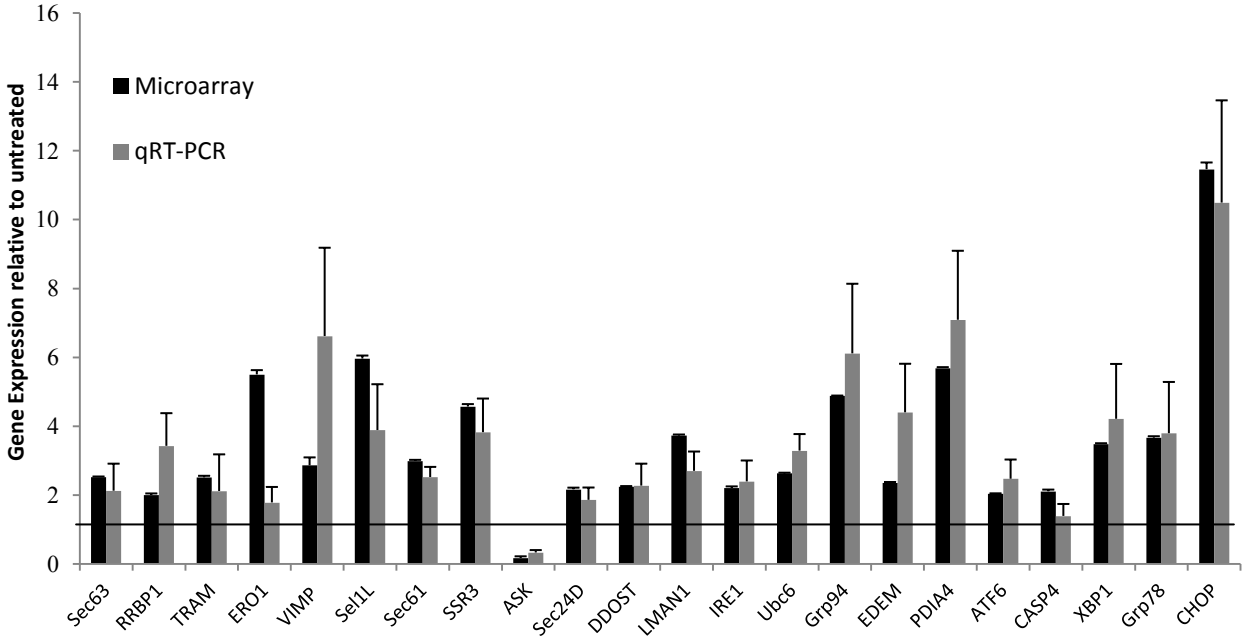

Figure 3.6 Validation of microarray fold change in gene expression by qPCR. The selected DEGs were analysed using qPCR. The fold changes of the DEGs obtained from the microarray (black) and qPCR (grey) were compared and normalized to the untreated control being a value of one **(A)** Bar graph comparing microarray with qPCR fold changes of bisPMB RNA sample. **(B)** Bar graph comparing the microarray and qPCR TG sample fold changes. The microarray DEGs were normalised relative to RMA normalization whereas the mRNA fold changes from the qPCR was normalised to GAPDH.

3.2.3 Functional enrichment analysis of microarray derived bisPMB and TG DEGs

3.2.3.1 Gene Ontology analysis

In order to mechanistically interpret the microarray gene expression data and determine the molecular events triggered by bisPMB or TG in WHCO1 cells, gene ontology (GO) analysis was performed. We generated GO using the WebGestalt web based software which uses published information on genes in the human genome and gene attributes to organize bisPMB or TG DEGs into various biological contexts. GOs are organised into three domains namely; biological processes, molecular function and cellular components. In addition, the Bonferroni test is applied to determine the adjusted *p*-value/false discovery rate (FDR). The FDR significance level cut off for the analysis performed in bisPMB or TG DEGs was set at $\alpha \leq 0.05$. This type of analysis enabled identification of the most prominent biological events in the bisPMB and TG samples.

We observed numerous GO biological processes enriched with bisPMB DEGs, these included metabolic process, biological regulation, response to stimuli, cell communication, multi-cellular organismal process, localization, development process, cellular component organization, death, multi-organism process, reproduction, cell proliferation and growth (figure 3.7). Higher resolution into specific biological processes was obtained using a directed acyclic graph (DAG). The DAG illustrated that the "activation of signalling protein activity involved in unfolded protein response" (UPR), was the most specific and significant (adjP/FDR of 2.95e-120) biological process enriched with bisPMB DEGs with the (figure 3.8). Thus, this demonstrated that bisPMB primarily affected genes involved in the UPR in WHCO1 cells. BisPMB also appeared to affect biological processes such as metabolic processes, which are commonly associated with cancer progression and response to treatment. Furthermore, the most specific biological process involved the unfolded protein response.

Overrepresented TG DEGs were found to be those involved in the metabolic process category, biological regulation and response to stimuli, multi-cellular organismal process, cellular component organizations, cell communication, localization, developmental process, cell death, cell proliferation, reproduction, multi-organism process and cell growth (figure 3.9). Further resolution into the most specifically enriched biological process converged on mitosis (FDR=3.97e-28) and DNA metabolic processes (FDR=1.74e-21); with 184 and 326 the TG DEGs forming part of these clusters respectively (figure 3.10). Ultimately, the bisPMB and TG samples were both found to deregulated similar biological process categories but the specific

mode of action of TG was related to cell division, which is essential in cancer proliferation and cell death and that of bPMB is UPR & ER stress.

In order to investigate the cellular components relevant to the bisPMB or TG DEGs, Bar Chart and Directed Acyclic Graphs were constructed. The cellular components from the bisPMB sample were found to include the membrane, nucleus, membrane enclosed lumen, cytosol, endomembrane system, macromolecular complex, endoplasmic reticulum, Golgi apparatus, mitochondrion, vesicle, cytoskeleton, cell projection, extracellular space, envelope, endosome, chromosome, vacuole, extracellular matrix, microbody and lipid particle (figure 3.11). The most specific and significant cellular components, under the membrane and membrane enclosed lumen category in the bisPMB sample, were the endoplasmic reticulum membrane and the endoplasmic reticulum lumen with FDR values of 1.21e-07 and 1.18e-02 respectively (figure 3.12). These significantly enriched cellular components fall in line with the biological processes data on the bisPMB sample as the UPR has been associated with genes localized in the ER membrane and lumen.

Comparably, the membrane, nucleus, membrane enclosed lumen, macromolecular complex, cytosol, endomembrane system, cytoskeleton, endoplasmic reticulum, mitochondrion, Golgi apparatus, cell projection, vesicle, chromosome, envelope, extracellular space, endosome, vacuole, extracellular matrix, microbody, ribosome, lipid particle and external encapsulating structure were the cellular components containing the TG DEGs (figure 3.13). The most specific and significantly enriched cellular components where TG DEGs were active included the “cytoplasmic part” with FDR of 3.75e-35, “intracellular organelle” (FDR= 9.25e-43) and in the “intracellular membrane- bound organelle” (FDR= 3.85e-51) (figure 3.14). This can be expected as the different stages of TG triggered events, such as ER stress, occur in the above mentioned cellular compartments. For example, the splicing of XBP-1 mRNA occurs in the “cytoplasmic part of the cell and the dissociation of GRP78/BIP from transmembrane proteins take place in the ER, and “intracellular organelle” or “intracellular membrane- bound organelle”.

The GO findings demonstrated that bisPMB and TG regulated similar biological processes and cellular components. However, bisPMB was primarily implicated in UPR while TG was implicated in mitosis and DNA metabolic processes. This provided a broad overview of intracellular mechanistic events occurring in both the bisPMB and TG samples. In order to gain more information into the underlying molecular events of the above mentioned biological processes, pathway analysis was conducted.

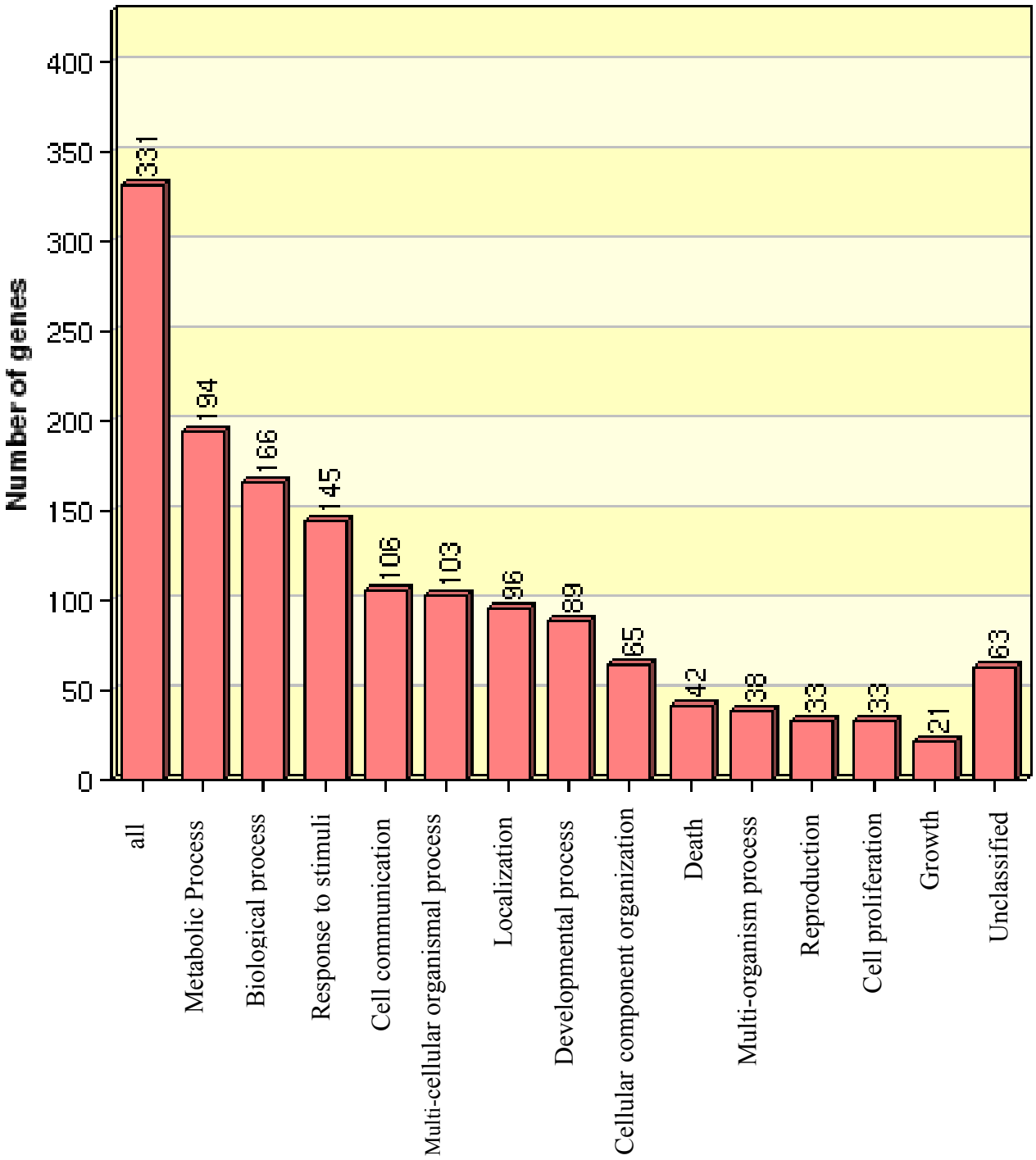

Figure 3.7 Bar graph representing Gene Ontology biological processes ancestral categories in the bisPMB sample. Each bar signifies broad ancestral biological process category and the numbers of bisPMB DEGs involved in each processes are displayed on top of each bar.

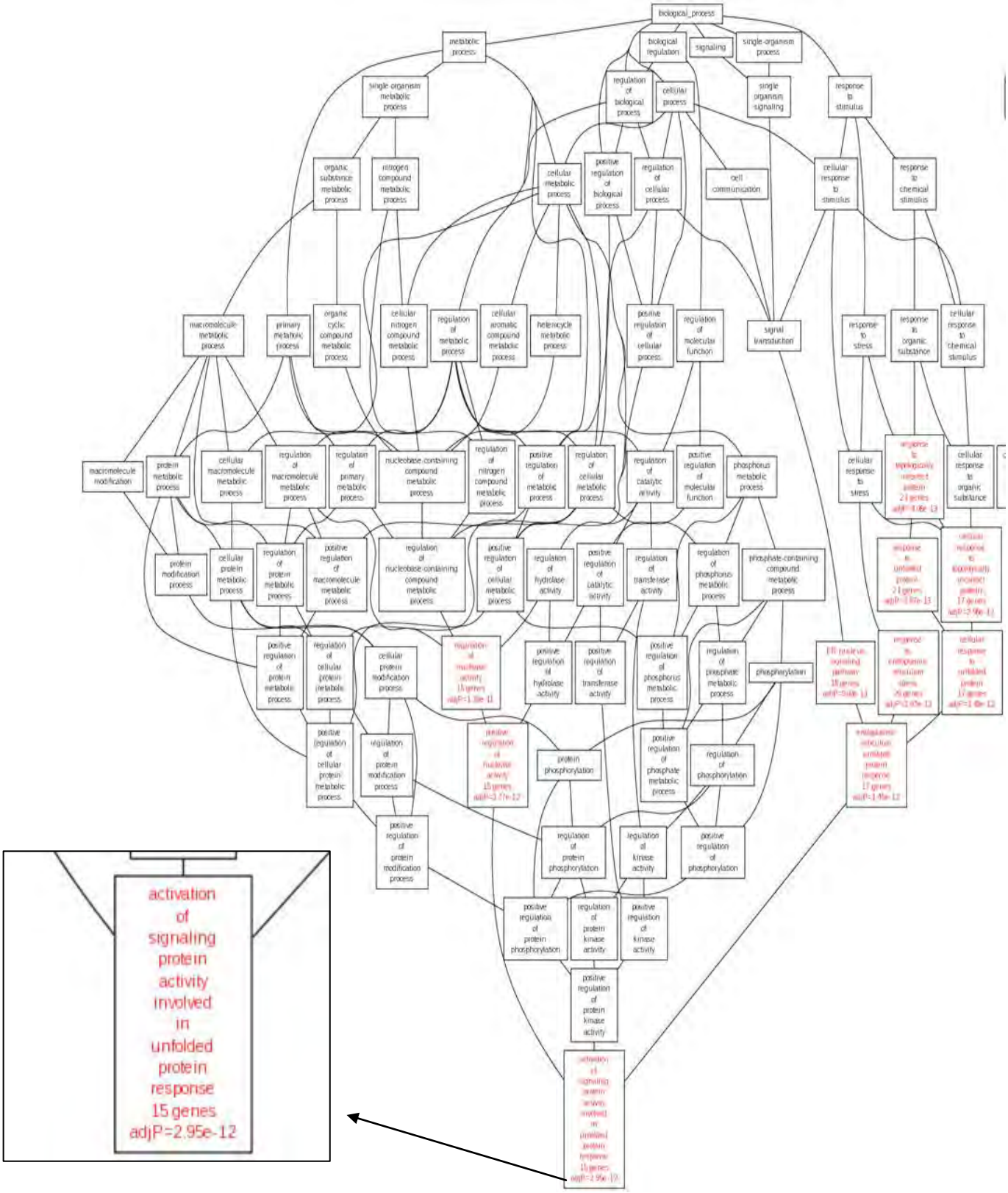

Figure 3.8. Gene Ontology biological processes significantly enriched in bisPMB sample. Directed acyclic graph (DAG) showing the hierarchical order, from ancestral to more specific biological processes. The biological processes highlighted in red indicate the significantly enriched categories. Bonferroni statistical test was used to calculate FDR ($p<0.05$).

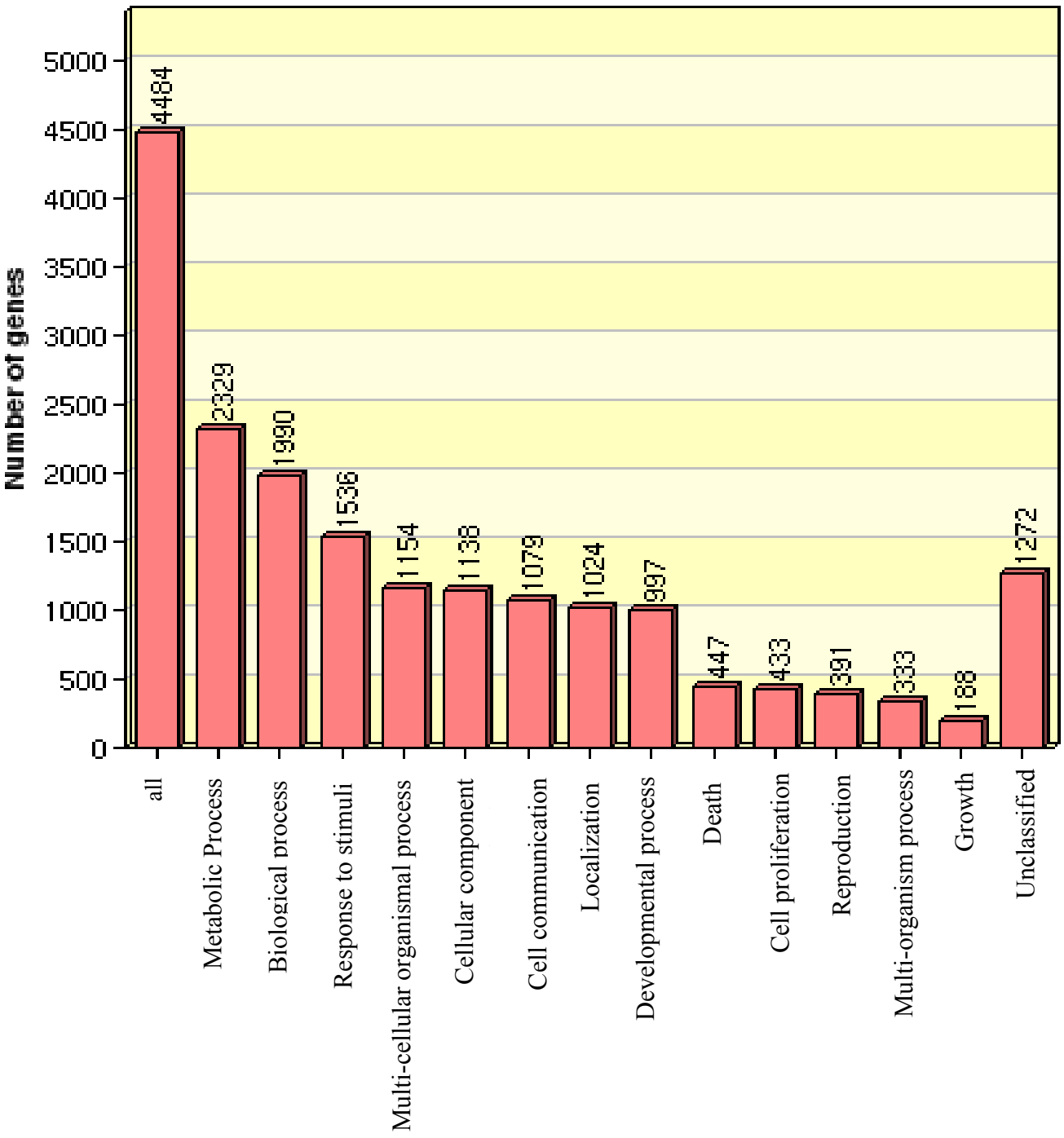

Figure 3.9 Bar graph representing Gene Ontology biological processes ancestral categories in the TG sample. Each bar signifies broad ancestral biological process category and the numbers of TG DEGs involved in each processes are displayed on top of each bar.

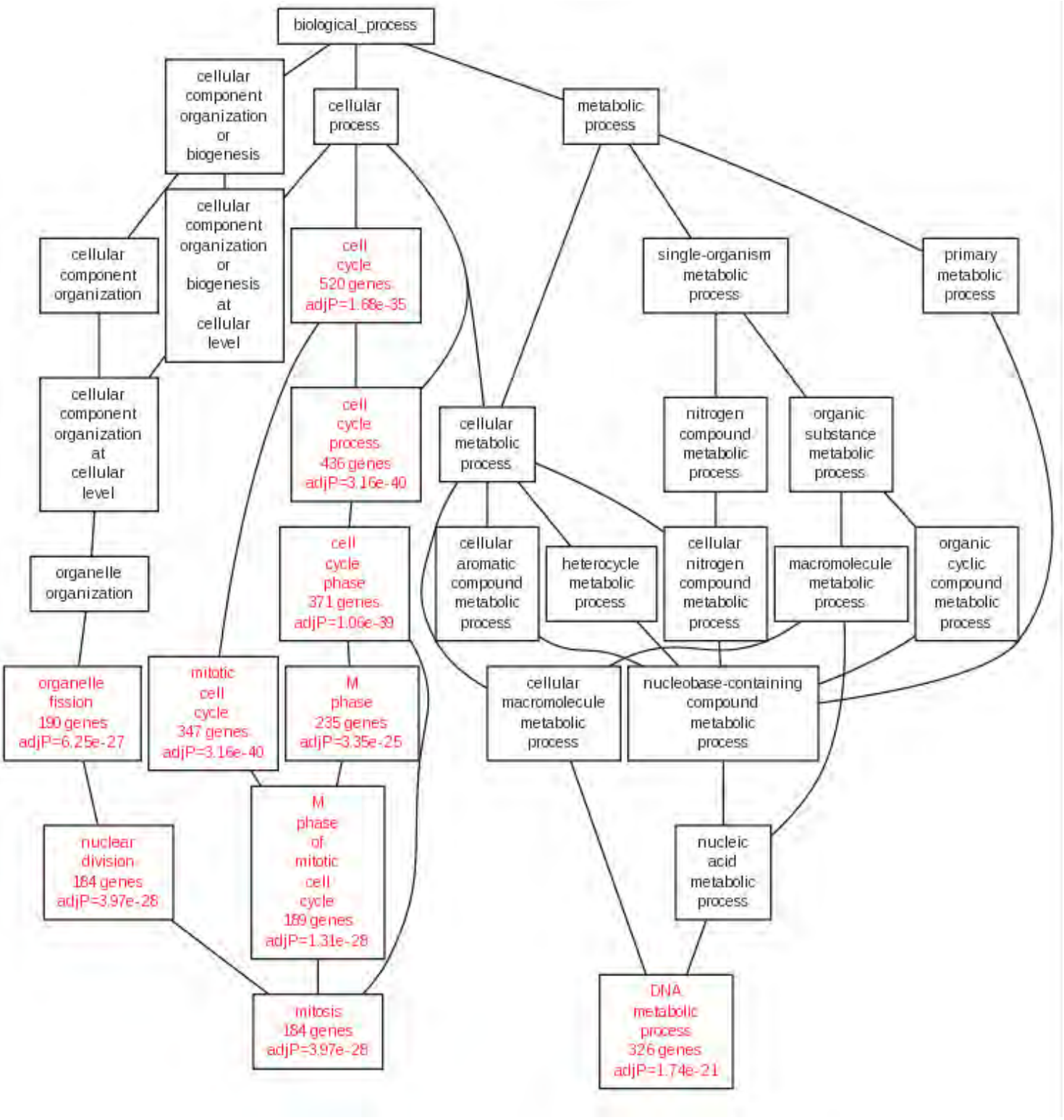

Figure 3.10. Gene Ontology biological processes significantly enriched in TG sample Directed acyclic graph (DAG) showing the hierarchical order of biological processes showing further resolution to more specific biological processes. The biological processes highlighted in red indicate the significantly enriched categories. Bonferroni statistical test was used to calculate FDR ($p<0.05$).

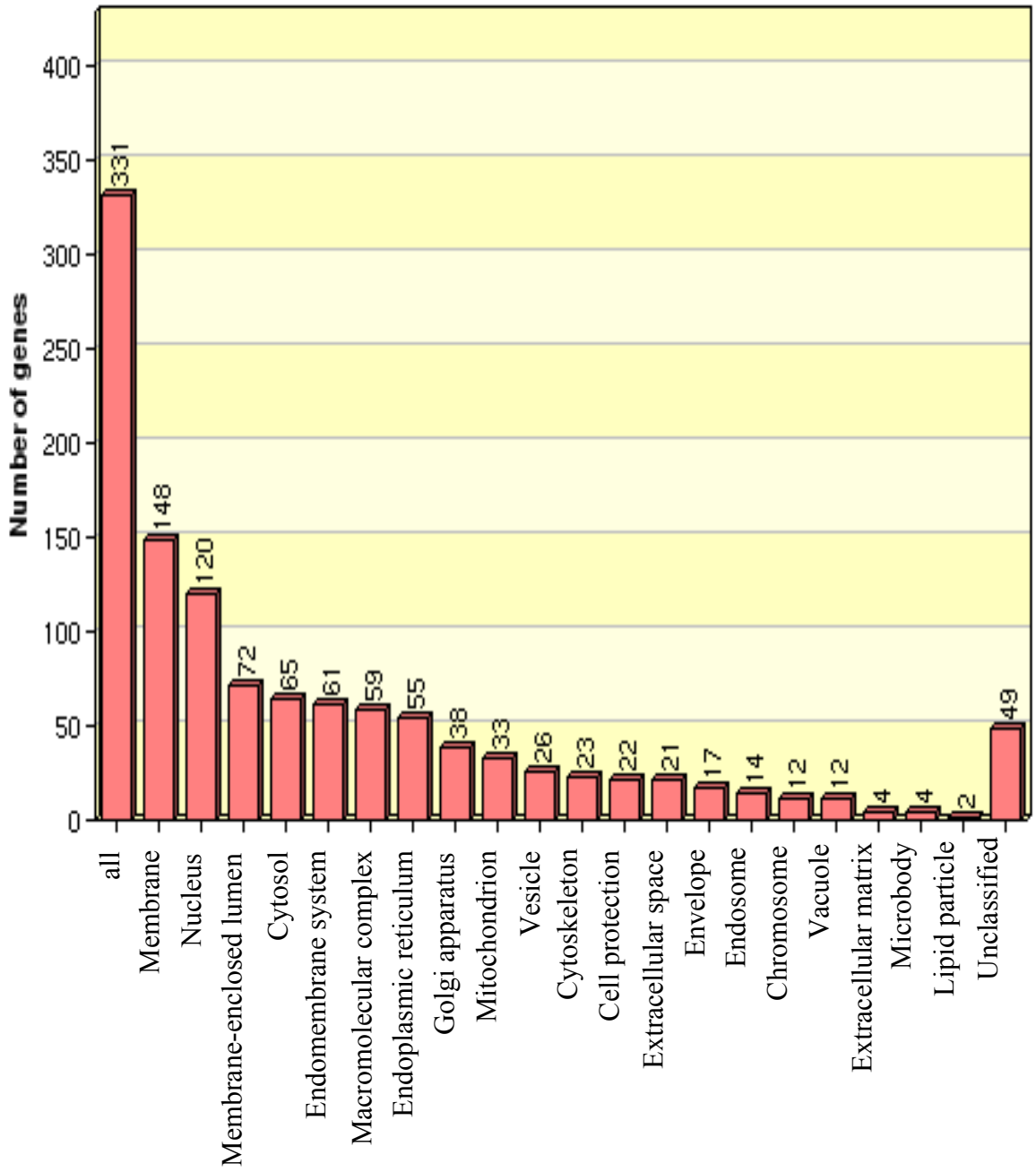

Figure 3.11 Bar graph representing Gene Ontology cellular component ancestral categories in the bisPMB sample. Each bar signifies broad ancestral cellular component and the numbers of bisPMB DEGs involved in each component are displayed on top of each bar.

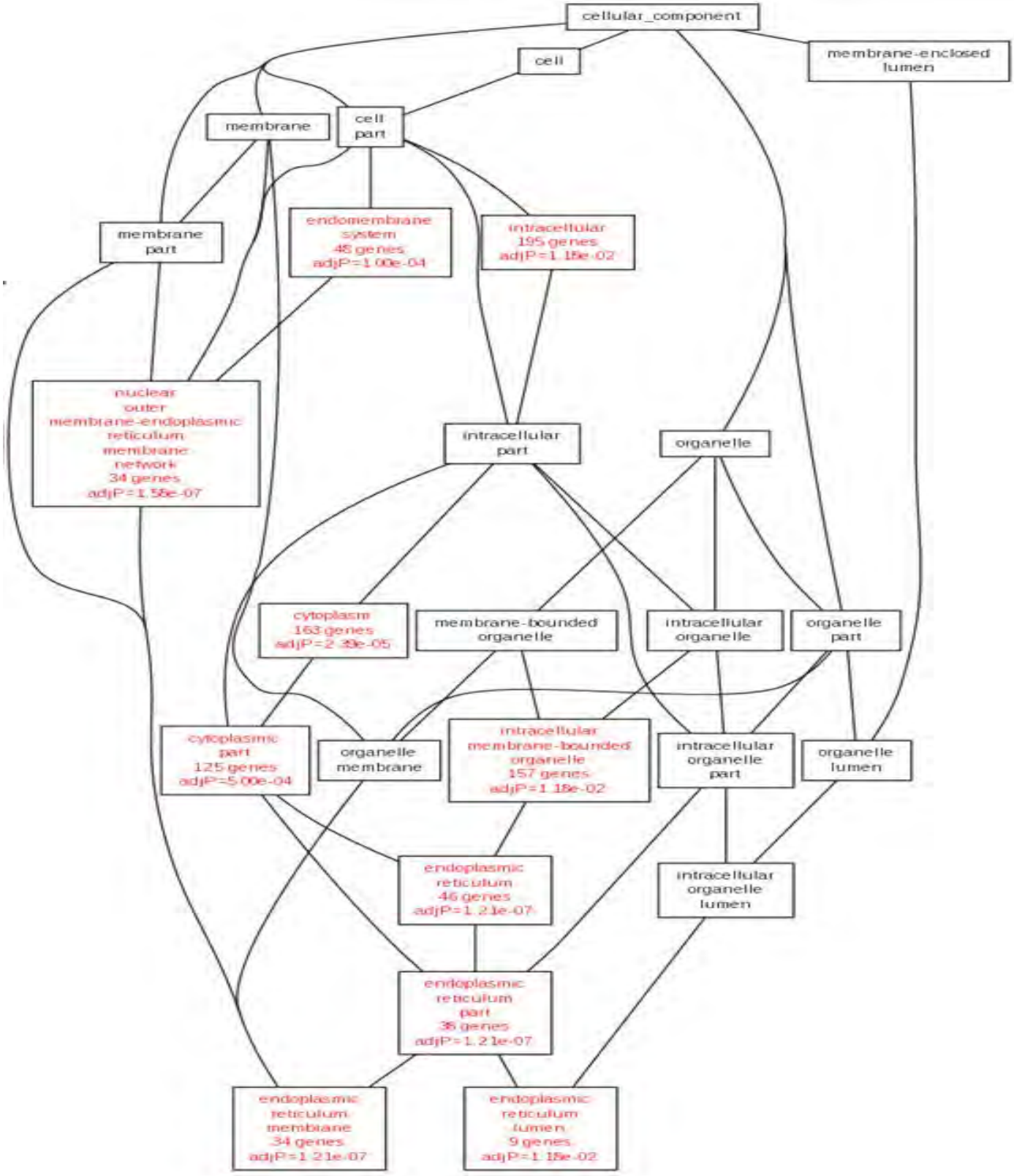

Figure 3.12. Gene Ontology cellular components significantly enriched in bisPMB. Directed acyclic graph (DAG) showing the hierarchical order of cellular components showing further resolution to more specific cellular components. The cellular components highlighted in red indicate the significantly enriched categories. Bonferroni statistical test was used to calculate FDR ($p<0.05$).

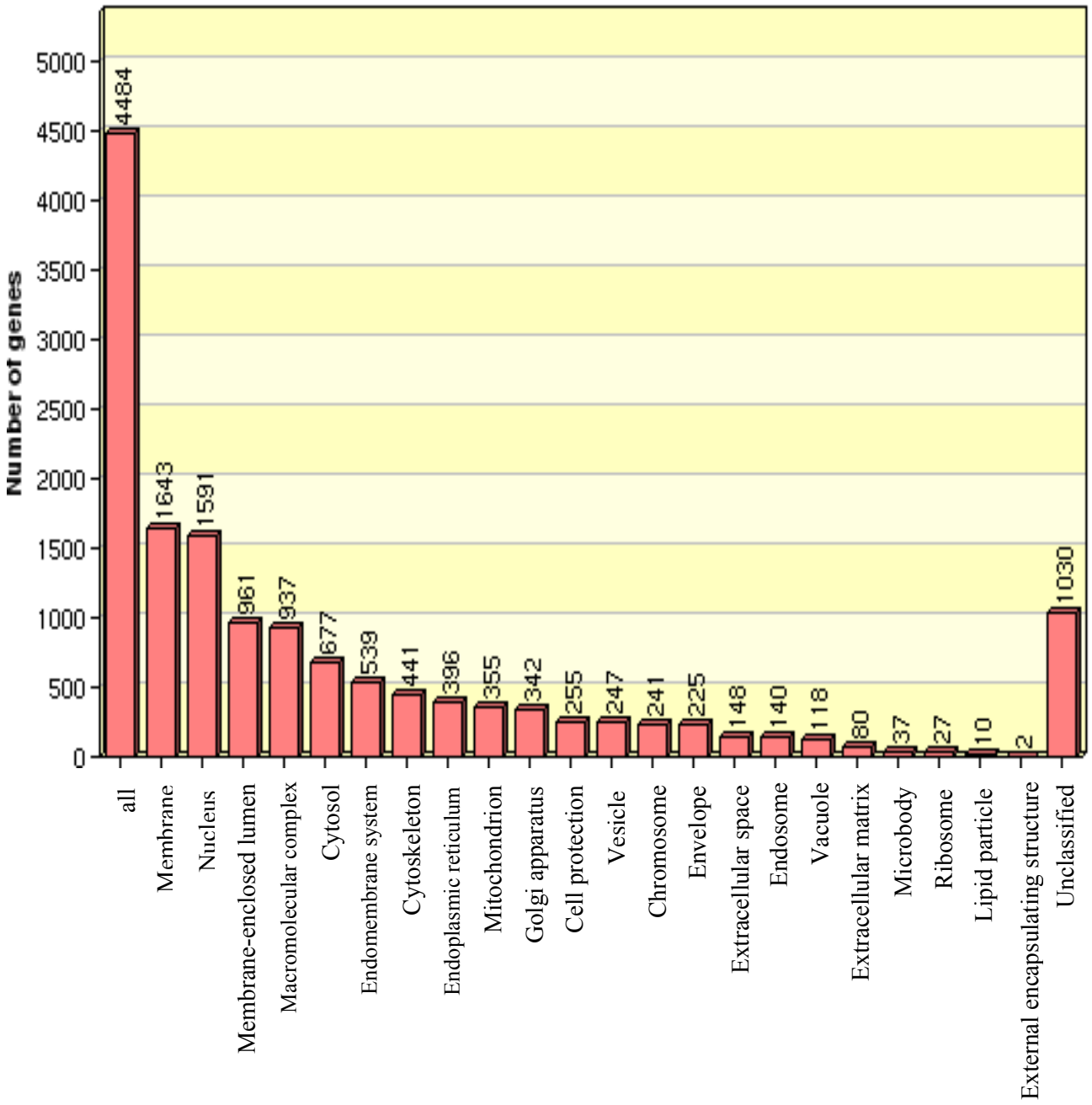

Figure 3.13. Bar chart representing Gene Ontology cellular component ancestral categories in the TG sample. Each bar signifies broad ancestral cellular component category and the numbers of TG DEGs involved in each component are displayed on top of each bar.

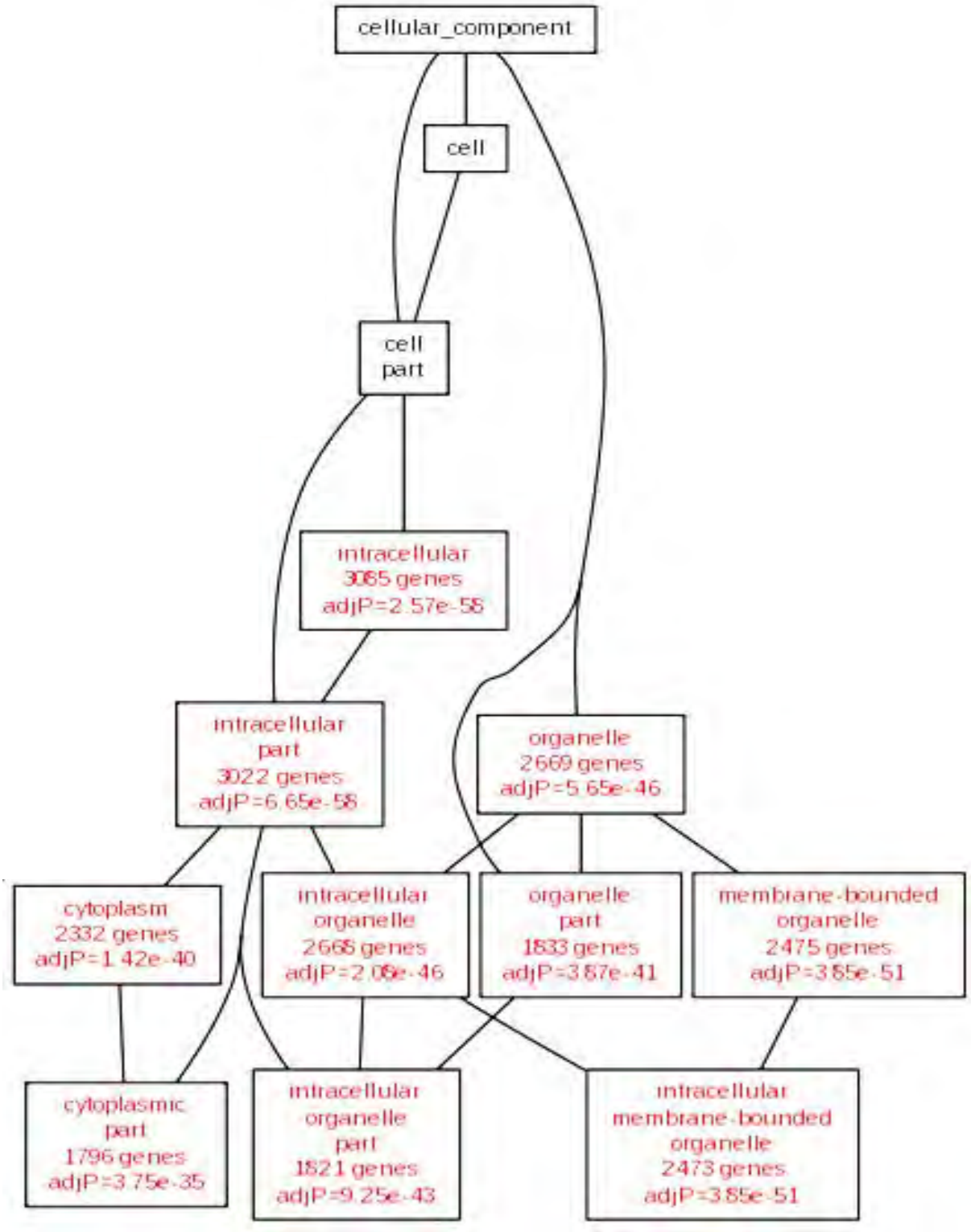

Figure 3.14 Gene Ontology cellular components significantly enriched in TG. Directed acyclic graph (DAG) showing the hierarchical order of biological processes showing further resolution to more specific cellular component. The cellular components highlighted in red indicate the significantly enriched categories. Bonferroni statistical test was used to calculate FDR ($p<0.05$).

3.2.3.2 Pathways Analysis

Examination of the molecular pathways activated by bisPMB or TG was conducted using the KEGG pathway network module and the ingenuity pathway analysis (IPA). Numerous KEGG pathways were found to contain bisPMB DEGs (figure 3.15). The three with the largest number of bisPMB DEGs included pathways in cancer, protein processing in the endoplasmic reticulum and the MAPK signalling pathways (figure 3.15). Similarly, the most significantly enriched KEGG pathways in the TG sample included protein processing in ER, cell cycle, pathways in cancer and MAPK signalling pathway (figure 3.16). Further resolution of the KEGG pathway network modules revealed the presence of ER Stress/UPR genes in the protein processing in the ER pathway category for both bisPMB & TG (figure 3.17). These pathways that formed part of the protein processing in the ER pathway category included; UPR, endoplasmic reticulum associated degradation (ERAD) and protein translocation pathways for both bisPMB & TG (figure 3.17). However, the number of bisPMB DEGs overrepresented in protein processing pathways in the ER was found to be much lower than the TG DEGs (figure 3.17 **A** and **B**).

The bisPMB DEGs represented in the UPR pathways were found to include ATF6, XBP-1, GRP78/BIP and CHOP, all of which were upregulated. Similarly, the TG DEGs that were represented in the UPR pathway were upregulated and they included the PERK, ATF6, IRE1, GADD34, CHOP and XBP-1. The ERAD DEGs such as EDEM, Ubc6 and VIMP were present in both bisPMB and TG sample (figure 3.17). Furthermore, the majority of the bisPMB DEGs represented in the protein translocation pathways were down regulated and these included the Sec63, TRAM, Sec24D and SSR3/TRAP but were upregulated in the TG sample. These findings suggest that WHCO1 cells respond to bisPMB by regulating genes involved in enhancing the UPR and ERAD, which promote protein folding to degrade terminally misfolded proteins. BisPMB also downregulated the genes that play a role in the import of proteins to the ER by down-regulating genes involved in the protein translocation pathways. In comparison, TG upregulated DEGs involved in the UPR, ERAD and the translocation pathway. Suggesting that bisPMB ad TG induces ER stress, however the ER stress mechanisms of these two compounds may not be identical.

Evidence for the significant deregulation of ER Stress and UPR pathways in the bisPMB and TG samples was provided by the canonical pathways generated with the ingenuity pathway analysis (IPA) software. Our results demonstrated that the ER Stress pathway was the most significantly enriched canonical pathway in the bisPMB sample, with 9.5 % down regulated and

23.8 % up regulated DEGs (figure 3.18). Comparatively, the ER Stress pathway was found to be one of the significantly enriched canonical pathways in the TG sample with 4.8 % down regulated and 38.1 % up regulated genes (figure 3.19). These findings demonstrate that activation of ER stress is one of the primary modes of action for bisPMB in WHCO1 cells and only one of the pathways activated in the TG sample..

Generally, bisPMB and TG DEGs shared the majority of the Kyoto encyclopaedia of genes and genomes (KEGG) pathways. TG elicited a stronger response compared to bisPMB in WHCO1 cells as more genes were deregulated by TG in each KEGG pathway. On the other hand, the ER stress and UPR pathway was more important than other pathways in the bisPMB sample as evidenced by the GO biological processes and IPA results. Furthermore, both bisPMB and TG samples displayed high number of DEGs in the "protein processing in the ER" KEGG pathway compared to the other pathways. This demonstrated that bisPMB and TG elicited similar responses in cancer cells.

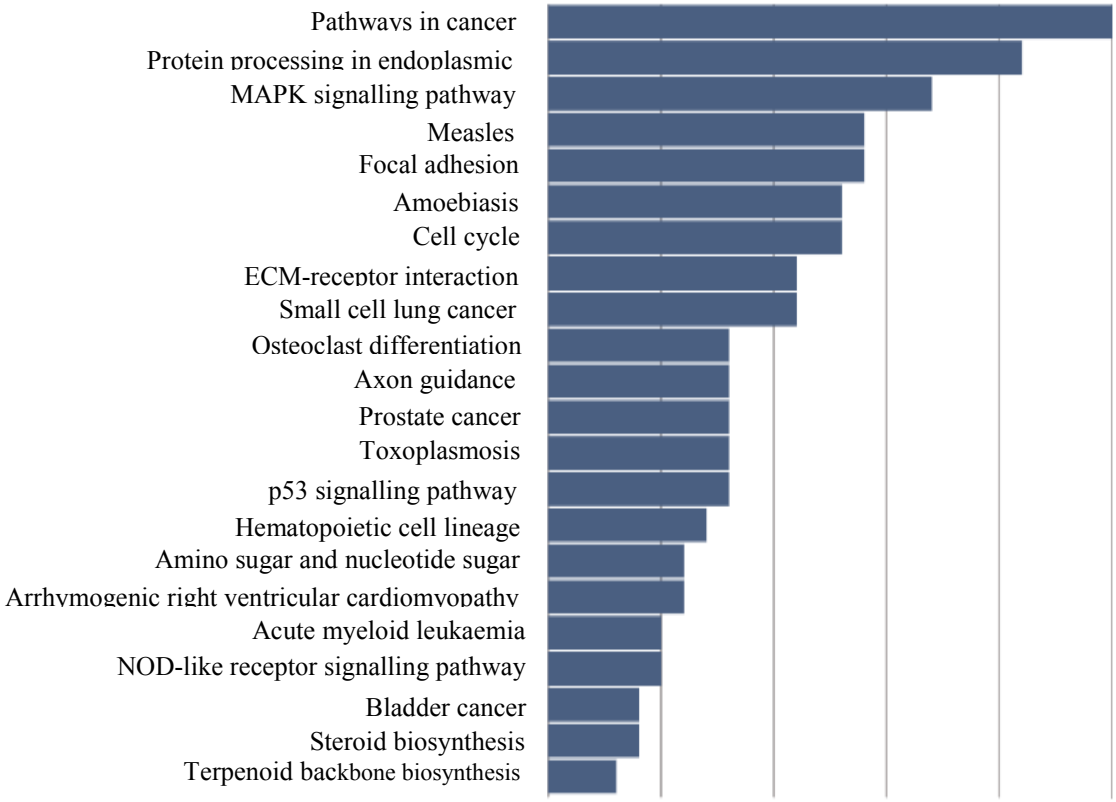

Figure 3.15 KEGG Pathways enriched with bisPMB DEGs. Bar chart indicating the number of DEGs represented in each pathway category. The names of the pathways are indicated on the y-axis and the number of DEGs present in each pathway is on the x-axis.

is on the x-axis.

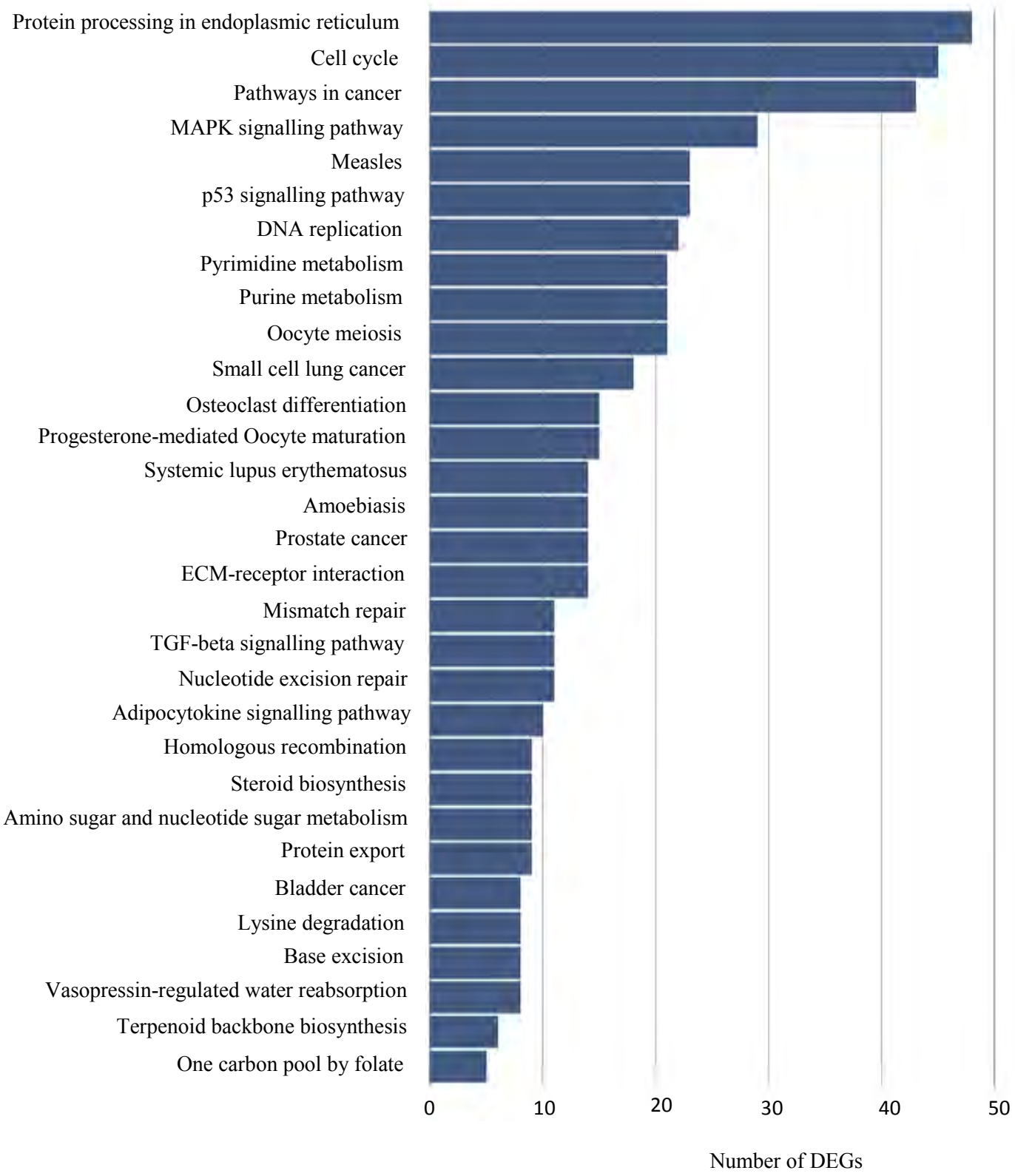

Figure 3.16 KEGG Pathways enriched with TG DEGs. Bar chart indicating the number of DEGs represented in each pathway category. The names of the pathways are indicated on the y-axis and the number of DEGs present in each pathway is on the x-axis.

A

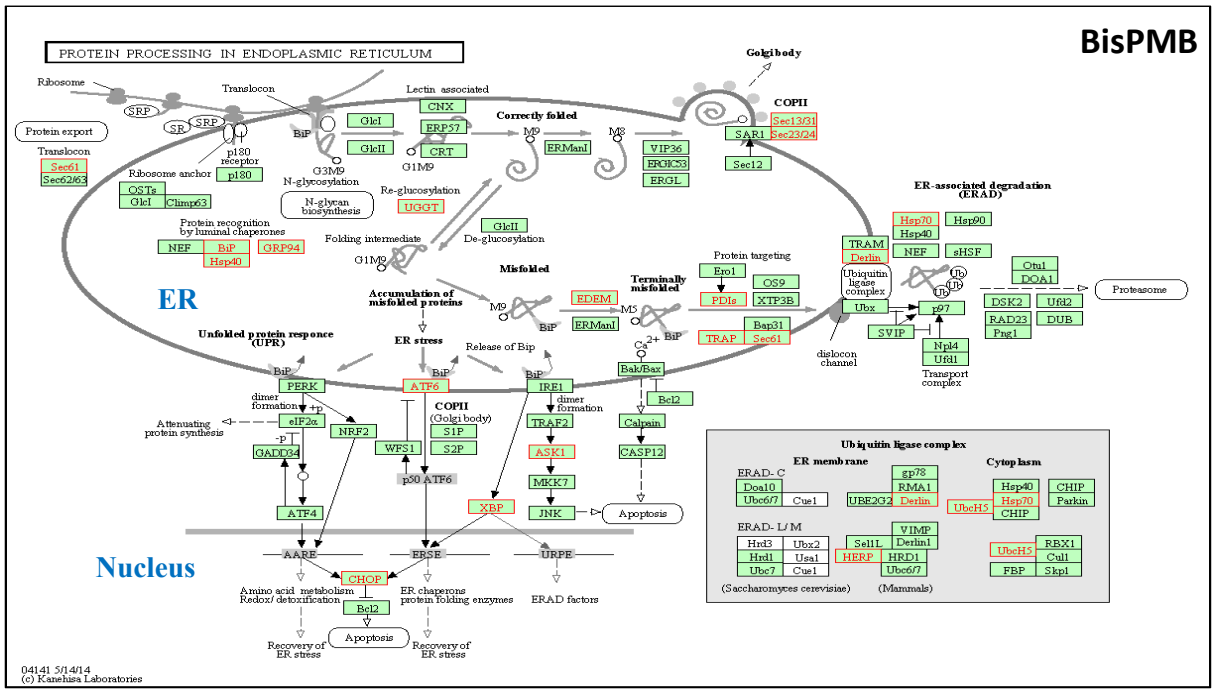

B

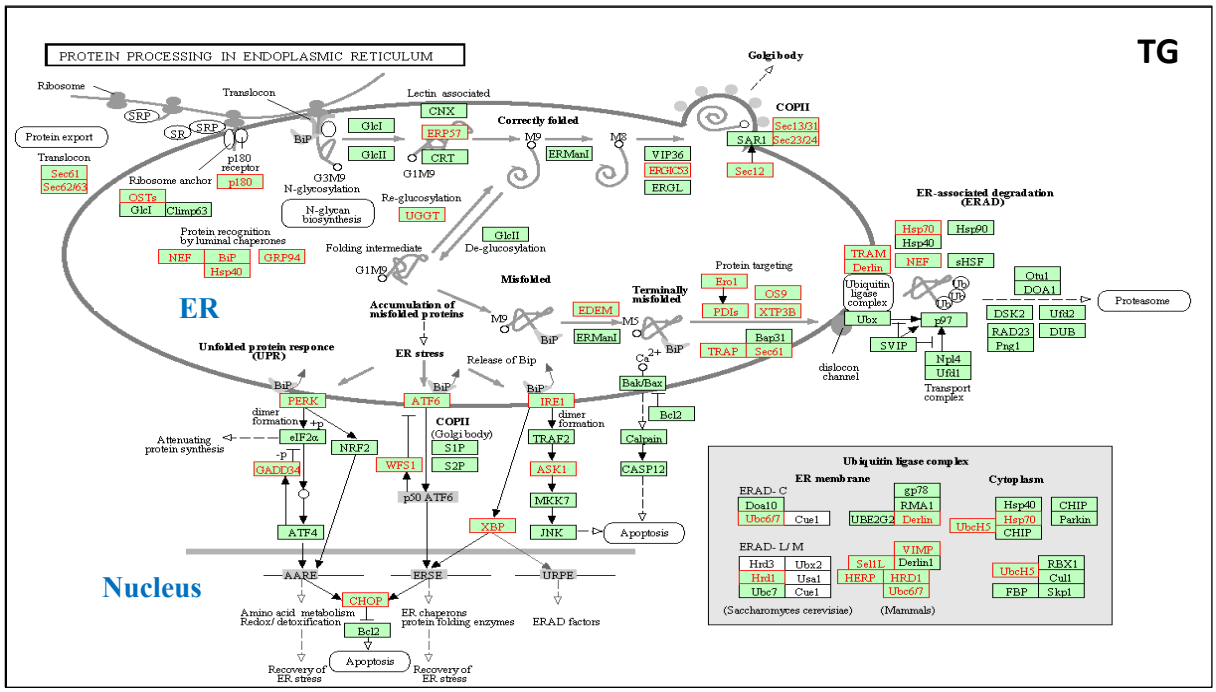

Figure 3.17 KEGG pathway map showing the significantly enriched protein processing in endoplasmic reticulum pathway. The WebGestalt program was used to generate the significantly enriched KEGG pathways from a list of imported DEGs. The KEGG pathway map is composed of green rectangular boxes which represent gene products such as protein or RNA. The names of the gene products are written in black and the DEGs found in the (**A**) bisPMB sample and (**B**) TG samples are highlighted in red in the protein processing in the endoplasmic reticulum pathway map.

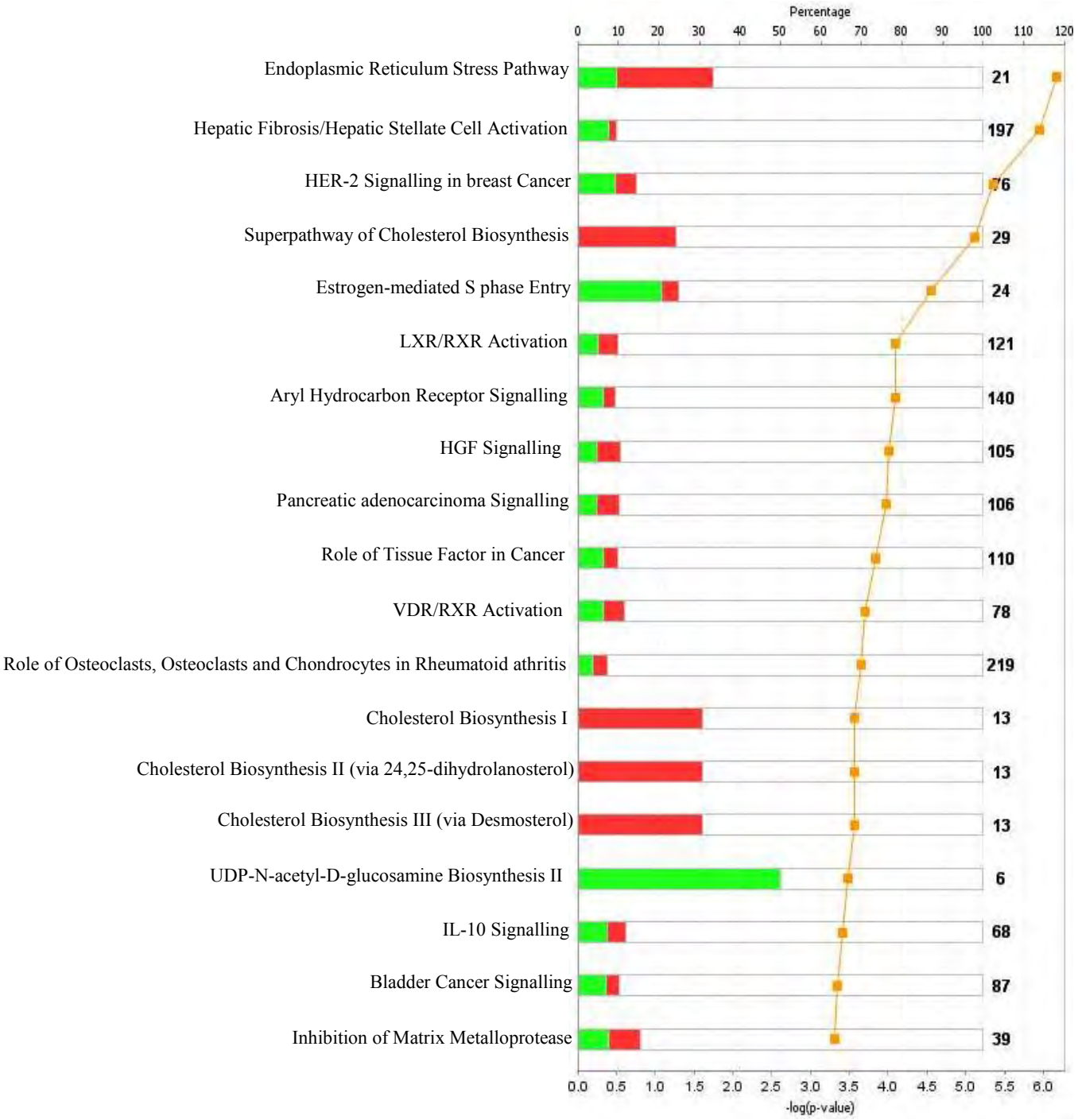

Figure 3.18 significantly deregulated canonical pathways in WHCO1 cells treated with BisPMB. The names of the deregulated pathways are written on the y-axis, each bar corresponds to each pathway. The coloured sections of each bar represent genes that overlap with the genes in each pathway, while the clear sections represent lack of overlap. The green bars show genes that are down regulated, while the red indicated up regulation. The numbers indicated at the top of each bar represent the total number of genes that are found in that particular pathway. The top x-axis indicates the percentage of genes in a data set that overlap with genes in a pathway, while the bottom x-axis represents the significance of the pathway as calculated with the Fischer's test and shown in –log (p-value). The yellow line illustrates the significance of each pathway. The bar graphs represent the canonical pathways generated from the bisPMB sample.

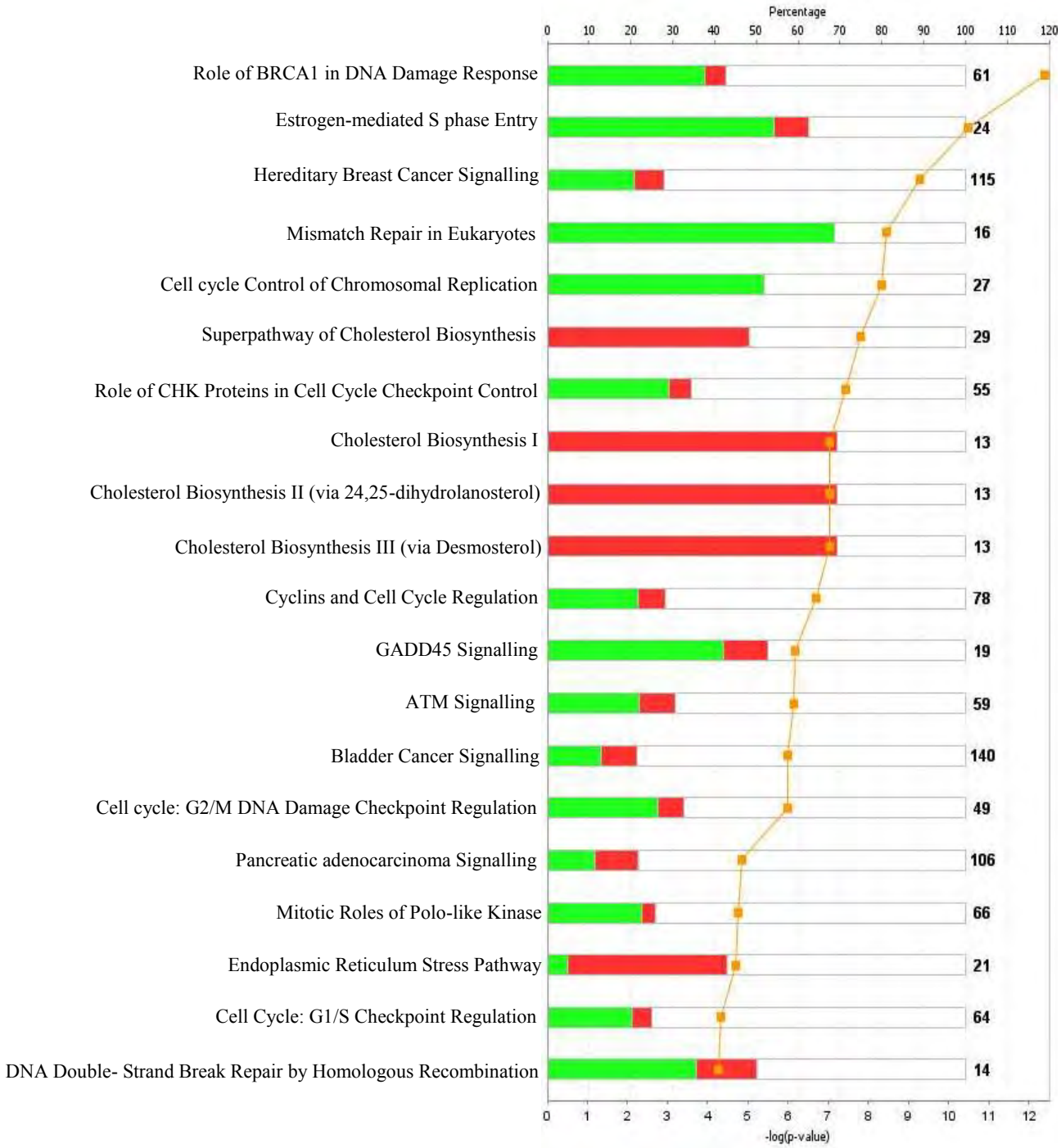

Figure 3.19 Significantly deregulated canonical pathways in WHCO1 cells treated with 1µM TG. The names of the deregulated pathways are written on the y-axis, each bar corresponds to each pathway. The coloured sections of each bar represent genes that overlap with the genes in each pathway, while the clear sections represent lack of overlap. The green bars show genes that are down regulated, while the red indicated up regulation. The numbers indicated at the top of each bar represents the total number of genes that are found in that particular pathway. The top x-axis indicates the percentage of genes in data set that overlap with genes in pathway, while the bottom x-axis represents the significance of the pathway as calculated with the Fischer's test and shown in –log (p-value). The yellow line illustrates the significance of each pathway. The bar graphs represent the canonical pathways generated from the TG sample.

3.2.3.3 Network Analysis

The gene network making up the ER stress pathway was generated using IPA, a web-based software that organizes gene expression data into pathways and networks using the IPA knowledge base (IPKB) for reference. The genes in the ER stress network include the ER transmembrane proteins IRE-1, PERK and ATF6, which are transducers of the UPR signalling pathway. We observed an upregulation of ATF6 while no change was observed in the transcription of IRE1 and PERK in the bisPMB sample (figure 3.20). Additionally, we observed an up regulation of molecular chaperones GRP78/BIP and GRP94; transcription factors CHOP and XBP1 and a down regulation of ASK and the PERK inhibitor p58i (figure 3.20).

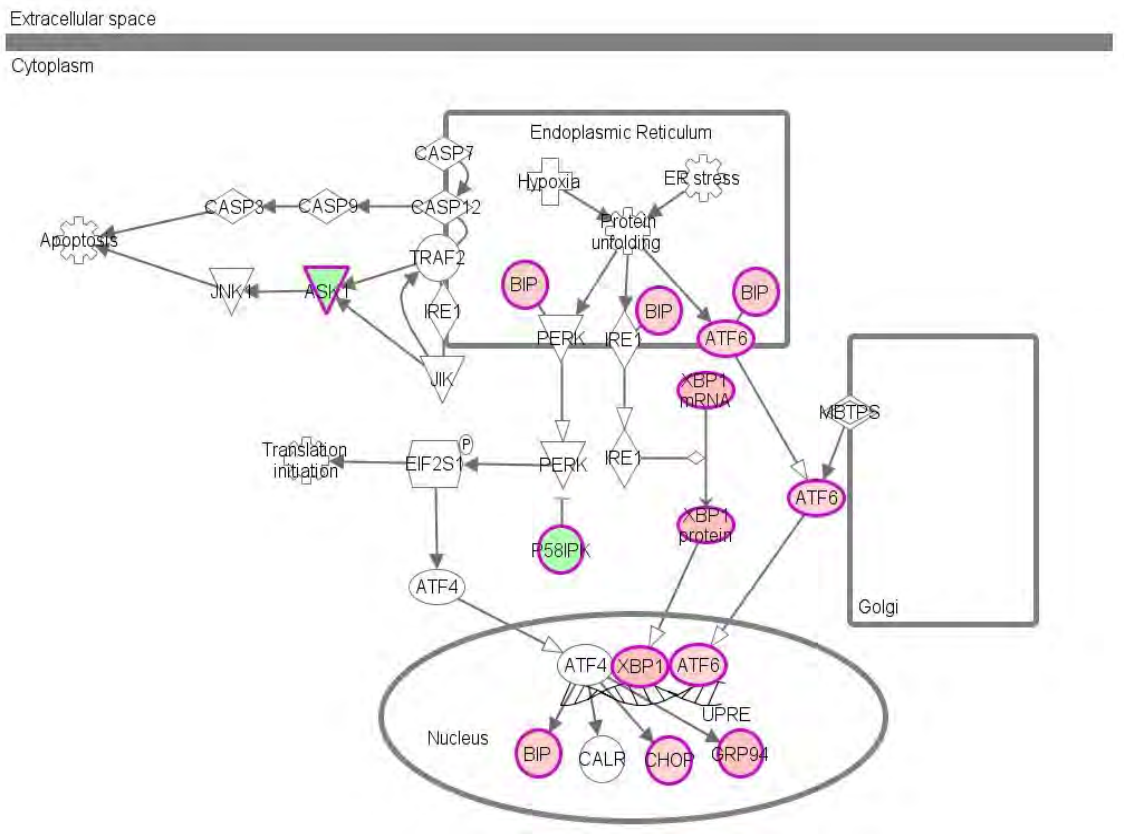

Figure 3.20 The gene network involved in the ER Stress pathway. The DEGs obtained from the bisPMB sample are highlighted in either green or red. Green indicates down regulated genes, while the red indicate the up regulated genes. The intensity of the red or green demonstrates the magnitude of the fold change. The cellular compartments are labelled inside the shape demarcating them.

Comparatively, all TG DEGs involved in the ER stress pathway network were found to be upregulated except for ASK1 (figure 3.21). Specifically, the transcription of IRE-1, ATF6 and PERK were upregulated in the TG sample, implying that all transmembrane proteins were

involved in TG ER stress/UPR pathways. Together, these results suggest that bisPMB may induce ER stress in WHCO1 cells, leading to subsequent increase in the transcription of the ATF6 gene. The subtle changes observed in the bisPMB sample can be attributed to the sub-toxic concentration used in these experiments. On the other hand, TG enhanced the transcription of all UPR target genes, which included IRE-1, ATF6 and PERK ER transmembrane proteins.

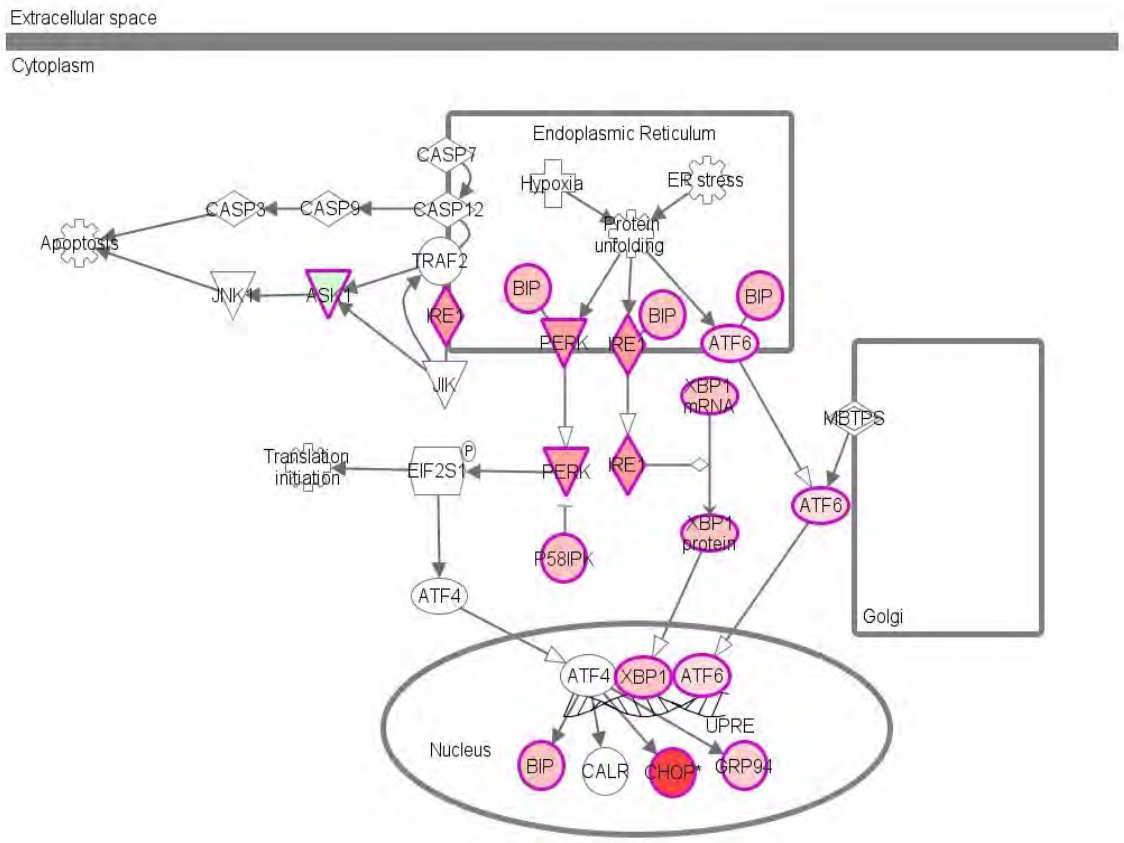

Figure 3.21 The gene network involved in the ER Stress pathway. The DEGs obtained from the TG sample are highlighted in either green or red. Green indicates down regulated genes, while the red indicate the up regulated genes. The intensity of the red or green indicates the magnitude of the fold change. The cellular compartments are labelled inside the shape demarcating them.

In order to identify genes that are functionally and physically related and underlie the observed pathways in the bisPMB and TG samples, relevant molecular gene networks were generated in IPA. IPA networks are named according to the molecular function categories that they mediate. Additionally, IPA ranks networks according to the number of DEGs it contains and the number of connections arising between the genes in each network. We observed that the most highly ranked molecular network in the bisPMB sample was named "Cellular Compromise, Cellular Function and Maintenance, Cellular Assembly and Organization" and was composed of 34

DEGs containing ER Stress DEGs ATF6, XBP1 and BiP (grp78 or HSPA5) (figure 3.22**A**). In addition, the DEG with the highest number of connections to other genes in this network was XBP-1 (figure 3.22**A**). This suggests that XBP-1 may be the most biologically relevant gene in this network, as it influenced the highest number of genes that are involved in various other cellular functions through its connections. The genes that were connected to XBP-1 included STARD5, GLGA4, SEC24D, FKBP14, EDEM2, EDEM1, PDIA4, HSP90B1, AFT6, SEC61A1, SRPRB, COPE, SSR3, SEC31A and HSPA5/GRP78/BIP. In the TG sample, the most highly ranked molecular gene network was composed of 35 DEGs and named the "cell cycle, cellular assembly and organization, DNA replication, Recombination and Repair". However, the DEG with the most connections to other genes, thus the most biologically relevant gene in the TG sample was the small ubiquitin –like modifier (SUMO2) gene (figure 3.23).

The IPA findings are consistent with the GO, KEGG and IPA results which suggest that bisPMB primarily triggers the ER stress/UPR pathway. In addition, the molecular gene network implies that the XBP-1 gene is central to regulating most of these intracellular functions by regulating the expression of the highest number of DEGs. Whereas the pathways important in TG treated WHCO1 cells are implicated the cell cycle and DNA damage.

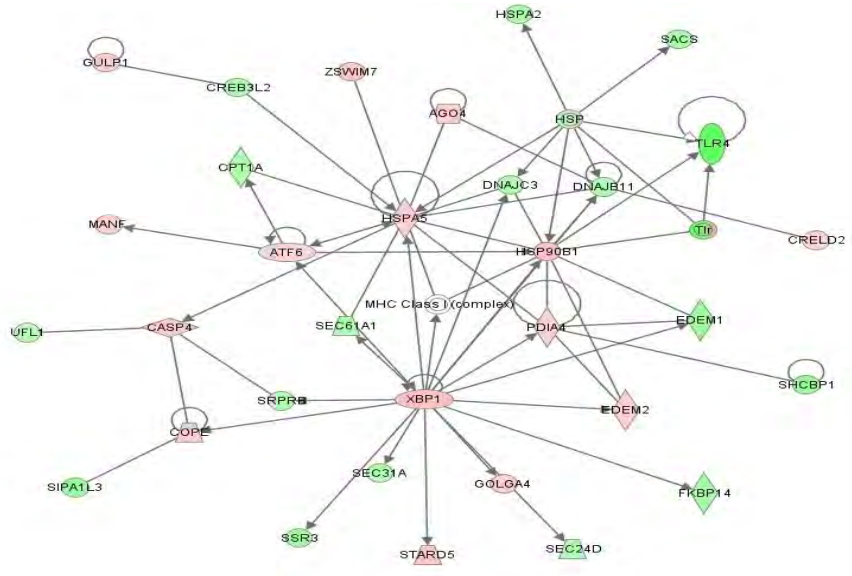

Figure 3.22 Cellular Compromise, Cellular Function and Maintenance, Cellular Assembly and Organization molecular gene network and functional categories for bisPMB. The highest ranked gene network containing bisPMB DEGs. Green indicates down-regulated genes and red are up-regulated. The lines connecting the genes indicate the biological relationship between the genes.

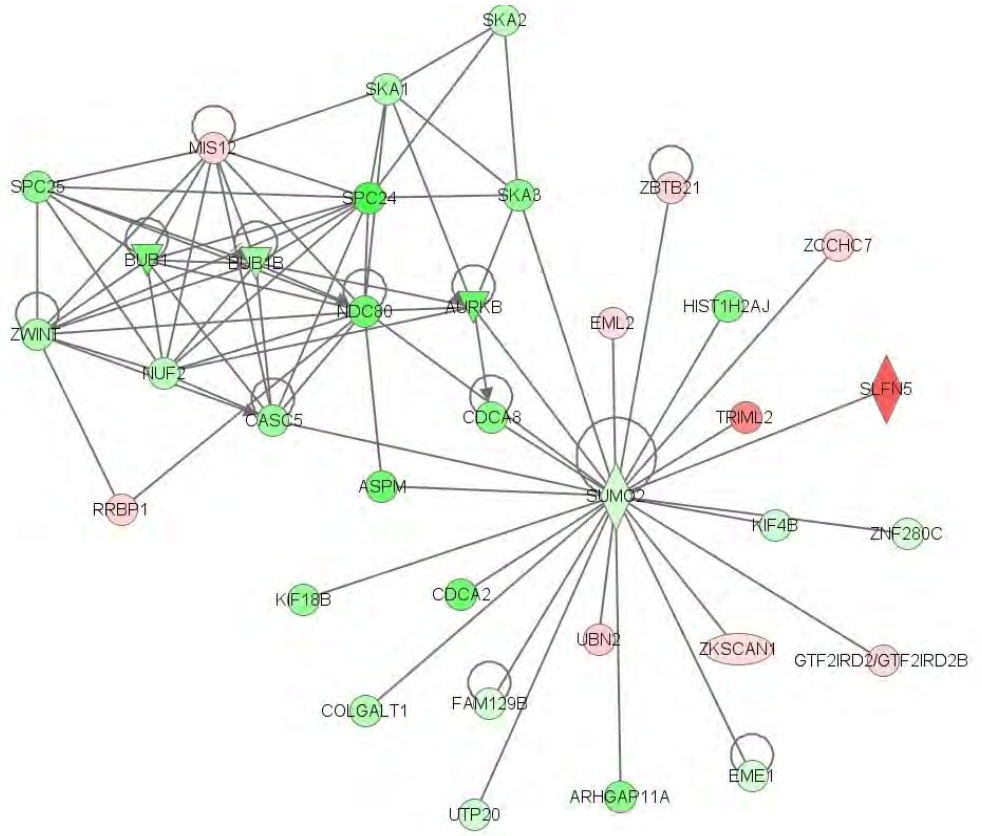

Figure 3.23 Cell cycle, cellular assembly and organization, DNA replication, Recombination and Repair. Molecular gene network containing TG DEGs. Gene highlighted in red are up-regulated and highlighted in green are down-regulated. The lines connecting the genes indicate biological relationship between the genes.

3.3 DISCUSSION

To gain insights into the genes deregulated in WHCO1 cells in response to bisPMB treatment, we investigated the change in gene transcription at a sub-toxic concentration of bisPMB. Based on the observation that ajoene targets and accumulates in the ER in MDA-MB-231 cells and induces GRP78/BIP expression (Kaschula et al., 2015); we hypothesized that the ajoene analogue bisPMB may induce ER stress in WHCO1 cells. To tests this hypothesis, we compared the gene transcriptional response of bisPMB to that of TG, a known ER stress inducer (Treiman et al., 1998d).

Gene transcriptional deregulation was assessed using cDNA microarray analysis, which revealed 488 and 6359 differentially expressed genes (DEGs) in WHCO1 cells treated with bisPMB and TG respectively at the 1.5 cut off. The higher number of DEGs observed in the TG

sample may be attributed to the cytotoxic concentration of TG used in this study compared to that chosen for bisPMB. The toxicity of the 1μM TG concentration was exemplified by its ability to induce apoptosis in WHCO1 cells by two fold. On the other hand, the low number of DEGs observed in the bisPMB sample is consistent with that reported for 10 μM ajoene in human leukaemia HL60 cells, in which only 28 genes were found to be differentially expressed from a cDNA microarray chip containing 2400 genes (Fang et al., 2002). The 10 μM ajoene concentration does not induce apoptosis in HL60 cells (Dirsch et al., 2002). Thus the number of DEGs observed could be attributed to the toxicity of the concentration used for bisPMB versus TG.

The microarray gene expression data obtained in this study was validated by q-RT PCR. For the validation, we used the same RNA sample that was submitted for microarray analysis and also performed q-RT PCR on independent samples 23 genes were chosen for validation that were found to be deregulated in both the bisPMB and the TG samples. The genes were selected because they formed part of the protein processing in the ER pathway. We observed consistency between cDNA microarray analysis and q-RT PCR in 19 of the 23 selected DEGs in the bisPMB sample. Comparably, none of the selected DEGs in the TG sample demonstrated inconsistencies between cDNA microarray analysis and q-RT PCR results. Discrepancies observed in the 4 selected DEGs in the bisPMB sample, (Ub6, DDOST, GRP94 and CASP4), may be accredited to factors including different normalisation methods between the two techniques (RMA method for microarray and GAPDH for q-RT PCR) and the low fold change (< 2 fold) observed in the microarray genes (Morey et al., 2006). For example, the cut off fold change in this study was set at 1.5 fold and the majority of the deregulated genes in the bisPMB sample displayed less than 2 fold change in gene expression. In contrast, the gene expression changes in the TG sample were all greater than two. Consequently, there was a greater reproducibility in the TG sample compared to the bisPMB sample. Nonetheless, the majority of the DEGs in both bisPMB and TG samples were reproducible, rendering the microarray data suitable for downstream analysis.

Gene expression data was then biologically interpreted using the functional enrichment analysis of Gene ontology (GO). Similarities were observed between bisPMB and TG, in which the biological process categories with the largest number of DEGs included metabolic processes, biological regulation and response to stimuli. These biological processes encompass DEGs such as CYP1A1 (cytochrome p450 family 1 subfamily A polypeptide 1), CDH13 (cadherin 13), MMP13 (matrix metallopeptidase), AXL (AXL receptor tyrosine kinase), XBP-1 (X box

binding protein 1) and IL8 (interleukin 8). These genes are involved in a range of well documented cellular functions such as inflammation, xenobiotic and drug metabolism, collagen degradation and the unfolded protein response. In addition, this observation is consistent with reports on ajoene induced anti-inflammatory properties (Schafer and Kaschula, 2014) and DAS altering the activity of cytochrome P450 enzymes in hepatic microsomes (Brady et al., 1988).

The most specific and significantly enriched GO biological process in the bisPMB sample was termed “activation of signalling protein activity involved in unfolded protein response”. The unfolded protein response (UPR) is a cytoprotective response triggered by ER stress as a result of an increase in misfolded proteins in the ER (Herr and Debatin, 2001, Hosoi et al., 2010, Hosoi and Ozawa, 2010). Data from our lab has illustrated that *Z*-ajoene enhances the expression of GRP78/BIP and promotes misfolded proteins and protein aggregation, in MDA-MB-231 breast cancer cells (Kaschula et al., 2015).These reports were consistent with our GO findings which suggest that the most significantly enriched cellular component in the bisPMB sample was the ER membrane and the ER lumen, a cellular location for UPR. For instance, the UPR involves the activation of three ER transmembrane proteins namely; PRK-like endoplasmic reticulum kinase (PERK), Inositol requiring enzyme 1/ ERN 1(IRE1) and activating transcription factor 6 (ATF6) (Schroder et al., 2005). The IRE1 and ATF6 pathways activate the transcription of genes that aid in protein folding such as chaperones and foldases (Han et al., 2009, Ye et al., 2000) which include GRP78/BIP and PDI and are located in the lumen of the ER (Wang and Tsou, 1993, Griesemer et al., 2014). Our findings and literature reports support bisPMB primarily triggering the UPR in WHCO1 cells,

In comparison, the most significantly enriched biological process in the TG sample was mitosis and DNA metabolic process with the most significantly enriched cellular components being located in the cytoplasm, intracellular organelle and intracellular membrane bound organelle. Although TG is an ER stress inducer, the TG concentration used in this study promoted the induction of apoptosis, which may account for the TG DEGs being involved in functions promoting cell death and affecting the cell cycle. TG is toxic to cancer cells at micromolar concentrations (Treiman et al., 1998a). GO analysis found that bisPMB primarily targets UPR activation in WHCO1 cells, while TG targets the cell cycle at the selected concentrations. In order to gain a better understanding of the molecular events underlying these broad cellular processes, pathway analysis was performed.

The KEGG pathway illustrated that pathways in cancer, protein processing in the ER and the mitogen activated protein kinase (MAPK) pathway were the most significantly enriched pathways in both bisPMB and TG samples. The deregulation of pathways in cancer in both samples was expected as this study was conducted in a cancer cell line. Moreover, bisPMB, ajoene and TG have been previously reported to have cytotoxic effects against various cancer cell lines (Dirsch et al., 2002, Kaschula et al., 2012, Dubois et al., 2013). In addition, the bisPMB and TG DEGs represented in the pathways in the cancer category included cyclin D1, cyclin E, and p27/KIP, which are all key players in cell cycle regulation. ER stress has been shown to inhibit cell cycle progression through the induction of p27 expression (Han et al., 2013). Therefore both bisPMB and TG may regulate pathways involved in cancer progression and cancer cell death.

The protein processing in the ER pathway was also deregulated in both bisPMB and TG treated WHCO1 cells. The similarities in WHCO1 cell response to bisPMB and TG in this pathway category was the upregulation of UPR and ERAD pathways. While the main difference was the deregulation of the DEGs in protein translocation pathway (Sec63, TRAM, Sec24D and SSR3/TRAP) that were upregulated in the TG sample and downregulated in the bisPMB sample. This finding was in line with the IPA analysis data that identified the ER stress pathway as the most significantly enriched canonical pathway in the bisPMB sample and one of the significantly enriched pathways in the TG sample. These observations implied that bisPMB may activate ER stress in WHCO1 cells. In agreement with these observations, ER stress has been suggested to play a role in the anti-apoptotic activity of the garlic OSCs DADS (Yang et al., 2009) and DATS (Wang et al., 2012) against human colon cancer and basal cell carcinoma cell lines.

In order to identify the DEGs that are biologically related to other genes within the ER stress pathway in both bisPMB and TG samples, we generated molecular gene networks using the IPA. The ER stress pathway gene network revealed that the PERK pathway may not be transcriptionally deregulated by bisPMB. Interestingly, p58i was down regulated in the bisPMB sample but up regulated in the TG sample. P58i is an ER resident HSP40 chaperone family member and an inhibitor of PERK (Lee et al., 1994, Polyak et al., 1996, Yan et al., 2002, Rutkowski et al., 2007). This suggests that PERK may not involved in UPR activation initiated by bisPMB but may be involved in TG treated WHCO1 cells although the microarray data is only a guide to generate an hypothesis and the response in bisPMB sample was low. Moreover, PERK pathway activation in the TG sample may in turn be regulated by p58i in WHCO1 cells.

We also observed no change in IRE-1 transcription but an increase in XBP-1 transcription in the bisPMB sample. The XBP1 mRNA is activated through splicing orchestrated by IRE1 endonuclease activity (Iwawaki and Akai, 2006, Koong et al., 2006, Han et al., 2009). Comparatively, TG displayed an upregulation of both IRE-1 and XBP-1. Furthermore, the transcriptional increase in XBP-1 indicates a possible mechanism to compensate for the un-spliced XBP-1 mRNA pool. An increase in XBP-1 activity has been associated with cancer cell proliferation and progression; moreover the inhibition of XBP-1 has led to the sensitization of multiple myeloma cells to ER Stress induced apoptosis (Koong et al., 2006, Chen et al., 2014). The data presented here suggests that bisPMB and TG increased XBP-1 transcription in WHCO1 cells.

We observed an increase in ATF6 transcription in the bisPMB sample. When ER stress is induced, the ATF6 transmembrane protein translocates to the Golgi apparatus and is cleaved by site 1 and 2 protease (sp1 and sp2). This generates the 50 kDa transcription factor, which regulates transcription of the ER resident chaperones and forms heterodimers with XBP-1 to regulate transcription of the ER associated degradation (ERAD) system (Yamamoto et al., 2007). ATF6α has been implicated in the pathogenesis of hepatocellular carcinomas (Arai et al., 2006). However, an anticancer agent desiprimine was found to activate ATF6 in C6 glioma cells (Ma et al., 2013). IRE1 is upstream of ATF6 activation during ER stress (Wang et al., 2000). The increase in ATF6 transcription during ER stress has been attributed to a possible positive feedback loop aimed at replenishing the ATF6 transmembrane protein (Koong et al., 2006). Therefore, the increase in ATF6 transcription in the bisPMB sample may be attributed to the activation of ATF6 and IRE1UPR pathway.

In addition to the PERK, IRE-1 and ATF6 UPR pathways, ER stress also activates another cytoprotective mechanism called endoplasmic reticulum associated degradation (ERAD). ERAD involves the removal of terminally misfolded proteins through degradation via the ubiquitin – proteasome system (Stolz and Wolf, 2010). Aberrations in protein ubiquitination have been associated with various types of cancer, such as the ubiquitin proteasome system (Grande et al., 2012, (Xu and Jaffrey, 2013). Furthermore, ubiquitin-proteasome degradation has been identified as a potential target for cancer treatment and prevention (Chen et al., 2010). We observed a deregulation of DEG's involved in the ERAD pathway including Ubc6 and EDEM in the bisPMB sample. This suggests that the ubiquitin-proteasome degradation system may be a possible target for bisPMB. Consistently, the Ub6 and EDEM also formed part of DEGs from the TG sample. Thus, ERAD may be triggered by both bisPMB and TG in WHCO1 cells.

Another pathway that we had observed to be enriched in the bisPMB and TG sample was the MAPK pathways. The MAPK includes p38, JNK and MEK/ERK. The p38 and JNK/MAPK pathways are associated with cellular stress and the induction of apoptosis, while MEK/ERK is associated with cell survival (Chang and Karin, 2001). The enrichment of these pathways may be caused by WHCO1 cancer cell stress response to bisPMB or TG. It is well known that cross-talk exists between the MAPK and ER stress pathways. JNK is activated in response to ER stress through the IRE1 transmembrane protein (Urano et al., 2000). Furthermore, the ATF6 UPR transmembrane protein is a p38 target for phosphorylation. For example, the p38 MAPK enhances the trans - activation activity of the ATF6 transcription factor (Thuerauf et al., 1998, Luo and Lee, 2002). Together, this implies that WHCO1 cells may respond to bisPMB and TG treatment by activating stress-associated pathways involving crosstalk between MAPK and ER stress pathways.

In addition to the ER stress and MAPK pathways, the cholesterol biosynthesis canonical pathways including the superpathway of cholesterol biosynthesis, cholesterol biosynthesis I, cholesterol biosynthesis II (via 24, 25- dihydrolanosterol) and cholesterol biosynthesis III (via Desmosterol) are upregulated in both the bisPMB and TG sample. Garlic derived compounds ajoene and allicin have been implicated in cholesterol biosynthesis. Ajoene has been reported to inhibit cholesterol synthesis in a liver homogenate (Sendl et al., 1992). Ajoene and allicin inhibited cholesterol biosynthesis in a concentration dependent manner at the stage of HMG-CoA-reductase and at a later stage of lanosterol 14 alpha-demethylase in HepG2 cells and rat hepatocytes (Gebhardt et al., 1994). Ajoene was also shown to inhibit cholesterol biosynthesis by affecting the 3-hydroxy-3-methyl-glutaryl coenzyme A (HMG-CoA) reductase and late enzymatic steps of the mevalonate (MVA) pathway (Ferri et al., 2003). It is likely that bisPMB inhibits cholesterol biosynthesis like ajoene. Thus the elevation in gene transcription of the genes involved in cholesterol biosynthesis canonical pathway in the bisPMB sample can be attributed to a negative feedback mechanism.

In order to demonstrate how DEGs relate with genes from different pathways, global molecular gene networks were generated with IPA. Genes have been suggested to interact physically or functionally as a network in order regulate molecular functions. The IPA ranks gene molecular networks according to the total number of genes in the network and the number of interactions between the genes forming part of the network. In addition, the IPA scores the gene networks

according to the number of DEGs included in the network with the most highly interconnected genes in high ranking networks affecting more cells functions called network hubs (Ravasz et al., 2002, Spirin and Mirny, 2003, Grigoryev et al., 2011). In this study, the most highly ranked and thus top scoring network in the bisPMB sample was the "cellular compromise, function and maintenance and cellular assembly and organization" network. The most interconnected DEG in this network was found to be XBP1. The genes that are interconnected with XBP1 are all involved in the protein processing pathway and are reported to be downstream targets of XBP-1 transcriptional activity. Thus, the direct interaction of the genes with XBP-1 is based on XBP-1 transcriptional activity. XBP1 regulates the transcription of Grp78 (HSPA5), PDI, EDEM1, EDEM2, Grp94 (HSP90B1) and DNAJC3 (p58i), which are involved in protein folding and degradation (Lee et al., 2003a, Koong et al., 2006, Yamamoto et al., 2007). Furthermore, XBP-1 also regulates the transcription of GOLGA4, SEC24D, FKBP14, SEC61A1, SRPRB, COPE and SSR3 in NIH-3T3 fibroblast cell line (Sriburi et al., 2007). These genes are involved in protein translocation into the ER and trafficking to the Golgi apparatus. On the other hand, ATF6 regulates the transcription of XBP-1 (Yoshida et al., 2001a, Sriburi et al., 2007) which suggests that XBP-1 plays a significant role in the WHCO1 cell response to bisPMB. Thus the early response of WHCO1 cells to sub-toxic concentrations of bisPMB may be primarily governed by XBP-1 transcription during UPR activation.

In comparison, the most highly ranked molecular network in the TG sample was called the "cell cycle, cellular assembly and organization, DNA replication, Recombination and Repair". The most interconnected gene within this network was found to be the small ubiquitin like modifier 2 (SUMO2), which binds to other proteins in order to post translationally modify them for DNA repair, mitosis and signal transduction (Schou et al., 2014, Gonzalez-Prieto et al., 2015). This finding is in line with the GO biological process reports in which TG was found to significantly enrich mitosis and DNA metabolic process, deregulate cell cycle KEGG pathway and deregulate the IPA canonical pathway "role of BRCA1 in DNA mediated response". The activation of this pathway has been reported to implicate DNA damage induced cell cycle checkpoint (Wu et al., 2010). Thus at the selected concentration, TG essentially regulates DNA damage and cell cycle functions in WHCO1 cells.

Here, we have demonstrated that bisPMB primarily deregulated genes involved in UPR signalling. Compared to other canonical pathways, the ER stress pathway was found to be the most significantly enriched pathway in both bisPMB and TG samples. Moreover, the molecular gene networks revealed that XBP-1 drove the molecular response in the bisPMB sample.

However, the SUMO2 gene regulated the response in the TG sample. Although TG also deregulated the ER stress pathway, as expected, it primarily mediated DNA damage and cell cycle pathways. This may be due to the cytotoxic concentration used. In hindsight, a nanomolar concentration of TG may have presented a better positive control to compare to a 3.5 μM concentration of bisPMB. In order to confirm the induction of ER stress/UPR and MAPK in bisPMB-treated WHCO1 cells, proteins and ER stress genes representing the UPR arms and MAPK were selected for further analysis.

CHAPTER 4: Role of UPR and MAPK signalling pathways in the cytotoxicity of bisPMB in WHCO1 cells

3.1 INTRODUCTION

The unfolded protein response (UPR) is made up of pro-survival intracellular pathways which are activated in response to ER stress. The role of UPR activation is to enable the cell to restore ER homeostasis (Schroder and Kaufman, 2005, Hetz, 2012). However, if ER stress persists, and homeostasis is not restored, the UPR pathways trigger apoptosis (Szegezdi et al., 2006). Emerging reports have illustrated that garlic OSC induce ER stress in cancer cells. Our lab has found that ajoene targets and accumulates in the ER of cancer cells where it *S*-thiolate numerous proteins to interfere with protein folding, resulting in an accumulation of misfolded protein aggregates. In support of this, ajoene was further found to increases levels of ubiquitinated proteins and to elevate GRP78/BIP expression levels in MDA-MB-231 breast cancer cells (Kaschula et al., 2015), supporting UPR induction. Furthermore, ER stress markers have been implicated in garlic OSC induced apoptosis. DADS and DATS triggered ER stress associated apoptosis in human basal cell carcinoma BCC and colon cancer COLO 205 cells respectively (Yang et al., 2009, Wang et al., 2012). Therefore ER stress and UPR activation may play an important role in garlic OSC cytotoxic activity.

Emerging evidence has demonstrated that UPR induced apoptosis is linked to MAPK signalling (Szegezdi et al., 2006, Darling and Cook, 2014). The most studied members of the MAPK pathway include the JNK1/2, MEK/ERK and p38. The JNK1/2 and p38 MAPK proteins belong to the stress activated protein kinase (SAPK) family of proteins which are activated by stress stimuli such as chemotherapeutic drugs and are associated with apoptosis (Raingeaud et al., 1995, Davis, 2000, Mhaidat et al., 2007). In contrast, the MEK/ERK pathway is a pro-survival pathway which has been implicated in apoptosis suppression (Erhardt et al., 1999). The garlic OSCs are reported to enhance the activation of MAPK *in vitro*. For example DADS, DATS and ajoene have been shown to activate the JNK, p38 and MEK/ERK signalling pathways in various cancer cell lines (Antlsperger et al., 2003, Xiao et al., 2004, Yang et al., 2006b, Shin et al., 2012, Shin et al., 2014).

Chapter 3 of this thesis showed that bisPMB, an ajoene analogue, primarily elicited transcriptional changes in genes that form part of the UPR pathway in the ER. In addition, bisPMB and TG, an ER stress inducer, significantly enriched protein processing in the ER and MAPK signalling

pathways. This suggests that the UPR and the MAPK signalling pathways may play a role in the cytotoxicity of bisPMB in WHCO1 cells. Thus, in this chapter, we investigated whether bisPMB induces activation of the UPR and MAPK signalling pathways by assessing changes in expression levels and certain posttranslational modifications of key proteins in these pathways. Furthermore inhibitors were used to further probe the importance of these pathways in the cytotoxic mechanism of action of bisPMB. TG, a well documented ER stress inducer, was used as a positive control in all experiments. For the experiments conducted in this chapter, we chose to use 7 μM bisPMB as it had been shown in chapter 1 to induce apoptosis.

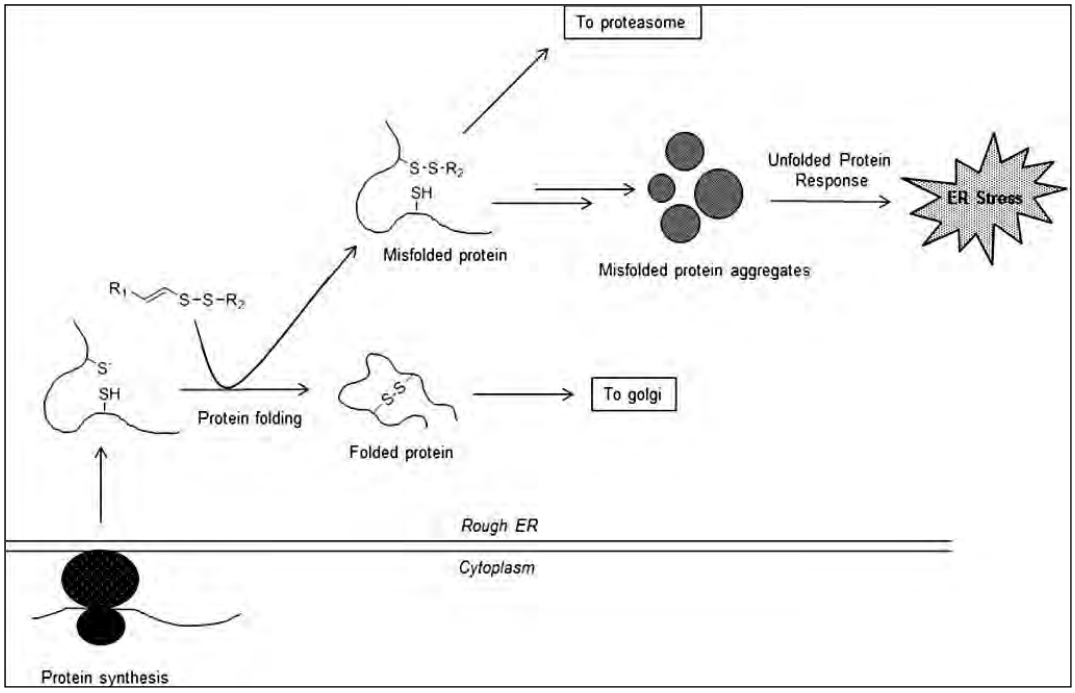

Figure 4.1 Schematic representation of the mechanism of action of ajoene in cells. Upon, ajoene treatment, nascent proteins form mixed disulphide bonds with ajoene (in this case: bisPMB), leading to protein misfolding. The misfolded proteins are either degraded via the ubiquitin proteosome system or they trigger UPR and ER stress activation. On the other hand, properly folded proteins are directed to the Golgi apparatus to the extracellular space or plasma membrane (Kaschula et al., 2015).

3.2 RESULTS

3.2.1 Expression of GRP78/BIP in bisPMB treated WHCO1 cells

In response to an accumulation of misfolded proteins in the ER, cells activate the UPR which results in increased expression of foldases and molecular chaperones including GRP78/BIP.

In order to determine if bisPMB affects the expression of GRP78/BIP, western blot analysis was performed as described in section 6.9. The total expression of GRP78/BIP (72 kDa and 78 kDa) was found to increase 4 - 5 fold in WHCO1 cells treated with bisPMB at the 7 μM concentration from 1 h and this was sustained up to 24 h. TG (1 μM) was used as a positive control and was found to trigger an approximate 5-fold increase in GRP78/BIP expression (figure 4.2).

Interestingly, the majority of the GRP78/BIP in bisPMB-treated cells was in the 72 kDa form as opposed to TG which was in the 78 kDa form. The clear increase in total GRP78/BIP expression supports bisPMB inducing UPR in WHCO1 cells.

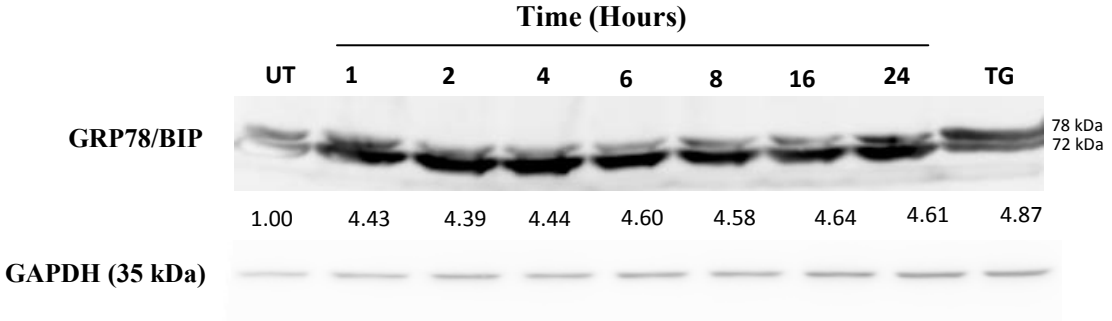

Figure 4.2 The induction of GRP78/BIP protein expression in bisPMB treated WHCO1 cells. Total cell lysate extracted from WHCO1 cells treated with 7 μM concentration of bisPMB for 1, 2, 4, 6, 8, 16 and 24 hours or 1μM TG for 24 hours, was analysed by western blot. The nitrocellulose membrane was subsequently probed with anti-GRP78 and anti-GAPDH antibodies. Relative quantities of total GRP78 (78 and 72 kDa) expression bands were normalised and quantified relative to GAPDH. This blot is representative of three independent experiments.

3.2.2 BisPMB increased protein ubiquitination in WHCO1 cells

One of the processes that occur in response to ER stress induced by an accumulation of misfolded proteins is ER associated degradation (ERAD). The ERAD attempts to recover ER homeostasis and reduce ER protein load, by eliminating misfolded proteins that can no longer be refolded (Oslowski and Urano, 2011). The ubiquitin proteasome system (UPS) forms an integral part of ERAD (Meusser et al., 2005), where misfolded proteins are ubiquitinated and targeted for degradation.

In order to ascertain whether bisPMB activates the UPR, the levels of ubiquitinated proteins in WHCO1 cells treated with bisPMB were detected using western blot analysis. There was no change in the level of protein ubiquitination between 2 - 4 hour post bisPMB treatments, compared to the untreated control. BisPMB treated WHCO1 cells were found to display an increase in ubiquitinated proteins between 6 - 24 hours compared to the untreated control, with maximal 5-fold between 8 and

16 hours (figure 4.3). No increase in the levels of Ub proteins were however observed in the 1 μM TG treated cells (figure 4.3). Although TG is an ER stress inducer, and thus expected to increase protein ubiquitination. The absence of change in protein ubiquitination in the TG sample can be attributed to the time point selected for TG treatment as ubiquitination appeared to be an early event for the bisPMB compound. All in all, these findings support bisPMB promoting ubiquitination of proteins in WHCO1 cells, which may suggest ERAD activation.

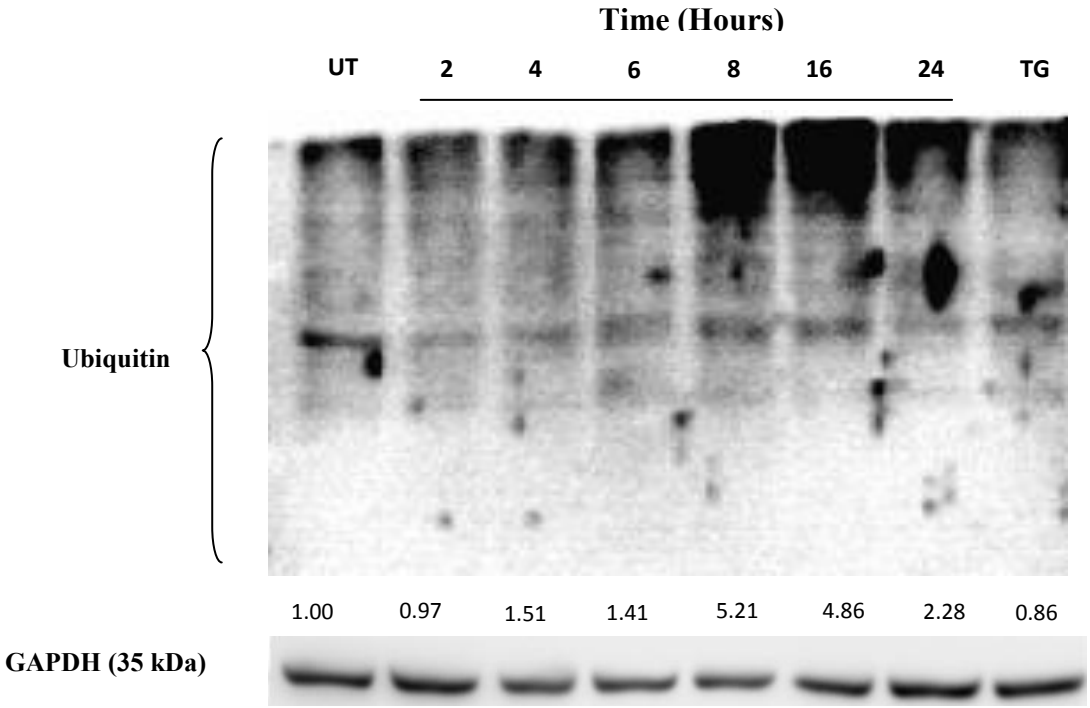

Figure 4.3 The induction of protein ubiquitination in bisPMB treated WHCO1 cells. Total cell lysate was collected from WHCO1 cells treated with bisPMB at the half 7 μM concentration for 2, 4, 6, 8, 16 and 24 hours or 1μM TG for 24 hours and analysed by western blot. The blot was probed with anti-ubiquitin and anti-GAPDH primary antibodies and quantitated relative to GAPDH. This blot is representative of three independent experiments.

Apart from increased GRP78/BIP expression and induction of ERAD, cells respond to the misfolded protein accumulation by activating the UPR. The UPR is activated through three transmembrane proteins PERK, IRE-1 and ATF6.

3.2.3 BisPMB increases ATF4 expression

The activation of the PERK/ATF4 UPR pathway leads to the phosphorylation and inactivation of eIF2α, which selectively enhances the translation of ATF4 (Lai et al., 2007). In order to examine

whether bisPMB activates the PERK/ATF4 pathway, the time-dependent expression of ATF4 in bisPMB treated WHCO1 cells was analysed and compared to TG. There is an initial decrease in ATF4 expression in WHCO1 cells after one hour of bisPMB treatment compared to the untreated. No changes were observed between 2 – 6 h compared to untreated control. BisPMB was found to trigger a time dependent increase in the expression of ATF4 in WHCO1 cells (figure 4.4). The increase in ATF4 protein levels was more pronounced in the later time points from 8 - 24 hours with maximal expression at 24 h, and in the 1 μM TG for 24 hours. From this data, it appears that bisPMB may mediate UPR signalling through the PERK/ATF4 signalling pathway.

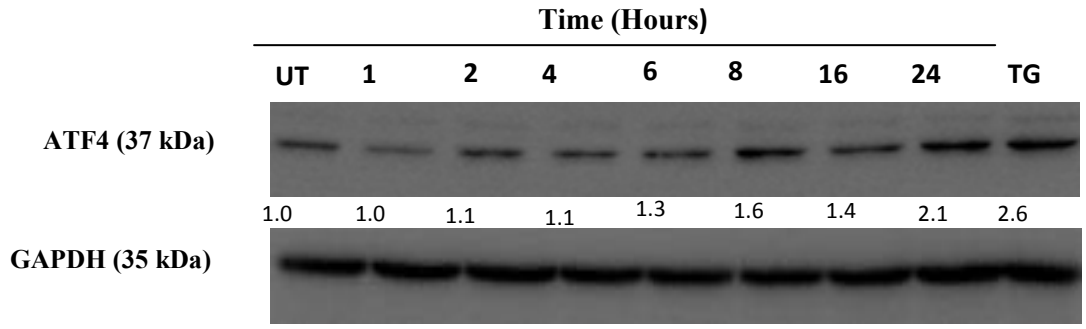

Figure 4.4. Time dependent increase of ATF4 protein expression in WHCO1 cells. Total cell lysate was extracted from WHCO1 cells treated with 7 μM concentration of bisPMB for 1, 2, 4, 6, 8, 16 and 24 hours or with 1 μM TG for 24 hours, and analysed by western blot. The membrane was probed with an anti-ATF4 antibody and GAPDH was used as a loading control. The protein levels were normalized and quantified relative to GAPDH levels. This blot is representative of 2 independent determinations.

3.2.4 BisPMB activates the ATF6 pathway

The UPR pathway is also activated through the ATF6 sensor. In response to ER stress, the ATF6 transmembrane protein is cleaved, by site specific proteases 1 and 2 in the Golgi apparatus, from a 90 kDa protein to a 50 kDa transcription factor (Ye et al., 2000). The activation of ATF6 was investigated in WHCO1 cells treated with bisPMB at the 7 μM concentration. No change was observed in the ATF6α 90 kDa expression levels between the untreated and after 1 hour bisPMB treatment in WHCO1 cells. On the other hand, bisPMB induced decrease in the protein levels of ATF6α (90kDa) between 2 - 24 hours compared to the untreated control (figure 4.5). There was no detectible ATF6 (90 kDa) at the time point 2 - 6 hours followed by a subsequent rise in ATF6α (90 kDa) expression was observed from 8 - 24 hours in the bisPMB treated sample. Additionally, TG-treated WHCO1 cells were also found to display decreased ATF6α (90 kDa) expression

(figure 4.5). Taken together, these results strongly imply that bisPMB, activates the ATF6 arm of UPR pathway in WHCO1 cells between 4 - 6h.

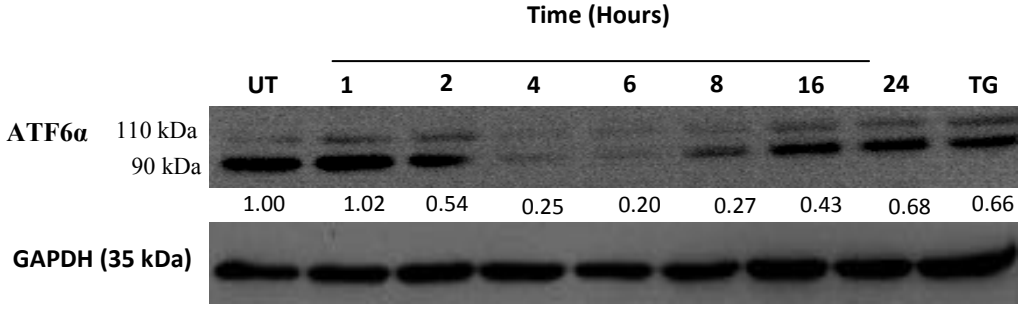

Figure 4.5 Time dependent decrease in ATF6α (90 kDa) protein expression in WHCO1 cells. Total cell lysate extracted from WHCO1 cells treated with 7 μM concentration of bisPMB for 1, 2, 4, 6, 8, 16 and 24 hours or 1 μM TG for 24 hours, and analysed by western blot. The membrane was probed with anti-ATF6α and GAPDH was used as a loading control. The protein levels were normalized and quantified relative to GAPDH. This blot is representative of 2 independent determinations

3.2.5 BisPMB activates the IRE-1/XBP-1 pathway

After observing ATF6 activation, the IRE-1/XBP-1 UPR pathway was examined in WHCO1 cells treated with bisPMB or TG. When activated, IRE-1 orchestrates cleavage of XBP1 mRNA. The resulting spliced XBP1 (XBP1s) mRNA variant is translated into a transcription factor that regulates the expression of certain ER stress genes. By RT-PCR bisPMB was found to cause an increase in XBP1 spliced variant between 1- 5 hour only but not at the later time points between 8 and 24h. In comparison, the TG control was also found to cause spliced XBP1 at the late 24 h time point (figure 4.6). These results suggest that bisPMB activates the IRE-1/ XBP-1 pathway and that endoribonuclease activity may be an early response in WHCO1 cells.

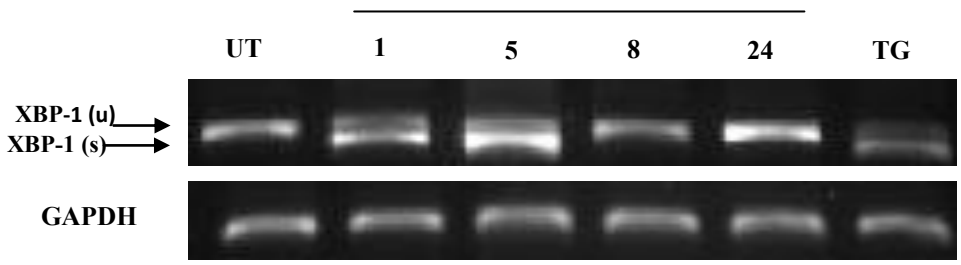

Figure 4.6 Time dependent splicing of XBP1 mRNA in bisPMB or TG treated WHCO1 cells. mRNA was extracted from WHCO1 cells incubated with bisPMB at 7 μM concentration for 1, 5, 8 and 24 hours or 1 μM TG for 24 hours. XBP1 and GAPDH gene expression was analysed by RT-PCR. The PCR products show the presence of the XBP-1s in WHCO1 cells treated with bisPMB for 1 - 5 hours or with 1μM TG for 24 hours. The blot above is representative of three independent experiments.

3.2.6 ER stress and cytotoxicity

3.2.6.1 BisPMB increases CHOP/GADD153 expression in a time dependent manner

When UPR is insufficient in establishing ER homeostasis, apoptosis is induced. All three UPR pathways i.e PERK/ATF4, ATF6 and IRE1/XBP-1 converge on the transcription of CHOP/GADD153 (Ma et al., 2002, Oyadomari and Mori, 2004), which is associated with ER stress induced apoptosis.

In order to determine if WHCO1 cells treated with 7 µM concentration of bisPMB induce the expression of CHOP/GADD153, western blot analysis was conducted. The CHOP/ GADD153 expression decreased between 1 - 6 hours of bisPMB treatment compared to the untreated control (figure 4.7). CHOP/GADD153 expression was then found to be elevated in WHCO1 cells treated with bisPMB between 8 -16 hours and 1 µM TG for 24 hours compared to the untreated control (figure. 4.7). These results show that both bisPMB and TG induce CHOP/GADD153 expression in WHCO1 cells.

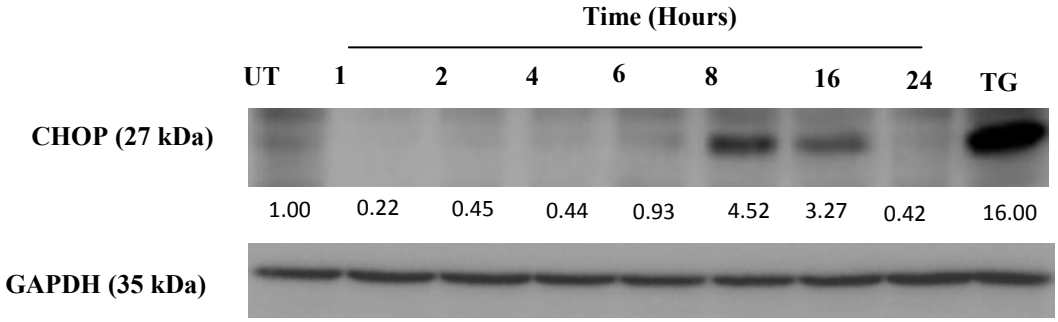

Figure 4.7 Time dependent increase of CHOP/GADD153 protein expression in bisPMB treated WHCO1 cells. Total cell lysate was collected from WHCO1 cells treated with bisPMB at the 7 µM concentration for 1, 2, 5, 8 and 24 hours or 1 µM TG for 24 hours and analysed by western blot. The blot was probed with anti-CHOP and anti-GAPDH antibodies and protein bands were quantified relative to untreated cells and the GAPDH loading control. This blot is representative of 2 independent determinations.

3.2.6.2 Silenced CHOP/GADD153 reverses the anti-proliferative activity of bisPMB

Seeing that bisPMB enhanced CHOP/GADD153 expression and that CHOP/GADD153 promotes ER stress induced apoptosis (Matsumoto et al., 1996, Oyadomari and Mori, 2004, Marciniak et al., 2004).We addressed the question of whether CHOP/GADD153 played a role in the inhibitory

effect of bisPMB in WHCO1 cell viability by silencing CHOP using siRNA and testing for WHCO1 cell viability following bisPMB treatment.

In order to validate the silencing of CHOP/GADD153 by siRNA, we stimulated CHOP/ GADD153 expression with bisPMB following pre-incubation with siCHOP and siControl. The siControl was used as a negative control for CHOP/ GADD153 silencing in this study. As expected, bisPMB enhanced the expression of CHOP compared to the untreated control. In addition, the combination of bisPMB and siControl also enhanced CHOP/ GADD153 expression compared to the untreated control. Ultimately, 60nM of CHOP/GADD153 siRNA was chosen as this concentration was found to reduce the expression of CHOP by approximately 3 folds compared to the bisPMB treated and the siRNA control (figure. 4.8). We were therefore able to show successful knockdown of the CHOP/GADD153 protein in WHCO1 cells.

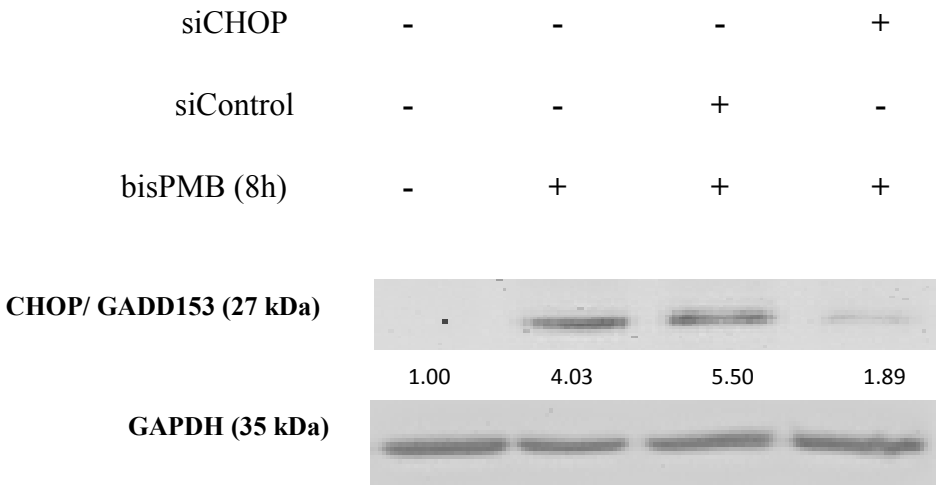

Figure 4.8 CHOP siRNA reduced protein expression of CHOP in WHCO1 cells treated with bisPMB. Total cell lysate was extracted from WHCO1 cells incubated with media only or 60 nM CHOP siRNA or 60 nM control siRNA and bisPMB for 8 hours and examined for CHOP protein expression by western blot. The blot was subsequently probed with anti-CHOP and anti-GAPDH antibodies and protein bands were quantified relative to the untreated control and to GAPDH. This blot is representative of 2 independent determinations.

Following the successful silencing of CHOP/GADD153, WHCO1 cells were incubated with bisPMB in combination with siCHOP or siControl for 24 hours and subjected to the MTT assay, which quantified WHCO1 cell viability. As expected the 7 μM concentration of bisPMB and 1 μM TG significantly reduced WHCO1 cell viability by 2 folds (figure 4.9). Furthermore, the siControl had no effect on the inhibitory effect of bisPMB and TG on WHCO1 cell viability. However, the siRNA mediated CHOP/GADD153 knockdown was found to completely abrogate the ability of bisPMB to inhibit WHCO1 cell viability; and this was not observed in the siControl or in the untreated cells (figure 4.9 **A**). Furthermore, CHOP was found to have a similar effect in

TG (figure 4.9 **B**) as seen for bisPMB. These findings demonstrate that CHOP/GADD153 plays a key role in both bisPMB and TG-mediated WHCO1 cytotoxicity.

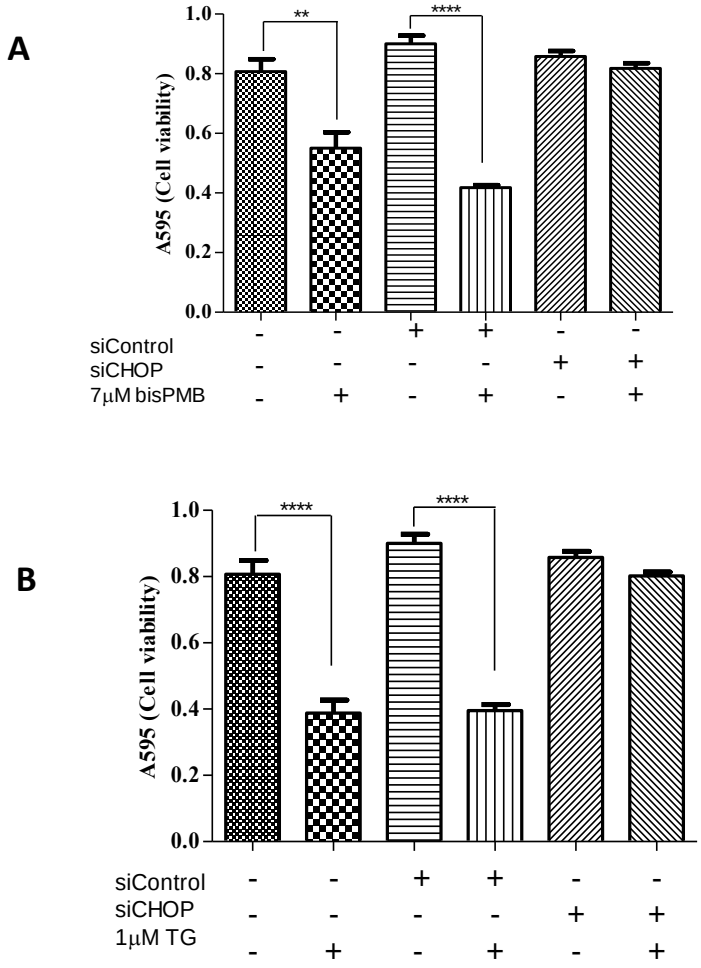

Figure 4.9 Reversal of bisPMB antiproliferative activity by CHOP knockdown. WHCO1 cells were incubated with control and CHOP siRNA prior to treatment with bisPMB at 7 μM concentration (A) or 1 μM TG (B) 24 hours and cell viability was determined using the MTT assay. Each column represents an average of three technical replicates ± SD although the graphs are representative of three independent experiments. A) Average cell viability in WHCO1 cells treated with bisPMB, in the presence of siControl and siCHOP. B) Average cell viability in WHCO1 cells treated with , TG, in the presence of siControl and siCHOP. A t-test statistical ** indicated *p*-value < 0.01, ****indicated *p*-value < 0.0001.

3.2.7 BisPMB induced MAPK signalling activation in WHCO1 cells

3.2.7.1 Induction of JNK activation by bisPMB in WHCO1 cells

ER stress induced apoptosis is linked to the JNK pathway, which in turn is triggered through the IRE-1 pathway. JNK pathway activation is commonly examined by measuring the phosphorylation levels of the JNK 1/2 MAPK proteins.

We observed that bisPMB increased JNK1/2 phosphorylation/activation in a time dependent manner compared to the untreated control with maximal activation at 8 h (figure 4.10). However, there was no change in the phosphorylated levels of JNK1/2 in TG treated WHCO1 cells compared to the untreated control. This data suggests that bisPMB induces JNK pathway activation in WHCO1 cells. The role played by JNK activation in bisPMB induced cytotoxicity was further examined using a SP600125 chemical inhibitor.

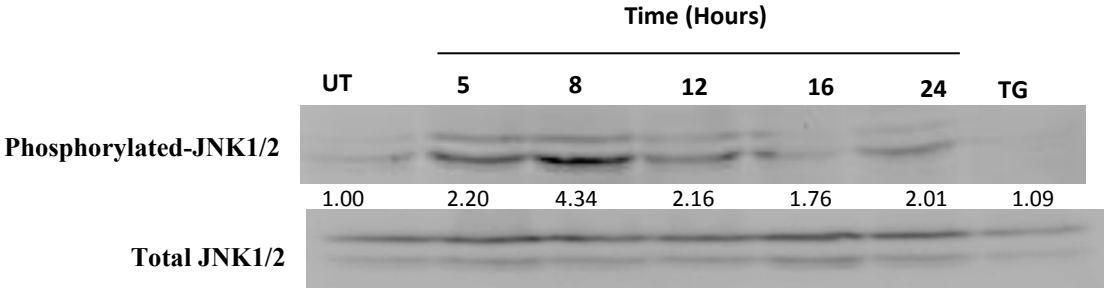

Figure 4.10 BisPMB induced JNK1/2 activation in WHCO1 cells. Total cell lysate was extracted from WHCO1 cells treated with bisPMB at the 7 μM concentration for 5, 8, 12, 16 and 24 hours or with 1 μM TG for 24 hours and analysed by western blot . The blot was probed using both anti-phosphorylated JNK1/2 and anti-JNK1/2 antibodies and protein bands were quantified and normalised relative to the untreated control and total JNK1/2. This blot is representative of 2 independent determinations.

3.2.7.2 Effect of JNK inhibition on bisPMB anti-proliferative activity

Prior to using the JNK inhibitor SP600125 in WHCO1 cells, the optimal concentration had to be established. The phosphorylation/activation of JNK was found to be progressively inhibited with increasing SP600125 concentration (figure 4.11) and 30 μM SP600125 was found to induce the greatest reduction of JNK phosphorylation.

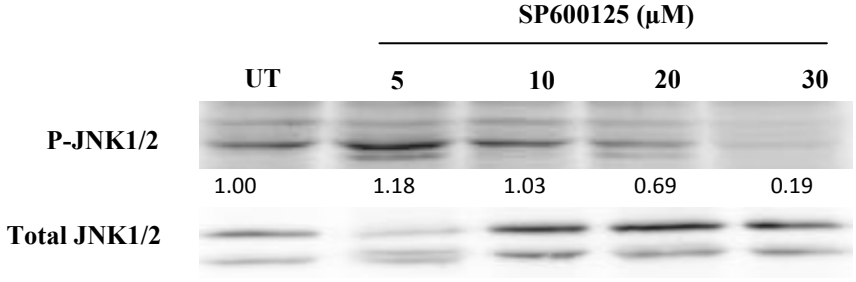

Figure 4.11 Inhibitor SP600125 reduces JNK1/2 phosphorylation in a concentration dependent manner. WHCO1 cells were incubated with 5, 10, 20 or 30 μM SB600125 for 24 hours. Total cell lysate was extracted and analysed by western blot. The membrane was subsequently probed with anti-phosphorylated JNK1/2 and l JNK1/2 primary antibodies. The phosphorylated and total JNK1/2 protein expression was quantified and normalised relative to untreated control and total JNK1/2. This blot is representative of 2 independent determinations.

Consequently, 30 µM SP600125 was selected for analysis of the role of JNK activation in bisPMB and TG cytotoxicity. Following pre-incubation with 30 µM SP600125, WHCO1 cells were incubated with bisPMB at 7 µM concentration or TG. The MTT assay was then performed in these cells to assess viability. The 30 µM SP600125 alone, had no effect of WHCO1 cell viability. WHCO1 cells were found to display a 47 % and 34 % decrease in cell viability respectively after treatment with bisPMB alone or in combination with SP600125 (figure 4.12). This demonstrated that the inhibition of JNK phosphorylation by SP600125 had no effect on bisPMB cytotoxic activity against WHCO1 cells. As previously observed, 1 µM TG significantly reduced WHCO1 cell viability by 2 folds. However, the inhibition of JNK activation completely reversed the cytotoxicity of TG in WHCO1 cells (figure 4.12). This demonstrated that the JNK pathway plays a key role in TG cytotoxic activity but not in bisPMB's inhibitory effect on WHCO1 cell viability.

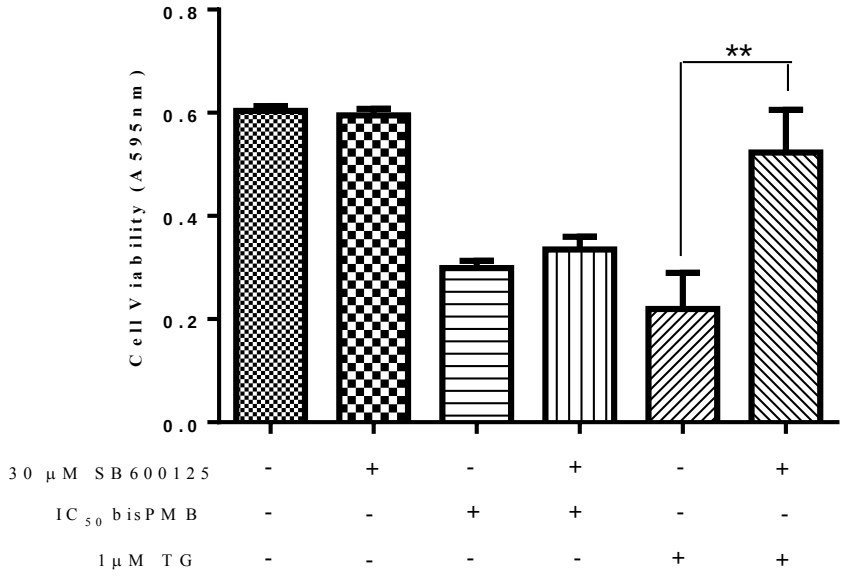

Figure 4.12 The effect of JNK inhibitor SB600125 bisPMB antiproliferative activity. WHCO1 cells were pre-incubated with 30 µM SB600125 and subsequently treated with the 7 µM concentration of bisPMB for 24 hours. WHCO1 cell viability was subsequently measured using the MTT assay. Each bar represents the average absorbance reading from four technical replicates and is representative of three independent experiments. A t-test statistical analysis was performed using GraphPad Prism and ** indicated *p*-value < 0.01.

3.2.8 BisPMB induces an increase in p38 activation

The p38 MAPK signal transduction pathway has been linked to apoptosis induction and is known to be activated in cells in response to external stimuli such as ER stress. In order to determine if the 7 μM concentration of bisPMB enhanced the activation of p38, western blot analysis was performed in WHCO1 cells. BisPMB was found to enhance the phosphorylation/activation of p38 in a time dependent manner (figure 4.13) which occurred within 2 hours and was sustained continually at a level of 4 fold up to 24 hours. TG was also found to increase p38 activation in WHCO1 cells compared to the untreated control.

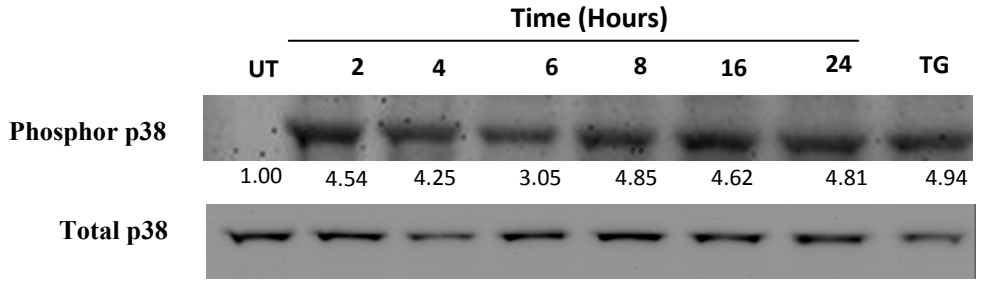

Figure 4.13 BisPMB induced p38 phosphorylation/activation in WHCO1 cells in a time dependent manner. Total cell lysate was extracted from WHCO1 cells treated with bisPMB at 7 μM concentration for 2, 4, 6, 8, 16, 24 hours and 1 μM TG for 24 hours and analysed by western blot. The membrane was subsequently probed with anti-phosphorylated p38 or total p38 antibodies and protein bands were and normalized to total p38. This blot is representative of 2 independent determinations.

3.2.8.1 The role of p38 MAPK on bisPMB induced anti-proliferative activity

The phosphorylated/activated form of p38 is commonly detected in stressed cells. In order to determine the concentration of the p38 inhibitor SB 203580 required to reverse the bisPMB induced phosphorylation of p38, whole cell lysate was extracted from cells pre-treated with varying concentrations of SB 203580 together with the 7 μM concentration of bisPMB. BisPMB alone and in combination with 10, 50 and 100 μM SB 203580 displayed elevated phosphorylated p38 expression levels compared to the untreated control (figure 4.14). SB 2035580 was found to reduce bisPMB induced p38 phosphorylation/activation in a concentration dependent manner in bisPMB treated cells (figure 4.14). Consequently, 100 μM of SB 203580 was found to display the lowest levels of bisPMB induced p38 phosphorylation, although it did not completely inhibit p38 phosphorylation, it was chosen as the concentration of inhibitor for the study as it did not induce a cytotoxic effect in WHCO1 cells.

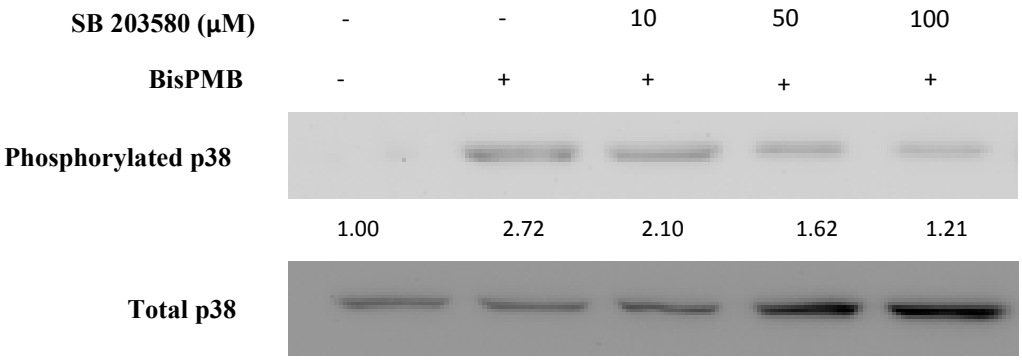

Figure 4.14 Inhibition of p38 activation with SB 203580 in WHCO1 cells treated with bisPMB. Total cell lysate was extracted from WHCO1 cells pre-treated with 10, 50 and 100 μM SB203580 followed by treatment with bisPMB at 7 μM concentration analysed using western blot. The membrane was subsequently probed with anti-phosphorylated p38 or Total p38 antibodies and protein bands were quantified and normalised relative to the untreated control and total p38. This blot is representative of 2 independent determinations.

In order to determine the role played by p38 activation in the cytotoxic effect of bisPMB in WHCO1 cells, cells were treated with bisPMB in the absence and presence of p38 inhibitor SB 203580 and cell viability was then evaluated using the MTT assay. The 100 μM SB 203580 alone did not have any effect on WHCO1 cell viability (figure 4.15). As expected, 7 μM concentration of bisPMB and 1 μM TG significantly reduced WHCO1 cell viability and the inhibition of p38 by SB 203580 was found not to affect the cytotoxic activity of bisPMB or TG in WHCO1 cells (figure 4.15). This demonstrated that p38 did not play a major role in bisPMB and TG cytotoxic effect in WHCO1 cells.

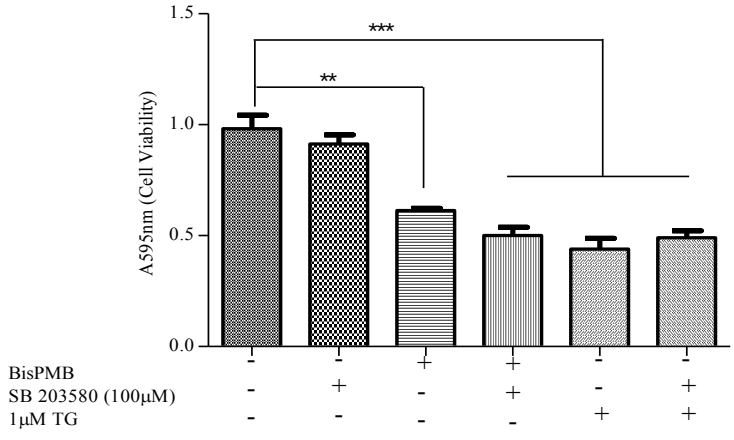

Figure 4.15 The role played by p38 on bisPMB and TG-induced cytotoxicity in WHCO1 cells. WHCO1 cells were pre-incubated with 100 μM SB203580 and treated with the 7 μM concentration of bisPMB or 1 μM TG for 24 hours. WHCO1 cell viability was measured using the MTT assay as described in section 6.2.2. Each bar represents the average absorbance reading from four technical replicates +- SD. This graph is representative of three independent experiments. A t-test and one-way ANOVA statistical analysis was performed using GraphPad Prism and ** indicated p-value < 0.01, *** indicated p-value < 0.0001.

3.2.9 MEK/ERK activation by bisPMB

The MEK/ERK pathway is known as a survival MAPK pathway and is activated by various garlic derived compounds such as ajoene (Antlsperger et al., 2003). The activation of the MEK/ERK pathways is usually evaluated by assessment of phosphorylated ERK1/2 MAPK. Total cell lysate extracted from WHCO1 cells treated with the 7 μM concentration of bisPMB or 1 μM TG was therefore analysed by western blot. BisPMB was found to enhance the ERK1/2 phosphorylated/activated levels in a time dependent manner compared to the untreated control and TG was also found to increase ERK1/2 phosphorylation (figure 4.16). BisPMB induced phosphorylation/activation of ERK1/2 was markedly pronounced within 5 minutes and with maximal induction at 4 hour (figure 4.16). However, the levels of phosphorylated ERK1/2 declined after 6 hours of bisPMB treatment with complete inactivation observed at 16 h. These results suggest that bisPMB induced transient, early activation of ERK1/2 activation while TG ERK1/2 activation was still observed at 24 hours.

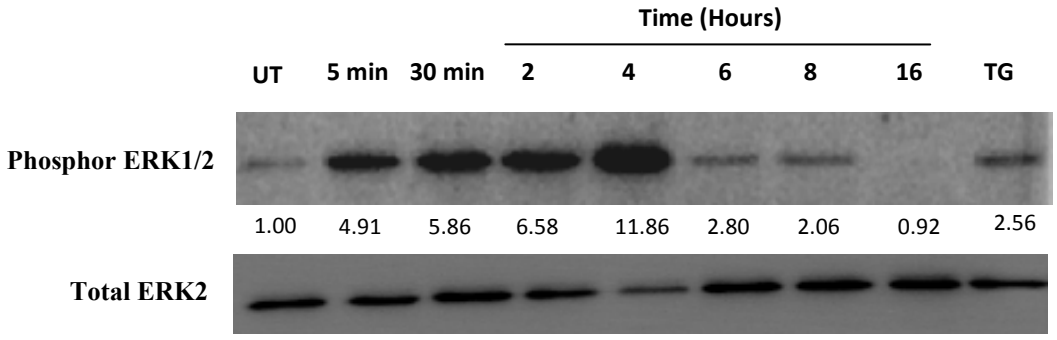

Figure 4.16 Time dependent activation of ERK in WHCO1 cells treated with bisPMB or TG. Total WHCO1 cell lysate was extracted and analysed by western blot as described in section 6.9. Antibodies against phosphorylated ERK1/2 and ERK2 were used for probing. Each bar represents the area density of the p-ERK1/2 protein band relative to the total ERK2 band. This blot is representative of three independent experiments.

3.2.9.1 The role of MEK/ERK signalling in bisPMB anti-proliferative activity

In order to determine the function of the MEK/ERK signal transduction pathway in the cytotoxic activity of bisPMB, specific MEK1/2 inhibitor, U0126 was used to block ERK1/2 activation.

Initially, a concentration dependent experiment for U0126 was performed in WHCO1 cells to ascertain the amount of U0126 required for MEK1/2 inhibition. The reduction in ERK1/2 phosphorylation was clearly visible in WHCO1 cells treated only with U0126. However, MEK1/2 inhibition was evident by the concentration dependent reduction in ERK1/2 phosphorylation in WHCO1 cells treated with bisPMB for 30 minutes (fig. 4.17). As a result, 10 μM U0126 was chosen as the most effective concentration as it resulted in the greatest reduction in ERK1/2 phosphorylation (figure 4.17).

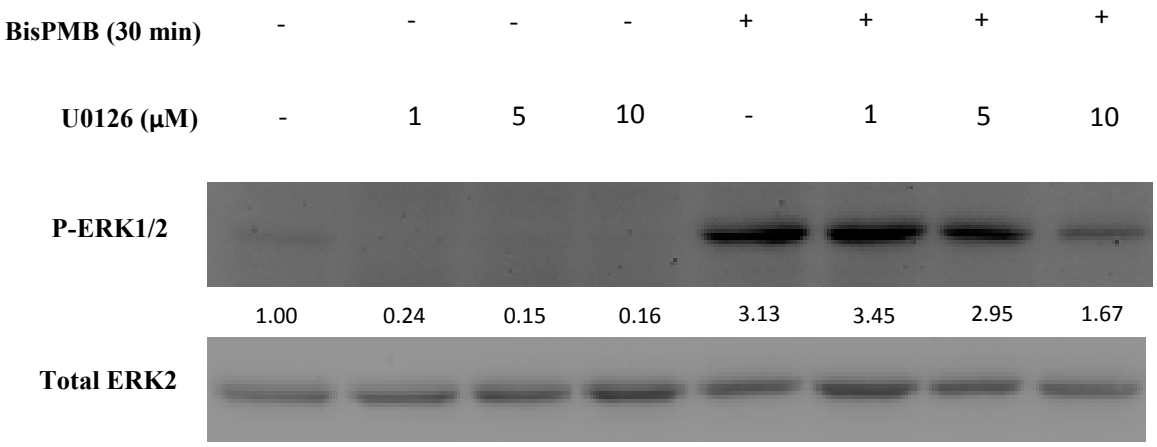

Figure 4.17 Concentration dependent inhibition of ERK1/2 phosphorylation with U0126. Following WHCO1 incubation with indicated concentrations of U0126, bisPMB and TG, cell lysate was extracted and analysed by western blot. The membrane was subsequently probed with anti-phosphorylated ERK1/2 or total ERK2 antibodies and protein bands were quantified and normalised relative to the untreated control and total ERK 2. This blot is representative of 2 independent determinations.

Following establishment of the optimal U0126 concentration, the role played by the MEK/ERK signal transduction pathway in the cytotoxic activity of bisPMB was investigated. The untreated control and 10 μM U0126 only treated WHCO1 cells displayed maximal cell viability. Furthermore, the 7 μM concentration of bisPMB significantly reduced the WHCO1 cell viability. Inhibition of the MEK1/2 using 10 μM U0126 was in fact found to display an increase in the cytotoxic behaviour of bisPMB in WHCO1 cells (figure 4.18). On the other hand, 1 μM TG reduced WHCO1 cell viability compared to the untreated control. However, MEK1/2 inhibition was found to have no effect on the cytotoxic activity of 1 μM TG (figure 4.18). These results suggest that the activation of the MEK/ERK pathway in bisPMB treated WHCO1 cells plays a pro-survival role. Therefore inhibition of MEK1/2 seemingly sensitizes WHCO1 cells to bisPMB

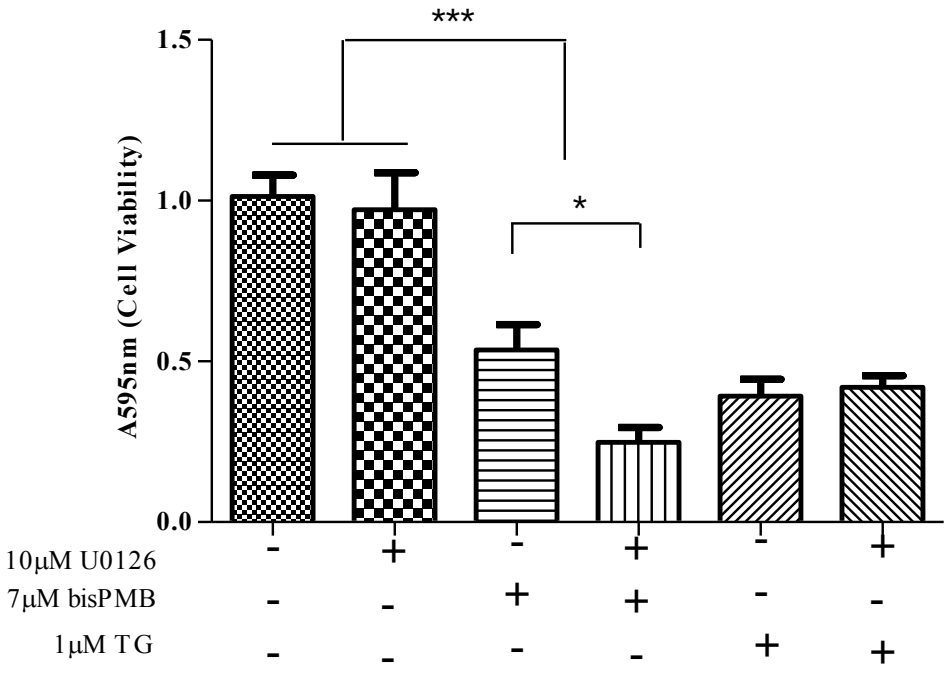

Figure 4.18 Inhibition of ERK1/2 increased the cytotoxic activity of bisPMB in WHCO1 cells. WHCO1 cells were pre-incubated with 10 μM U0126 and subsequently treated with the 7 μM concentration of bisPMB or 1 μM TG for 24 hours. WHCO1 cell viability was subsequently measured using the MTT assay. Each bar represents the average absorbance reading from three technical replicates. This graph is representative of three independent experiments. A t-test and one-way ANOVA statistical analysis was performed using GraphPad Prism and * indicated p-value < 0.05 and *** indicated p – value < 0.0001.

3.3 DISCUSSION

ER stress and the MAPK signalling pathways have been implicated in the cytotoxic mechanism of action of garlic derived DAS, DADS and DATS, (Das et al., 2007, Yang et al., 2009, Wang et al., 2012). In addition, garlic derived ajoene is reported to activate MAPK in human leukaemia HL60 cells (Antlsperger et al., 2003) and enhances the expression of ER stress marker GRP78/BIP in MDA-MB-231 cells (Kaschula et al., 2015). However the role played by the ER stress and UPR in these cytotoxic effects is not clear. Moreover, the role played by MAPK, ER stress and UPR has not been clearly defined for bisPMB.

We followed up from Chapter 3, where bisPMB was observed to primarily target the UPR. Here we show that bisPMB, an ajoene analogue, induced UPR and MAPK signalling pathways in WHCO1 cells in a time dependent manner. Throughout the study, bisPMB was compared with

thapsigargin because it is a well known ER stress inducer and is widely used as an ER stress positive control (Treiman et al., 1998d).

Prior to this study, our lab have been the first to demonstrate that ajoene localises to the ER of MDA-MB-231 breast cancer cells (Kaschula et al., 2015). We also found that ajoene disrupts protein folding and enhances the expression of GRP78/BIP (Kaschula et al., 2015). In response to ER stress, cells enhance the expression of molecular chaperones such as GRP78/BIP to aid the folding of misfolded proteins and restore ER homeostasis (Gething, 1999). The garlic compounds DATS and DADS have been shown to increase the expression of the ER resident molecular chaperone GRP78/BIP in basal cell carcinoma BCC and COLO 205 cells respectively (Yang et al., 2009, Wang et al., 2012). Thus garlic derived OSC DADS, DATS and ajoene may act via a similar mechanism to trigger ER stress in different cancer cell lines.

Consistent with reports on OSC induced GRP78/BIP expression; in this chapter we have shown that bisPMB mediated a fivefold increase in the GRP78/BIP expression at levels comparable to the thapsigargin positive control in WHCO1 cells. The GRP78/BIP antibody used detected both the 72 and 78 kDa GRP78/BIP protein bands, where the 72 kDa band was found to be more pronounced in bisPMB treated WHCO1 cells than in thapsigargin treated cells. This has been observed in other cancer cell lines as the 72 and 78 kDa GRP78/BIP proteins were also detected in untreated and Faclarindiol treated human colon cancer HCT 116 cells. The 72 kDa GRP78/BIP protein is referred to as the GRP78/BIP isoform and is present in certain cancer cells (Rauschert et al., 2008, Shani et al., 2008, Hammadi et al., 2013). The 72 kDa GRP78/BIP protein is reported to be the product of deglycosylation of the 82 kDa GRP78/BIP protein isoform (Rauschert et al., 2008, Shani et al., 2008). The higher expression of the 72 kDa GRP78/BIP in bisPMB compared to the TG treated WHCO1 cells imply that bisPMB may possibly increase deglycosylation or most likely inhibit GRP78/BIP glycosylation more than TG. *Ultimately, both bisPMB and TG increased GRP78/BIP overall expression, demonstrating that both compounds induced ER stress.* Cells undergoing ER stress promote the degradation of terminally misfolded proteins through ER associated degradation (ERAD) (Meusser et al., 2005). The execution of ERAD involves the activation of ubiquitin proteosome system UPS. Proteins targeted for destruction via the UPS are labelled by multiple ubiquitin molecules resulting in poly ubiquitination. These poly ubiquitinated proteins are then targeted to 26S proteosome for degradation (Glickman and Ciechanover, 2002). We observed that bisPMB increased the expression levels of ubiquitinated proteins in WHCO1 cells at in a time dependent manner. Suggesting that bisPMB enhanced protein ubiquitination and targeting of misfolded proteins for degradation. These results are in agreement with those found

for ajoene in MDA-MB-231 cells (Kaschula et al., 2015). On the other hand, TG did not alter the ubiquitination of proteins in WHCO1 cells. This could be attributed to the 24 hour time point at which TG induced protein ubiquitination was investigated, as the UPS event is reported to be short lived (Hershko and Ciechanover, 1998). Furthermore, to our knowledge, TG has not been reported to enhance protein ubiquitination. Our data therefore supports the idea of cancer cells restoring ER homeostasis by enhancing the expression of GRP78/BIP and triggering the ERAD process in response to bisPMB treatment. These observations imply an increase in misfolded proteins in bisPMB treated cells as the UPS is reported to degrade misfolded proteins (Glickman and Ciechanover, 2002).

In response to an accumulation of misfolded proteins, ER stress ensues and in turn activates the UPR which is orchestrated through three ER transmembrane proteins namely PERK, ATF6 and IRE-1(Li et al., 2011). Following ER stress activation, PERK phosphorylates eIF2α which leads to a reduction in global protein synthesis (Koumenis et al., 2002) and to the selective enhancement of ATF4 translation (Harding et al., 2000). ATF4 expression is often used as a marker for PERK pathway activation, even though several other kinases such as GCN2, HRI and PKR, are also reported to be responsible for phosphorylation of eIF-2α and subsequent enhancement of ATF4 translation (Donnelly et al., 2013). However, under ER stress conditions ATF4 enhanced protein expression is considered a good indicator of PERK activation (Ohoka et al., 2005, Rouschop et al., 2010). In this work, bisPMB and TG were found to increase the expression of ATF4 in a time dependent manner. These results imply that the PERK/ATF4 pathway is activated by bisPMB and TG in WHCO1 cells. Moreover, this observation is consistent with reports that demonstrate that the DATTS increases the expression of ATF4 in human colon cancer cells (Saidu et al., 2013).

The second UPR transmembrane protein is ATF6; whose activation is characterized by ATF6 (90kDa) transmembrane protein cleavage to ATF6 (50kDa) transcription factor by site specific proteases in the Golgi apparatus (Ye et al., 2000). ATF6 (50kDa) regulates the expression of ER stress genes involved in cell survival (Yoshida et al., 2001a). BisPMB was found to reduce the expression of ATF6 p90 in a time dependent manner, with the maximal reduction observed between 4 to 6 hours of bisPMB treatment. The reduction of ATF6α p90 was also observed in the TG treated WHCO1 cells. This suggested that bisPMB enhanced the cleavage of ATF6 p90 to give rise to ATF6 p50. However, ATF6 p50 could not be detected with the antibody used in this study. The reduction of ATF6 full length pre-cursor has been used to monitor ATF6 activation in A549 cells exposed to hypoxic conditions (Gewandter et al., 2009). Moreover, the activation of ATF6 in MDA-MD-231 breast cancer cell lines has also been observed for other anticancer

compounds such as Taxol (Notte et al., 2015). Thus, bisPMB enhanced the activation of ATF6 in WHCO1 cells. The increase in ATF6 activation has been implicated in the induction of ER resident chaperones and XBP-1 mRNA, which is activated by the IRE-1 transmembrane protein (Yoshida et al., 2001a, Yamamoto et al., 2007).

The XBP1/IRE1 UPR pathway is essential for proper protein folding and protein degradation in the ER (Lee et al., 2003a). The activation of the IRE1/ XBP1 pathway is characterized by IRE1 induced XBP1 mRNA splicing to produce spliced XBP-1 (XBP-1s) (Iwawaki and Akai, 2006, Koong et al., 2006, Han et al., 2009). In Hela cells, XBP1 mRNA is reported to be spliced in response to ER stress induced by TG (Yoshida et al., 2001a). BisPMB was found to transiently induce mRNA XBP-1 splicing at 8 h; whereas TG was found to induce XBP-1 splicing at 24 hours. This suggests that bisPMB and TG enhanced IRE-1 endoribonuclease activity but the transient activation of XBP-1 in bisPMB treated WHCO1 cells is possibly due to regulation of IRE-1 RNAse activity. The IRE-1 RNAse activity is regulated by its direct interaction with BAX, BAK, PUMA and BIM (Hetz et al., 2006, Rodriguez et al., 2012). For example, double knockout of PUMA and BIM in mouse embryonic fibroblast cells resulted in the transient activation of XBP-1 (Rodriguez et al., 2012).

ER stress induced apoptosis is mainly orchestrated by the CHOP and the JNK pathways (Urano et al., 2000, Marciniak et al., 2004), however all UPR pathways converge on the transcription of CHOP/GADD153 (Oyadomari and Mori, 2004). CHOP/GADD153 is the downstream target of ATF4, ATF6 and XBP-1s and has been reported to regulate the transcription of genes involved in cellular survival and death and to elicit intracellular pro-apoptotic protein-protein interactions (Matsumoto et al., 1996, Zinszner et al., 1998, McCullough et al., 2001, Yamaguchi and Wang, 2004). BisPMB was found to increase CHOP/GADD153 expression in WHCO1 cells, in a time dependent manner. This observation was found to be in agreement with that reported for DADS and DATS in human colon cancer and basal cell carcinoma cells respectively (Yang et al., 2009, Wang et al., 2012). As expected, TG enhanced CHOP /GADD153 expression in WHCO1 cells. This result is consistent with TG induced upregulation of CHOP/GADD153 in human colon cancer cells HCT116 (Yamaguchi and Wang, 2004). To test whether CHOP plays an important role in bisPMB cytotoxicity in WHCO1 cells, the effect of siRNA knockdown of CHOP/GADD153 was assessed in bisPMB and TG treated WHCO1 cells. We found that expression of CHOP/GADD153 was a key determinant in the cytotoxicity of bisPMB in WHCO1 cells. Thus far, there have been no reports on the role of CHOP/ GADD153 on OSC cytotoxic activities in cancer cells. On the other hand, we found that CHOP/GADD153 also play a central

role in TG cytotoxic activity. This consistent with the observation that CHOP/GADD153 siRNA knock down reduces TG apoptotic activity against human colon cancer HCT 116 cell line (Yamaguchi and Wang, 2004). Altogether, these findings demonstrated that CHOP/GADD153 plays a critical role in bisPMB and TG cytotoxicity in WHCO1 cells.

We then addressed the question of whether JNK plays a role in the cytotoxic activity of bisPMB and TG. The JNK pathway is a member of the MAPK pathways and is known as a stress activated protein kinase (SAPK). In this study, bisPMB was found to induce a transient increase in JNK phosphorylation/activation. This observation is consistent with that for ajoene and DADS which are reported to induce JNK activation in HL60 and COLO 205 cells respectively (Antlsperger et al., 2003, Yang et al., 2009). Furthermore, ER stress associated apoptosis inducing agents: thapsigargin, tunicamycin and dithiothreitol are reported to induce JNK activation in rat acinar AR42J cells (Urano et al., 2000). This suggests that the JNK pathway is activated by bisPMB and that it may be involved in bisPMB's cytotoxic activity. However, JNK inhibition was found to have no effect on the cytotoxicity of bisPMB in WHCO1 cells. This implies that JNK activation does not play a major role in bisPMB induced cytotoxic effects in WHCO1 cells. Interestingly, JNK inhibition played a more significant role for TG. These findings suggest that the duration of JNK activation is related to its role in apoptosis induction. For example, transient JNK activation (approximately 5 hours) was not involved in ajoene induced apoptosis in human leukaemia cells, whereas sustained JNK activation in DATS treated bladder cancer cells played a major role in its apoptotic induction (Antlsperger et al., 2003, Shin et al., 2014). Since bisPMB lead to JNK activation, other MAPK signalling pathways such as MEK/ERK and p38 were also investigated, as they have been previously shown to interact with each other and with the UPR pathways. Furthermore, the microarray data in Chapter 3 demonstrated that the MAPK signalling pathways were also significantly deregulated by bisPMB and TG in WHCO1 cells.

The p38 MAPK signalling pathways are reported to be involved in apoptosis induction by inflammatory cytokines and stress inducing chemotherapeutic agents (Obata et al., 2000, Ranganathan et al., 2006, Cuenda and Rousseau, 2007, Yang et al., 2013). In addition, the interaction of p38 activation and UPR has been reported. The substrates of p38 MAPK include the MAP kinase activated protein kinase 2, MAPK interacting kinase 1 (Mnk1), MAPK interacting kinase 1 (Mnk2) and components of the ER stress pathways such as activating transcription factor 6 (ATF6), Nrf2, c-Jun, XBP-1 and CHOP (Cohen, 1997, Ben-Levy et al., 1998, Thuerauf et al., 1998, Ma and Hendershot, 2004, Ranganathan et al., 2006). Several studies have suggested that CHOP is phosphorylated by p38 at the trans-activation sites (Wang and Ron, 1996, Darling and

Cook, 2014). Furthermore, the transcriptional activity of ATF6 is reported to be enhanced by phosphorylation with p38 MAPK in myocardial cells, promoting the transcription of GRP78/BIP (Thuerauf et al., 1998). In contrast, the p38 MAPK pathway has also been shown to be activated downstream of the PERK/ATF4 UPR pathway. It has been suggested that the natural compound seletinite induced PERK/ATF4 pathway inhibit HSp90, a negative regulator of p38, resulting in enhanced p38 MAPK activity in human promyelocytic leukaemia NB4 cells (Jiang et al., 2014). We observed that bisPMB increased phosphorylated p38 MAPK expression levels in WHCO1 cells. However, the inhibition of phosphorylated p38 with the SB203580 chemical inhibitor showed no effect on bisPMB and TG cytotoxic activity against. These findings are consistent with reports showing that p38 does not play a major role in ajoene induced apoptosis in human promyeloleukemia cells (Antlsperger et al., 2003). From these reports and our observations, it can be said that the observed ATF6 activation by bisPMB may be influenced by p38 MAPK. However, the central role of CHOP/GADD153 in bisPMB cytotoxic activity against WHCO1 cells may not influenced by p38 MAPK phosphorylation.

We then investigated the role played by the MEK/ERK pathway on bisPMB or TG induced cytotoxic activity in WHCO1 cells. The activation of the MEK/ERK pathway is known to be associated with cell survival. We demonstrated that bisPMB markedly enhanced the phosphorylation/activation of ERK1/23.5 μM in a time dependent manner and to a lesser extent in the TG treated sample. The transient activation of ERK1/2 activation has also been observed in ajoene treated human promyeloleukemia cells (Antlsperger et al., 2003). Furthermore, the elevation of ERK1/2 activation is possibly due to the initial pro-survival response of the cells to bisPMB induced stress because the inhibition of ERK1/2 activation with the specific MEK1/2 inhibitor U0126 led to an increase in bisPMB induced cytotoxicity. This observation is consistent with the protective effect of ERK1/2 pathway from ajoene induced apoptosis in HL-60 leukaemia cells (Antlsperger et al., 2003). Interestingly, the protective role of the MEK/ERK pathway was not observed in the TG treated sample, suggesting that the MEK/ERK pathway did not have a significant effect for TG.

The findings presented in this Chapter support our hypothesis that bisPMB induced ER stress/ UPR and MAPK signalling pathways in WHCO1 cells. BisPMB increased the expression of pro-survival UPR associated events such as ubiquitination and an increased expression in GRP78/BIP and activation of the UPR pathways. As expected, ERK1/2 protected WHCO1 cells against bisPMB cytotoxic activity. On the other hand, CHOP played a key role in bisPMB induced cytotoxicity but JNK and p38 MAPK signalling pathways were activated but not key for

cytotoxicity. Whereas, CHOP and JNK activation were seemingly required for TG induced cytotoxic activity.

Thus far, widely studied molecular mechanisms of garlic derived OSC include the induction of the mitochondrial dependent caspase cascade, activation of mitogen activated protein kinase (MAPK) pathways, intracellular calcium mobilization and enhancement of reactive oxygen species (ROS) production in various cancer cells. However, ER stress induction by garlic OSC is not a widely held hypothesis. To our knowledge, our lab was the first to show that ajoene targets the ER, promotes the accumulation of protein aggregates, increases protein ubiquitination and enhances GRP78/BIP expression in MDA-MB-231 breast cancer cells (Kaschula et al., 2015).

The findings from this chapter provided new insights into the mechanism of action of bisPMB in WHCO1 cancer cells. It showed that CHOP plays a central role in bisPMB inhibitory activity and that ERK1/2 reduced the cytotoxic activity of bisPMB in WHCO1 cells.

CHAPTER 5: GENERAL DISCUSSION, CONCLUSION AND FUTURE WORK

5.1 GENERAL DISCUSSION

This thesis investigated the role played by UPR and MAPK signalling pathways in bisPMB induced cytotoxic activity against oesophageal cancer WHCO1 cells. The findings of this study provided insight into the mechanisms of action of bisPMB as a potential therapeutic against OC cancer.

In vitro and *in vivo* studies have reported ajoene induced cytotoxic activity against a variety of cancer cell lines (Li et al., 2002a, Hassan, 2004). BisPMB is an ajoene analogue that is found to be more active than ajoene against various cancer cells lines, with best potency and selectivity against esophageal cancer WHCO1 cells (Hunter et al., 2008, Kaschula et al., 2011). In line with these reports, we found the anti-proliferative activity of bisPMB in WHCO1 cells to be time and concentration dependent with similar 7 μM values in the three oesophageal cancer cell lines tested (WHCO1, WHCO6 and KYSE30 cells). The potency of bisPMB was found to be greater than cisplatin at inhibiting oesophageal cancer cell proliferation (Tanaka et al., 2010). Therefore bisPMB shows chemotherapeutic potential .

We found that bisPMB induces a concentration dependent G_2/M cell cycle arrest and apoptosis in WHCO1 cells. The ability of anticancer agents to promote cell cycle arrest and apoptosis is key in managing the uncontrollable growth of cancer cells due to their ability to evade cell cycle check points and apoptosis (Hanahan and Weinberg, 2011). Ajoene has been shown to induce G_2/M cell cycle arrest and apoptosis in human leukaemia HL-60 cells (Dirsch et al., 2002, Li et al., 2002a), basal cell carcinoma TE354T (Tilli et al., 2003) and the prostate cancer DU145 cell line (Xiao et al., 2004). We found that bisPMB was more potent than ajoene at inducing cell cycle arrest and apoptosis. For example, cell cycle arrest and apoptotic activity of ajoene in human leukaemia HL60 cells was observed at a 40 μM concentration (Li et al., 2002a). Whereas we observed bisPMB induced G_2/M cell cycle arrest in WHCO1 cells at 7 μM concentration (7 μM) further demonstrating that bisPMB has an enhanced potency against cancer cell cytotoxicity.

We found that the antiproliferative activity of bisPMB was five times more pronounced and apoptosis was enhanced in WHCO1 cells compared to the normal oesophageal epithelial Het-1A cells. This was consistent with previous reports from our lab that bisPMB demonstrates enhanced anti-proliferative activity against a variety of cancer cell lines compared to their normal counterparts with the largest fold change selectivity of 2.9 for WHCO1 compared to normal EPC2 cells (Kaschula et al., 2011). In the case of ajoene, there are several reports that demonstrate selective cytotoxicity for cancer cells. Specifically, ajoene is reported to be more active against Burkitt lymphoma BJA-B than baby hamster kidney BHK21 (Scharfenberg et al., 1990) and against human leukaemia HL60, breast cancer MCF-7, nasopharyngeal KB, hepatocellular Bel 7402, gastric cancer BGC 823 and colon cancer HCT than kidney marsupial PtK2 cells (Li et al., 2002a). The human leukemic HL60 cell line is reported to be more sensitive to ajoene induced apoptosis than normal peripheral mononuclear blood PBMC cells from healthy donors (Dirsch et al., 1998). Selectivity is a necessary characteristic for cancer drugs as it can heighten the effect of the agent at low concentrations (Mencher and Wang, 2005). In addition, cancer cell selectivity by anticancer agents also minimizes toxic side effects to normal cells (Rao et al., 2013). Thus our findings provide further evidence that bisPMB may be a good candidate for the treatment of OC because it's selectively for cancer cells.

Following the above mentioned *in vitro* cytotoxicity observations; we performed mechanistic studies to unravel the molecular mechanisms underlying bisPMB induced cytotoxic activity in WHCO1 cells. Structure-activity studies revealed the vinyl disulfide group to be the pharmacophore for bisPMB in WHCO1 OC cancer cell line (Kaschula et al., 2012). Further reports support the hypothesis that ajoene and related garlic OSC induce their cytotoxic effects through *S*-thiolation of cellular thiols via mixed disulfide formation (Gargouri et al., 1989, Gallwitz et al., 1999, Hosono et al., 2005, Kaschula et al., 2012). We have recently found that ajoene targets the endoplasmic reticulum in breast cancer MDA-MB-231 cells where it *S*-thiolate numerous protein targets and interferes with protein folding (Kaschula et al., 2015). This effect was found to increase the expression of GRP78/BIP in the MDA-MB-231 breast cancer cell line (Kaschula et al., 2015). GRP78/BIP, an ER resident chaperone, is commonly indicative of ER stress and unfolded protein response (UPR) . Consistent with these reports, our gene expression study demonstrated that bisPMB primarily targets the UPR mainly driven by XBP-1. The role of XBP-1 in cancer thus far has been pro-survival (Chen et al., 2014). Since the bisPMB concentration used in this the gene expression study displays

minimal toxicity to the cells, it can be suggested that the initial response of WHCO1 cells to bisPMB is pro-survival to counteract the imbalance caused by bisPMB entrance into the cell.

In addition, we found that bisPMB and the ER stress inducer TG affected some common pathways in WHCO1 cells. These common pathways included the protein processing in the endoplasmic pathway, pathways in cancer and the MAPK signalling pathways. The protein processing in the ER pathway was inclusive of the ER stress pathway, which was found to be the most significantly enriched pathway in the bisPMB sample. UPR pathways have been implicated in crosstalks with the MAPK pathways and garlic OSCs are known to activate the MAPK signalling pathways (Antlsperger et al., 2003, Shin et al., 2012, Darling and Cook, 2014). In addition, there is some emerging evidence that garlic OSC may also induce ER stress in cancer cells. ER stress was activated by DADS in human colon cancer cells COLO 205 (Yang et al., 2009) and by DATS in basal cell carcinoma BCC cells (Wang et al., 2012).

We found that BisPMB and TG deregulate ER stress/UPR pathways in a time dependent manner as evidenced by the increase in ATF4 expression, GRP78/BIP expression and decreased ATF6 p90 expression as well as increased splicing of XBP-1mRNA in WHCO1 cells. This confirmed the Gene Ontology data, which showed that bisPMB primarily induces UPR activation in WHCO1 cells. The ER stress pathway is increasingly been studied as a target for cancer therapy (Boelens et al., 2007), as the triggering of ER stress in already stressed cancer cells may sensitise the cells to apoptosis. Thus, the activation of ER stress by bisPMB may potentiate its effects as an anticancer agent.

Prolonged UPR is known to trigger ER stress induced apoptosis, which is associated with the induction of CHOP and the activation of the JNK signalling pathway (Urano et al., 2000, Matsumoto et al., 2013). We observed a time dependent induction of CHOP and JNK1/2 phosphorylation/activation. Furthermore, siRNA silencing of CHOP abolished the cytotoxic activity of bisPMB and TG in WHCO1 cells; illustrating that CHOP is a central regulator in bisPMB induced cytotoxic activity in WHCO1 cells. CHOP has been reported to play a critical role in TG induced apoptosis in prostate cancer cell lines LNCaP, A2780S and DU145 (Yamaguchi and Wang, 2004). On the other hand, the inhibition of JNK activation was found to have no effect on bisPMB induced cytotoxicity, implying that JNK activation is secondary to CHOP induction and not critical for cytotoxicity. Our finding is supported by that in the literature in which inhibition of JNK activation by the JNK 1-3 inhibitor SP600125 did not alter ajoene induced apoptosis in HL-60 cell lines (Antlsperger et al., 2003). This

suggested that BisPMB induced cytotoxic activity required CHOP but not JNK MAPK activation in WHCO1 cells, whereas TG required CHOP and JNK activation to induce its cytotoxic activity against WHCO1 cells. This is the first time that cytotoxicity of garlic-related disulfides has been exclusively linked to UPR and induction of CHOP.

Like the JNK signalling pathway, other MAPK family members such as p38 and ERK1/2 have been implicated in ER stress induced apoptosis. BisPMB was found to induce a time dependent phosphorylation/activation of p38 and ERK1/2 MAPK. This is in line with ajoene and *Z*-ajoene induced p38 and ERK1/2 phosphorylation/activation in human leukaemia HL-60 cells (Antlsperger et al., 2003) and human glioblastoma multiforme cancer stem cells (Jung et al., 2014). The inhibition of p38 MAPK had no effect on bisPMB cytotoxicity. However, the inhibition of ERK signalling pathway with U0126 MEK1/2 inhibitor enhanced the cytotoxic activity of bisPMB. This may be explained by the MEK/ERK pathway playing a pro-survival role in response to bisPMB as the MEK/ERK pathway promotes cell survival, differentiation and proliferation (Yang et al., 2013). Also, MEK/ERK pathway has been implicated downstream of ER stress activation. IRE-1 induced ERK1/2 activation is reported to enhance the proliferation of gastric cancer cells under ER stress conditions (Zhang et al., 2009). Chronic ER stress promotes tumour progression of hepatocellular carcinoma cells through enhancement of the activation of ERK pathway (Dai et al., 2009). The MEK/ERK activation may diminish the cytotoxic activity of bisPMB as breast and lung cancer cell lines resist thapsigargin or tunicamycin induced ER stress induced cell death by activating the MEK/ERK pathway to promote cancer cell survival (Hu et al., 2004). Moreover, the inhibition of the MEK/ERK pathway is reported to enhance the anticancer activity of known chemotherapeutic drugs such as cisplatin and paclitaxel in non small cell lung cancer (NSCLC) cell lines A549, H460 and H1703 (MacKeigan et al., 2000, Kim et al., 2015). In addition, the inhibition of MEK/ERK pathway by U0126 and PD 98059 enhanced ajoene induced apoptosis in HL-60 cell (Antlsperger et al., 2003). From these observations, it is clear that the MEK/ERK pathway opposes the effect of cancer cell killing agents, including bisPMB.

The modulation of multiple intracellular pathways by anticancer agents is beneficial to cancer therapy as the cancer disease is characterised by the abnormal functioning of numerous molecular events (Hanahan and Weinberg, 2011). In addition, anticancer drugs targeting multiple pathways are reported to re-establish the balance caused by abnormality of disrupted molecular events that underlie tumour progression (Mencher and Wang, 2005). For this

thesis, BisPMB was found to activate key components of the UPR and MAPK pathways at different time points. The initial response appears to be pro-survival as the data collected at the early time points (2 – 6 hours) showed that bisPMB had no effect on WHCO1 cell viability and a dramatic increase in ERK1/2 activation, ATF6 cleavage and XBP-1 splicing. This seems to be orchestrated by IRE1 as both XBP-1 and ERK1/2 have been reported to be downstream of IRE1 activation (Lee et al., 2003a, Zhang et al., 2009, Iwawaki and Akai, 2006). At the later time points (8 – 24 hours), we found that bisPMB induced a decrease in WHCO1 cell viability which correlated with an increase in protein ubiquitination, CHOP, JNK activation, p38 activation and ATF4. Thus far, it can be said that CHOP and the MEK/ERK pathways may play a significant role in bisPMB induced cytotoxic activities in WHCO1 cells. Thus, bisPMB may be a good target for OC therapy because it influences the activity of multiple pathways.

We previously found that ajoene targets the endoplasmic reticulum, where it *S*-thiolate newly synthesized proteins (Kaschula et al., 2015), disrupting the protein's ability to fold. This would lead to an increase in misfolded proteins in the ER, resulting in ER stress and subsequent UPR activation. We observed that bisPMB induced activation of UPR was accompanied by an increased GRP78/BIP protein expression and protein ubiquitination (figure 5.1). Moreover, bisPMB induced UPR pathways including ATF6, IRE-1 and PERK facilitate an increase in the transcription factor CHOP/GADD153, which reduced WHCO1 cell viability (figure 5.1). Simultaneously, the MEK/ERK pathway counteracted the anti-proliferative activity of bisPMB. Although, bisPMB activated the JNK and p38 MAPK, they were not central to its cytotoxic activity (figure 5.1).

Identification of novel intracellular pathways is vital for rational drug combination design in cancer therapy as drug synergism is often attained by drugs that target different pathways (Clark et al., 2010). In this thesis, the ER stress and MAPK pathways were shown to act as the primary targets for bisPMB cytotoxic activity. Numerous ER stress inducing anticancer agents such as cisplatin, carboplatin and thapsigargin based pro-drug G202, have been shown to have positive outcomes in cancer patients (Tombal et al., 2000, Rabik et al., 2008, Brozovic et al., 2013, Antonarakis and Carducci, 2010, Michelangeli and East, 2011). Since the MEK/ERK pathway counteracts the cytotoxic activity of bisPMB, combination of bisPMB with agents that inhibit the MEK/ERK pathway such as Vermurafenib, Trametinib, MEK162, AZD6244, SCH772984 in different phases of drug development (Samatar and Poulikakos, 2014), may be useful in therapy for OC treatment.

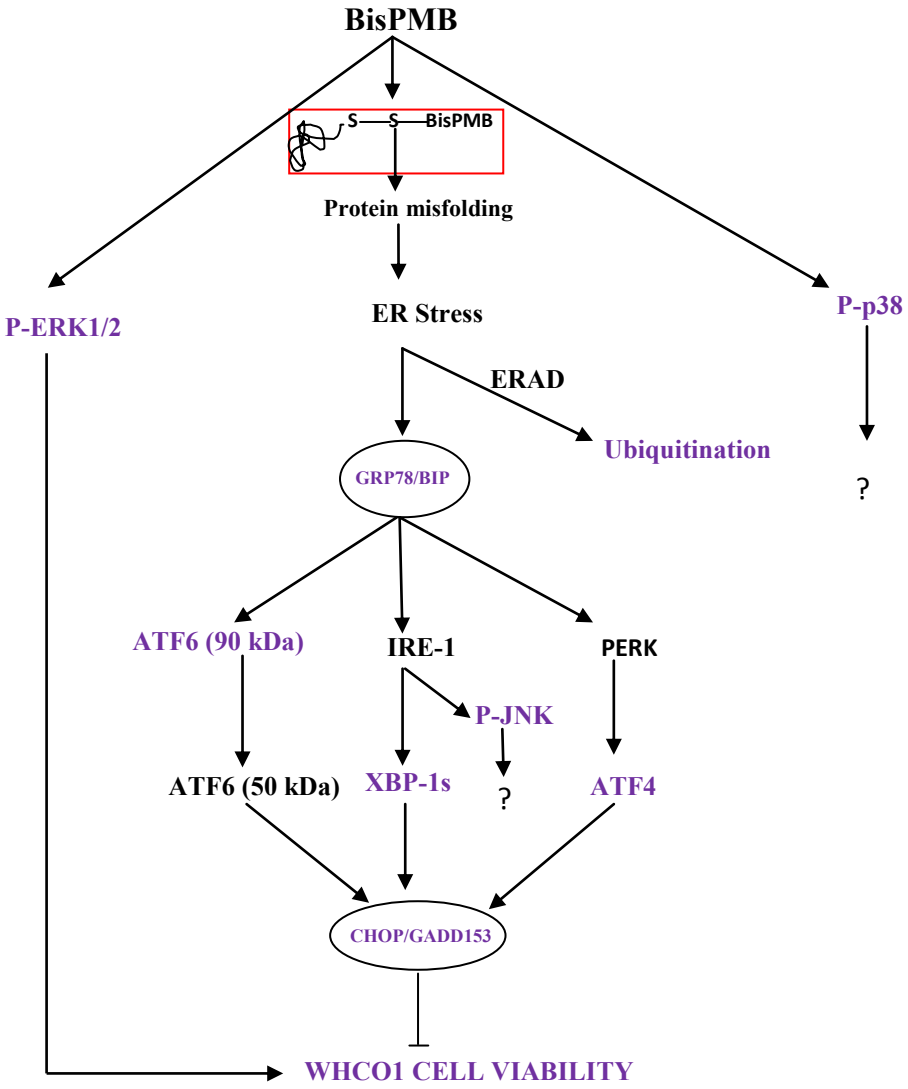

Figure 5.1 Schematic representation of summary of the key findings of this study in WHCO1 cells treated with bisPMB. The red box indicates the proposed bisPMB induced protein *S*-thiolation in the endoplasmic reticulum of WHCO1 cells. The arrows and entities in black represent pathways and cellular processes documented in the literature. In purple are the pathways and findings identified in this thesis.

5.2 CONCLUSION

This thesis provided insights into the intracellular pathways contributing to the cytotoxicity of bisPMB in WHCO1 cells. It also demonstrated that WHCO1 cell response to bisPMB shared similarities with TG, an ER stress inducer.

We showed that bisPMB induced its cytotoxic activity in oesophageal cancer cells by inhibiting cell viability, inducing G_2/M cell cycle arrest, apoptosis and late stage apoptosis/ secondary necrosis. We then demonstrated that bisPMB primarily targets the UPR at sub-toxic concentrations. Furthermore, bisPMB activated the ER stress/UPR and MAPK pathways. Moreover, CHOP/GADD153 and ERK1/2 were critical to the cytotoxic activity of bisPMB in WHCO1 cells.

Even though ER stress and MAPK are activated in bisPMB treated WHCO1 cells, it is unlikely that they may be solely responsible for bisPMB's cytotoxicity. The findings of this thesis contribute to the current understanding of the molecular mechanisms underlying the anticancer activity of bisPMB and its parent compound, ajoene. Consequently, a comprehensive understanding of bisPMB underlying molecular events may serve as a vital tool in rational design of anticancer drug combinations with ajoene or bisPMB.

5.3 FUTURE WORK

5.3.1 Drug combinations

Since the cytotoxic activity of bisPMB was found to be reduced by ERK1/2 activation and enhanced by CHOP, it would be interesting to evaluate synergism in drug combinations of bisPMB and clinically used MEK/ERK inhibitors. The MEK/ERK inhibitors that can be used in these experiments include the Vermurafenib, Trametinib, MEK162, AZD6244, and SCH772984. In addition to the above mentioned anti-cancer drugs,cisplatin, a commonly used drug for oesophageal cancer has been shown to induce ER stress in human melanoma 224 and colon cancer HCT116 cell lines (Mandic et al., 2003). The induction of ER stress has been documented to enhance the efficiency of cisplatin chemotherapeutic effect (Xu et al., 2014). Thus, the effect of the combination of cisplatin with another ER stress inducing compound like bisPMB on treatment of oesophageal cancer should be evaluated. For the future experiments of this study, bisPMB and cisplatin can be used in combination to treat oesophageal cell lines and assessed whether the combination has a synergistic, antagonistic or additive effect.

5.3.2 Animal studies

The cytotoxic effect and the data on the molecular mechanisms of bisPMB in oesophageal cancer cells observed in this thesis demonstrate bisPMB as a promising OC cell killing agent. In the drug discovery process, *in vivo* studies are conducted following *in vitro* tests. In addition, reports on *in vivo* mouse models studies conducted in both wild type (CHOP+/+) and knockout (CHOP-/-) mice. Thus, the next step would be to perform animal studies on WHCO1 cell engrafted mice and monitor change in tumour size.

5.3.3 ROS Production and inhibition of calcium ATPase

ROS plays a major role in therapy cancer cell death (Benhar et al., 2002) and mediates OSC induced apoptosis in cancer cells. ROS production is key in ajoene induced apoptosis in human lymphoma U937 cells (Kelkel et al., 2012), leukaemia HL60 (Dirsch et al., 1998) and adipocytes 3T3-L1(Yang et al., 2006b).In addition ROS accumulation is reported to trigger ER stress in prostate cancer cell lines treated with Shikonin (Gara et al., 2015). Thus the ability for bisPMB to increase ROS production in WHCO1 cells should be evaluated.

Garlic OSC, DADS was found to inhibit the growth of human colon, lung and skin cancer by reducing the expression of calcium ATPase activity and consequently increasing intracellular calcium levels (Sundaram and Milner, 1996). Since TG induces ER stress by inhibiting the Ca ATPase, it would be interesting to test whether bisPMB had any effect on the expression of Ca^{2+} ATPase. Therefore, future experiments should include the detection of Calcium ATPase expression and activity levels.

CHAPTER 6: MATERIALS AND METHODS

6.1 Cell Culture

6.1.1 Cell lines used in the project

The experiments in this study were conducted in human oesophageal squamous epithelial carcinoma cell lines WHCO1, WHCO6 and KYSE30. The SV40 large T-antigen immortalised Het1-A cell line was used as a normal epithelial control cell line. WHCO1 and WHCO6 were derived from biopsies of South African patients (Veal & Thornly, 1989). The KYSE30 cell line was derived from the middle intra-thoracic oesophagus of a 64 year old Japanese man (Shimada et al., 1992). Het1-A cell line, immortalized with SV40 large T-antigen,was derived from a 25 year old black male and obtained from the American type culture collection (ATCC® CLR-2692™)(Stoner et al., 1991). All the cells were grown in Dulbecco's Modified Eagle medium (DMEM) (Gibco®, Life Technologies, USA) supplemented with 10% foetal bovine serum (FBS)((HyClone™ ,GE Healthcare Life Sciences, USA), 100 U/ml penicillin and 100µg/ml streptomycin (Pen strep) (Biochrom, Berlin, Germany) (complete media). The cells were maintained in a 37°C incubator with 5% carbon dioxide in 95% humidity.

6.1.2 Sub-culturing

Cells were cultured in complete media. Confluent (80%) cells were split at 1:3 ratio into 100mm culture dishes. For the splitting procedure; adherent cells were rinsed with phosphate buffer saline (PBS) (pH7.5) and lifted with 0.5% Trypsin 0.53mM Ethylenediaminetetraacetic acid (EDTA) in PBS. The 0.5% Trypsin/EDTA was then deactivated by adding equal volume of DMEM/FCS to the detached cells. The cells were then transferred to a 12 ml tube and spun at 4000 rpm for 3 minutes (Hettich®EBA 20 Centrifuge, sigma-Aldrich, USA). The supernatant was removed and discarded and the pellet resuspended in DMEM/FCS and cultured in100mm culture dishes.

6.1.3 Freezing/Thawing of cells

For long term storage, the cells were frozen in liquid nitrogen. The culture medium was removed from adherent cells which were then detached with 0.5% Trypsin/EDTA for 3

minutes. An equal volume of DMEM/FCS was added to detached trypsinised cells. The cells were centrifuged at 4000rpm for 3 minutes and the pellet was resuspended in freeze down media (DMEM supplemented with 20% foetal calf serum FCS and 10% dimethyl sulfoxide (DMSO), Sigma Aldrich, USA). A volume of 10 µl of the resuspended cells was subsequently stained with tryphan blue (Molecular Probes®, life technologies, USA), counted using cells countess counter with countess glass slides (Invitrogen™, Life technologies, USA) and $1X10^6$ cells are aloquoted in cryotubes. The aliquot tubes were then placed at -80°C for 24 hours and transferred to the liquid nitrogen tank for long term storage.

6.1.4 Thawing protocol

When required, cells were removed from the nitrogen storage and immediately thawed in a 37˚C water bath. The cells were then transferred to 12 ml falcon tubes and centrifuged at 4000rpm for 3 minutes; this was followed by the removal of the freeze down media. The cells were resuspended in fresh complete medium and cultured in 100mm culture dishes.

6.1.5 Mycoplasma Test

I order to ensure cells were mycoplasma free, cells were cultured in pen/strep free DMEM media. The cells were then spun at 4000rpm for 3 minutes and supernatant was removed. Following the resuspension of cells with pen strep free media, drops of the cells were added to sterile cover slip which were transferred to a 6 well plate and incubated at 37˚C incubator for 1 hour. After incubation, the full media was added carefully to each well and incubated at 37˚C overnight. Subsequent to the overnight incubation, a fixative solution was added twice to each well and incubated at room temperature for a few seconds. Distilled water was used to rinse off the fixative solution and then the cover slips were incubated with the staining solution for no longer than 30 seconds. The stain was washed off with distilled water and placed face down onto the glass slide. The slide was then viewed under an Olympus florescent microscope (Olympus© X81S8F, Japan) at 100X magnification, and images were captured using digital camera (Olympus© X81S8F, Japan).

6.1.6 Morphology

The cells were seeded at a density of $5x10^4$ cells per well in a 6 well plate and allowed to attach overnight at 37˚C. The following day, the cells were treated with 3.5 µMor 7 µM or 14 µM of bisPMB for 24 hours or 0.1% DMSO for 24 hours. The images of the cells were

subsequently captured using an Olympus SC30 digital camera (Olympus© SC30, Japan) at 10 and 20 x magnification. Phase contrast images were then captured using a microscope digital camera (Olympus© SC30, Japan) and analysed with the analysis getIT image analysis software (Olympus© SC30, Japan).

6.2 Cell viability assays

6.2.1 WST assay

The WST-1 assay was used to quantify cell proliferation. The water soluble tetrazolium (WST) (Roche, Indianapolis, IN, USA) salt is cleaved by metabolically active cells to form formazan. Briefly, 2.5 x 10^3 cells/well were seeded in a 96 well culture plate (SPL life sciences, Korea) and allowed to settle overnight. Following incubation with the test compound 10µl/well of wst reagent was added onto the cells and incubated at 37℃ for 4 hours. The colorimetric intensity of the formazan was measured at the absorbance of 450nm, with a reference reading of 650nm using the Multiskan FC multi well plate reader (Thermo scientific, USA). The data obtained from the absorbance readings was presented as mean ± SD of quadruplicate technical replicates using GraphPad Prism version 5.01 software.

6.2.2 MTT assays

The MTT assay was used to indirectly measure cell proliferation by quantifying the viability of metabolically active cells (Mosmann, 1983). Viable cells reduce the yellow tetrazolium salt to blue-purple formazan crystals, with the aid of the cofactors nicotinamide adenine dinucleotide phosphate (NADPH) and nicotinamide adenine dinucleotide (NADH). The MTT assay was carried out by seeding 2.5 x 10^3 cells/ well to a final volume of 90µl in a 96 well culture plate (SPL life sciences, Korea). Following the desired incubation with the test compound, 10µl of thiazol blue tetrazolium bromide (MTT) (Sigma Aldrich, USA) was added to the cells and incubated at 37°C for 4 hours. The blue formazan crystals that resulted from the reduction of the yellow MTT by viable cells were solubilised with 100µM sodium lauryl sulphate (SLS) for 16 hours at 37℃. The resulting colorimetric intensity was measured at the absorbance of 595nm with Multiskan FC multi-well reader (Thermo scientific, USA). The data obtained from the absorbance readings was presented as mean ± SD of quadruplicate technical replicates using GraphPad Prism version 5.01 software.

6.3 Cytotoxicity assays

6.3.1 IC_{50} determination

The IC_{50} in WHCO1, WHCO6, KYSE30 and Het-1a cells were determined by seeding 2.5 x 10^3 cells /well in 96 well culture plates and allowed to attach overnight. A twofold dilution series of the bisPMB dissolved in DMSO was prepared and then added to the cells at 1:1000 dilutions, to achieve 0.1% DMSO final concentration. The cells were subsequently incubated with the bisPMB for 24 or 48 hours, depending on time point of the IC_{50} determination. Following treatment, 10µl MTT reagent (Roche, Indianapolis, IN, USA) was added to the cells and incubated at 37˚C for 4 hours, after which 100µl solubilisation reagent (SLS) was added to the cells. The plates were then incubated overnight and read at 595nm with the Multiskan FC multiwell reader (Thermo scientific, USA).

6.3.2 IC_{50} Data Analysis

The IC_{50} and 95% confidence interval (CI) were derived from quadruplicate data retrieved from the Multiskan FC multiwell reader (Thermo scientific, USA). The data was analysed with version 5.0 of GraphPad prism version 5.01 software (GraphPad Prism software Inc., San Diego, USA). The values obtained from the absorbance readings were presented as mean ± SD, log transformed and fitted onto a non linear regression log (inhibitor) vs. response equation in order to construct a sigmoidal dose response curve.

6.3.3 Lactate dehydrogenase (LDH) assay

The quantification of cell cytotoxicity was performed with the lactate dehydrogenase activity assay kit (Roche Diagnostics, Mannheim Germany). The LDH assay was carried out as described in the manufacturer's instructions. Briefly, 3 x 10^3 WHCO1 cells per well were seeded in a 96 well culture plate and allowed to attach at 37˚C overnight. The following day, WHCO1 cells were treated with 1µM or 10µM bisPMB dissolved in DMSO or 0.1% DMSO for 3h, 6h, 24h and 48 hours. Lysis buffer was added to the cells followed by incubation at room temperature for 15 minutes with gentle shaking. The reaction mixture (see appendix A) was prepared according to the manufacturer instructions and added to the lysate. The absorbance was read at 492 nm with the reference wavelength of 620 nm, with a Multiskan FC multiwell reader (Thermo scientific, USA) and analysed using GraphPad Prism version

5.0 (GraphPad Prism software Inc., San Diego, USA). The assay was conducted in quadruplicate and data was presented as mean ± SD.

6.4 Histone associated DNA fragmentation apoptosis assay

Apoptosis was detected using the Cell death Detection Elisa ^{PLUS} kit (Roche Diagnostics, Mannheim Germany), which quantified cytoplasmic mono and oligonucleotides in cells undergoing apoptosis. The histone associated DNA fragmentation apoptosis assay was carried our according to manufacturer's instructions. Briefly, 5×10^3 cells/ well were seeded in a 96 well culture plate and allowed to attach at 37°C overnight. Following the 24 hour treatment of the cells with bisPMB or 0.1% DMSO, the 96 well culture plate was centrifuged for 10 minutes at $200\times g$. Subsequently, 50µl of the supernatant was removed from each well, followed by the addition of the lysis buffer and 30 minute incubation at 25℃. After cell lysis was complete, 20µl of the cell lysate was transferred to a streptavidin coated 96 well culture plate and then 80µl of immunoreagent containing anti-histone-biotin, anti-DNA-POD (anti- DNA horse radish peroxidise) and incubation buffer was added. The 96 well culture plate was then incubated on a shaker (200 rpm) at 25℃ for 2 hours covered with an adhesive foil. This was followed by the removal of the immunoreagent and washing of the wells with incubation buffer. 100µl of ABTS solution was subsequently added to the wells incubated for 10 minutes while shaking at 200rpm. Following the colourimetric development, 100µl of ABTS stop solution was added to stop the reaction and then the absorbance of developed colour intensity was measured at 405nm with the reference wavelength of 492nm using the Multiskan FC multiwell plate reader (Thermo scientific, USA). The data obtained from the absorbance readings was presented as mean ± SD of triplicate technical replicates using GraphPad Prism version 5.01 software.

6.5 Cell cycle analysis

The effect of the bisPMB on the cell cycle was determined by fluorescence activated cell sorting (FACS) analysis in cells stained with propidium iodide. Briefly, 1×10^6 WHCO1 cells were seeded in a 100mm culture dish and allowed to attach overnight at 37°C. Following the treatment of with bisPMB for 24 hours, the cells were harvested (including floating cells) with 0.5% Trypsin EDTA, fixed with 70% ethanol and stored at -20°C for up to two weeks. Cells were then spun at 4000rpm for 5 minutes and washed twice with 1 × PBS. After the washing step, the cells were incubated with 50µg/ml RNase A (Roche,

Indianapolis, IN, USA) for 15 minutes at 37°C and stained with the propidium iodide staining solution. The flow cytometer (FACScalibur®, Becton Dickinson (BD) Biosciences, San Jose, CA) was used to count 50000 cells for each analysis. The analysis of the cell cycle data was carried out using the ModFit 3.0 software (Verity, Topsham, ME).

6.6 Transient knock down of CHOP in WHCO1 cells

In order to attenuate the expression of CHOP in WHCO1 cells we used CHOP specific small interfering (siRNA). Briefly, 1.5×10^5 WHCO1 cells are seeded in a 12 well culture plate and allowed to settle overnight at 37˚C. Afterwards, the cells were washed with 1× PBS and then incubated with the transfection solution containing transfectin (TransFectin™ Lipid reagent, BIO-RAD, Hercules, CA) and 40nM CHOP siRNA (Sigma- Aldrich, USA) or control siRNA (Santa Cruz Biotechnology, USA) in serum free DMEM. Six hours post transfection; the transfection media were removed and replaced with complete DMEM.

6.7 Polymerase chain reaction (PCR)

6.7.1 RNA Extraction

Total RNA was isolated from cells using the phenol-chloroform extraction method (Chomczynski and Sacchi, 1987). Briefly, 1 x 10^6 cells were seeded in 100mm culture dishes and allowed to attach overnight. The cells were then incubated with the compound of interest for the desired experimental period. Following treatment, the media was removed from the cells and then the cells were rinsed twice with ice cold PBS. Subsequently, 1ml of QIAzol® lysis reagent (QIAGEN, Venlo, Netherlands) was added to the cells and immediately scraped off with a cell scraper (Greiner Bio-One, Monroe, NC). The cell lysate was then homogenised by passing it through a pipette several times, transferred it to a 1.5µl eppindorfs and incubated it on ice. This was followed by the addition of 200µl of chloroform and subsequent incubation for 3 minutes. The samples were then centrifuged at 12 000 rpm for 15 minutes . After the separation of phases, the top aqueous phase was transferred to a clean 1.5ml eppie and mixed with Isopropanol in order to precipitate the RNA from the solution. The RNA was subsequently washed with 75% diethylpyrocarbonate (DEPC) (Sigma Aldrich, USA) ethanol. The RNA pellet was air dried for 10 minutes and resuspended with 30µl DEPC treated water. The RNA sample preparation was followed up with 5 minute incubation at 55˚C in the heating blocks, to dissolve the RNA. For long term storage, the RNA was then preserved at -80℃.

6.7.2 RNA clean up

RNA clean up was carried out using the RNeasy mini kit (QIAGEN, Venlo, The Netherlands). The RNA clean up was carried out as described by the manufacturer. Subsequent to dissolving the RNA in DEPC water, the volume was adjusted to 100µl with RNAse free water. The RTL buffer (see appendix A) and 100% ethanol was used to precipitate the RNA with a Qiashredder (QIAGEN, Venlo, The Netherlands) and washed with 70% ethanol. RNAse free water was then used to elute the RNA from the column.

6.7.3 RNA Quantification

Total RNA concentration was measured using the Nanodrop 2000 (Thermo Fischer Scientific, USA). The absorbance was measured at the wavelength 260 and 280nm RNA that had A260/280 ratio between 1.8 - 2.0 was considered pure.

6.7.4 Formaldehyde gel electrophoresis for RNA quality evaluation

The quality of the RNA was assessed by 1.5% formaldehyde gel electrophoresis. 1.5gof agarose powder (Roche Diagnostics, Mannheim Germany) was dissolved in 4-Morpholinepropanesulfonic acid (MOPS) by heating. After cooling of the solution formaldehyde and 0.001% of ethedium bromide (Sigma Aldrich, USA) was added to the solution and allowed to set on the casting tray. Approximately 2µg of RNA was loaded onto the formaldehyde gel and separated at 100V for 30 minutes. The gel was visualised under UV in the UVP BioSpectrum™500 Imaging System (UVP, LCC Upland, CA, USA) and images were captured using the CCD camera (Canon Inc., Tokyo).

6.7.5 Complementary DNA synthesis

RNA was reverse transcribed using the ImpromII Reverse transcription system (Promega© Inc, Madison, WI, USA) kit. Complementary DNA (cDNA) synthesis was performed according to the manufacturer instructions. Briefly, 3µg of RNA was mixed with 50µM oligo-dT $_{(15)}$ primer, 10mM dNTPs and nuclease free water and incubated at 70℃ for 10 minutes. This was followed by the addition of master mix, contains 1.5 mM $MgCl_2$, dNTPs, RNAse inhibitor (RNAsin), 5× first strand reaction buffer and reverse transcriptase (RT),

and incubation at 42℃ for 2 hours, followed by heat inactivation at 70℃ for 10 minutes. For long term storage, cDNA was stored at -20℃.

6.7.6 Quantitative PCR

Quantitative polymerase chain reaction (qPCR) was conducted in order to measure the relative change in gene transcription. Briefly, 2 × KAPA^{TM} SYBR® fast qPCR master mix (KAPA BIOSYSTEMS, Boston, Massachusetts), RNAse free water, 0.5µmol forward and reverse primers (see appendix B) and cDNA were loaded onto low profile 96 well culture plate (SPL Life Sciences, Korea). Glyceraldehyde 3- phosphate dehydrogenase (GAPDH) primers were used as a reference for each experiment. Following brief centrifugation of the 96 well plates, the light cycler 480 (Roche, Mannheim Germany) was then used for PCR amplification. Each qPCR experiment had four technical replicates and at least two biological replicates.

6.7.7 Relative Quantification

The threshold cycle (C_t) values obtained from the light cycler 480 were used to calculate fold changes in gene expression. The $2^{-\Delta\Delta Ct}$ method was used to calculate fold change in gene expression (Yuan et al., 2006). This method normalizes the gene of interest with a reference gene such as GAPDH and then calculates the difference in gene expression between two experimental conditions for example treated (T) versus untreated (UT). This method assumes that the amplification efficiency of each experiment is 2. Therefore the fold induction is equal to $2^{-\Delta\Delta Ct}$ and $\Delta\Delta Ct = [C_t\,(\text{gene of interest})_{UT} - C_t\,(\text{reference gene})_{UT}] - [C_t\,(\text{gene of interest})_{T} - C_t\,(\text{reference gene})_{T}]$.

6.8 Microarray

6.7.2 RNA Preparation

In order to investigate the effect of bisPMB on WHCO1 gene expression and to ascertain if bisPMB induced ER stress, the microarray analysis was conducted. Total RNA was extracted from WHCO1 cells treated with 3.5 µM bisPMB concentration, 1µM Thapsigargin or incubated in DMEM for 24 hours. Each experiment was conducted in quadruplicate.

6.8.2 Quality Control of RNA and microarray

The quality control (QC) and microarray analysis was performed at the Centre for Proteomic and Genomic Research (CPGR). Twelve RNA samples were analysed using the nanodrop ND1000 spectrophotometer (Thermo Fischer Scientific, USA) and the Agilent 2100 Bioanalyser Eukaryotic Total RNA Nano Assay (Agilent Technologies, Germany) with an internal control RNA sample ~ 20ng/µl bieng included. The nanodrop was used to measure the sample concentration and the presence of possible contaminants and the Agilent 2100 Bioanalyser Nano assay was used determine RNA integrity and suitability (Panaro et al., 2000). The RNA Integrity Number (RIN) number was used to evaluate the suitability of the RNA sample (Schroeder et al., 2006). RNA samples with a RIN of 7.00 – 10.00 were considered suitable for further processing. The RNA samples were then processed and hybridized to the Affymetrix Human Gene ST 2.0 chip, which contains over 24 000 probe sets. Briefly, total RNA was converted into biotin labelled complementary RNA (cRNA) transcribed from cDNA. The cRNA was then hybridized onto the Affymetrix human gene ST 2.0 array and stained. The quantification of fluorescent intensity and distribution patterns of transcripts was obtained with the GeneChip® Scanner 3000 7G, from which the Affymetrix CEL files were generated.

6.8.3 Data analysis

The Affymetrix CEL files containing the raw intensities of the probe set were imported onto the Partek® Genomics

Suite™ software version 6.6 (Partek Inc., St Louis, MI, USA). The data loaded onto the Partek® software was assigned to categorical comparison groups based on the biological replicates of the samples. The samples were subsequently subjected to the robust multi array average (RMA) method, which was used for normalization, background correction and summarization of the probe intensity values. The principal component analysis (PCA) and the hierarchical clustering were generated in order to demonstrate the clustering of biological replicates, identification of outliers and reproducibility of the samples. After that the 2 way Analysis Of Variance (ANOVA) between the untreated and bisPMB or thapsigargin treated samples *p*-values were calculated to measure significance of differentially expressed genes (DEGs). These p-values were further corrected using the Bonferroni test for false discovery rate (FDR). Additionally, the cut off for the significantly deregulated genes was set at -1.5 to + 1.5 fold and FDR *p*-value <0.05. The DEG list generated using these parameters were then used for functional enrichment analysis. The DEG list generated was used to construct a

Venn diagram, using the Partek® Genomics Suite™ software version 6.6, to visualize DEGs that are uniquely expressed or shared between the bisPMB and TG samples.

6.8.4 Functional Enrichment Analysis

The DEGs were inputted onto the web based integrated system GEne SeT AnaLysis Toolkit (WebGestalt) at http://bioinfo.vanderbilt.edu/webgestalt. WebGestalt was used to identify the significantly enriched gene ontologies (GO) and KEGG pathways from the DEG list (Wang et al., 2013). Furthermore the ingenuity pathway analysis (IPA) software was used to generate significantly enriched canonical pathways and interactive gene networks http://www.ingenuity.com (Viswanathan et al., 2008).

6.9 Western blotting

Western blot analysis was performed in order to quantify any change in protein levels or detection of post translational modifications induced by treatment in cells.

6.9.2 Protein Extraction

3×10^6 WHCO1 cells were seeded in 145mm culture dishes and treated with bisPMB or 0.1% DMSO for desired periods. Subsequently, cells were washed with cold 1 × PBS and lysed using 1 × Ripa buffer (Cell Signalling Technology, USA) supplemented with proteinase inhibitor (Roche, Mannheim Germany). Rubber cell scrapers (Greiner Bio-One, Monroe, NC) were used to scrape the lysate off the culture dish. After which, the lysate was transferred to 1.5ml eppendorf tubes, incubated on ice for 30 minutes and sonicated twice for 10 seconds. Subsequently, the whole cell lysate was centrifuged at 14000rpm for 5 minutes at 4℃ and transferred to a new 1.5ml eppendorf tube for storage at -20℃.

6.9.3 Protein Quantification

Protein quantification was performed using the Pierce® Bradford Protein Assay kit (Thermo Fischer Scientific, USA). Protein concentration was determined through the use of a standard curve from a serial dilution of bovine serum albumin (BSA) standards. 25µl of BSA standards and 2.5µl of cell lysate was seeded on a 96 well culture plate and mixed with the

Bradford coomassie reagent followed by 30 minute incubation at 37℃. The intensity of the colour was measured with the Multiskan FC multiwall plate reader (Thermo scientific, USA) at the absorbance value of 595nm.

6.9.4 Sodium dodecasulfate Polyacrylamide gel electrophoresis (SDS-PAGE)

6.9.4.1 Polyacrylamide Gel Electrophoresis

Proteins in whole cell lysate were separated on sodium dodecasulfate polyacrylamide gel electrophoresis (SDS-PAGE). The 1.5mm spacer glass plates (Bio-Rad, California, USA) were assembled into casting clamps (Bio-Rad, California, USA) for set up. After set up, 4% stacking and 6% to 10% separating gel (table 6.2) were prepared and loaded onto the glass plates. Subsequently, 50µg of protein was mixed with reducing 4× loading buffer and boiled at 95℃ for 5 minutes was then separated by electrophoresis at 150V for 1 hour.

Table 6.2 Reagents and volumes required for the preparation of the stacking and separating gel for western blot

Reagents	4% Stacking gel	6 % Separating gel	10 % Separating gel
Distilled H_2O	3.65ml	4.09ml	2.75ml
Tris buffer	0.625ml	3.75ml	3.75ml
30% bisacrylamide	0.650ml	2ml	3.35ml
10% SDS	50µl	100µl	100µl
10% APS	25µl	50µl	50µl
TEMED	5µ	5µl	5µl

6.9.4.2 Protein Transfer to nitrocellulose membrane

Once protein separation was completed, the proteins were transferred onto a 0.2µm nitrocellulose membrane (Bio-Rad, California, USA). The gel, nitrocellulose membrane, filter paper and sponges were used to make a sandwich in electrophoresis cassette (Bio-Rad, California, USA). This sandwich was then placed in transfer apparatus in the presence of 1 × transfer buffer. The transfer of protein was then performed at 100V on ice for 1 hour. After the transfer, the membrane is washed for 10 minutes with Tris-Buffered Saline / 0.1% Tween

20 (TBST) (see appendix A) on a shaker and briefly stained with the ponceau stain (Sigma Aldrich, USA) to check for protein loading and transfer efficiency.

6.9.4.3 Probing with primary and secondary antibody

Following the quality testing of protein transfer, the nitrocellulose membrane was blocked by 5% fat free powder milk (Clover, South Africa) dissolved in 1 × Tris-Buffered Saline / 0.1% Tween 20 (TBST) (Sigma Aldrich, USA) for 1 hour at room temperature in a shaker. The nitrocellulose membrane was then incubated with primary antibody (table 6.3) in 5% fat free powder milk (Clover, South Africa) dissolved in 1 × Tris-Buffered Saline / 0.1% Tween 20 (TBST) (Sigma Aldrich, USA) at 4℃ overnight. Subsequently the TBST was used to wash the membrane 3 X 15 minutes in order to remove excess primary antibody prior to incubation with secondary antibody (table 6.3) containing horse radish peroxidise (HRP) for 1 hour at room temperature. The chemiluminescent (LumiGloReserve, KPL Incorporated, USA) substrate solutions A and B prepared in a 1:2 ratio was added to the nitrocellulose membrane. The protein on the membrane was visualised under UV light in the dark room of the UVP BioSpectrum™500 Imaging System (UVP, LCC Upland, CA, USA), captured by the CCD camera (Canon Inc., Tokyo) and analysed with the Visionworks LS Acquasition analysis software (UVP, LCC Upland, CA, USA).

6.9.4.4 Protein Band Quantitation

The bands in the image captured by the UVP CCD camera were quantified using image J software. Once the western blot image has been opened with image J, the “analyze” tab was selected in order to choose the “gels” drop option. Following the selection of the “gels” option, a rectangle that covers the band of the first lane of each gel is drawn using the “rectangular selection”. The same rectangle is used to demarcate the band area in all the lanes of the image. Once an area of interest is outlined in each lane it is numbered using the control command in order to identify the lane. The density data from the band are is used to generate histograms of each lane, where the peaks of the histograms correspond to intensity of the band. The density data from the band are is used to generate histograms of each lane, where the peaks of the histograms correspond to intensity of the band. The value of the intensity of each band is then normalised to the intensity value of a loading control such as GAPDH.

6.9.5 Antibodies

Table 6.3 The sources of Primary and Secondary antibodies and their dilutions used for western blot analysis. P-JNK/p38/ERK indicates antibodies that detect phosphorylated forms of the proteins.

Protein	Supplier	Catalogue number	Dilution	Blocking	Source
GAPDH	Santa Cruz Biotechnology	sc-25778	1:1000	5% milk in TBST	Rabbit
CHOP	Cell Signaling Technology	D46F1	1:1000	5% milk in TBST	Rabbit
ATF4	Sigma Aldrich	SAB2500130	2mg/ml	5% milk in TBST	Goat
ATF6α	Santa Cruz Biotechnology	sc-22799	1:500	5% milk in TBST	Rabbit
UBIQUITIN	Santa Cruz Biotechnology	sc-9133	1:500	5% milk in TBST	Rabbit
JNK1/2	Cell Signaling Technology	9252	1:1000	5% milk in TBST	Rabbit
P-JNK1/2	Cell Signaling Technology	9251	1:1000	5% milk in TBST	Rabbit
GRP78	Sigma Aldrich	G9043	1:4000	5% milk in TBST	Rabbit
P- P38	Cell Signalling Technology	9211	1:500	5% milk in TBST	Rabbit
P38	Cell Signaling Technology	9212	1:1000	5% milk in TBST	Rabbit
P-ERK1/2	Cell Signaling Technology	9106	1:500	5% BSA in TBST	Mouse
ERK 2	Santa Cruz Biotechnology	Sc153	1:1000	5% milk in TBST	Rabbit

6.10 Kinase inhibition

In order to determine the significance of the role played by activated JNK and MEK-ERK signal transduction pathways, chemical inhibitors U0126 (MEK1/2 inhibitor) and SP600125 (JNK1/2 inhibitor) were used to inhibit the pathways. Briefly, 3.5×10^5 were seeded in 6 well culture plates and allowed to settle overnight. Different concentrations of U0126 (1µM, 5µM or 10µM) and SP600125 (5µM, 10µM, 20µM or 30µM) were used in order to determine the optimal concentrations required for inhibition of the JNK and MEK-ERK signal transduction pathways.

REFERENCES

AFAQ, F., ADHAMI, V. M., AHMAD, N. & MUKHTAR, H. 2003. Inhibition of ultraviolet B-mediated activation of nuclear factor kappaB in normal human epidermal keratinocytes by green tea Constituent (-)-epigallocatechin-3-gallate. *Oncogene,* 22**,** 1035-44.

AGARWAL, K. C. 1996. Therapeutic actions of garlic constituents. *Medical Research Reviews,* 16**,** 111-24.

ALI, B. H. & AL MOUNDHRI, M. S. 2006. Agents ameliorating or augmenting the nephrotoxicity of cisplatin and other platinum compounds: a review of some recent research. *Food and Chemical Toxicology,* 44**,** 1173-83.

ALLUM, W. H., STENNING, S. P., BANCEWICZ, J., CLARK, P. I. & LANGLEY, R. E. 2009. Long-term results of a randomized trial of surgery with or without preoperative chemotherapy in esophageal cancer. *Journal of Clinical Oncology,* 27**,** 5062-7.

AMAGASE, H. & MILNER, J. A. 1993. Impact of various sources of garlic and their constituents on 7,12-dimethylbenz[a]anthracene binding to mammary cell DNA. *Carcinogenesis,* 14**,** 1627-31.

AMAGASE, H., PETESCH, B. L., MATSUURA, H., KASUGA, S. & ITAKURA, Y. 2001. Intake of garlic and its bioactive components. *Journal of Nutrition,* 131**,** 955S-62S.

ANDERSEN, T. B., LOPEZ, C. Q., MANCZAK, T., MARTINEZ, K. & SIMONSEN, H. T. 2015. Thapsigargin--from Thapsia L. to mipsagargin. *Molecules,* 20**,** 6113-27.

ANTLSPERGER, D. S., DIRSCH, V. M., FERREIRA, D., SU, J. L., KUO, M. L. & VOLLMAR, A. M. 2003. Ajoene-induced cell death in human promyeloleukemic cells does not require JNK but is amplified by the inhibition of ERK. *Oncogene,* 22**,** 582-9.

ANTONARAKIS, E. S. & CARDUCCI, M. A. 2010. Future directions in castrate-resistant prostate cancer therapy. *Clinical Genitourin Cancer,* 8**,** 37-46.

ARAI, M., KONDOH, N., IMAZEKI, N., HADA, A., HATSUSE, K., KIMURA, F., MATSUBARA, O., MORI, K., WAKATSUKI, T. & YAMAMOTO, M. 2006. Transformation-associated gene regulation by ATF6 alpha during hepatocarcinogenesis. *Febs Letters,* 580**,** 184-190.

BANERJEE, S., BUESO-RAMOS, C. & AGGARWAL, B. B. 2002. Suppression of 7,12-dimethylbenz(a)anthracene-induced mammary carcinogenesis in rats by resveratrol: role of nuclear factor-kappaB, cyclooxygenase 2, and matrix metalloprotease 9. *Cancer Research,* 62**,** 4945-54.

BARABAS, K., MILNER, R., LURIE, D. & ADIN, C. 2008. Cisplatin: a review of toxicities and therapeutic applications. *Veterinary and Comparative Oncology,* 6**,** 1-18.

BEHREND, L., HENDERSON, G. & ZWACKA, R. M. 2003. Reactive oxygen species in oncogenic transformation. *Biochemical Society Transactions,* 31**,** 1441-4.

BEN-LEVY, R., HOOPER, S., WILSON, R., PATERSON, H. F. & MARSHALL, C. J. 1998. Nuclear export of the stress-activated protein kinase p38 mediated by its substrate MAPKAP kinase-2. *Current Biology,* 8**,** 1049-57.

BENHAR, M., ENGELBERG, D. & LEVITZKI, A. 2002. ROS, stress-activated kinases and stress signaling in cancer. *EMBO Reports,* 3**,** 420-5.

BHARTI, A. C., DONATO, N., SINGH, S. & AGGARWAL, B. B. 2003. Curcumin (diferuloylmethane) down-regulates the constitutive activation of nuclear factor-kappa B and IkappaBalpha kinase in human multiple myeloma cells, leading to suppression of proliferation and induction of apoptosis. *Blood,* 101**,** 1053-62.

BIANCHINI, F. & VAINIO, H. 2001. Allium vegetables and organosulfur compounds: do they help prevent cancer? *Environtal Health Perspectives,* 109**,** 893-902.

BLEIBERG, H., CONROY, T., PAILLOT, B., LACAVE, A. J., BLIJHAM, G., JACOB, J. H., BEDENNE, L., NAMER, M., DE BESI, P., GAY, F., COLLETTE, L. & SAHMOUD, T. 1997. Randomised phase II study of cisplatin and 5-fluorouracil (5-FU) versus cisplatin alone in advanced squamous cell oesophageal cancer. *European Journal of Cancer,* 33**,** 1216-20.

BLOCK, E., AHMAD, S., CATALFAMO, J. L., JAIN, M. K. & APITZCASTRO, R. 1986. Antithrombotic Organosulfur Compounds from Garlic - Structural, Mechanistic, and Synthetic Studies. *Journal of the American Chemical Society,* 108**,** 7045-7055.

BLOCK, E., NAGANATHAN, S., PUTMAN, D. & ZHAO, S. H. 1992. Allium Chemistry - Hplc Analysis of Thiosulfinates from Onion, Garlic, Wild Garlic (Ramsoms), Leek, Scallion, Shallot, Elephant (Great-Headed) Garlic, Chive, and Chinese Chive - Uniquely High Allyl to Methyl Ratios in Some Garlic Samples. *Journal of Agricultural and Food Chemistry,* 40**,** 2418-2430.

BOELENS, J., LUST, S., OFFNER, F., BRACKE, M. E. & VANHOECKE, B. W. 2007. Review. The endoplasmic reticulum: a target for new anticancer drugs. *In Vivo,* 21**,** 215-26.

BOSSET, J. F., GIGNOUX, M., TRIBOULET, J. P., TIRET, E., MANTION, G., ELIAS, D., LOZACH, P., OLLIER, J. C., PAVY, J. J., MERCIER, M. & SAHMOUD, T. 1997. Chemoradiotherapy followed by surgery compared with surgery alone in squamous-cell cancer of the esophagus. *New England Journal of Medicine,* 337**,** 161-7.

BOULTON, T. G., NYE, S. H., ROBBINS, D. J., IP, N. Y., RADZIEJEWSKA, E., MORGENBESSER, S. D., DEPINHO, R. A., PANAYOTATOS, N., COBB, M. H. & YANCOPOULOS, G. D. 1991. Erks - a Family of Protein-Serine Threonine Kinases That Are Activated and Tyrosine Phosphorylated in Response to Insulin and Ngf. *Cell,* 65**,** 663-675.

BRADY, J. F., LI, D. C., ISHIZAKI, H. & YANG, C. S. 1988. Effect of diallyl sulfide on rat liver microsomal nitrosamine metabolism and other monooxygenase activities. *Cancer Research,* 48**,** 5937-40.

BROZOVIC, A., VUKOVIC, L., POLANCAC, D. S., ARANY, I., KOBERLE, B., FRITZ, G., FIKET, Z., MAJHEN, D., AMBRIOVIC-RISTOV, A. & OSMAK, M. 2013. Endoplasmic Reticulum Stress Is Involved in the Response of Human Laryngeal Carcinoma Cells to Carboplatin but Is Absent in Carboplatin-Resistant Cells. *Plos One,* 8.

BRUSH, M. H., WEISER, D. C. & SHENOLIKAR, S. 2003. Growth arrest and DNA damage-inducible protein GADD34 targets protein phosphatase 1 alpha to the endoplasmic reticulum and promotes dephosphorylation of the alpha subunit of eukaryotic translation initiation factor 2. *Molecular and Cell Biology,* 23**,** 1292-303.

BUCCIANTINI, M., GIANNONI, E., CHITI, F., BARONI, F., FORMIGLI, L., ZURDO, J., TADDEI, N., RAMPONI, G., DOBSON, C. M. & STEFANI, M. 2002. Inherent toxicity of aggregates implies a common mechanism for protein misfolding diseases. *Nature,* 416**,** 507-11.

CAI, L., XU, G., SHI, C., GUO, D., WANG, X. & LUO, J. 2015. Telodendrimer nanocarrier for co-delivery of paclitaxel and cisplatin: A synergistic combination nanotherapy for ovarian cancer treatment. *Biomaterials,* 37**,** 456-68.

CALFON, M., ZENG, H., URANO, F., TILL, J. H., HUBBARD, S. R., HARDING, H. P., CLARK, S. G. & RON, D. 2002. IRE1 couples endoplasmic reticulum load to secretory capacity by processing the XBP-1 mRNA. *Nature,* 415**,** 92-6.

CARRASCO, D. R., SUKHDEO, K., PROTOPOPOVA, M., SINHA, R., ENOS, M., CARRASCO, D. E., ZHENG, M., MANI, M., HENDERSON, J., PINKUS, G. S., MUNSHI, N., HORNER, J., IVANOVA, E. V., PROTOPOPOV, A., ANDERSON, K. C., TONON, G. & DEPINHO, R. A. 2007. The differentiation and stress response factor XBP-1 drives multiple myeloma pathogenesis. *Cancer Cell,* 11**,** 349-60.

CHANDRA-KUNTAL, K., LEE, J. & SINGH, S. V. 2013. Critical role for reactive oxygen species in apoptosis induction and cell migration inhibition by diallyl trisulfide, a cancer chemopreventive component of garlic. *Breast Cancer Research and Treatment,* 138**,** 69-79.
CHANG, L. & KARIN, M. 2001. Mammalian MAP kinase signalling cascades. *Nature,* 410**,** 37-40.

CHAUHAN, D., SINGH, A. V., CICCARELLI, B., RICHARDSON, P. G., PALLADINO, M. A. & ANDERSON, K. C. 2010. Combination of novel proteasome inhibitor NPI-0052 and lenalidomide trigger in vitro and in vivo synergistic cytotoxicity in multiple myeloma. *Blood,* 115**,** 834-45.

CHEN, C. Y., HUANG, C. F., TSENG, Y. T. & KUO, S. Y. 2012. Diallyl disulfide induces Ca2+ mobilization in human colon cancer cell line SW480. *Archives of Toxicology,* 86**,** 231-8.

CHEN, X., ILIOPOULOS, D., ZHANG, Q., TANG, Q., GREENBLATT, M. B., HATZIAPOSTOLOU, M., LIM, E., TAM, W. L., NI, M., CHEN, Y., MAI, J., SHEN, H., HU, D. Z., ADORO, S., HU, B., SONG, M., TAN, C., LANDIS, M. D., FERRARI, M., SHIN, S. J., BROWN, M., CHANG, J. C., LIU, X. S. & GLIMCHER, L. H. 2014. XBP1 promotes triple-negative breast cancer by controlling the HIF1alpha pathway. *Nature,* 508**,** 103-7.

CHIAVARINI, M., MINELLI, L. & FABIANI, R. 2015. Garlic consumption and colorectal cancer risk in man: a systematic review and meta-analysis. *Public Health Nutrition***,** 1-10.

CHIU, T. H., LAN, K. Y., YANG, M. D., LIN, J. J., HSIA, T. C., WU, C. T., YANG, J. S., CHUEH, F. S. & CHUNG, J. G. 2013. Diallyl Sulfide Promotes Cell-Cycle Arrest Through the p53 Expression and Triggers Induction of Apoptosis Via Caspase- and Mitochondria-Dependent Signaling Pathways in Human Cervical Cancer Ca Ski Cells. *Nutrition and Cancer-an International Journal,* 65**,** 505-514.

CHOMCZYNSKI, P. & SACCHI, N. 1987. Single-step method of RNA isolation by acid guanidinium thiocyanate-phenol-chloroform extraction. *Analytical Biochemistry,* 162**,** 156-9.
CLARK, A., ELLIS, M., ERLICHMAN, C., LUTZKER, S. & ZWIEBEL, J. 2010. Development of rational drug combinations with investigational targeted agents. *Oncologist,* 15**,** 496-9.

COHEN, D. J. & LEICHMAN, L. 2015. Controversies in the treatment of local and locally advanced gastric and esophageal cancers. *Journal of Clinical Oncology,* 33**,** 1754-9.

COHEN, P. 1997. The search for physiological substrates of MAP and SAP kinases in mammalian cells. *Trends in Cell Biology,* 7**,** 353-61.

COOPER, J. S., GUO, M. D., HERSKOVIC, A., MACDONALD, J. S., MARTENSON, J. A., JR., AL-SARRAF, M., BYHARDT, R., RUSSELL, A. H., BEITLER, J. J., SPENCER, S., ASBELL, S. O., GRAHAM, M. V. & LEICHMAN, L. L. 1999. Chemoradiotherapy of locally advanced esophageal cancer: long-term follow-up of a prospective randomized trial (RTOG 85-01). Radiation Therapy Oncology Group. *JAMA,* 281**,** 1623-7.

COTTON, R. G., LANGER, R., LEONG, T., MARTINEK, J., SEWRAM, V., SMITHERS, M., SWANSON, P. E., QIAO, Y. L., UDAGAWA, H., UENO, M., WANG, M., WEI, W. Q. & WHITE, R. E. 2014. Coping with esophageal cancer approaches worldwide. *Annals of the New York Academy of Sciences,* 1325**,** 138-58.

CRAGG, G. M. 1998. Paclitaxel (Taxol): a success story with valuable lessons for natural product drug discovery and development. *Medicinal Research Reviews,* 18**,** 315-31.

CRAGG, G. M. & NEWMAN, D. J. 2005. Plants as a source of anti-cancer agents. *Journal of Ethnopharmacology,* 100**,** 72-79.

CRAGG, G. M., NEWMAN, D. J. & SNADER, K. M. 1997. Natural products in drug discovery and development. *Journal of Natural Products,* 60**,** 52-60.

CREDLE, J. J., FINER-MOORE, J. S., PAPA, F. R., STROUD, R. M. & WALTER, P. 2005. On the mechanism of sensing unfolded protein in the endoplasmic reticulum. *Proceedings of National Academy of Science United States of America,* 102**,** 18773-84.

CUENDA, A. & ROUSSEAU, S. 2007. p38 MAP-kinases pathway regulation, function and role in human diseases. *Biochimica et Biophysica Acta,* 1773**,** 1358-75.

DAI, R., CHEN, R. & LI, H. 2009. Cross-talk between PI3K/Akt and MEK/ERK pathways mediates endoplasmic reticulum stress-induced cell cycle progression and cell death in human hepatocellular carcinoma cells. *International Journal of Oncology,* 34**,** 1749-57.

DANDARA, C., ROBERTSON, B., DZOBO, K., MOODLEY, L. & PARKER, M. I. 2015. Patient and tumour characteristics as prognostic markers for oesophageal cancer: a retrospective analysis of a cohort of patients at Groote Schuur Hospital. *European Journal of Cardio-Thoracic Surgery*.

DARLING, N. J. & COOK, S. J. 2014. The role of MAPK signalling pathways in the response to endoplasmic reticulum stress. *Biochimica et Biophysica Acta,* 1843**,** 2150-63.

DAS, A., BANIK, N. L. & RAY, S. K. 2007. Garlic compounds generate reactive oxygen species leading to activation of stress kinases and cysteine proteases for apoptosis in human glioblastoma T98G and U87MG cells. *Cancer,* 110**,** 1083-95.

DASARI, S. & TCHOUNWOU, P. B. 2014. Cisplatin in cancer therapy: molecular mechanisms of action. *European Journal of Pharmacology,* 740**,** 364-78.

DASGUPTA, P. & BANDYOPADHYAY, S. S. 2013. Role of di-allyl disulfide, a garlic component in NF-kappaB mediated transient G2-M phase arrest and apoptosis in human leukemic cell-lines. *Nutrition and Cancer,* 65**,** 611-22.

DAVIS, J. N., KUCUK, O. & SARKAR, F. H. 1999. Genistein inhibits NF-kappa B activation in prostate cancer cells. *Nutrition and Cancer,* 35**,** 167-74.

DAVIS, R. J. 2000. Signal transduction by the JNK group of MAP kinases. *Cell,* 103**,** 239-52.

DENMEADE, S. R., JAKOBSEN, C. M., JANSSEN, S., KHAN, S. R., GARRETT, E. S., LILJA, H., CHRISTENSEN, S. B. & ISAACS, J. T. 2003. Prostate-specific antigen-activated thapsigargin prodrug as targeted therapy for prostate cancer. *Journal of the National Cancer Institute,* 95**,** 990-1000.

DESAI, P. B., VYAS, J. J., SHARMA, S., DESHPANDE, R. K., BADWE, R. A., ADVANI, S. H., SAIKIA, T., DINSHAW, K. A. & SANTHI SWAROOP, V. 1989. Combined treatment modalities in esophageal cancer. *Seminars in Surgical Oncology,* 5**,** 365-9.

DIRSCH, V. M., ANTLSPERGER, D. S., HENTZE, H. & VOLLMAR, A. M. 2002. Ajoene, an experimental anti-leukemic drug: mechanism of cell death. *Leukemia,* 16**,** 74-83.

DIRSCH, V. M., GERBES, A. L. & VOLLMAR, A. M. 1998. Ajoene, a compound of garlic, induces apoptosis in human promyeloleukemic cells, accompanied by generation of reactive oxygen species and activation of nuclear factor kappaB. *Molecular Pharmacology,* 53**,** 402-7.

DOAN, N. T., PAULSEN, E. S., SEHGAL, P., MOLLER, J. V., NISSEN, P., DENMEADE, S. R., ISAACS, J. T., DIONNE, C. A. & CHRISTENSEN, S. B. 2015. Targeting thapsigargin towards tumors. *Steroids,* 97**,** 2-7.

DONNELLY, N., GORMAN, A. M., GUPTA, S. & SAMALI, A. 2013. The eIF2alpha kinases: their structures and functions. *Cellular and Molecular Life Sciences* 70**,** 3493-511.

DUBOIS, C., VANDEN ABEELE, F., SEHGAL, P., OLESEN, C., JUNKER, S., CHRISTENSEN, S. B., PREVARSKAYA, N. & MOLLER, J. V. 2013. Differential effects of thapsigargin analogues on apoptosis of prostate cancer cells: complex regulation by intracellular calcium. *FEBS JOURNAL,* 280**,** 5430-40.

EDGE, S. B. & COMPTON, C. C. 2010. The American Joint Committee on Cancer: the 7th edition of the AJCC cancer staging manual and the future of TNM. *Annals of Surgical Oncology,* 17**,** 1471-4.

ERHARDT, P., SCHREMSER, E. J. & COOPER, G. M. 1999. B-Raf inhibits programmed cell death downstream of cytochrome c release from mitochondria by activating the MEK/Erk pathway. *Molecular and Cell Biology,* 19**,** 5308-15.

FERRI, N., YOKOYAMA, K., SADILEK, M., PAOLETTI, R., APITZ-CASTRO, R., GELB, M. H. & CORSINI, A. 2003. Ajoene, a garlic compound, inhibits protein prenylation and arterial smooth muscle cell proliferation. *Br J Pharmacol,* 138**,** 811-8.

FILOMENI, G., AQUILANO, K., ROTILIO, G. & CIRIOLO, M. R. 2003. Reactive oxygen species-dependent c-Jun NH2-terminal kinase/c-Jun signaling cascade mediates neuroblastoma cell death induced by diallyl disulfide. *Cancer Research,* 63**,** 5940-9.

FLEIGE, S. & PFAFFL, M. W. 2006. RNA integrity and the effect on the real-time qRT-PCR performance. *Molecular Aspects of Medicine,* 27**,** 126-39.

FLEISCHAUER, A. T., POOLE, C. & ARAB, L. 2000. Garlic consumption and cancer prevention: meta-analyses of colorectal and stomach cancers. *The American Journal of Clinical Nutrition,* 72**,** 1047-52.

FREEDMAN, R. B., HIRST, T. R. & TUITE, M. F. 1994. Protein disulphide isomerase: building bridges in protein folding. *Trends in Biochemical Sciences,* 19**,** 331-6.

GALLUZZI, L., SENOVILLA, L., VITALE, I., MICHELS, J., MARTINS, I., KEPP, O., CASTEDO, M. & KROEMER, G. 2012. Molecular mechanisms of cisplatin resistance. *Oncogene,* 31**,** 1869-83.
GALLUZZI, L., VITALE, I., MICHELS, J., BRENNER, C., SZABADKAI, G., HAREL-BELLAN, A., CASTEDO, M. & KROEMER, G. 2014. Systems biology of cisplatin resistance: past, present and future. *Cell Death and Disease,* 5**,** e1257.

GALLWITZ, H., BONSE, S., MARTINEZ-CRUZ, A., SCHLICHTING, I., SCHUMACHER, K. & KRAUTH-SIEGEL, R. L. 1999. Ajoene is an inhibitor and subversive substrate of human glutathione reductase and Trypanosoma cruzi trypanothione reductase: crystallographic, kinetic, and spectroscopic studies. *Journal of Medicinal Chemistry,* 42**,** 364-72.

GAO, C. M., TAKEZAKI, T., DING, J. H., LI, M. S. & TAJIMA, K. 1999. Protective effect of allium vegetables against both esophageal and stomach cancer: a simultaneous case-referent study of a high-epidemic area in Jiangsu Province, China. *Japanese Journal of Clinical Oncology,* 90**,** 614-21.

GARA, R. K., SRIVASTAVA, V. K., DUGGAL, S., BAGGA, J. K., BHATT, M., SANYAL, S. & MISHRA, D. P. 2015. Shikonin selectively induces apoptosis in human prostate cancer cells through the endoplasmic reticulum stress and mitochondrial apoptotic pathway. *Journal of Biomedical Science,* 22**,** 26.

GARDNER, B. M. & WALTER, P. 2011. Unfolded proteins are Ire1-activating ligands that directly induce the unfolded protein response. *Science,* 333**,** 1891-4.

GARGOURI, Y., MOREAU, H., JAIN, M. K., DE HAAS, G. H. & VERGER, R. 1989. Ajoene prevents fat digestion by human gastric lipase in vitro. *Biochimica et Biophysica Acta,* 1006**,** 137-9.
GEBHARDT, R., BECK, H. & WAGNER, K. G. 1994. Inhibition of cholesterol biosynthesis by allicin and ajoene in rat hepatocytes and HepG2 cells. *Biochim Biophys Acta,* 1213**,** 57-62.
GETHING, M. J. 1999. Role and regulation of the ER chaperone BiP. *Seminars in Cell & Developmental Biology,* 10**,** 465-72.

GEWANDTER, J. S., STAVERSKY, R. J. & O'REILLY, M. A. 2009. Hyperoxia augments ER-stress-induced cell death independent of BiP loss. *Free Radical Biology and Medicine,* 47**,** 1742-52.

GLICKMAN, M. H. & CIECHANOVER, A. 2002. The ubiquitin-proteasome proteolytic pathway: destruction for the sake of construction. *Physiological Reviews,* 82**,** 373-428.

GOLDBERG, A. L. 2003. Protein degradation and protection against misfolded or damaged proteins. *Nature,* 426**,** 895-9.

GONZALEZ-PRIETO, R., CUIJPERS, S. A., LUIJSTERBURG, M. S., VAN ATTIKUM, H. & VERTEGAAL, A. C. 2015. SUMOylation and PARylation cooperate to recruit and stabilize SLX4 at DNA damage sites. *EMBO Reports,* 16**,** 512-9.

GRAHAM, A. J., SHRIVE, F. M., GHALI, W. A., MANNS, B. J., GRONDIN, S. C., FINLEY, R. J. & CLIFTON, J. 2007. Defining the optimal treatment of locally advanced esophageal cancer: a systematic review and decision analysis. *Annals of Thoracic Surgery,* 83**,** 1257-64.

GRAHAM, J. G., QUINN, M. L., FABRICANT, D. S. & FARNSWORTH, N. R. 2000. Plants used against cancer - an extension of the work of Jonathan Hartwell. *Journal of Ethnopharmacology,* 73**,** 347-377.

GREEN, D. R. & KROEMER, G. 2004. The pathophysiology of mitochondrial cell death. *Science,* 305**,** 626-9.

GRIESEMER, M., YOUNG, C., ROBINSON, A. S. & PETZOLD, L. 2014. BiP clustering facilitates protein folding in the endoplasmic reticulum. *PLOS Computational Biology,* 10**,** e1003675.

GRIGORYEV, Y. A., KURIAN, S. M., HART, T., NAKORCHEVSKY, A. A., CHEN, C., CAMPBELL, D., HEAD, S. R., YATES, J. R., 3RD & SALOMON, D. R. 2011. MicroRNA regulation of molecular networks mapped by global microRNA, mRNA, and protein expression in activated T lymphocytes. *Journal of Immunology,* 187**,** 2233-43.

GUAN, D., WANG, H., LI, V. E., XU, Y., YANG, M. & SHEN, Z. 2009. N-glycosylation of ATF6beta is essential for its proteolytic cleavage and transcriptional repressor function to ATF6alpha. *Journal of Cellular Biochemistry,* 108**,** 825-31.

GUZMAN, M., DUARTE, M. J., BLAZQUEZ, C., RAVINA, J., ROSA, M. C., GALVE-ROPERH, I., SANCHEZ, C., VELASCO, G. & GONZALEZ-FERIA, L. 2006. A pilot clinical study of Delta(9)-tetrahydrocannabinol in patients with recurrent glioblastoma multiforme. *British Journal of Cancer,* 95**,** 197-203.

HALPERIN, L., JUNG, J. & MICHALAK, M. 2014. The many functions of the endoplasmic reticulum chaperones and folding enzymes. *IUBMB Life,* 66**,** 318-26.

HAMMADI, M., OULIDI, A., GACKIERE, F., KATSOGIANNOU, M., SLOMIANNY, C., ROUDBARAKI, M., DEWAILLY, E., DELCOURT, P., LEPAGE, G., LOTTEAU, S., DUCREUX, S., PREVARSKAYA, N. & VAN COPPENOLLE, F. 2013. Modulation of ER stress and apoptosis by endoplasmic reticulum calcium leak via translocon during unfolded protein response: involvement of GRP78. *The FASEB Journal,* 27**,** 1600-9.

HAN, C., JIN, L., MEI, Y. & WU, M. 2013. Endoplasmic reticulum stress inhibits cell cycle progression via induction of p27 in melanoma cells. *Cell Signal,* 25**,** 144-9.

HAN, D., LERNER, A. G., VANDE WALLE, L., UPTON, J. P., XU, W. H., HAGEN, A., BACKES, B. J., OAKES, S. A. & PAPA, F. R. 2009. IRE1 alpha Kinase Activation Modes Control Alternate Endoribonuclease Outputs to Determine Divergent Cell Fates. *Cell,* 138**,** 562-575.

HAN, S. S., KEUM, Y. S., SEO, H. J., CHUN, K. S., LEE, S. S. & SURH, Y. J. 2001. Capsaicin suppresses phorbol ester-induced activation of NF-kappaB/Rel and AP-1 transcription factors in mouse epidermis. *Cancer Letters,* 164**,** 119-26.

HANAHAN, D. & WEINBERG, R. A. 2011. Hallmarks of cancer: the next generation. *Cell,* 144**,** 646-74.

HANSON, B. E. & VESOLE, D. H. 2009. Retaspimycin hydrochloride (IPI-504): a novel heat shock protein inhibitor as an anticancer agent. *Expert Opinion on Investigational Drugs,* 18**,** 1375-83.

HARADA, H., NAKAGAWA, H., OYAMA, K., TAKAOKA, M., ANDL, C. D., JACOBMEIER, B., VON WERDER, A., ENDERS, G. H., OPITZ, O. G. & RUSTGI, A. K. 2003. Telomerase induces immortalization of human esophageal keratinocytes without p16INK4a inactivation. *Mol Cancer Res,* 1**,** 729-38.

HARDING, H. P., NOVOA, I., ZHANG, Y., ZENG, H., WEK, R., SCHAPIRA, M. & RON, D. 2000. Regulated translation initiation controls stress-induced gene expression in mammalian cells. *Molecular Cell,* 6**,** 1099-108.

HARTWELL, J. L. 1969a. Plants used against cancer. A survey. *Lloydia,* 32**,** 78-107.

HARTWELL, J. L. 1969b. Plants used against cancer. A survey. *Lloydia,* 32**,** 153-205.

HARTWELL, J. L. 1969c. Plants used against cancer. A survey. *Lloydia,* 32**,** 247-96.

HARTWELL, J. L. 1971. Plants used against cancer. A survey. *Lloydia,* 34**,** 386-425.

HASSAN, H. T. 2004. Ajoene (natural garlic compound): a new anti-leukaemia agent for AML therapy. *Leukemia Research,* 28**,** 667-71.

HEATH, E. I., HILLMAN, D. W., VAISHAMPAYAN, U., SHENG, S., SARKAR, F., HARPER, F., GASKINS, M., PITOT, H. C., TAN, W., IVY, S. P., PILI, R., CARDUCCI, M. A., ERLICHMAN, C. & LIU, G. 2008. A phase II trial of 17-allylamino-17-demethoxygeldanamycin in patients with hormone-refractory metastatic prostate cancer. *Clinical Cancer Research,* 14**,** 7940-6.

HEBERT, D. N. & MOLINARI, M. 2007. In and out of the ER: protein folding, quality control, degradation, and related human diseases. *Physiological Reviews,* 87**,** 1377-408.

HENDRICKS, D. & PARKER, M. I. 2002. Oesophageal cancer in Africa. *IUBMB Life,* 53**,** 263-8.

HERMAN-ANTOSIEWICZ, A., KIM, Y. A., KIM, S. H., XIAO, D. & SINGH, S. V. 2010. Diallyl Trisulfide-Induced G2/M Phase Cell Cycle Arrest in DU145 Cells Is Associated with Delayed Nuclear Translocation of Cyclin-Dependent Kinase 1. *Pharmaceutical Research,* 27**,** 1072-1079.

HERR, I. & DEBATIN, K. M. 2001. Cellular stress response and apoptosis in cancer therapy. *Blood,* 98**,** 2603-14.

HERSEY, P. & ZHANG, X. D. 2008. Adaptation to ER stress as a driver of malignancy and resistance to therapy in human melanoma. *Pigment Cell & Melanoma Research,* 21**,** 358-67.
HERSHKO, A. & CIECHANOVER, A. 1998. The ubiquitin system. *Annual Review of Biochemistry,* 67**,** 425-79.

HETZ, C. 2012. The unfolded protein response: controlling cell fate decisions under ER stress and beyond. *Nature Reviews Molecular Cell Biology,* 13**,** 89-102.

HETZ, C., BERNASCONI, P., FISHER, J., LEE, A. H., BASSIK, M. C., ANTONSSON, B., BRANDT, G. S., IWAKOSHI, N. N., SCHINZEL, A., GLIMCHER, L. H. & KORSMEYER, S. J. 2006. Proapoptotic BAX and BAK modulate the unfolded protein response by a direct interaction with IRE1alpha. *Science,* 312**,** 572-6.

HIBI, M., LIN, A., SMEAL, T., MINDEN, A. & KARIN, M. 1993. Identification of an oncoprotein- and UV-responsive protein kinase that binds and potentiates the c-Jun activation domain. *Genes & Development,* 7**,** 2135-48.

HIROTA, M., KITAGAKI, M., ITAGAKI, H. & AIBA, S. 2006. Quantitative measurement of spliced XBP1 mRNA as an indicator of endoplasmic reticulum stress. *Journal of Toxicological Sciences,* 31**,** 149-56.

HOCHREITER-HUFFORD, A. & RAVICHANDRAN, K. S. 2013. Clearing the dead: apoptotic cell sensing, recognition, engulfment, and digestion. *Cold Spring Harbor perspectives in biology,* 5**,** a008748.

HORWITZ, S. B. 1994. Taxol (paclitaxel): mechanisms of action. *Annals of Oncology,* 5 Suppl 6**,** S3-6.

HOSOI, T., KUME, A., OTANI, K., OBA, T. & OZAWA, K. 2010. A unique modulator of endoplasmic reticulum stress-signalling pathways: the novel pharmacological properties of amiloride in glial cells. *British Journal of Pharmacology,* 159**,** 428-37.

HOSOI, T. & OZAWA, K. 2010. Endoplasmic reticulum stress in disease: mechanisms and therapeutic opportunities. *Clinical Science,* 118**,** 19-29.

HOSONO, T., FUKAO, T., OGIHARA, J., ITO, Y., SHIBA, H., SEKI, T. & ARIGA, T. 2005. Diallyl trisulfide suppresses the proliferation and induces apoptosis of human colon cancer cells through oxidative modification of beta-tubulin. *Journal of Biological Chemistry,* 280**,** 41487-93.

HU, P., HAN, Z., COUVILLON, A. D. & EXTON, J. H. 2004. Critical role of endogenous Akt/IAPs and MEK1/ERK pathways in counteracting endoplasmic reticulum stress-induced cell death. *Journal of Biological Chemistry,* 279**,** 49420-9.

HUNG, F. M., SHANG, H. S., TANG, N. Y., LIN, J. J., LU, K. W., LIN, J. P., KO, Y. C., YU, C. C., WANG, H. L., LIAO, J. C., LU, H. F. & CHUNG, J. G. 2014. Effects of diallyl trisulfide on induction of apoptotic death in murine leukemia WEHI-3 cells in vitro and alterations of the immune responses in normal and leukemic mice in vivo. *Environmental Toxicology*.

HUNTER, R., KASCHULA, C. H., PARKER, M. I., CAIRA, M. R., RICHARDS, P., TRAVIS, S., TAUTE, F. & QWEBANI, T. 2008. Substituted ajoenes as novel anti-cancer agents. *Bioorganic & Medicinal Chemistry Letters,* 18**,** 5277-9.

IMAI, J., IDE, N., NAGAE, S., MORIGUCHI, T., MATSUURA, H. & ITAKURA, Y. 1994. Antioxidant and radical scavenging effects of aged garlic extract and its constituents. *Planta Medica,* 60**,** 417-20.

IRIZARRY, R. A., HOBBS, B., COLLIN, F., BEAZER-BARCLAY, Y. D., ANTONELLIS, K. J., SCHERF, U. & SPEED, T. P. 2003. Exploration, normalization, and summaries of high density oligonucleotide array probe level data. *Biostatistics,* 4**,** 249-64.

ISHIKAWA, K., NAGANAWA, R., YOSHIDA, H., IWATA, N., FUKUDA, H., FUJINO, T. & SUZUKI, A. 1996. Antimutagenic effects of ajoene, an organosulfur compound derived from garlic. *Bioscience, Biotechnology, and Biochemistry,* 60**,** 2086-8.

IWAWAKI, T. & AKAI, R. 2006. Analysis of the XBP1 splicing mechanism using endoplasmic reticulum stress-indicators. *Biochemical and Biophysical Research Communications,* 350**,** 709-15.

JAKOBSEN, T. H., VAN GENNIP, M., PHIPPS, R. K., SHANMUGHAM, M. S., CHRISTENSEN, L. D., ALHEDE, M., SKINDERSOE, M. E., RASMUSSEN, T. B., FRIEDRICH, K., UTHE, F., JENSEN, P. O., MOSER, C., NIELSEN, K. F., EBERL, L., LARSEN, T. O., TANNER, D., HOIBY, N., BJARNSHOLT, T. & GIVSKOV, M. 2012. Ajoene, a sulfur-rich molecule from garlic, inhibits genes controlled by quorum sensing. *Antimicrobial Agents and Chemotherapy,* 56**,** 2314-25.

JEKUNEN, A. P., CHRISTEN, R. D., SHALINSKY, D. R. & HOWELL, S. B. 1994. Synergistic interaction between cisplatin and taxol in human ovarian carcinoma cells in vitro. *British Journal of Cancer,* 69**,** 299-306.

JIANG, Q., LI, F., SHI, K., WU, P., AN, J., YANG, Y. & XU, C. 2014. Involvement of p38 in signal switching from autophagy to apoptosis via the PERK/eIF2alpha/ATF4 axis in selenite-treated NB4 cells. *Cell Death and Disease,* 5**,** e1270.

JIN, Z. Y., WU, M., HAN, R. Q., ZHANG, X. F., WANG, X. S., LIU, A. M., ZHOU, J. Y., LU, Q. Y., ZHANG, Z. F. & ZHAO, J. K. 2013. Raw garlic consumption as a protective factor for lung cancer, a population-based case-control study in a Chinese population. *Cancer Prevention Research,* 6**,** 711-8.

JUNG, Y., PARK, H., ZHAO, H. Y., JEON, R., RYU, J. H. & KIM, W. Y. 2014. Systemic approaches identify a garlic-derived chemical, Z-ajoene, as a glioblastoma multiforme cancer stem cell-specific targeting agent. *Molecules and Cells,* 37**,** 547-53.

KAJA, S., PAYNE, A. J., SINGH, T., GHUMAN, J. K., SIECK, E. G. & KOULEN, P. 2015. An optimized lactate dehydrogenase release assay for screening of drug candidates in neuroscience. *Journal of Pharmacological and Toxicological Methods,* 73**,** 1-6.

KASCHULA, C. H., HUNTER, R., COTTON, J., TUVERI, R., NGARANDE, E., DZOBO, K., SCHAFER, G., SIYO, V., LANG, D., KUSZA, D. A., DAVIES, B., KATZ, A. A. & PARKER, M. I. 2015. The garlic compound ajoene targets protein folding in the endoplasmic reticulum of cancer cells. *Molecular Carcinogenesis*.

KASCHULA, C. H., HUNTER, R., HASSAN, H. T., STELLENBOOM, N., COTTON, J., ZHAI, X. Q. & PARKER, M. I. 2011. Anti-proliferation activity of synthetic ajoene analogues on cancer cell-lines. *Anti-Cancer Agents in Medicinal Chemistry,* 11**,** 260-6.

KASCHULA, C. H., HUNTER, R. & PARKER, M. I. 2010. Garlic-derived anticancer agents: structure and biological activity of ajoene. *Biofactors,* 36**,** 78-85.

KASCHULA, C. H., HUNTER, R., STELLENBOOM, N., CAIRA, M. R., WINKS, S., OGUNLEYE, T., RICHARDS, P., COTTON, J., ZILBEYAZ, K., WANG, Y., SIYO, V., NGARANDE, E. & PARKER, M. I. 2012. Structure-activity studies on the anti-proliferation activity of ajoene analogues in WHCO1 oesophageal cancer cells. *European Journal of Medicinal Chemistry,* 50**,** 236-54.

KATO, H. & NAKAJIMA, M. 2013. Treatments for esophageal cancer: a review.*General Thoracic and Cardiovascular Surgery*61**,** 330-5.

KAWASAKI, E. S. 2006. The end of the microarray Tower of Babel: will universal standards lead the way? *Journal of Biomolecular Techniques,* 17**,** 200-6.

KELKEL, M., CERELLA, C., MACK, F., SCHNEIDER, T., JACOB, C., SCHUMACHER, M., DICATO, M. & DIEDERICH, M. 2012. ROS-independent JNK activation and multisite phosphorylation of Bcl-2 link diallyl tetrasulfide-induced mitotic arrest to apoptosis. *Carcinogenesis,* 33**,** 2162-71.

KELSEN, D. P., GINSBERG, R., PAJAK, T. F., SHEAHAN, D. G., GUNDERSON, L., MORTIMER, J., ESTES, N., HALLER, D. G., AJANI, J., KOCHA, W., MINSKY, B. D. & ROTH, J. A. 1998. Chemotherapy followed by surgery compared with surgery alone for localized esophageal cancer. *The New England Journal of Medicine,* 339**,** 1979-84.

KIM, E. Y., KIM, A., KIM, S. K. & CHANG, Y. S. 2015. AZD6244 inhibits cisplatin-induced ERK1/2 activation and potentiates cisplatin-associated cytotoxicity in K-ras G12D preclinical models. *Cancer Letters,* 358**,** 85-91.

KIM, Y. A., XIAO, D., XIAO, H., POWOLNY, A. A., LEW, K. L., REILLY, M. L., ZENG, Y., WANG, Z. & SINGH, S. V. 2007. Mitochondria-mediated apoptosis by diallyl trisulfide in human prostate cancer cells is associated with generation of reactive oxygen species and regulated by Bax/Bak. *Molecular Cancer Therapeutics* 6**,** 1599-609.

KIM, Y. H., SHIN, S. W., KIM, B. S., KIM, J. H., KIM, J. G., MOK, Y. J., KIM, C. S., RHYU, H. S., HYUN, J. H. & KIM, J. S. 1999. Paclitaxel, 5-fluorouracil, and cisplatin combination chemotherapy for the treatment of advanced gastric carcinoma. *Cancer,* 85**,** 295-301.

KIMBARIS, A. C., SIATIS, N. G., DAFERERA, D. J., TARANTILIS, P. A., PAPPAS, C. S. & POLISSIOU, M. G. 2006. Comparison of distillation and ultrasound-assisted extraction methods for the isolation of sensitive aroma compounds from garlic (Allium sativum). *Ultrason Sonochem,* 13**,** 54-60.

KNOWLES, L. M. & MILNER, J. A. 2003. Diallyl disulfide induces ERK phosphorylation and alters gene expression profiles in human colon tumor cells. *Journal of Nutrition,* 133**,** 2901-2906.

KODALI, R. T. & ESLICK, G. D. 2015. Meta-analysis: does garlic intake reduce risk of gastric cancer? *Nutrition and Cancer,* 67**,** 1-11.

KOONG, A. C., CHAUHAN, V. & ROMERO-RAMIREZ, L. 2006. Targeting XBP-1 as a novel anti-cancer strategy. *Cancer biology & therapy,* 5**,** 756-9.

KOSHY, M., ESIASHVILLI, N., LANDRY, J. C., THOMAS, C. R., JR. & MATTHEWS, R. H. 2004. Multiple management modalities in esophageal cancer: combined modality management approaches. *Oncologist,* 9**,** 147-59.

KOUMENIS, C., NACZKI, C., KORITZINSKY, M., RASTANI, S., DIEHL, A., SONENBERG, N., KOROMILAS, A. & WOUTERS, B. G. 2002. Regulation of protein synthesis by hypoxia via activation of the endoplasmic reticulum kinase PERK and phosphorylation of the translation initiation factor eIF2 alpha. *Molecular and Cellular Biology,* 22**,** 7405-7416.

KWON, K. B., YOO, S. J., RYU, D. G., YANG, J. Y., RHO, H. W., KIM, J. S., PARK, J. W., KIM, H. R. & PARK, B. H. 2002. Induction of apoptosis by diallyl disulfide through activation of caspase-3 in human leukemia HL-60 cells. *Biochemical Pharmacology,* 63**,** 41-7.

LAI, E., TEODORO, T. & VOLCHUK, A. 2007. Endoplasmic reticulum stress: signaling the unfolded protein response. *Physiology (Bethesda),* 22**,** 193-201.

LAWSON, L. D. & GARDNER, C. D. 2005. Composition, stability, and bioavailability of garlic products used in a clinical trial. *Journal of Agricultural and Food Chemistry,* 53**,** 6254-61.

LAWSON, L. D., WANG, Z. J. & HUGHES, B. G. 1991. Identification and HPLC quantitation of the sulfides and dialk(en)yl thiosulfinates in commercial garlic products. *Planta Medica,* 57**,** 363-70.

LEE, A. H., IWAKOSHI, N. N. & GLIMCHER, L. H. 2003a. XBP-1 regulates a subset of endoplasmic reticulum resident chaperone genes in the unfolded protein response. *Molecular and Cell Biology,* 23**,** 7448-59.

LEE, P., WONG, A. F., BURRIS, H. A., PAPADOPOULOS, K., SAUSVILLE, E. A., ROSEN, P. J., MENDELSON, D. S., INFANTE, J. R., PATNAIK, A. & GORDON, M. S. 2010. Updated results of a phase Ib/II study of carfilzomib (CFZ) in patients (pts) with relapsed malignancies. *Journal of Clinical Oncology,* 28.

LEE, S. N., KIM, N. S. & LEE, D. S. 2003f. Comparative study of extraction techniques for determination of garlic flavor components by gas chromatography-mass spectrometry. *Anal Bioanal Chem,* 377**,** 749-56.

LEE, T. G., TANG, N., THOMPSON, S., MILLER, J. & KATZE, M. G. 1994. The 58,000-dalton cellular inhibitor of the interferon-induced double-stranded RNA-activated protein kinase (PKR) is a member of the tetratricopeptide repeat family of proteins. *Molecular and Cell Biology,* 14**,** 2331-42.

LEI, K. & DAVIS, R. J. 2003. JNK phosphorylation of Bim-related members of the Bcl2 family induces Bax-dependent apoptosis. *Proceedings of National Academy of Science United States of America,* 100**,** 2432-7.

LI, D., LI, L., LI, P., LI, Y. & CHEN, X. 2015. Apoptosis of HeLa cells induced by a new targeting photosensitizer-based PDT via a mitochondrial pathway and ER stress. *Onco Targets Ther,* 8**,** 703-11.

LI, M., CIU, J. R., YE, Y., MIN, J. M., ZHANG, L. H., WANG, K., GARES, M., CROS, J., WRIGHT, M. & LEUNG-TACK, J. 2002a. Antitumor activity of Z-ajoene, a natural compound purified from garlic: antimitotic and microtubule-interaction properties. *Carcinogenesis,* 23**,** 573-9.

LI, M., MIN, J. M., CUI, J. R., ZHANG, L. H., WANG, K., VALETTE, A., DAVRINCHE, C., WRIGHT, M. & LEUNG-TACK, J. 2002o. Z-ajoene induces apoptosis of HL-60 cells: involvement of Bcl-2 cleavage. *Nutrition and Cancer,* 42**,** 241-7.

LI, X., ZHANG, K. & LI, Z. 2011. Unfolded protein response in cancer: the physician's perspective. *J Hematol Oncol,* 4**,** 8.

LIN, H. L., YANG, J. S., YANG, J. H., FAN, S. S., CHANG, W. C., LI, Y. C. & CHUNG, J. G. 2006. The role of Ca2+ on the DADS-induced apoptosis in mouse-rat hybrid retina ganglion cells (N18). *Neurochem Res,* 31**,** 383-93.

LING, H., LU, L. F., HE, J., XIAO, G. H., JIANG, H. & SU, Q. 2014. Diallyl disulfide selectively causes checkpoint kinase-1 mediated G2/M arrest in human MGC803 gastric cancer cell line. *Oncology Reports,* 32**,** 2274-82.

LISBONA, F., ROJAS-RIVERA, D., THIELEN, P., ZAMORANO, S., TODD, D., MARTINON, F., GLAVIC, A., KRESS, C., LIN, J. H., WALTER, P., REED, J. C., GLIMCHER, L. H. & HETZ, C. 2009. BAX inhibitor-1 is a negative regulator of the ER stress sensor IRE1alpha. *Molecular Cell,* 33**,** 679-91.

LIU, J., LIN, R. I. & MILNER, J. A. 1992. Inhibition of 7,12-dimethylbenz[a]anthracene-induced mammary tumors and DNA adducts by garlic powder. *Carcinogenesis,* 13**,** 1847-51.

LONGLEY, D. B., HARKIN, D. P. & JOHNSTON, P. G. 2003. 5-fluorouracil: mechanisms of action and clinical strategies. *Nature Reviews Cancer,* 3**,** 330-8.

LUO, J., SOLIMINI, N. L. & ELLEDGE, S. J. 2009. Principles of cancer therapy: oncogene and non-oncogene addiction. *Cell,* 136**,** 823-37.

LUO, S. & LEE, A. S. 2002. Requirement of the p38 mitogen-activated protein kinase signalling pathway for the induction of the 78 kDa glucose-regulated protein/immunoglobulin heavy-chain binding protein by azetidine stress: activating transcription factor 6 as a target for stress-induced phosphorylation. *Biochemical Journal,* 366**,** 787-95.

MA, J., HOU, L. N., RONG, Z. X., LIANG, P., FANG, C., LI, H. F., QI, H. & CHEN, H. Z. 2013. Antidepressant desipramine leads to C6 glioma cell autophagy: implication for the adjuvant therapy of cancer. *Anti-Cancer Agents in Medicinal Chemistry,* 13**,** 254-60.

MA, Y., BREWER, J. W., DIEHL, J. A. & HENDERSHOT, L. M. 2002. Two distinct stress signaling pathways converge upon the CHOP promoter during the mammalian unfolded protein response. *Journal of Molecular Biology,* 318**,** 1351-65.

MA, Y. & HENDERSHOT, L. M. 2004. The role of the unfolded protein response in tumour development: friend or foe? *Nature Reviews Cancer,* 4**,** 966-77.

MACKAY, S. & STEFANOU, G. 2006. Management of oesophageal carcinoma. *Australian Family Physician,* 35**,** 202-6.

MACKEIGAN, J. P., COLLINS, T. S. & TING, J. P. 2000. MEK inhibition enhances paclitaxel-induced tumor apoptosis. *Journal of Biological Chemistry,* 275**,** 38953-6.

MANDIC, A., HANSSON, J., LINDER, S. & SHOSHAN, M. C. 2003. Cisplatin induces endoplasmic reticulum stress and nucleus-independent apoptotic signaling. *Journal of Biological Chemistry,* 278**,** 9100-6.

MARCINIAK, S. J., YUN, C. Y., OYADOMARI, S., NOVOA, I., ZHANG, Y., JUNGREIS, R., NAGATA, K., HARDING, H. P. & RON, D. 2004. CHOP induces death by promoting protein synthesis and oxidation in the stressed endoplasmic reticulum. *Genes & Development,* 18**,** 3066-77.

MASUDA, M., SUZUI, M., LIM, J. T., DEGUCHI, A., SOH, J. W. & WEINSTEIN, I. B. 2002. Epigallocatechin-3-gallate decreases VEGF production in head and neck and breast carcinoma cells by inhibiting EGFR-related pathways of signal transduction. *Journal of Experimental Therapeutics and Oncology,* 2**,** 350-9.

MATSUMOTO, H., MIYAZAKI, S., MATSUYAMA, S., TAKEDA, M., KAWANO, M., NAKAGAWA, H., NISHIMURA, K. & MATSUO, S. 2013. Selection of autophagy or apoptosis in cells exposed to ER-stress depends on ATF4 expression pattern with or without CHOP expression. *Biology Open,* 2**,** 1084-90.

MATSUMOTO, M., MINAMI, M., TAKEDA, K., SAKAO, Y. & AKIRA, S. 1996. Ectopic expression of CHOP (GADD153) induces apoptosis in M1 myeloblastic leukemia cells. *FEBS Letters,* 395**,** 143-7.

MCCULLOUGH, K. D., MARTINDALE, J. L., KLOTZ, L. O., AW, T. Y. & HOLBROOK, N. J. 2001. Gadd153 sensitizes cells to endoplasmic reticulum stress by down-regulating Bcl2 and perturbing the cellular redox state. *Molecular and Cell Biology,* 21**,** 1249-59.

MEHTA, R. G., STEELE, V., KELLOFF, G. J. & MOON, R. C. 1991. Influence of thiols and inhibitors of prostaglandin biosynthesis on the carcinogen-induced development of mammary lesions in vitro. *Anticancer Research,* 11**,** 587-91.

MENCHER, S. K. & WANG, L. G. 2005. Promiscuous drugs compared to selective drugs (promiscuity can be a virtue). *BMC Clinical Pharmacology,* 5**,** 3.

MENG, S., ZHANG, X., GIOVANNUCCI, E. L., MA, J., FUCHS, C. S. & CHO, E. 2013. No association between garlic intake and risk of colorectal cancer. *Cancer Epidemiology,* 37**,** 152-5.

MEUSSER, B., HIRSCH, C., JAROSCH, E. & SOMMER, T. 2005. ERAD: the long road to destruction. *Nature Cell Biology,* 7**,** 766-72.

MHAIDAT, N. M., ZHANG, X. D., JIANG, C. C. & HERSEY, P. 2007. Docetaxel-induced apoptosis of human melanoma is mediated by activation of c-Jun NH2-terminal kinase and inhibited by

the mitogen-activated protein kinase extracellular signal-regulated kinase 1/2 pathway. *Clinical Cancer Research,* 13**,** 1308-14.

MICHELANGELI, F. & EAST, J. M. 2011. A diversity of SERCA Ca2+ pump inhibitors. *Biochemical Society Transactions,* 39**,** 789-97.

MINDEN, A., LIN, A. N., SMEAL, T., DERIJARD, B., COBB, M., DAVIS, R. & KARIN, M. 1994. C-Jun N-Terminal Phosphorylation Correlates with Activation of the Jnk Subgroup but Not the Erk Subgroup of Mitogen-Activated Protein-Kinases. *Molecular and Cellular Biology,* 14**,** 6683-6688.

MODEM, S., DICARLO, S. E. & REDDY, T. R. 2012. Fresh Garlic Extract Induces Growth Arrest and Morphological Differentiation of MCF7 Breast Cancer Cells. *Genes Cancer,* 3**,** 177-86.

MOREY, J. S., RYAN, J. C. & VAN DOLAH, F. M. 2006. Microarray validation: factors influencing correlation between oligonucleotide microarrays and real-time PCR. *Biological Procedures Online,* 8**,** 175-93.

MORI, K. 2009. Signalling pathways in the unfolded protein response: development from yeast to mammals. *Journal of Biochemistry,* 146**,** 743-50.

MORI, K., OGAWA, N., KAWAHARA, T., YANAGI, H. & YURA, T. 2000. mRNA splicing-mediated C-terminal replacement of transcription factor Hac1p is required for efficient activation of the unfolded protein response. *Proceedings of National Academy of Science United States of America,* 97**,** 4660-5.

MOSMANN, T. 1983. Rapid colorimetric assay for cellular growth and survival: application to proliferation and cytotoxicity assays. *Journal of Immunology Methods,* 65**,** 55-63.

MOURIA, M., GUKOVSKAYA, A. S., JUNG, Y., BUECHLER, P., HINES, O. J., REBER, H. A. & PANDOL, S. J. 2002. Food-derived polyphenols inhibit pancreatic cancer growth through mitochondrial cytochrome C release and apoptosis. *International Journal of Cancer,* 98**,** 761-9.

MUNCHBERG, U., ANWAR, A., MECKLENBURG, S. & JACOB, C. 2007. Polysulfides as biologically active ingredients of garlic. *Organic & Biomolecular Chemistry,* 5**,** 1505-18.

MUNDAY, R. & MUNDAY, C. M. 1999. Low doses of diallyl disulfide, a compound derived from garlic, increase tissue activities of quinone reductase and glutathione transferase in the gastrointestinal tract of the rat. *Nutrition and Cancer,* 34**,** 42-8.

MURAI, M., INOUE, T., SUZUKI-KARASAKI, M., OCHIAI, T., RA, C., NISHIDA, S. & SUZUKI-KARASAKI, Y. 2012. Diallyl trisulfide sensitizes human melanoma cells to TRAIL-induced cell death by promoting endoplasmic reticulum-mediated apoptosis. *International Journal of Oncology,* 41**,** 2029-37.

NAKAGAWA, H., TSUTA, K., KIUCHI, K., SENZAKI, H., TANAKA, K., HIOKI, K. & TSUBURA, A. 2001. Growth inhibitory effects of diallyl disulfide on human breast cancer cell lines. *Carcinogenesis,* 22**,** 891-7.

NAKAGAWA, T. & YUAN, J. 2000. Cross-talk between two cysteine protease families. Activation of caspase-12 by calpain in apoptosis. *Journal of Cell Biology,* 150**,** 887-94.

NAZNIN, M. T., AKAGAWA, M., OKUKAWA, K., MAEDA, T. & MORITA, N. 2008. Characterization of E- and Z-ajoene obtained from different varieties of garlics. *Food Chemistry,* 106**,** 1113-1119.

NGUYEN, D. T., KEBACHE, S., FAZEL, A., WONG, H. N., JENNA, S., EMADALI, A., LEE, E. H., BERGERON, J. J., KAUFMAN, R. J., LAROSE, L. & CHEVET, E. 2004. Nck-dependent activation of extracellular signal-regulated kinase-1 and regulation of cell survival during endoplasmic reticulum stress. *Molecular Biology of the Cell,* 15**,** 4248-60.

NICASTRO, H. L., ROSS, S. A. & MILNER, J. A. 2015. Garlic and onions: their cancer prevention properties. *Cancer Prevention Research,* 8**,** 181-9.

NISHITOH, H., MATSUZAWA, A., TOBIUME, K., SAEGUSA, K., TAKEDA, K., INOUE, K., HORI, S., KAKIZUKA, A. & ICHIJO, H. 2002. ASK1 is essential for endoplasmic reticulum stress-induced neuronal cell death triggered by expanded polyglutamine repeats. *Genes & Development,* 16**,** 1345-55.

NOBILI, S., LIPPI, D., WITORT, E., DONNINI, M., BAUSI, L., MINI, E. & CAPACCIOLI, S. 2009. Natural compounds for cancer treatment and prevention. *Pharmacological Research,* 59**,** 365-78.

NOTTE, A., REBUCCI, M., FRANSOLET, M., ROEGIERS, E., GENIN, M., TELLIER, C., WATILLON, K., FATTACCIOLI, A., ARNOULD, T. & MICHIELS, C. 2015. Taxol-induced unfolded protein response activation in breast cancer cells exposed to hypoxia: ATF4 activation regulates autophagy and inhibits apoptosis. *International Journal of Biochemistry and Cell Biology,* 62**,** 1-14.

O'CONNOR, O. A., STEWART, A. K., VALLONE, M., MOLINEAUX, C. J., KUNKEL, L. A., GERECITANO, J. F. & ORLOWSKI, R. Z. 2009. A phase 1 dose escalation study of the safety and pharmacokinetics of the novel proteasome inhibitor carfilzomib (PR-171) in patients with hematologic malignancies. *Clinical Cancer Research,* 15**,** 7085-91.

OBATA, T., BROWN, G. E. & YAFFE, M. B. 2000. MAP kinase pathways activated by stress: the p38 MAPK pathway. *Critical Care Medicine,* 28**,** N67-77.

OHOKA, N., YOSHII, S., HATTORI, T., ONOZAKI, K. & HAYASHI, H. 2005. TRB3, a novel ER stress-inducible gene, is induced via ATF4-CHOP pathway and is involved in cell death. *EMBO JOURNAL,* 24**,** 1243-55.

OOMMEN, S., ANTO, R. J., SRINIVAS, G. & KARUNAGARAN, D. 2004. Allicin (from garlic) induces caspase-mediated apoptosis in cancer cells. *European Journal of Pharmacology,* 485**,** 97-103.

OSLOWSKI, C. M. & URANO, F. 2011. Measuring ER stress and the unfolded protein response using mammalian tissue culture system. *Methods in Enzymology,* 490**,** 71-92.

OYADOMARI, S. & MORI, M. 2004. Roles of CHOP/GADD153 in endoplasmic reticulum stress. *Cell Death & Differentiation,* 11**,** 381-9.

PACEY, S., GORE, M., CHAO, D., BANERJI, U., LARKIN, J., SARKER, S., OWEN, K., ASAD, Y., RAYNAUD, F., WALTON, M., JUDSON, I., WORKMAN, P. & EISEN, T. 2012. A Phase II trial of 17-allylamino, 17-demethoxygeldanamycin (17-AAG, tanespimycin) in patients with metastatic melanoma. *Investigational New Drugs* 30**,** 341-9.

PANARO, N. J., YUEN, P. K., SAKAZUME, T., FORTINA, P., KRICKA, L. J. & WILDING, P. 2000. Evaluation of DNA fragment sizing and quantification by the agilent 2100 bioanalyzer. *Clinical Chemistry,* 46**,** 1851-3.

PAPANDREOU, I., DENKO, N. C., OLSON, M., VAN MELCKEBEKE, H., LUST, S., TAM, A., SOLOW-CORDERO, D. E., BOULEY, D. M., OFFNER, F., NIWA, M. & KOONG, A. C. 2011. Identification of an Ire1alpha endonuclease specific inhibitor with cytotoxic activity against human multiple myeloma. *Blood,* 117**,** 1311-4.

PARK, K. K., CHUN, K. S., LEE, J. M., LEE, S. S. & SURH, Y. J. 1998. Inhibitory effects of [6]-gingerol, a major pungent principle of ginger, on phorbol ester-induced inflammation, epidermal ornithine decarboxylase activity and skin tumor promotion in ICR mice. *Cancer Letters,* 129**,** 139-44.

PERCHELLET, J. P., PERCHELLET, E. M., ABNEY, N. L., ZIRNSTEIN, J. A. & BELMAN, S. 1986. Effects of garlic and onion oils on glutathione peroxidase activity, the ratio of reduced/oxidized glutathione and ornithine decarboxylase induction in isolated mouse epidermal cells treated with tumor promoters. *Cancer Biochemistry Biophysics,* 8**,** 299-312.
PETERSON, L. E. 2002. CLUSFAVOR 5.0: hierarchical cluster and principal-component analysis of microarray-based transcriptional profiles. *Genome Biology,* 3**,** SOFTWARE0002.

PETRASCH, S., WELT, A., REINACHER, A., GRAEVEN, U., KONIG, M. & SCHMIEGEL, W. 1998. Chemotherapy with cisplatin and paclitaxel in patients with locally advanced, recurrent or metastatic oesophageal cancer. *British Journal of Cancer,* 78**,** 511-4.

PLUMMER, S. M., HOLLOWAY, K. A., MANSON, M. M., MUNKS, R. J., KAPTEIN, A., FARROW, S. & HOWELLS, L. 1999. Inhibition of cyclo-oxygenase 2 expression in colon cells by the chemopreventive agent curcumin involves inhibition of NF-kappaB activation via the NIK/IKK signalling complex. *Oncogene,* 18**,** 6013-20.

POLYAK, S. J., TANG, N., WAMBACH, M., BARBER, G. N. & KATZE, M. G. 1996. The P58 cellular inhibitor complexes with the interferon-induced, double-stranded RNA-dependent protein kinase, PKR, to regulate its autophosphorylation and activity. *Journal of Biological Chemistry,* 271**,** 1702-7.

PRITCHARD, A. L. & HAYWARD, N. K. 2013. Molecular pathways: mitogen-activated protein kinase pathway mutations and drug resistance. *Clinical Cancer Research,* 19**,** 2301-9.

PYRKO, P., KARDOSH, A., LIU, Y. T., SORIANO, N., XIONG, W., CHOW, R. H., UDDIN, J., PETASIS, N. A., MIRCHEFF, A. K., FARLEY, R. A., LOUIE, S. G., CHEN, T. C. & SCHONTHAL, A. H. 2007a. Calcium-activated endoplasmic reticulum stress as a major component of tumor cell death induced by 2,5-dimethyl-celecoxib, a non-coxib analogue of celecoxib. *Molecular Cancer Therapeutics* 6**,** 1262-75.

PYRKO, P., SCHONTHAL, A. H., HOFMAN, F. M., CHEN, T. C. & LEE, A. S. 2007b. The unfolded protein response regulator GRP78/BiP as a novel target for increasing chemosensitivity in malignant gliomas. *Cancer Research,* 67**,** 9809-16.

RAASI, S. & WOLF, D. H. 2007. Ubiquitin receptors and ERAD: a network of pathways to the proteasome. *Seminars in Cell & Developmental Biology,* 18**,** 780-91.

RABIK, C. A., FISHEL, M. L., HOLLERAN, J. L., KASZA, K., KELLEY, M. R., EGORIN, M. J. & DOLAN, M. E. 2008. Enhancement of cisplatin [cis-diammine dichloroplatinum (II)] cytotoxicity by O6-benzylguanine involves endoplasmic reticulum stress. *Journal of Pharmacology and Experimental Therapeutics,* 327**,** 442-52.

RAINGEAUD, J., GUPTA, S., ROGERS, J. S., DICKENS, M., HAN, J., ULEVITCH, R. J. & DAVIS, R. J. 1995. Pro-inflammatory cytokines and environmental stress cause p38 mitogen-activated protein kinase activation by dual phosphorylation on tyrosine and threonine. *Journal of Biological Chemistry,* 270**,** 7420-6.

RANGANATHAN, A. C., ZHANG, L., ADAM, A. P. & AGUIRRE-GHISO, J. A. 2006. Functional coupling of p38-induced up-regulation of BiP and activation of RNA-dependent protein kinase-like endoplasmic reticulum kinase to drug resistance of dormant carcinoma cells. *Cancer Research,* 66**,** 1702-11.

RAO, B., LAIN, S. & THOMPSON, A. M. 2013. p53-Based cyclotherapy: exploiting the 'guardian of the genome' to protect normal cells from cytotoxic therapy. *British Journal of Cancer,* 109**,** 2954-8.

RAUSCHERT, N., BRANDLEIN, S., HOLZINGER, E., HENSEL, F., MULLER-HERMELINK, H. K. & VOLLMERS, H. P. 2008. A new tumor-specific variant of GRP78 as target for antibody-based therapy. *Laboratory Investigation,* 88**,** 375-86.

RAVASZ, E., SOMERA, A. L., MONGRU, D. A., OLTVAI, Z. N. & BARABASI, A. L. 2002. Hierarchical organization of modularity in metabolic networks. *Science,* 297**,** 1551-1555.

REDDY, B. S., RAO, C. V., RIVENSON, A. & KELLOFF, G. 1993. Chemoprevention of colon carcinogenesis by organosulfur compounds. *Cancer Research,* 53**,** 3493-8.

RICE, T. W., BLACKSTONE, E. H. & RUSCH, V. W. 2010. 7th edition of the AJCC Cancer Staging Manual: esophagus and esophagogastric junction. *Annals of Surgical Oncology,* 17**,** 1721-4.

RICE, T. W., BLACKSTONE, E. H., RYBICKI, L. A., ADELSTEIN, D. J., MURTHY, S. C., DECAMP, M. M. & GOLDBLUM, J. R. 2003. Refining esophageal cancer staging. *Journal of Thoracic and Cardiovascular Surgery,* 125**,** 1103-13.

RICHARDSON, P. G., BADROS, A. Z., JAGANNATH, S., TARANTOLO, S., WOLF, J. L., ALBITAR, M., BERMAN, D., MESSINA, M. & ANDERSON, K. C. 2010. Tanespimycin with bortezomib: activity in relapsed/refractory patients with multiple myeloma. *British Journal of Haematology,* 150**,** 428-437.

RICHTER, C., GOGVADZE, V., LAFFRANCHI, R., SCHLAPBACH, R., SCHWEIZER, M., SUTER, M., WALTER, P. & YAFFEE, M. 1995. Oxidants in mitochondria: from physiology to diseases. *Biochimica et Biophysica Acta,* 1271**,** 67-74.

RODRIGUEZ, D. A., ZAMORANO, S., LISBONA, F., ROJAS-RIVERA, D., URRA, H., CUBILLOS-RUIZ, J. R., ARMISEN, R., HENRIQUEZ, D. R., CHENG, E. H., LETEK, M., VAISAR, T., IRRAZABAL, T., GONZALEZ-BILLAULT, C., LETAI, A., PIMENTEL-MUINOS, F. X., KROEMER, G. & HETZ, C. 2012. BH3-only proteins are part of a regulatory network that control the sustained signalling of the unfolded protein response sensor IRE1alpha. *EMBO JOURNAL,* 31**,** 2322-35.

RON, D. & WALTER, P. 2007. Signal integration in the endoplasmic reticulum unfolded protein response. *Nature Reviews Molecular Cell Biology,* 8**,** 519-29.

ROUSCHOP, K. M., VAN DEN BEUCKEN, T., DUBOIS, L., NIESSEN, H., BUSSINK, J., SAVELKOULS, K., KEULERS, T., MUJCIC, H., LANDUYT, W., VONCKEN, J. W., LAMBIN, P., VAN DER KOGEL, A. J., KORITZINSKY, M. & WOUTERS, B. G. 2010. The unfolded protein response protects human tumor cells during hypoxia through regulation of the autophagy genes MAP1LC3B and ATG5. *Journal of Clinical Investigation,* 120**,** 127-41.

RUTKOWSKI, D. T., KANG, S. W., GOODMAN, A. G., GARRISON, J. L., TAUNTON, J., KATZE, M. G., KAUFMAN, R. J. & HEGDE, R. S. 2007. The role of p58IPK in protecting the stressed endoplasmic reticulum. *Molecular Biology of the Cell,* 18**,** 3681-91.

SAIDU, N. E., ABU ASALI, I., CZEPUKOJC, B., SEITZ, B., JACOB, C. & MONTENARH, M. 2013. Comparison between the effects of diallyl tetrasulfide on human retina pigment epithelial cells (ARPE-19) and HCT116 cells. *Biochimica et Biophysica Acta,* 1830**,** 5267-76.

SAKAMOTO, K., LAWSON, L. D. & MILNER, J. A. 1997. Allyl sulfides from garlic suppress the in vitro proliferation of human A549 lung tumor cells. *Nutrition and Cancer,* 29**,** 152-6.

SAMATAR, A. A. & POULIKAKOS, P. I. 2014. Targeting RAS-ERK signalling in cancer: promises and challenges. *Nature Reviews Drug Discovery,* 13**,** 928-42.

SAN MIGUEL, J. F., SCHLAG, R., KHUAGEVA, N. K., DIMOPOULOS, M. A., SHPILBERG, O., KROPFF, M., SPICKA, I., PETRUCCI, M. T., PALUMBO, A., SAMOILOVA, O. S., DMOSZYNSKA, A., ABDULKADYROV, K. M., SCHOTS, R., JIANG, B., MATEOS, M., ANDERSON, K. C., ESSELTINE, D. L., LIU, K., CAKANA, A., VAN DE VELDE, H., RICHARDSON, P. G. & INVESTIGATORS, V. T. 2008. Bortezomib plus melphalan and prednisone for initial treatment of multiple myeloma. *New England Journal of Medicine,* 359**,** 906-917.

SANO, R. & REED, J. C. 2013. ER stress-induced cell death mechanisms. *Biochimica et Biophysica Acta,* 1833**,** 3460-70.

SARASTE, A. 1999. Morphologic criteria and detection of apoptosis. *Herz,* 24**,** 189-95.

SAYBASILI, H., YUKSEL, M., HAKLAR, G. & YALCIN, A. S. 2001. Effect of mitochondrial electron transport chain inhibitors on superoxide radical generation in rat hippocampal and striatal slices. *Antioxidants and Redox Signaling,* 3**,** 1099-104.

SCHAFER, G. & KASCHULA, C. H. 2014. The immunomodulation and anti-inflammatory effects of garlic organosulfur compounds in cancer chemoprevention. *Anti-Cancer Agents in Medicinal Chemistry,* 14**,** 233-40.

SCHARFENBERG, K., WAGNER, R. & WAGNER, K. G. 1990. The cytotoxic effect of ajoene, a natural product from garlic, investigated with different cell lines. *Cancer Letters,* 53**,** 103-8.

SCHIENE, C. & FISCHER, G. 2000. Enzymes that catalyse the restructuring of proteins. *Current Opinion in Structural Biology,* 10**,** 40-5.

SCHLANSKY, B., DIMARINO, A. J., LOREN, D., INFANTOLINO, A., KOWALSKI, T. & COHEN, S. 2006. A survey of oesophageal cancer: pathology, stage and clinical presentation. *Alimentary Pharmacology & Therapeutics,* 23**,** 587-593.

SCHOU, J., KELSTRUP, C. D., HAYWARD, D. G., OLSEN, J. V. & NILSSON, J. 2014. Comprehensive Identification of SUMO2/3 Targets and Their Dynamics during Mitosis. *Plos One,* 9.

SCHRODER, M. & KAUFMAN, R. J. 2005. The mammalian unfolded protein response. *Annual Review of Biochemistry,* 74**,** 739-89.

SCHROEDER, A., MUELLER, O., STOCKER, S., SALOWSKY, R., LEIBER, M., GASSMANN, M., LIGHTFOOT, S., MENZEL, W., GRANZOW, M. & RAGG, T. 2006. The RIN: an RNA integrity number for assigning integrity values to RNA measurements. *BMC Molecular Biology,* 7**,** 3.

SCHUBERT, U., ANTON, L. C., GIBBS, J., NORBURY, C. C., YEWDELL, J. W. & BENNINK, J. R. 2000. Rapid degradation of a large fraction of newly synthesized proteins by proteasomes. *Nature,* 404**,** 770-4.

SEKI, T., TSUJI, K., HAYATO, Y., MORITOMO, T. & ARIGA, T. 2000. Garlic and onion oils inhibit proliferation and induce differentiation of HL-60 cells. *Cancer Letters,* 160**,** 29-35.

SEN, S. & D'INCALCI, M. 1992. Apoptosis. Biochemical events and relevance to cancer chemotherapy. *FEBS Letters,* 307**,** 122-7.

SENDL, A., SCHLIACK, M., LOSER, R., STANISLAUS, F. & WAGNER, H. 1992. Inhibition of cholesterol synthesis in vitro by extracts and isolated compounds prepared from garlic and wild garlic. *Atherosclerosis,* 94**,** 79-85.

SHANI, G., FISCHER, W. H., JUSTICE, N. J., KELBER, J. A., VALE, W. & GRAY, P. C. 2008. GRP78 and Cripto form a complex at the cell surface and collaborate to inhibit transforming growth factor beta signaling and enhance cell growth. *Molecular and Cell Biology,* 28**,** 666-77.

SHEEN, L. Y., CHEN, H. W., KUNG, Y. L., LIU, C. T. & LII, C. K. 1999. Effects of garlic oil and its organosulfur compounds on the activities of hepatic drug-metabolizing and antioxidant enzymes in rats fed high- and low-fat diets. *Nutrition and Cancer,* 35**,** 160-6.

SHEN, J., CHEN, X., HENDERSHOT, L. & PRYWES, R. 2002. ER stress regulation of ATF6 localization by dissociation of BiP/GRP78 binding and unmasking of Golgi localization signals. *Developmental Cell,* 3**,** 99-111.

SHI, Y. 2001. A structural view of mitochondria-mediated apoptosis. *Nature Structural & Molecular Biology,* 8**,** 394-401.

SHIMADA, Y., IMAMURA, M., WAGATA, T., YAMAGUCHI, N. & TOBE, T. 1992. Characterization of 21 newly established esophageal cancer cell lines. *Cancer,* 69**,** 277-84.

SHIN, D. Y., KIM, G. Y., HWANG, H. J., KIM, W. J. & CHOI, Y. H. 2014. Diallyl trisulfide-induced apoptosis of bladder cancer cells is caspase-dependent and regulated by PI3K/Akt and JNK pathways. *Environmental Toxicology Pharmacol,* 37**,** 74-83.

SHIN, D. Y., KIM, G. Y., LEE, J. H., CHOI, B. T., YOO, Y. H. & CHOI, Y. H. 2012. Apoptosis induction of human prostate carcinoma DU145 cells by diallyl disulfide via modulation of JNK and PI3K/AKT signaling pathways. *International Journal of Molecular Sciences,* 13**,** 14158-71.
SHIRYAEV, S. A., CHELTSOV, A. V., GAWLIK, K., RATNIKOV, B. I. & STRONGIN, A. Y. 2011. Virtual ligand screening of the National Cancer Institute (NCI) compound library leads to the allosteric inhibitory scaffolds of the West Nile Virus NS3 proteinase. *ASSAY and Drug Development Technologies,* 9**,** 69-78.

SHUDA, M., KONDOH, N., IMAZEKI, N., TANAKA, K., OKADA, T., MORI, K., HADA, A., ARAI, M., WAKATSUKI, T., MATSUBARA, O., YAMAMOTO, N. & YAMAMOTO, M. 2003. Activation of the ATF6, XBP1 and grp78 genes in human hepatocellular carcinoma: a possible involvement of the ER stress pathway in hepatocarcinogenesis. *Journal of Hepatology,* 38**,** 605-14.

SHUKLA, Y. & KALRA, N. 2007. Cancer chemoprevention with garlic and its constituents. *Cancer Letters,* 247**,** 167-81.

SIEGERS, C. P., STEFFEN, B., ROBKE, A. & PENTZ, R. 1999. The effects of garlic preparations against human tumor cell proliferation. *Phytomedicine,* 6**,** 7-11.

SINGH, A. & SHUKLA, Y. 1998a. Antitumor activity of diallyl sulfide in two-stage mouse skin model of carcinogenesis. *Biomedical and Environmental Sciences* 11**,** 258-63.

SINGH, A. & SHUKLA, Y. 1998b. Antitumour activity of diallyl sulfide on polycyclic aromatic hydrocarbon-induced mouse skin carcinogenesis. *Cancer Letters,* 131**,** 209-14.

SINGH, S. & AGGARWAL, B. B. 1995. Activation of transcription factor NF-kappa B is suppressed by curcumin (diferuloylmethane) [corrected]. *Journal of Biological Chemistry,* 270**,** 24995-5000.

SOMDYALA, N. I., PARKIN, D. M., SITHOLE, N. & BRADSHAW, D. 2015. Trends in cancer incidence in rural Eastern Cape Province; South Africa, 1998-2012. *International Journal of Cancer,* 136**,** E470-4.

SONG, M. S., PARK, Y. K., LEE, J. H. & PARK, K. 2001. Induction of glucose-regulated protein 78 by chronic hypoxia in human gastric tumor cells through a protein kinase C-epsilon/ERK/AP-1 signaling cascade. *Cancer Research,* 61**,** 8322-30.

SONI, K. B., LAHIRI, M., CHACKRADEO, P., BHIDE, S. V. & KUTTAN, R. 1997. Protective effect of food additives on aflatoxin-induced mutagenicity and hepatocarcinogenicity. *Cancer Letters,* 115**,** 129-33.

SPIRIN, V. & MIRNY, L. A. 2003. Protein complexes and functional modules in molecular networks. *Proceedings of National Academy of Science United States of America,* 100**,** 12123-8.

SRIBURI, R., BOMMIASAMY, H., BULDAK, G. L., ROBBINS, G. R., FRANK, M., JACKOWSKI, S. & BREWER, J. W. 2007. Coordinate regulation of phospholipid biosynthesis and secretory pathway gene expression in XBP-1(S)-induced endoplasmic reticulum biogenesis. *Journal of Biological Chemistry,* 282**,** 7024-34.

STAHL, M., STUSCHKE, M., LEHMANN, N., MEYER, H. J., WALZ, M. K., SEEBER, S., KLUMP, B., BUDACH, W., TEICHMANN, R., SCHMITT, M., SCHMITT, G., FRANKE, C. & WILKE, H. 2005. Chemoradiation with and without surgery in patients with locally advanced squamous cell carcinoma of the esophagus. *Journal of Clinical Oncology,* 23**,** 2310-7.

STEFANI, M. & DOBSON, C. M. 2003. Protein aggregation and aggregate toxicity: new insights into protein folding, misfolding diseases and biological evolution. *Journal of Molecular Medicine-Jmm,* 81**,** 678-699.

STEIN, C. A. 1999. Mechanisms of action of taxanes in prostate cancer. *Seminars in Oncology,* 26**,** 3-7.

STOLZ, A. & WOLF, D. H. 2010. Endoplasmic reticulum associated protein degradation: a chaperone assisted journey to hell. *Biochimica et Biophysica Acta,* 1803**,** 694-705.

STONER, G. D., KAIGHN, M. E., REDDEL, R. R., RESAU, J. H., BOWMAN, D., NAITO, Z., MATSUKURA, N., YOU, M., GALATI, A. J. & HARRIS, C. C. 1991. Establishment and characterization of SV40 T-antigen immortalized human esophageal epithelial cells. *Cancer Research,* 51**,** 365-71.

STOREY, J. D. 2002. A direct approach to false discovery rates. *Journal of the Royal Statistical Society Series B-Statistical Methodology,* 64**,** 479-498.

SUBBARAMAIAH, K., CHUNG, W. J., MICHALUART, P., TELANG, N., TANABE, T., INOUE, H., JANG, M., PEZZUTO, J. M. & DANNENBERG, A. J. 1998. Resveratrol inhibits cyclooxygenase-2 transcription and activity in phorbol ester-treated human mammary epithelial cells. *Journal of Biological Chemistry,* 273**,** 21875-82.

SUBBARAMAIAH, K., MICHALUART, P., CHUNG, W. J., TANABE, T., TELANG, N. & DANNENBERG, A. J. 1999. Resveratrol inhibits cyclooxygenase-2 transcription in human mammary epithelial cells. *Annals of the New York Academy of Sciences,* 889**,** 214-23.

SUNDARAM, S. G. & MILNER, J. A. 1996. Diallyl disulfide inhibits the proliferation of human tumor cells in culture. *Biochimica et Biophysica Acta,* 1315**,** 15-20.

SURH, Y. J. 2003. Cancer chemoprevention with dietary phytochemicals. *Nature Reviews Cancer,* 3**,** 768-780.

SZEGEZDI, E., LOGUE, S. E., GORMAN, A. M. & SAMALI, A. 2006. Mediators of endoplasmic reticulum stress-induced apoptosis. *EMBO Reports,* 7**,** 880-5.

TACCHINI, L., DANSI, P., MATTEUCCI, E. & DESIDERIO, M. A. 2000. Hepatocyte growth factor signal coupling to various transcription factors depends on triggering of Met receptor and protein kinase transducers in human hepatoma cells HepG2. *Experimental Cell Research,* 256**,** 272-81.

TADI, P. P., LAU, B. H., TEEL, R. W. & HERRMANN, C. E. 1991. Binding of aflatoxin B1 to DNA inhibited by ajoene and diallyl sulfide. *Anticancer Research,* 11**,** 2037-41.

TAKAYANAGI, S., FUKUDA, R., TAKEUCHI, Y., TSUKADA, S. & YOSHIDA, K. 2013. Gene regulatory network of unfolded protein response genes in endoplasmic reticulum stress. *Cell Stress Chaperones,* 18**,** 11-23.

TANAKA, N., KIMURA, H., FARIED, A., SAKAI, M., SANO, A., INOSE, T., SOHDA, M., OKADA, K., NAKAJIMA, M., MIYAZAKI, T., FUKUCHI, M., KATO, H., ASAO, T., KUWANO, H., SATOH, T., OIKAWA, M., KAMIYA, T. & ARAKAWA, K. 2010. Quantitative analysis of cisplatin sensitivity of human esophageal squamous cancer cell lines using in-air micro-PIXE. *Cancer Science,* 101**,** 1487-92.

TANIMUKAI, H., KANAYAMA, D., OMI, T., TAKEDA, M. & KUDO, T. 2013. Paclitaxel induces neurotoxicity through endoplasmic reticulum stress. *Biochemical and Biophysical Research Communications,* 437**,** 151-5.

TAYLOR, P., NORIEGA, R., FARAH, C., ABAD, M. J., ARSENAK, M. & APITZ, R. 2006. Ajoene inhibits both primary tumor growth and metastasis of B16/BL6 melanoma cells in C57BL/6 mice. *Cancer Letters,* 239**,** 298-304.

TESKE, B. F., WEK, S. A., BUNPO, P., CUNDIFF, J. K., MCCLINTICK, J. N., ANTHONY, T. G. & WEK, R. C. 2011. The eIF2 kinase PERK and the integrated stress response facilitate activation of ATF6 during endoplasmic reticulum stress. *Molecular Biology of the Cell,* 22**,** 4390-405.

THASTRUP, O., CULLEN, P. J., DROBAK, B. K., HANLEY, M. R. & DAWSON, A. P. 1990. Thapsigargin, a tumor promoter, discharges intracellular Ca2+ stores by specific inhibition of the endoplasmic reticulum Ca2(+)-ATPase. *Proceedings of National Academy of Science United States of America,* 87**,** 2466-70.

THUERAUF, D. J., ARNOLD, N. D., ZECHNER, D., HANFORD, D. S., DEMARTIN, K. M., MCDONOUGH, P. M., PRYWES, R. & GLEMBOTSKI, C. C. 1998. p38 Mitogen-activated protein kinase mediates the transcriptional induction of the atrial natriuretic factor gene through a serum response element. A potential role for the transcription factor ATF6. *Journal of Biological Chemistry,* 273**,** 20636-43.

TILLI, C. M., STAVAST-KOOY, A. J., VUERSTAEK, J. D., THISSEN, M. R., KREKELS, G. A., RAMAEKERS, F. C. & NEUMANN, H. A. 2003. The garlic-derived organosulfur component ajoene decreases basal cell carcinoma tumor size by inducing apoptosis. *Archives of Dermatological Research,* 295**,** 117-23.

TIRASOPHON, W., WELIHINDA, A. A. & KAUFMAN, R. J. 1998. A stress response pathway from the endoplasmic reticulum to the nucleus requires a novel bifunctional protein kinase/endoribonuclease (Ire1p) in mammalian cells. *Genes & Development,* 12**,** 1812-24.

TOMBAL, B., WEERARATNA, A. T., DENMEADE, S. R. & ISAACS, J. T. 2000. Thapsigargin induces a calmodulin/calcineurin-dependent apoptotic cascade responsible for the death of prostatic cancer cells. *Prostate,* 43**,** 303-17.

TONG, D. K. & LAW, S. 2009. Management of oesophageal cancer. *Indian Journal of Surgery,* 71**,** 317-25.

TREIMAN, M., CASPERSEN, C. & CHRISTENSEN, S. B. 1998a. A tool coming of age: thapsigargin as an inhibitor of sarco-endoplasmic reticulum Ca(2+)-ATPases. *Trends in Pharmacological Sciences,* 19**,** 131-5.

TREIMAN, M., CASPERSEN, C. & CHRISTENSEN, S. B. 1998d. A tool coming of age: thapsigargin as an inhibitor of sarcoendoplasmic reticulum Ca2+-ATPases. *Trends in Pharmacological Sciences,* 19**,** 131-135.

TURATI, F., PELUCCHI, C., GUERCIO, V., LA VECCHIA, C. & GALEONE, C. 2015. Allium vegetable intake and gastric cancer: a case-control study and meta-analysis. *Molecular Nutrition & Food Research,* 59**,** 171-9.

UEMURA, A., OKU, M., MORI, K. & YOSHIDA, H. 2009. Unconventional splicing of XBP1 mRNA occurs in the cytoplasm during the mammalian unfolded protein response. *Journal of Cell Science,* 122**,** 2877-86.

UNDERWOOD, T. J., DEROUET, M. F., WHITE, M. J., NOBLE, F., MOUTASIM, K. A., SMITH, E., DREW, P. A., THOMAS, G. J., PRIMROSE, J. N. & BLAYDES, J. P. 2010. A comparison of primary oesophageal squamous epithelial cells with HET-1A in organotypic culture. *Biol Cell,* 102**,** 635-44.

URANO, F., WANG, X., BERTOLOTTI, A., ZHANG, Y., CHUNG, P., HARDING, H. P. & RON, D. 2000. Coupling of stress in the ER to activation of JNK protein kinases by transmembrane protein kinase IRE1. *Science,* 287**,** 664-6.

URBA, S. G., ORRINGER, M. B., TURRISI, A., IANNETTONI, M., FORASTIERE, A. & STRAWDERMAN, M. 2001. Randomized trial of preoperative chemoradiation versus surgery alone in patients with locoregional esophageal carcinoma. *Journal of Clinical Oncology,* 19**,** 305-13.

VAN HUIZEN, R., MARTINDALE, J. L., GOROSPE, M. & HOLBROOK, N. J. 2003. P58IPK, a novel endoplasmic reticulum stress-inducible protein and potential negative regulator of eIF2alpha signaling. *Journal of Biological Chemistry,* 278**,** 15558-64.

VISWANATHAN, G. A., SETO, J., PATIL, S., NUDELMAN, G. & SEALFON, S. C. 2008. Getting started in biological pathway construction and analysis. *PLOS Computational Biology,* 4**,** e16.
WALTER, P. & JOHNSON, A. E. 1994. Signal Sequence Recognition and Protein Targeting to the Endoplasmic-Reticulum Membrane. *Annual Review of Cell Biology,* 10**,** 87-119.

WALTER, P. & RON, D. 2011. The unfolded protein response: from stress pathway to homeostatic regulation. *Science,* 334**,** 1081-6.

WANG, C. C. & TSOU, C. L. 1993. Protein disulfide isomerase is both an enzyme and a chaperone. *FASEB Journal,* 7**,** 1515-7.

WANG, H. C., HSIEH, S. C., YANG, J. H., LIN, S. Y. & SHEEN, L. Y. 2012. Diallyl trisulfide induces apoptosis of human basal cell carcinoma cells via endoplasmic reticulum stress and the mitochondrial pathway. *Nutrition and Cancer,* 64**,** 770-80.

WANG, H. C., YANG, J. H., HSIEH, S. C. & SHEEN, L. Y. 2010a. Allyl sulfides inhibit cell growth of skin cancer cells through induction of DNA damage mediated G2/M arrest and apoptosis. *Journal of Agricultural and Food Chemistry,* 58**,** 7096-103.

WANG, J., DUNCAN, D., SHI, Z. & ZHANG, B. 2013. WEB-based GEne SeT AnaLysis Toolkit (WebGestalt): update 2013. *Nucleic Acids Research,* 41**,** W77-83.

WANG, X. Z. & RON, D. 1996. Stress-induced phosphorylation and activation of the transcription factor CHOP (GADD153) by p38 MAP Kinase. *Science,* 272**,** 1347-9.

WANG, Y., SHEN, J., ARENZANA, N., TIRASOPHON, W., KAUFMAN, R. J. & PRYWES, R. 2000. Activation of ATF6 and an ATF6 DNA binding site by the endoplasmic reticulum stress response. *Journal of Biological Chemistry,* 275**,** 27013-20.

WANG, Y. B., QIN, J., ZHENG, X. Y., BAI, Y., YANG, K. & XIE, L. P. 2010b. Diallyl trisulfide induces Bcl-2 and caspase-3-dependent apoptosis via downregulation of Akt phosphorylation in human T24 bladder cancer cells. *Phytomedicine,* 17**,** 363-8.

WEI, Y., PATTINGRE, S., SINHA, S., BASSIK, M. & LEVINE, B. 2008. JNK1-mediated phosphorylation of Bcl-2 regulates starvation-induced autophagy. *Molecular Cell,* 30**,** 678-88.
WHITMARSH, A. J., SHORE, P., SHARROCKS, A. D. & DAVIS, R. J. 1995. Integration of Map Kinase Signal-Transduction Pathways at the Serum Response Element. *Science,* 269**,** 403-407.
WONG, R. & MALTHANER, R. 2000. Esophageal cancer: a systematic review. *Current Problems in Cancer,* 24**,** 297-373.

WU, J., LU, L. Y. & YU, X. 2010. The role of BRCA1 in DNA damage response. *Protein Cell,* 1**,** 117-23.

WU, X. J., KASSIE, F. & MERSCH-SUNDERMANN, V. 2005. The role of reactive oxygen species (ROS) production on diallyl disulfide (DADS) induced apoptosis and cell cycle arrest in human A549 lung carcinoma cells. *Mutation Research* 579**,** 115-24.

XIAO, D., CHOI, S., JOHNSON, D. E., VOGEL, V. G., JOHNSON, C. S., TRUMP, D. L., LEE, Y. J. & SINGH, S. V. 2004. Diallyl trisulfide-induced apoptosis in human prostate cancer cells involves c-Jun N-terminal kinase and extracellular-signal regulated kinase-mediated phosphorylation of Bcl-2. *Oncogene,* 23**,** 5594-606.

XIAO, D., HERMAN-ANTOSIEWICZ, A., ANTOSIEWICZ, J., XIAO, H., BRISSON, M., LAZO, J. S. & SINGH, S. V. 2005. Diallyl trisulfide-induced G(2)-M phase cell cycle arrest in human prostate cancer cells is caused by reactive oxygen species-dependent destruction and hyperphosphorylation of Cdc 25 C. *Oncogene,* 24**,** 6256-68.

XIAO, D., ZENG, Y., HAHM, E. R., KIM, Y. A., RAMALINGAM, S. & SINGH, S. V. 2009. Diallyl trisulfide selectively causes Bax- and Bak-mediated apoptosis in human lung cancer cells. *Environmental and Molecular Mutagenesis,* 50**,** 201-12.

XU, B., MONSARRAT, B., GAIRIN, J. E. & GIRBAL-NEUHAUSER, E. 2004. Effect of ajoene, a natural antitumor small molecule, on human 20S proteasome activity in vitro and in human leukemic HL60 cells. *Fundamental & Clinical Pharmacology,* 18**,** 171-80.

XU, G. & JAFFREY, S. R. 2013. Proteomic identification of protein ubiquitination events. *Biotechnology & genetic engineering reviews,* 29**,** 73-109.

XU, Y., WANG, C. & LI, Z. 2014. A new strategy of promoting cisplatin chemotherapeutic efficiency by targeting endoplasmic reticulum stress. *Molecular and Clinical Oncology,* 2**,** 3-7.
YADAV, R. K., CHAE, S. W., KIM, H. R. & CHAE, H. J. 2014. Endoplasmic reticulum stress and cancer. *Journal of Cancer Prevention,* 19**,** 75-88.

YAMAGUCHI, H. & WANG, H. G. 2004. CHOP is involved in endoplasmic reticulum stress-induced apoptosis by enhancing DR5 expression in human carcinoma cells. *Journal of Biological Chemistry,* 279**,** 45495-502.

YAMAMOTO, K., SATO, T., MATSUI, T., SATO, M., OKADA, T., YOSHIDA, H., HARADA, A. & MORI, K. 2007. Transcriptional induction of mammalian ER quality control proteins is mediated by single or combined action of ATF6alpha and XBP1. *Developmental Cell,* 13**,** 365-76.

YAN, W., FRANK, C. L., KORTH, M. J., SOPHER, B. L., NOVOA, I., RON, D. & KATZE, M. G. 2002. Control of PERK eIF2alpha kinase activity by the endoplasmic reticulum stress-induced molecular chaperone P58IPK. *Proceedings of National Academy of Science United States of America,* 99**,** 15920-5.

YANG, C. S., CHHABRA, S. K., HONG, J. Y. & SMITH, T. J. 2001. Mechanisms of inhibition of chemical toxicity and carcinogenesis by diallyl sulfide (DAS) and related compounds from garlic. *Journal of Nutrition,* 131**,** 1041S-5S.

YANG, J. S., CHEN, G. W., HSIA, T. C., HO, H. C., HO, C. C., LIN, M. W., LIN, S. S., YEH, R. D., IP, S. W., LU, H. F. & CHUNG, J. G. 2009. Diallyl disulfide induces apoptosis in human colon cancer cell line (COLO 205) through the induction of reactive oxygen species, endoplasmic reticulum stress, caspases casade and mitochondrial-dependent pathways. *Food and Chemical Toxicology,* 47**,** 171-9.

YANG, J. S., KOK, L. F., LIN, Y. H., KUO, T. C., YANG, J. L., LIN, C. C., CHEN, G. W., HUANG, W. W., HO, H. C. & CHUNG, J. G. 2006a. Diallyl disulfide inhibits WEHI-3 leukemia cells in vivo. *Anticancer Research,* 26**,** 219-25.

YANG, J. Y., DELLA-FERA, M. A., NELSON-DOOLEY, C. & BAILE, C. A. 2006b. Molecular mechanisms of apoptosis induced by ajoene in 3T3-L1 adipocytes. *Obesity (Silver Spring),* 14**,** 388-97.

YANG, S. H., SHARROCKS, A. D. & WHITMARSH, A. J. 2013. MAP kinase signalling cascades and transcriptional regulation. *Gene,* 513**,** 1-13.

YE, J., RAWSON, R. B., KOMURO, R., CHEN, X., DAVE, U. P., PRYWES, R., BROWN, M. S. & GOLDSTEIN, J. L. 2000. ER stress induces cleavage of membrane-bound ATF6 by the same proteases that process SREBPs. *Molecular Cell,* 6**,** 1355-64.

YE, Y., YANG, H. Y., WU, J., LI, M., MIN, J. M. & CUI, J. R. 2005. [Z-ajoene causes cell cycle arrest at G2/M and decrease of telomerase activity in HL-60 cells]. *Zhonghua Zhong Liu Za Zhi,* 27**,** 516-20.

YIN, X., ZHANG, R., FENG, C., ZHANG, J., LIU, D., XU, K., WANG, X., ZHANG, S., LI, Z., LIU, X. & MA, H. 2014. Diallyl disulfide induces G2/M arrest and promotes apoptosis through the p53/p21 and MEK-ERK pathways in human esophageal squamous cell carcinoma. *Oncology Reports,* 32**,** 1748-56.

YOSHIDA, H., MATSUI, T., YAMAMOTO, A., OKADA, T. & MORI, K. 2001a. XBP1 mRNA is induced by ATF6 and spliced by IRE1 in response to ER stress to produce a highly active transcription factor. *Cell,* 107**,** 881-91.

YOSHIDA, H., OKADA, T., HAZE, K., YANAGI, H., YURA, T., NEGISHI, M. & MORI, K. 2001g. Endoplasmic reticulum stress-induced formation of transcription factor complex ERSF including NF-Y (CBF) and activating transcription factors 6alpha and 6beta that activates the mammalian unfolded protein response. *Molecular and Cell Biology,* 21**,** 1239-48.

YUAN, J. S., REED, A., CHEN, F. & STEWART, C. N., JR. 2006. Statistical analysis of real-time PCR data. *BMC Bioinformatics,* 7**,** 85.

ZHANG, L. J., CHEN, S., WU, P., HU, C. S., THORNE, R. F., LUO, C. M., HERSEY, P. & ZHANG, X. D. 2009. Inhibition of MEK blocks GRP78 up-regulation and enhances apoptosis induced by ER stress in gastric cancer cells. *Cancer Letters,* 274**,** 40-6.

ZHANG, Y. S., CHEN, X. R. & YU, Y. N. 1989. Antimutagenic effect of garlic (Allium sativum L.) on 4NQO-induced mutagenesis in Escherichia coli WP2. *Mutation Research* 227**,** 215-9.

ZHU, B., ZOU, L., QI, L., ZHONG, R. & MIAO, X. 2014. Allium vegetables and garlic supplements do not reduce risk of colorectal cancer, based on meta-analysis of prospective studies. *Clinical Gastroenterology and Hepatology,* 12**,** 1991-2001 e1-4; quiz e121.

ZINSZNER, H., KURODA, M., WANG, X., BATCHVAROVA, N., LIGHTFOOT, R. T., REMOTTI, H., STEVENS, J. L. & RON, D. 1998. CHOP is implicated in programmed cell death in response to impaired function of the endoplasmic reticulum. *Genes & Development,* 12**,** 982-95.

APPENDIX A

RECIPES

Acrylamide/Bisacrylamide Solution (30%)

To make the stork solution, 29g of acrylamide and 1g of bisacrylamide were dissolved in 100ml of distilled water and stored at 4℃ away from light.

7.5M Ammonium acetate, pH7.4

57.81g of ammonium acetate were dissolved in 60ml of distilled water and the pH was adjusted to pH 7.4.

10 % Ammonium persulfate (APS):

100 mg APS was dissolved in 1 ml double-distilled water, and stored at 4 °C.

Coomassie staining solution:

0.5 g Coomassie BB was diluted in 200 ml methanol, 100 ml acetic acid and 400 ml double-distilled water. It autoclaved and stored at room temperature.

Destaining solution:

100 ml acetic acid, 100 ml methanol and 800 ml double-distilled water were mixed and stored at room temperature.

Dulbecco's minimal eagle media (DMEM):

DMEM Powder with catalogue number 12800-017 was prepared according to the manufacturer's instructions.

6X DNA Loading Dye:

25mg of bromophenol blue, 25mg of xylene cyanol FF and 4mg of sucrose were dissolved in 9ml of distilled water. The dye was subsequently stored at -20℃.

0.5 M EDTA (pH 8.0):

37.22 g Na2EDTA·2H2O was added to 140 ml of distilled water. The pH was adjusted to 8.0 and then distilled water was added to a final volume of 200 ml. The solution was subsequently autoclaved and stored at room temperature.

Ethedium Bromide:

10µl of stork solution (10mg/ml) was added to 200ml distilled water, to obtain a 0.5mg/ml final concentration.

Freeze down media:

7ml of fetal bovine serum (FBS), 2ml DMEM and 1ml Dimethylsulphoxide (DMSO).

Membrane stripping solution:

To make 1 M Glycine, 37.5g of glycine was added to 400ml of distilled water. The solution was then adjusted to pH 2.5. Distilled water was added up to 500ml final volume, and then stored at room temperature.

MOWIOL® 4-88 mounting medium:

75 g MOWIOL 4-88 ® (Calbiochem) mounting medium was diluted in 300 ml 1× PBS and stirred for 16 hours at room temperature. After that, 150 ml glycerol was added to the solution and then it was stirred for an additional 16 hours at room temperature. The solution was subsequently centrifuged for 15 minutes at 4000 rpm and the pH was adjusted to pH8. The supernatant was then stored at - 20 °C and n-Propylgallate supplement was added.

5 % Non-fat blocking solution:

3.3 mg non-fat milk powder was dissolved in 30 ml TBST

5 mg/ml 3-[4, 5-dimethylthiazol]-2,5-diphenyltetrazolium bromide (MTT):

100 mg MTT (3-[4, 5-dimethylthiazol]-2, 5-diphenyltetrazolium bromide) (Sigma) added to 20ml of 1 x PBS at pH 7.5 (under sterile condition). The solution was then stored at 4 °C away from light, and used within a month.

Penicillin G/Streptomycinsulfate:

For the preparation of the penicillin G/streptomycinsulfate solution, 604 mg (999620 IU) penicillin G and 1316 mg (1000160 IU) streptomycinsulfate was dissolved in 100 ml double-distilled water, and filter sterilised.

10 × Phosphate Buffer Saline (PBS) (pH 7.5):

For a 10 × PBS preparation NaCl (Merck), KCl (Merck), Na2HPO4 (Merck) and KH2PO4 (Merck) powders were diluted in double distilled water to 1.37 M , 27 mM, 43 mM and 14 mM respectively, and finally calibrated to a final pH of 7.5.

Ponseau staining solution:

The Ponseau (usb®) staining solution was prepared by diluting Ponseau powder and acetic acid in double-distilled water to 0.2 % and 5 % respectively.

Propidium iodide (PI) staining solution:

Stocks of 100% Triton X-100, 1 M MgCl2, 1 M NaCl, 0.1 M PIPES and 1 mg/ml PI were diluted in 20 ml double-distilled water to give a final concentration of 0.1 % Triton X-100, 2 mM MgCl2, 0.1 M NaCl, 10 mM PIPES and 0.01 mg/ml PI. The solution was stored in a 50 ml Falcon tube and covered with foil as it is sensitive to light.

4 X Protein loading buffer:

24 ml 1 M Tris at pH 6.8, 4 ml 20 % SDS, 0.2 ml 0.1 % bromophenol blue and 4 ml glycerol were mixed. 50 µl bromophenol blue (Merck) was added after the solution was diluted to a 1 x concentration.

10 × Running buffer:

Tris, glycine and SDS were diluted in double distilled water to a final concentration of 240 mM, 1.92M and 35 mM respectively.

10 % Sodium dodecyl sulphate (SDS):

10 g SDS was dissolved in 80 ml double-distilled water, then made to a final volume of 100 ml with double-distilled water.

10 % Solubilisation reagent: Sodium Lauryl Sulfate (SLS):

5 ml 1 M HCl was added to 50 g SLS (MERCK). The solution was further diluted with double distilled water to a final volume of 500 ml.

4 % Stacking gel:

0.63 ml 1 M Tris (Merck) at pH 6.8, 0.65 ml 30 % acrylamide/bisacrylamide (Sigma®) and 50 µl 10 % SDS (Merck) was diluted in 3.65 ml double-distilled water. Immediately before adding to the gel tray, 25 µl 10 % ammonium persulfate (APS) (MERCK) and 5 µl TEMED (Sigma) was added to the solution.

8 % stacking gel:

For the preparation of 8 % stacking gel, 3.75 ml 1 M Tris at pH 8.8, 2.7 ml 30 % Acrylamide/bisacrylamide and 100 µl 10 % SDS was diluted in 3.39 ml double-distilled water. Immediately before adding to the gel tray, 50 µl 10 % ammonium persulfate (APS) and 5 µl TEMED was added to the solution.

TBST (TBS-tween):

To make up TBST, 50 ml 1 M tris-base, 20 ml 5 M NaCl and 250 µl Tween-20 was dissolved in 100 ml double-distilled water, and stored at room temperature.

10 × Transfer buffer:

3.03 Tris and 14.5 glycine (Merck) were diluted to a final concentration of 24 mM and 193 mM respectively in 1 L double distilled water.

Tris-buffered saline (TBS):

3.03 g Tris (pH 7.5) and 9 g NaCl was added to final concentrations of 25 mM and 0.9 % (w/v) respectively in 1 L double-distilled water.

1 M Tris pH 6.8 (per litre):

Add 121 g Tris base to 800 ml double-distilled water, adjust the pH to 6.8, and add double distilled water to 1 L, then autoclave.

1 M Tris pH 7.5 (per litre):

Add 121 g Tris base to 800 ml double-distilled water, adjust the pH to 7.5, and add double distilled water to 1 L, then autoclave.

1 M Tris pH 8.0 (per litre):

Add 121 g Tris base to 800 ml double-distilled water, adjust the pH to 8.0, and add double distilled water to 1 L, then autoclave.

1 M Tris pH 8.8 (per litre):

Add 121 g Tris base to 800 ml double-distilled water, adjust the pH to 8.8, and add double distilled water to 1 L, then autoclave.

Trypsin:

Trypsin is made up by adding 0.5 g trypsin powder to 0.2 g EDTA powder, and making up to a total volume of 1 L with PBS buffer. The pH of the solution was adjusted to 7.4 and the solution was filter sterilised.

APPENDIX B

Primer sequences of genes amplified with qRT-PCR and the amplicon size. The sequences were designed using the NCBI/Primer-BLAST.

Gene Symbol	Forward Primer (5' – 3')	Reverse Primer (5' – 3')	Annealing Temperature (℃)
gapdg	GCCTGCTTCACCACCTTC	GGCTCTCCAGAACATCATCC	60
sec63	TTCCAGTTGTTGTGGGCTCTT	CAGAAGCTCCAGCCAAAACC	60
ddost	CGGACAAGCCTATCACCCAG	TGCCTGTCTGGGAATACCTCT	60
rrbp1	GGCAGACCTCCTAGTGAAAG	GAGTTTTCGCCATCTCCTTGC	58
llman1	CAGAATCCAAGATGGCGGGA	GGAATAGCATTCCCCGCGT	58
Ire1	GCCTAGTCAGTTCTGCGTCC	GCTGGTACTTCCAAAAATCCCG	60
ssr3	CTCAAGCACAAAGTAGCACAGA	GACCACGACCAGGAACAGAG	59
tram	GCGATTCGCAAGAAAAGCAC	TTGTTCTTCTGTTGCTGGGAGG	60
ero1	GGTGCTTCTGCCAGGTTAGTG	GTCCCTTCTTCCACACTGGC	60
vimp	GGATGAGGCTAAGAATCTTGTAGA	GTAATTACACTGCTCAAGGCTC	57
sel1l	GAAACCAGCTTTGACCGCCA	AGCCCCACTTTTCATCTGCT	60
ubc6	GATCATTACCATGCGCAGCC	TCGACCATTAGCCGTTAGGAG	60
sec61	ATTTCCAGGGCTTCCGAGTG	CGAGCTGAGAGCATTTGGGA	60
grp94	CTGCTCCACGTGGTCTGTTT	GATCATCTGAGTCCACCACACC	60
edem	TGTTCACAACAGAGGGACAC	CAGGTACACGATTGCAGTTGG	58
pdiA4	CACCAGAAGTCACGCTTGTGTTGA	AGGAGAACGCTTGCTGAGCTCCTT	60
ask	CCCTGGAAACCCTGCATTTTG	GAGTCCGAGTTAGTATCACAG	55
sec24D	GAGAAAGGGTTTGACGTGGC	CAAAAGAAGTCTGTTCCCGCTC	59
atf6	ACGGAGTATTTTGTCCGCCT	AGCAAAGAGAGCAGAATCCCAA	59

casp4	TGTTCCCTATGGCAGAAGGC	TGTCCTGCCATACGTTGCTT	57
xbp-1s	TTACGAGAGAAAACTCATGGCC	GGGTCCAAGTTGTCCAGAATGC	55
grp78/bip	GACATCAAGTTCTTGCCGTT	CTCATAACATTTAGGCCAGC	50
ddit3/chop	CCAGCAGAGGTCACAAGCAC	GGGAATGACCACTCTGTTTC	55